



National Centre
for the Replacement
Refinement & Reduction
of Animals in Research



University of
Nottingham
UK | CHINA | MALAYSIA

Modelling changes in excitability of the peripheral nervous system using compartmentalised microfluidic culture

Thesis submitted for the degree of Doctor of Philosophy

Alice Marie Rockliffe

Student ID 4308748

January 2021

Declaration

I confirm that the work in this thesis is my own. Images from other sources, or work that has been generated through collaborative projects, have been otherwise acknowledged in the text.

Alice Marie Rockliffe

Table of Figures:

Figure 1.2.1: Comparison of neuronal phenotypes. 1A) A multipolar neuron phenotype, typically observed by cortical neurons in the CNS. 1B) A Pseudounipolar neuron, most commonly recognised as the phenotype of the neurons of the dorsal root ganglion.	18
Figure 1.4.1: A simplified representation of a myelinated neuron in the PNS, made using BioRender.....	21
Figure 1.4.2: Distribution of voltage gate channel isoforms at the paranodal and nodal regions. This image has been taken from (Rasband and Peles, 2016) as a recreation from (Lakke, 1997).....	23
Figure 1.4.3: An overview of the action potential.	24
Figure 1.5.1: The changes in paw withdrawal threshold associated with development of peripheral sensitisation and hyperalgesia.	31
Figure 1.6.1 A) simplified diagram of a cross section of the fibres of the DRG showing relative subpopulations of neuronal fibres.....	33
Figure 1.6.2: An simplified overview of the fibres of the DRG (Susuki, 2010). There is a wide variability in the range of stimuli that can activate the neurons of the DRG in pain based processing. Whilst the role of C- and A δ fibres in nociceptive processing is widely explored, there is also evidence for function of the larger diameter A β fibres as both mechanoreceptors and nociceptors.....	34
Figure 1.7.1: A) Subcellular localization of potassium channels in murine DRG neuron (Tsantoulas and McMahon, 2014).....	46
Figure 1.10.1: An overview of the canonical pathway of microRNA biogenesis, made using Biorender.....	58
Figure 2.2.1: Example scan of cytokine array membrane exposed to M1-like media for 10-minutes.	68
Figure 2.2.2: Schematic showing the design of a two channel microfluidic device with microgroove length 150 μ M separating the microfluidically isolated compartments, image taken from Xona microfluidics.	71
Figure 2.4.1 The dual luciferase reporter system using pmiRGlo and expression of firefly luciferase (FLuc) to quantify miR-mimic binding to a protein sequence of interest in vector	80

Figure 3.1.1: Interactions between distinct parts of a nociceptor with different types of non-neuronal cells, (R. R. Ji, Chameessian and Zhang, 2016) 95

Figure 3.2.1: Separating channels to demonstrate migration of those cells stained with DAPI nuclear stain through the microgrooves of a two-channel microfluidic device. Where DAPI nuclear staining was localised to both the axonal and the somal compartment of these devices, the microfluidic isolation was lost ,rendering them useless. 103

Figure 3.2.2: Attempting to optimise neonatal rat culture in microfluidic devices. Addition of DAPI nuclear stain showed migration of non-neuronal cells through the microgrooves, meaning microfluidic isolation of these cultures was lost. Anti-mitotics were added to attempt to reduce the ratio of non-neuronal cells in culture; 105

Figure 3.2.3: Dual-staining of DRG neurons cultured from E16.5 murine tissue in a two-channel microfluidic device. No migration of cells through the microgrooves was observed, the DAPI nuclear stain (blue) remained localised to the somal compartment. 20X magnification. Red= Acetylated Tubulin, Blue= DAPI 106

Figure 3.2.4: Immunofluorescent staining of E16.5 mouse DRG neurons at DiV5 in culture to compare methods of culture. 107

Figure 3.3.1: Bright-field imaging at 20X of a healthy culture of monocytes isolated from bone marrow of adult mouse femur tissue. Imaged at DiV7. Cells have attached to the plastic and showed an elongated phenotype 110

Figure 3.3.2: Multiple methods of coating for culturing bone derived monocytes in the lateral compartment of microfluidic devices were investigated to ensure cell adhesion without migration through the microgrooves: 111

Figure 3.3.3: Overview for the role of the metabolism of L-arginine in characterising the phenotype of macrophages. In vivo, *this switch between arginine and orthinine metabolism can be used to characterise the phenotype of inflammatory cells* (See Mosser and Zhang., 2008) 114

Figure 3.3.4: Exposure to inflammatory stimuli for 24H induced a quantifiable change in macrophage phenotype: 116

Figure 3.4.1: Determination of the purity of a microglial culture isolated from embryonic spinal cord tissue. 122

Figure 3.4.2: Exposure to inflammatory mediators induced significant changes in the phenotype of spinal cord derived microglial cells.....	124
Figure 4.2.1: Schematic representation of the differences between stimulating the axons in compartmentalised microfluidic culture versus the whole cell population in a standard dissociated plate culture.	134
Figure 4.2.2: By measuring change in fluorescence as a proxy for cell excitability, the effects of KCL stimulation on evoked Ca ²⁺ transients was quantified in two different DRG neuron culture systems:.....	137
Figure 5.1.1: An overview of a hyperalgesic priming model <i>in vivo</i> , as used previously by members of the Dajas-Bailador laboratory.....	165
Figure 5.1.2: The results of a preliminary microarray showing upregulation of miR-138-5p in tissue extracted from adult rat primed tissue in the chronic phase of hyperalgesia (Clare Martin, 2016). <i>Saline control N=1, Carrageenan primed tissue N=2.</i>	167
Figure 5.3.1: Culturing cells in semi-permeable "Twiss" inserts for RNA extraction.....	171
Figure 5.3.2: Exposure of axons to inflammatory media significantly increased the expression of miR-138-5p in the soma	172
Figure 5.3.3: Incubation of the axons with either M1-like or M2-like media in the presence of the miR-138 inhibitor induced no significant change in the amplitude of Ca ²⁺ transients and neuronal excitability compared to those observed following incubation of the axons with a non-targeting control.....	175
Figure 5.4.1: <i>miR-138 inhibition in the axonal compartment induced a significant decrease in Ca²⁺ transients in the soma following axonal stimulation with KCL (25mM): Legend continued overleaf...</i>	180
Figure 5.4.2: miR-138 inhibition in the axonal compartment did not induce a significant decrease in Ca ²⁺ transients recorded in the soma following axonal stimulation with Capsaicin (200nM):	182
Figure 5.4.3; Prolonged inhibition of miR-138 in the soma of DRG sensory neurons did not evoke significant changes in neuronal excitability:.....	185
Figure 5.4.4: Prolonged inhibition of miR-138 in the soma of DRG sensory neurons did not evoke significant changes in neuronal excitability:.....	187
Figure 5.4.5: Developing a pipeline for bioinformatic searches of predicted targets overlapping with miR-138-5p.....	189

Figure 5.4.6: : Based on seed sequence expression in the 3'UTR, ion channels of interest were shortlisted and subsequently validated as predicted targets of miR-138-5p. . 191

Figure 5.4.7: Dual staining immunofluorescence from a dissociated plate-based culture of DRG neurons at DiV5 showing high relative expression of Kv1.2 at the terminals (40X.) 194

Figure 5.4.8: Preliminary results from a luciferase reporter assay at N=1: Results show %Change in fluorescence detected when cells were treated with 50nM miR-138 mimic for 48-hours. All 7-targets were previously validated using Sanger sequencing to locate the sequence of interest inserted into the pmiRGlo vector. Only the 4-targets marked with an asterix were carried forward to N=4, where they showed reduction in fLuc activity in the dual luciferase reporter assay. 196

Figure 5.4.9: Transfection with miR-138 mimic and pmiRGlo with the target site inserted showed a reduction in firefly luciferase activity for four targets of interest..... 198

Figure 5.4.10: A site-directed mutagenesis assay demonstrated a loss of function with mutation of the seed sequence for miR-138-5p in the 3'UTR. Transfection with the miR-138 mimic and the mutated DNA sequenced did not induce a reduction in firefly luciferase activity in the dual luciferase assay, (N=3.) No significant difference in fLuc activity was detected between the LNA control and the SDM miR-138-5p targets, therefore validating the presence of a binding site in the 3'UTR of Kv1.2 for miR-138-5p. 199

Figure 5.4.11: Prolonged incubation of the axonal compartment (24-hours) with 100nM siRNA for Kv1.2 evoked small changes in neuronal excitability relative to the non-targeting siRNA control sequence. Evoked change in excitability was not deemed statistically significant at N=7 biological replicates..... 201

Figure 7.1.1: Measuring non-neuronal cell migration in microfluidic cultures; 213

Figure 7.2.1: Results of a 40-target cytokine array using inverted densitometry for a semi-quantitative analysis of the fold change in the most highly expressed cytokines present in different media subtypes. N=2, error bars representing the standard deviation of the fold change. 214

Figure 7.3.1: Looking at the overlay between Iba-1 and the green latex bead as a marker for how the phagocytic activity of microglial cells is dependent on phenotype. 218

Figure 7.5.1: Quantification of localised effects of inflammatory mediators on expression of miR-138-5p in pooled samples of RNA	221
Figure 7.7.1: Plasmid map for pmiRGlo (Promega).....	222

Table of Contents:

1	<i>Introduction and literature review</i>	15
1.1	The nervous system:	15
1.2	The Neuron	17
1.3	The Axon:	18
1.4	The Action Potential:	20
1.5	Disruptions to the action potential:	26
1.5.1	An overview of pain:	26
1.5.2	Peripheral Sensitisation and the DRG neurons:	28
1.5.3	The switch from acute to chronic pain:	29
1.6	Neurons of the pain pathways:	32
1.6.1	Dorsal Root Ganglion Neurons (DRGs):	32
1.6.2	A summary of the activity of fibres within the DRG:	33
1.7	Receptors expressed on the nociceptors:	36
1.7.1	Transient receptor potential channels (TRP):	37
1.7.2	Other TRP channels and pain:	40
1.7.3	Voltage Gated Sodium Channels:	41
1.7.4	Potassium Channels:	44
1.8	Role of non-neuronal cells in nociception:	46
1.8.1	Non-Neuronal Cells:	46
1.8.2	Macrophages:	47
1.8.3	Microglial cells:	50
1.9	Protein turnover and local translation in the nervous system:	52
1.10	MicroRNA:	55

1.10.1	MicroRNAs as regulators of translation in the nervous system:	55
1.10.2	Biogenesis of microRNA:	57
1.10.3	Association with the RNA Induced Silencing Complex:	59
1.10.4	Other pathways for microRNA Biogenesis:	60
1.10.5	Utilising the miRNA seed sequence for target recognition in a signalling pathway:	61
1.11	Summary and aims of this thesis:	62
2	<i>Materials and Methods</i>	63
2.1.1	Animals	63
2.1.2	Cell culture:	63
2.2	Cell Culture based protocols:	63
2.2.1	Coating of plates, dishes and coverslips	63
2.2.2	In vitro culture of bone marrow derived macrophages:	64
2.2.3	Microglial Culture in vitro:	69
2.2.4	In vitro culture of dorsal root ganglion:	70
2.3	Functional studies with DRG in microfluidic chambers:	72
2.3.1	Calcium Imaging:	72
2.4	MicroRNA functional analysis tools:	78
2.4.1	MicroRNA 'power' inhibitors;	78
2.4.2	Small interfering RNA (siRNA):	78
2.4.3	Target prediction using Bioinformatics:	79
2.4.4	Target validation using Luciferase assay:	79
2.5	TRIZOL extraction of RNA:	85
2.5.1	Extraction of RNA fractions from porous trans-well inserts:	87
2.5.2	Quantitative polymerase chain reaction (qPCR):	87
2.5.3	cDNA Synthesis:	87
2.5.4	qPCR using SYBR green:	87
2.6	Immunofluorescent staining of primary cells:	89
2.6.1	Quantifying relative expression of protein markers using immunofluorescence:	

3	<i>In Vitro modelling of nociceptive cellular connectivity using compartmentalised microfluidic culture systems</i>	92
3.1	Introduction	92
3.1.1	Peripheral Sensitization of DRG neurons	93
3.1.2	Hyperalgesic priming and the transition from acute to chronic pain	95
3.1.3	Modelling Nociceptive networks in vitro:	96
3.1.4	Experimental aims of the chapter:	101
3.2	Results and Discussion:	102
3.2.1	Culture of DRG neurons in compartmentalised microfluidic chambers:	102
3.3	Culture of inflammatory macrophage cells:	110
3.3.1	Culture of Macrophages in microfluidics:	111
3.3.2	Polarization of macrophages in vitro:	112
3.3.3	Discussion and conclusions from the culture and polarization of macrophages in vitro:	117
3.4	In vitro culture of spinal cord microglia as a model for inflammatory cells in the CNS:	120
3.4.1	Polarizing microglial cells in vitro	123
3.4.2	Discussion and conclusions from the development of in vitro culture method of spinal cord derived microglial cells:	125
3.5	Chapter conclusions:	127
4	<i>Investigation of changes in DRG excitability using a compartmentalised microfluidic model</i>	129
4.1	Introduction:	129
4.1.1	Using evoked Ca ²⁺ transients as a reporter for changes in neuronal excitability:	129
4.1.2	The effect of inflammation on neuron excitability and calcium transients in neurons:	131
4.1.3	Modelling in vitro responses to an acutely applied stimulus	132
4.1.4	Experimental aims and objectives of the chapter:	133

4.2	Part A: Axonal stimulation of embryonic DRG cultures in microfluidic devices evokes rapid Ca²⁺ transients and changes in cell excitability:	133
4.2.1	Stimulation of the axons with potassium chloride in a compartmentalised microfluidic device evoked Ca ²⁺ transients in the soma:	134
4.2.2	Capsaicin evokes increase in neuronal excitability by stimulation of C-like fibres in vitro:	138
4.2.3	The peak excitability of a cell was affected by the cross-sectional cell area of the DRG neuron:	142
4.3	Part B: Macrophage dependent changes in neuronal excitability and Ca²⁺ transients:	146
4.3.1	Acute axonal addition of polarized macrophage media evoked changes in DRG neuronal excitability:	147
4.3.2	Acute stimulation with macrophage media induced changes in the amplitude of a subsequent stimulation with KCL :	149
4.3.3	Prolonged exposure of the axon terminals to polarised macrophage media induced quantifiable changes in neuronal excitability	152
4.4	Discussion and chapter conclusions:	156
5	<i>miR-138-5p regulates DRG excitability</i>	163
5.1	Introduction:	163
5.1.1	microRNA and pain:	164
5.1.2	miR-138-5p and pain:	165
5.2	Materials:	167
5.2.1	LNA technology:	167
5.3	Part A: Investigation of miR-138-5p in modulating the excitability of small fibre DRG neurons	170
5.3.1	Part A objectives:	170
5.3.2	Exposure of axons to inflammatory media demonstrated upregulation of miR-138-5p in the soma:	170
5.3.3	Functional analysis of the dual effect of inflammatory mediators and miR-138-5p on neuronal excitability:	173

5.4	Part B: Molecular and cellular analysis of the mechanisms underlying the effect of miR-138-5p on sensitization of peripheral neurons:	178
5.4.1	Part B objectives:	178
5.4.2	Inhibition of miR-138-5p expression in the axonal compartment of compartmentalised microfluidic devices reduced evoked Ca ²⁺ transients and changes in neuronal excitability:	179
5.4.3	Inhibition of miR-138-5p in the somal compartment did not reduce KCl or Capsaicin-evoked increase in neuronal excitability:	185
5.4.4	Bioinformatic prediction for targets with roles in regulating neuronal excitability by interaction with miR-138-5p:	188
5.4.5	Luciferase reporter assay:	195
5.4.6	Treatment of axons with small interfering RNA (siRNA) for Kv1.2 demonstrated partial rescue of the decrease in excitability induced by miR-138-5p inhibition:	200
5.4.7	Discussion and Chapter Conclusions:	202
6	<i>General Discussion and Conclusions</i>	205
6.1	Role of the DRG neurons in peripheral neuropathy:	205
6.2	Investigation of inflammation on the amplitude of evoked Ca²⁺ transients in the soma of sensory neurons:	206
6.3	The role of microRNA in regulation of sensory neuron excitability:	207
6.4	Dysregulation of potassium channels in disease and neuropathy:	209
6.5	Concluding remarks:	209
6.6	Implications of this study on future work:	211
6.6.1	Investigation of neuronal excitability on inflammation:	211
6.6.2	Investigation of the targets for miR-138-5p in regulating neuronal excitability:	212
7	<i>Appendices</i>	213
7.1	Reduction in the concentration of GDNF did not prevent non-neuronal cell migration	213
7.2	Composition of polarized macrophage media:	213

7.3	Microglial Phagocytosis assay:	217
7.4	Analysing changes in morphology dependent on cellular phenotype:	218
7.5	The stimulation of axons by cytokines used to polarize macrophages did not evoke a significant increase Ca²⁺ transients:	219
7.6	QPCRs from Pooled samples:	221
7.7	pmiRGlo Plasmid Map (Promega):	222
7.8	miR-138-5p binding sites in the 3'UTR of Kv1.2:	222
	<i>Bibliography</i>	223

Acknowledgments:

I would like to take this opportunity to acknowledge all those people who have supported me throughout this PhD, it's hard to find the words to explain my gratitude.

Firstly, I would like to thank NC3Rs for sponsoring this work, I have always been proud to work on this project. I would like to thank Dr. Dajas-Bailador and Dr. Gareth Hathway at the University of Nottingham for giving me this opportunity, I will always be thankful for their guidance over the past three years. I would also like to thank Dr. Angus Brown for seeing potential in me, and encouraging me to pursue a career in science- sometimes we all need someone to give us a nudge in the right direction.

I first started at the University of Nottingham in 2013, and in many ways, it became like a second home to me over the years. I would particularly like to thank Dr. Alex Rathbone and Dr. Cristiano Lucci of the Dajas-Bailador lab for their invaluable guidance and support. On my first day Dr. Lucci taught me how to dissect DRG neurons, and in my last week I taught him to image DRG neurons for Ca^{2+} signalling. Thank you for being so patient and understanding- were it not for your support I would not be where I am today. A special thanks also goes to Asta Tranholm, for being the best friend I could have asked for, I am already missing our daily coffee break!

My deepest gratitude goes to my family- in particular to my sisters Kate and Lucy, and my parents Catrina and John. I will never be able to express how grateful I am for your unconditional love and support. I would also like to thank my grandparents, whose generosity helped to support me throughout my whole university experience. Thank you all for always encouraging me to follow my dreams, I hope that what I have achieved makes you proud.

Last but not least I would like to thank my better half George, I would not be where I am today without your never-ending support.

Abstract:

This thesis describes the use of compartmentalised microfluidic devices to investigate changes in neuronal excitability. All studies carried out in this work were completed in line with principles of the NC3Rs (reduction, replacement and refinement). Particular interest was given to the study of the excitability of dorsal root ganglion neurons (DRGs) in the context of pain-based signalling. This also included the *in vitro* culture and characterisation of non-neuronal cells involved in inflammation and nociception.

Current methods for *In vitro* modelling of pain pathways often fails to replicate the unique morphology of the DRG neurons. These pseudo-unipolar neurons detect nociceptive stimuli at the peripheral terminals, and transduce long range action-potentials to higher processing centres in the central nervous system. Unlike *in vivo* modelling of pain behaviours, *in vitro* models of nociception provide the capacity to monitor changes in neuronal function at a cellular and molecular level. However, until the development of technology such as microfluidics, the standard methods of culture failed to isolate the axons from the soma.

The primary aim of this project was to develop a model capable of replicating the complex microenvironment that terminals of the DRG neurons encounter during the development and onset of pain. This involved the optimisation of cell culture methods for inflammatory cells used to induce changes in neuronal excitability, both from the context of the peripheral terminals, or from the CNS if desired. At a molecular level, the microfluidic model was also used to investigate the role of small non-coding RNA (microRNAs) on regulating DRG excitability in the context of nociception. This Thesis hypothesises that voltage-gated potassium channels form an interesting target for a microRNA of interest. However, it is widely acknowledged that microRNAs regulate the expression of multiple mRNAs.

The use of functional studies using the microfluidic model have shown here that there are differences in the way in which a neuron responds to a stimulus, dependent on whether it is applied locally to the axon or the soma. Live cell imaging was used to measure evoked changes in Ca^{2+} transients as a proxy for cell excitability. As well as significant differences in the response to depolarising agents such as potassium chloride (KCL), the use of biologically relevant stimuli to the study of nociception was also developed. The culture of inflammatory cells such as bone marrow derived macrophages led to the development of cytokine-rich media which was used to evoke changes in neuronal excitability. By exploiting the microfluidic

nature of the device, subsequent investigations to the role of microRNA 138-5p in regulating neuronal excitability were undertaken. The use of cell permeable microRNA inhibition showed a reduction in cell excitability if applied locally to the axons. Bioinformatics led to the development of Kv1.2 as a potential target for miR-138-5p *in vivo*, which could explain the effects of miR-138-5p in modulating excitability of the DRGs.

The findings in this work have demonstrated the potential for development of more biologically relevant *in vitro* models using microfluidic compartmentalised cell culture. For example, fluidic isolation has characterised the role of miR-138-5p in regulating DRG excitability at the axons.

1 Introduction and literature review

The formation of precise axonal connections between the peripheral and central nervous system is essential for successful function related development. The cells of the nervous system form multiple connections in early development, which are systematically pruned to form a complex network for effective signal transduction. In this way a sensory stimulus is detected by cells of the peripheral nervous system, and action potentials rapidly propagated to the central nervous system, whereupon an appropriate motor response is induced. This cell signalling is particularly important for complex multi-cellular processes such as pain, where transduction of a noxious stimuli into an electrical signal relies on compartmentalisation and polarisation of neuronal networks.

1.1 The nervous system:

The central nervous system consists of the brain and the spinal cord, where all neurons are encased by up to 30 sheaths of myelin formed by oligodendrocytes. All other neuronal tissue forms the peripheral nervous system; these neurons are both sensory and motor in nature and propagate action potentials into the central nervous system where it is processed accordingly. Dependent on the function of the nerve, the neurons in the peripheral nervous system may or may not be myelinated. Dependent on the function of the nerve, the neurons in the peripheral nervous system may or may not be myelinated. For example, both small diameter unmyelinated C-fibers, and myelinated A δ fibers are involved in nociceptive processing, but remain silent in the absence of a nocifensive stimulus (Yam *et al.*, 2018). The obvious advantage of myelination is the capacity for saltatory conduction, where the action potential appears to 'jump' between the unmyelinated nodes on the axon. However, whether a nerve is myelinated by Schwann cells is not dependent on the axon diameter, but rather on the expression of neuregulin-1, an epidermal growth factor (Nave and Salzer, 2006). The profiling of neurons within the specific areas of the nervous system demonstrates that neurons develop in accordance with their function. For example, those neurons that are highly involved in movement express high levels of dopaminergic receptors and appear to be more prevalent in the frontal lobe of the cortex. In order to understand these pathologies, it

is therefore essential to investigate the structure and function of the building block of the nervous system, the neuron.

The nervous system is highly complex and first develops within the first 2 to 8 weeks of embryo development (Elshazzly and Caban, 2019). Although formation of the neural plate begins early in embryogenesis, the nervous system continues to grow, and axonal connections continue to form even throughout post-natal development (*Discovering the Brain*, 1992). Once formed, the human brain is estimated to contain 10^{15} neurons as early as aged 3 (Drachman, 2005). At which point, the nervous system undergoes systematic 'pruning' to ensure that axonal connections are meaningful and propagate action potentials in the most effective way possible (Cowan *et al.*, 1984; Meier, Finch and Evan, 2000; Low and Cheng, 2006). The selective re-structuring of the connections in the human brain is at its core a good example of natural selection. The plasticity of the nervous system in early post-natal development occurs in multiple ways. More commonly, cells undergo apoptosis due to changes in the surrounding environment (Yuan, Lipinski and Degterev, 2003). And this programmed cell death reduces unnecessary competition for potential synaptic targets. However, it has also been demonstrated that surrounding growth factors and neurotrophins, such as NGF, may not solely be involved in maintaining cell viability, but also regulating axon development and survival (Singh and Miller, 2005). It is for this reason that such growth factors and cytokines are of particular interest in the development of pathologies like pain, whereby the activity of sensory neurons appears to become dysfunctional due to changes in the surrounding environment.

It is widely acknowledged that most of the nervous system does not generally acquire new neurons post-natally, although there is evidence to suggest that in certain areas adult neurogenesis has been detected in rodent modelling (Lei *et al.*, 2019). This doctrine was first defined in 1965 (Altman and Das, 1965). Since then it has been demonstrated that the genesis of new neurons in adult rodent brains is limited largely to the hippocampal and subventricular zones (Ming and Song, 2011). Furthermore, it has been demonstrated that neurogenesis in the adult human brain is even further limited than that of the rodent CNS. Most notably, in rodents and other mammals neuroblasts appear to migrate from the subventricular zone to the olfactory bulb. However, in humans no new neurons were detected here after development of the adult CNS (Bergmann *et al.*, 2012). In summary, we should be wary when

directly comparing rodent tissue to the CNS of humans. For example, there is also evidence that axons of existing neurons readily regenerate following peripheral nerve injury. Although the axonal connections of the central nervous system (CNS) do not readily regenerate, the neurons of the peripheral nervous system (PNS) have been shown to (Huebner and Strittmatter, 2009).

1.2 The Neuron

The nervous system is comprised of multiple cell types, including neurons (10^{15}) and non-neuronal cells such as glial cells. It was previously estimated that glial cells outnumbered neurons by a factor of 10:1 (HYDEN, 1962) but more recent histological data has suggested otherwise. More accurate cell counting techniques have demonstrated that it is more likely that the glial cell to neuron ratio is around 1:1, with around 86.1 billion neuronal cells and 84.6 billion non-neuronal cells (Azevedo *et al.*, 2009; von Bartheld, Bahney and Herculano-Houzel, 2016). Furthermore, whilst neurons do not continue to divide, and rarely self-regenerate following injury, the glial cells readily proliferate upon injury.

The signalling and cellular excitability of neuronal cells in the PNS forms the basis of this thesis, although we also investigated how the excitability of these cells can be modulated by non-neuronal cells such as immune cells. Therefore, it must be acknowledged early that the neurons cannot function as discrete entities, efficient function of the nervous system relies on multiple layers of cell-to-cell communication.

The majority of neurons acquire a highly polarised morphology in development, often corresponding to the functional of a neuron in the nervous system. Unlike multipolar neurons (figure 1.2.1A) found in the CNS, the neurons of the dorsal root ganglion (DRG) develop an unusual pseudo-unipolar structure (see figure 1.2.1B, below.) Classically it is understood that the dendrites receive information and transmit it to the soma, whilst the axon carries action potentials away from the cell body, towards a receptor cell. The diagram below shows how this flow of information is propagated along the cell via action potentials.

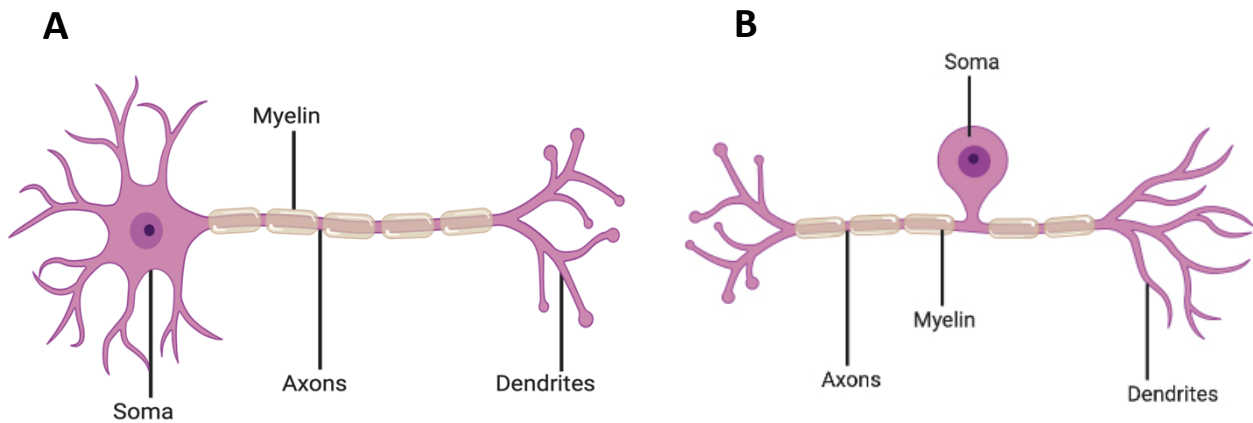


Figure 1.2.1: Comparison of neuronal phenotypes. 1A) A multipolar neuron phenotype, typically observed by cortical neurons in the CNS. 1B) A Pseudounipolar neuron, most commonly recognised as the phenotype of the neurons of the dorsal root ganglion.

1.3 The Axon:

The axons, or nerve fibres are long processes along which action potentials are rapidly propagated for effective cell communication. For example, in some areas of the human body, axons can be up to one metre long, running from the base of the spinal cord to the end of the foot. Primarily the axons are connective structures through which complex neuronal networks are formed for effective cell-to-cell signalling. Therefore, the transduction and transmission of electrical impulses along the axon is essential for rapid neuronal signalling. However, due to the highly polarized nature of the neurons, the axons are also critical in the bidirectional transport of signalling molecules for successful neuronal signalling. Unlike the action potential which is only transported in one direction along the axon, the movement of specific axonal components can require either anterograde (e.g. Kinesin) or retrograde (e.g. Dynein) transport of molecules. Although similar processes of macromolecular transport can be observed in other cells, the scale of protein trafficking observed in the neurons is unique due to the elongated axons and polarized phenotype of the cell.

In general, anterograde transport is essential to transport newly synthesised proteins to a target of interest, whilst retrograde transport simultaneously clears the cell of misfolded or damaged molecules. Microtubule motor proteins drive the movement of molecules along the

axons, inclusive of organelles, endosomes and RNA vesicles. Where kinesin proteins drive the movement of molecules away from the soma, proteins such as dynein are responsible for retrograde transport. However, the purification of axonal endosomes have exhibited the presence of both motor proteins (Hendricks *et al.*, 2010). Therefore, it is understandable that the bi-directional transport of macromolecules is essential not only for the development of the nervous system, but also to prevent pathological degeneration.

The “neurotrophic factor hypothesis” was postulated in 1968, following the result that removal of chick hindlimbs led to a reduction in motor and sensory neurons (Hamburger and Levi-Montalcini, 1949; Levi-Montalcini, 1987). This hypothesis suggested the presence of target-derived neurotrophins was required for the survival of neurons, and ultimately led to the characterization of nerve growth factor (NGF.) Injection of radio-labelled NGF into the axonal terminals led to the discovery that NGF could later be detected in the soma, a result which was confirmed both *in-vitro* and *in-vivo* (MacInnis and Campenot, 2002). Furthermore, the addition of NGF to the axonal compartment of compartmentalised cultures promoted the growth of axons over time (Campenot, 1982). However, since then the family of proteins referred to as neurotrophins has been further investigated and is also known to incorporate BDNF, NT-3 and NT-4/5. These neurotrophins have regulatory roles in both the peripheral and central nervous systems, with established roles in both axonal guidance and nerve regeneration.

Anterograde transport has been most clearly defined using metabolic labelling techniques in the cell (Weiss, 1967). Manipulating the cytoskeleton demonstrated that microtubules are essential for rapid movement along the axons, whilst pulse-chase labelling in motor neurons led to the discovery of multiple phases involved in anterograde transport along the axons (Griffin *et al.*, 1976). Furthermore, the rate of transport appears to be dependent on the function and size of the molecule. Organelles have been shown to move at 400mm/day, whereas cytoskeletal proteins move away from the soma much more slowly (<8mm/day) (Maday *et al.*, 2014). Of particular interest to this project is the anterograde transport of mRNA and microRNA along the axons of sensory nerves. Local protein synthesis is essential for functional cell-to-cell signalling. Although it is evident that localization of specific mRNA within distinct neuronal compartments is important for neuronal function, the mechanisms

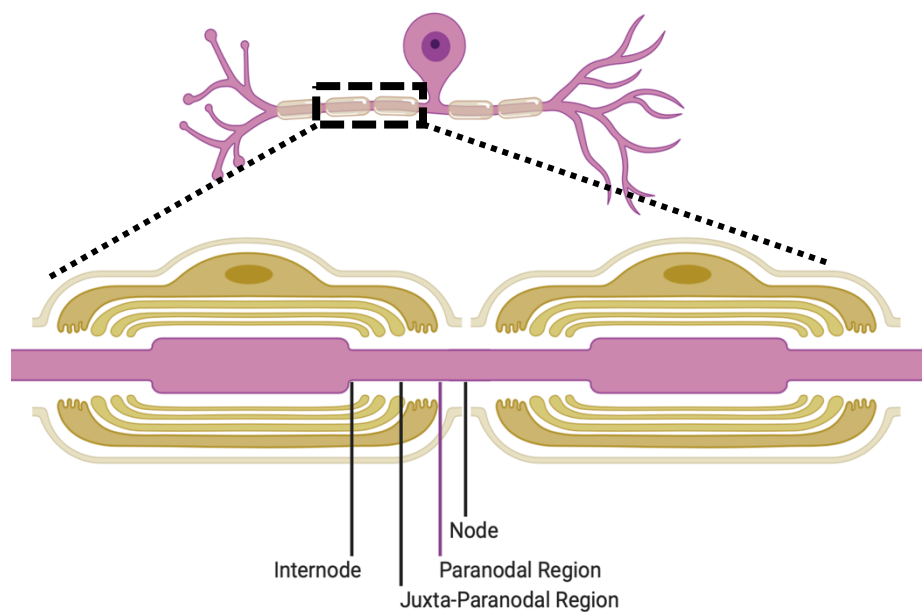
by which this is regulated have yet to be elucidated (Holt, C. E., and Schuman, 2013). Meanwhile microRNAs act as negative regulators of mRNA translation, and the pathway for biogenesis of mature miRNA is discussed in detail below. However, precursor microRNA molecules have been identified both in the soma and the distal compartments of the axon in sensory neurons (Kim, H. H., Kim, P., Phay, M., and Yoo, 2015; Rotem *et al.*, 2017). As such, it is understandable that anterograde transport of microRNA and mRNA is important in regulation of gene expression in neurons.

1.4 The Action Potential:

The action potential underlies all electrophysiological neuronal cell-to-cell signalling. The action potential is an 'all-or-nothing' response, with the resting membrane potential typically measuring -60-70mV (as shown in figure 1.4 below.) Therefore, an action potential will only be generated if the membrane is sufficiently depolarized. For example, when a stimulus such as TRPV1 binds receptor at the terminal of the DRG, a small influx in Na⁺ ions is triggered and the membrane potential is brought closer to the threshold potential of -20mV. This small influx of Na⁺ is known as a generator potential but unlike the action potential, these generator potentials have graded responses. There are four main classes of tactile mechanoreceptors that relay extracellular stimuli such as touch or pressure, to intracellular signal transduction via mechanically gated ion channels. These tactile mechanoreceptors are found in the superficial laminae, and deeper layers of the skin. One such example is the Pacinian corpuscles (Abraira and Ginty, 2013). Upon mechanical disruption of these receptors, ions flow into the cell causing electrical depolarization and generator potentials. When the influx of sodium ions associated with stimulation is sufficient to reach threshold potential, the membrane rapidly and completely depolarizes to +40mV. This depolarization is rapidly followed by repolarization of the membrane by efflux of K⁺ ions. This transient switch in membrane potential is known as the action potential (Hammond, 2015). Figures 1.4.1- 1.4.3 show the depolarisation phase of the action potential is associated with the influx of sodium ions (Na⁺), whilst the repolarisation phase is dependent on the efflux of potassium (K⁺) ions. Following depolarisation, the neuron enters a refractory period, in which an action potential cannot be produced because the sodium channels are closed (and do not open) and the membrane is undergoing repolarisation via efflux of K⁺.

Rapid cell communication is required between cells of the nervous system for effective signal transduction followed by an appropriate response. A good example of this is the reflex response; if you hold your hand over an open flame, action potentials are rapidly propagated along the nerves of the PNS to the CNS so that your motor neurons are activated, and you remove your hand from harm. For this reason, action potentials must be propagated in the most efficient way possible, and therefore most of the nerves in the body are myelinated.

A



B

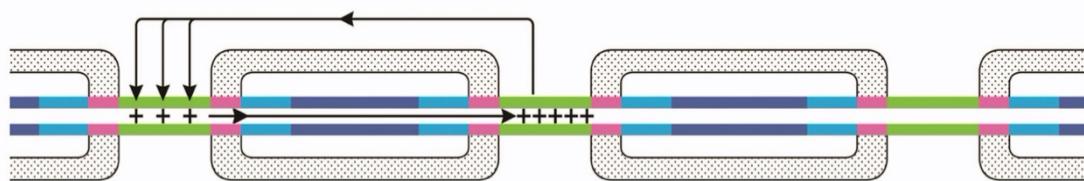


Figure 1.4.1: A simplified representation of a myelinated neuron in the PNS, made using BioRender.

A) The insert demonstrates how the myelination is not continuous, but there are unmyelinated nodes where the ionic capacitance is higher, and the action potential can pass through the membrane easily. B) The flow of current through a neuron during saltatory conduction of an action potential. Images taken from (Uncini and Kuwabara, 2015)

In the neurons of the PNS, the myelination of fibres is formed by polarised, longitudinal Schwann cells ensheathing the axon (Salzer, 2003; Pereira, Lebrun-Julien and Suter, 2012). In

development of the PNS, axons signal to glial precursors, initiating Schwann cell migration and survival (Perlin *et al.*, 2011). Both the axons and the surrounding Schwann cells release bi-directional trophic signals throughout life to support cell survival (Jessen and Mirsky, 2005; Pereira, Lebrun-Julien and Suter, 2012). Critically, the myelination of the axons by the Schwann cells helps to regulate the axon cytoskeleton as well as the rate of transport along the axon. Myelin provides a high resistance, low capacitance barrier that enables saltatory conduction of ions between the unmyelinated nodes of Ranvier (Hillman and Hillman, 1986; Salzer, 2003). Effectively, the action potential appears to 'jump' between the nodes, where the ions cannot pass through the myelin sheath surrounding the axon:

Myelination of the axon is clearly important in propagation of the action potential and irreversible de-myelination of nerves is an underlying factor of pathologies such as Multiple Sclerosis (Moalem and Tracey, 2006a; Popescu and Lucchinetti, 2012; Huang, Chen and Zhang, 2017). The loss of myelin surrounding axons damages the exposed fibre, reducing the efficiency of action potential propagation, as well as reducing the capability of the neuron to traffic proteins efficiently. The lipidic nature of myelin gives the neuron a low capacitance at regions where the Schwann cells surround the axon. Therefore, ions must cross the membrane solely at the unmyelinated regions known as the Nodes of Ranvier. The expression of voltage-gated channels for sodium and potassium at these regions is therefore also instrumental in maintaining successful propagation of the action potential.

In the PNS, it has been demonstrated that there is selective expression of subsets of voltage gated ion channels, dependent on the presence of surrounding Schwann cells.

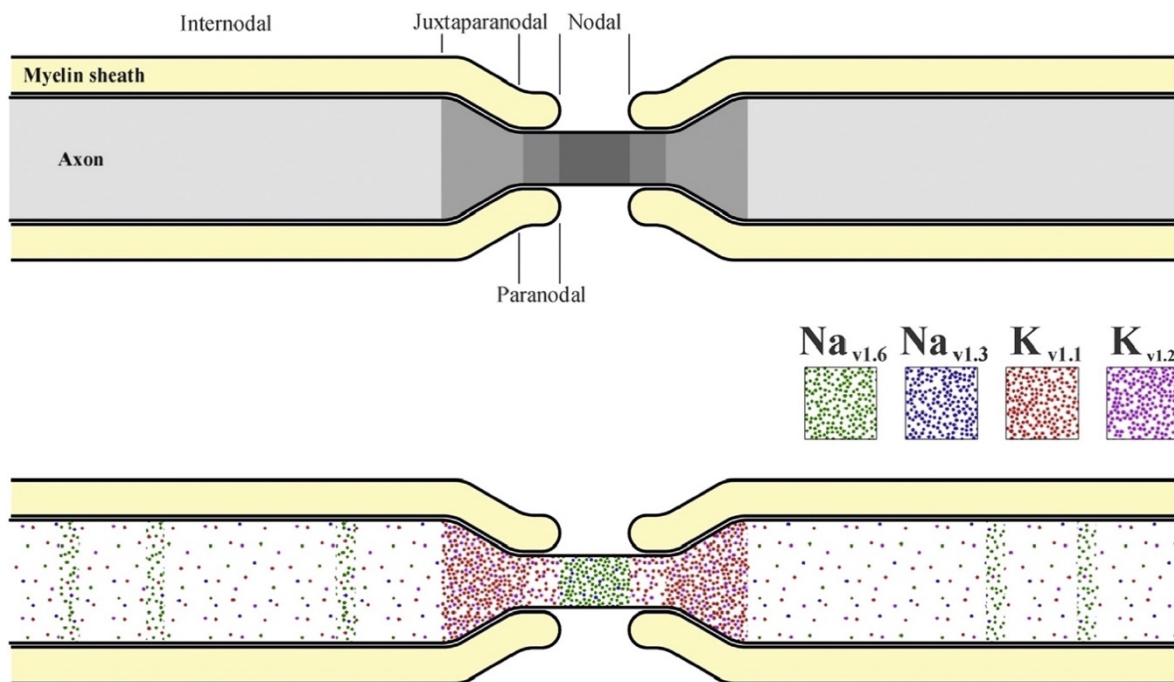


Figure 1.4.2: Distribution of voltage gate channel isoforms at the paranodal and nodal regions. This image has been taken from (Rasband and Peles, 2016) as a recreation from (Lakke, 1997).

Figure 1.4.2 demonstrates that whilst the propagation of action potentials is reliant upon the presence of voltage gated channels at the node, the expression of relevant proteins is not uniform (Rasband and Peles, 2016). This differential expression of ion channels is essential in the development of functional distinctions in sensory neurons.

The rapid influx of sodium ions in the depolarising phase of the action potential is essential for reaching threshold potential. However, evidence has shown that not all subtypes of voltage-gated channels open at the same time, see figure 1.4.3. Nociceptive fibres express both tetrodotoxin (TTX) sensitive and TTX resistant subtypes of channels. Genes encoding the TTX-R channels NaV1.8 and NaV1.9 were initially deemed exclusively expressed in sensory neurons (Akopian, Sivilotti and Wood, 1996). Additionally, immunocytochemistry has demonstrated higher expression of TTX-R channels in unmyelinated fibres of the DRG, in the soma, axon and nerve terminals (Fjell *et al.*, 2000; Fang *et al.*, 2002). Since TTX-R and TTX-S channels have very different kinetics with relation with activation and inactivation, it is understandable that there is differential activity throughout the action potential (Elliott and Elliott, 1993). Higher expression of TTX-R polymodal nociceptors has been deemed to underlie activity dependent slowing of conduction in the nociceptors in response to a range of nociceptive stimuli (Jonas *et al.*, 2020).

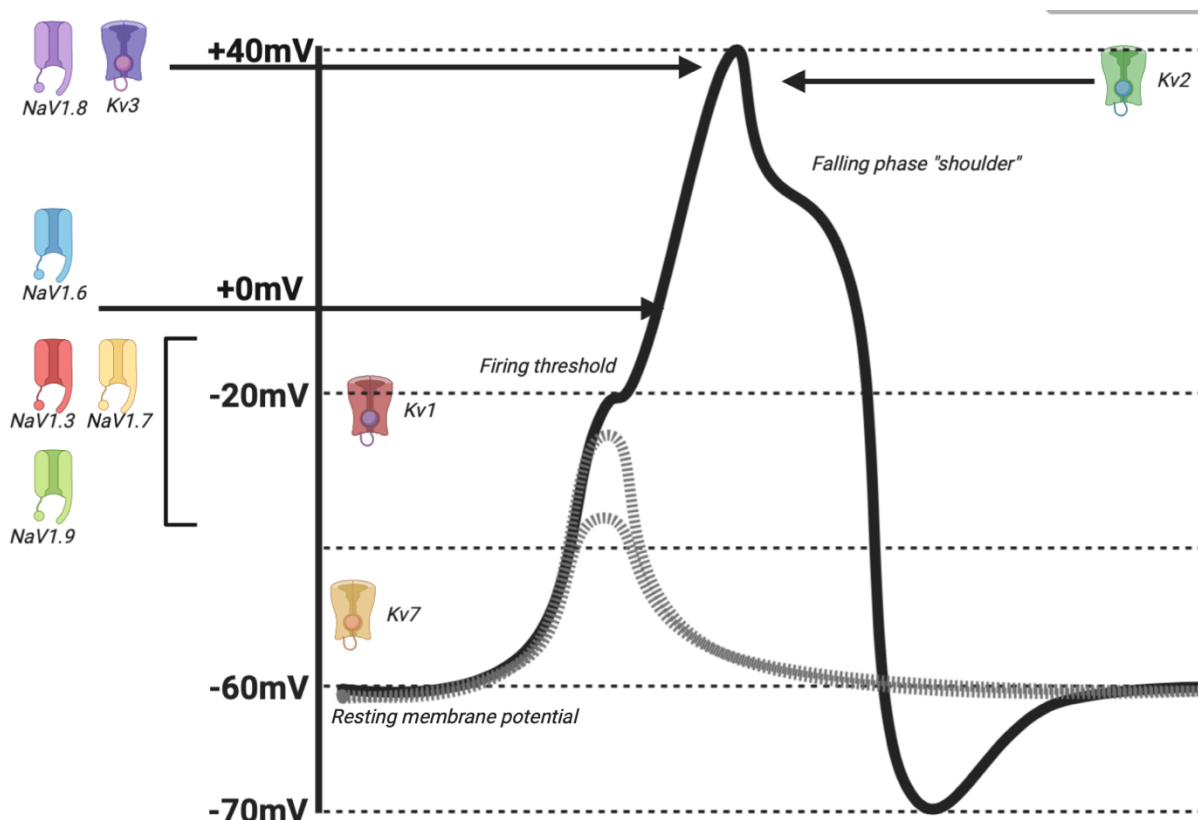


Figure 1.4.3: An overview of the action potential.

Voltage-Gated sodium channels are open during the depolarizing phase, and rapid influx of sodium ions increases the membrane potential. In contrast, the re-polarization of the membrane is largely due to the opening of voltage-gated potassium channels, and efflux of potassium from the cell. Evidence for the roles of subsets of voltage gated channels has been acquired from relevant literature (Tsantoulas and McMahon, 2014; Dib-Hajj, Geha and Waxman, 2017)

Patch clamping has shown that initial depolarization is resultant from TTX-S sodium currents; where these channels (NaV1.3 and NaV1.7 in particular) activate rapidly but are also inactivated before the membrane potential has peaked. TTX-R channels are also activated and reach maximal amplitude during the rising phase of the action potential. However, these channels (especially NaV1.8, as shown by figure 1.4.3) do not completely inactivate during the re-polarization of the membrane. It is thought that these TTX-R channels are largely responsible for a “shoulder” in the falling phase (Blair and Bean, 2002). Particularly in smaller diameter nociceptors it has been shown that TTX-R are responsible for most of the influx of Na⁺ during the depolarizing phase, whilst at low temperatures NaV1.8 are solely responsible for the initiation of the action potential (Zimmermann *et al.*, 2007). It has also been demonstrated that there is a high composition of NaV at the unmyelinated region of the Node

of Ranvier, in particular Nav1.1 and Nav1.6 in the CNS (Rios *et al.*, 2003; Duflocq *et al.*, 2008), although the Nav1.6 isoform is also highly clustered at the node in the nerves of the PNS (Caldwell *et al.*, 2000; Rasband and Peles, 2016).

Where the movement of sodium ions into the neuron is known to initiate the action potential, the movement of potassium channels out of the axon returns the neuron to its resting state. In particular the resting membrane potential is known to be regulated by two-pore potassium channels, and members of the Kv7 family, as shown in figure 1.4.3. This figure only suggests the association of voltage gated potassium channels with regulating the action potential, but it is evident that other isoforms of potassium channel are also involved in ionic conductance across the neuron membrane. This includes two-pore potassium channels, as well as calcium-activated potassium channels, and inward rectifiers (Tsantoulas and McMahon, 2014). The voltage gated potassium channel is by far the largest family of potassium channels, with over 40 genes in humans (Gutman *et al.*, 2005). Pharmacological evidence has demonstrated a heterogeneous nature of the voltage-gate potassium channel family. Therefore, it is likely that a range of Kv channels are expressed in cells, each of which rectifies the action potential with unique biophysical properties. Six distinct K⁺ currents have been observed in the neurons of the DRG, 3 of which appear to be unique to small diameter fibres, or nociceptors (Everill, Rizzo and Kocsis, 1998; Everill and Kocsis, 1999). Several voltage gated potassium channels cluster in the juxta-paranodal regions, in particular those isoforms of the Kv1 family, to regulate neuronal excitability (Rasband *et al.*, 2001). Although there is abundant evidence for the role of NaV, TRP and even H⁺ sensitive channels on the surface of the sensory neurons of the DRG, there is relatively little in comparison on the diverse range of Kv channels expressed on these neurons. The myelinated nerve fibres of the DRG appear to predominantly express isoforms of the Kv1 family, with particular interest to Kv1.1 and Kv1.2. These channels form complexes to maintain internodal resting potential (Wang *et al.*, 1993; Rasband *et al.*, 1998). Neuropathic pain models using spinal nerve ligation (SNL) of L5-L6, has demonstrated the effect of potassium channels on sensory nerve excitability. In the ipsilateral fibres of L5-L6 the expression of Kv1 channels was significantly reduced, where in comparison little change in expression in the uninjured L4 fibres (Rasband *et al.*, 2001). Furthermore, induced axotomy demonstrated a significant decrease in the expression of these channels in medium diameter fibres of the DRGs. In particular, the downregulation of Kv1.1 has been linked to reduced firing

threshold, and consequentially mechanical allodynia (Xian and Nicol, 2007; Hao *et al.*, 2013). In contrast, the activity of Kv1.2 has been linked to regulation of the membrane potential by augmenting firing rate (Tsantoulas and McMahon, 2014). Additionally, the mechanosensitive effects of Kv1.2 have not only been detected in the myelinated fibres of the DRG, but also linked to C-fibre activity.

1.5 Disruptions to the action potential:

Repetitive and controlled regulation of the action potential along the axon is essential for cell-to-cell communication via synapses, even at a long distance. The movement of ions across the membrane is tightly regulated such that resting membrane potential always returns to -60mV. Therefore, dysregulation of the action potential can induce downstream effects, disrupting sensory and motor function. One such family of pathologies in which disruption to the action potential is implicated is pain. Pain is defined by IASP as ‘an unpleasant sensory and emotional experience associated with actual or potential tissue damage, or described in terms of such damage.’ Underlying a painful physical sensation is altered cell signalling of sensory neurons, in particular the nociceptive fibres of the DRGs. At a cellular level this is often caused by a change in the conductance of the axons, where cell membranes may become hyper- or hypoexcitable, and consequentially the action potential is not efficiently propagated. Nociception can be defined as the ability to detect noxious stimuli, and in humans activation of the nociceptive neurons usually evokes a downstream sensation of physical pain.

1.5.1 An overview of pain:

From a physiological perspective pain is an evolutionary response that provides a protective role against noxious stimuli. This physiological response is comprised of both an emotional response, and the unpleasant physical sensation associated with pain, known as nociception (Basbaum *et al.*, 2009). Generally the pathway involving physical detection of a noxious stimuli has been determined to have three main parts.

1. The first stage involves exposure and subsequent detection of a stimulus via binding of receptors (e.g. Capsaicin at TRPV1) on terminals of the DRG neurons. Activation of

these receptors bring the membrane closer to threshold potential, in order to depolarize the membrane and generate an action potential.

2. An action potential is propagated along the active nociceptors and integrated into the superficial laminae of the dorsal horn, where the sensory neurons of the DRGs terminate. *(In wound healing, non-neutrophilic CD11b+ cells (most likely macrophages) sensitize pseudounipolar DRG neurons via the release of pro-inflammatory cytokines, NGF and histamine (Ghasemlou et al., 2015) with the ability to change the sensitivity of these neurons following nerve injury.)*
3. From here, the action potential is transmitted through pain pathways of the central nervous system. These include the ascending pathways to higher processing centres (such as the thalamus and the cortex,) and the descending pathways of pain where action potentials are transmitted via the spinal cord to the reflex organs (Yam et al., 2018).

A good example involves the myotactic (stretch) reflex following tapping the patellar tendon with a hammer. It is important to note that from the point at which a stimulus is detected by the sensory afferent fibres, to the response from a motor efferent fibre, there are several other cell types indirectly involved in signal transduction. *Other withdrawal reflexes, including the nociceptive withdrawal response (e.g. removing your hand from an open flame) are polysynaptic, including one or more synaptic connections between the afferent and efferent fibres.)*

*NB: This is a generalised overview of the **typical** steps involved in the perception of pain. However, it is worth noting that the physical response to detection of a noxious stimuli can occur prior to integration in the CNS. It has been demonstrated that decerebration of mice, rats and rabbits has not removed the withdrawal reflex in these animals. Removal of the forebrain in rats did not appear to impair the ability of these animals to respond relatively normally to a noxious stimulus. For example, decerebrate rats still showed normal withdrawal responses, vocalization and licking at the site of injury. In this regard the behaviour of the decerebrate animals was almost identical to a healthy control. However, removal of the frontal cortex and thalamus induced limitations in the normal behaviour of these rats. Whilst they responded appropriately to a noxious stimuli, immediately afterwards these animals returned to normal grooming behaviours. Even following contact thermal injury where the*

ipsilateral paw was extremely sensitive, these animals continued with normal behaviours (e.g grooming) and demonstrated no sustained response to protect the site of the injury. These results suggested that the sensory component of the pain pathway was intact and functional, but the reactive component was now abnormal where the cortex was removed (Woolf, 1984)

However, it is also evident that there is a pathological component to the development of pain often underlying multiple disorders, such as arthritis. In this context, the pain elicited by inflammation or even injury to the nervous system evokes a pathophysiological response. The sensitisation of firstly the peripheral nociceptors, and subsequently the ascending pathways of the pain pathways in the central nervous system induces changes in signalling of the nociceptive neurons. The International Association for the Study of Pain (IASP) determined that pain can be classified according to the region of the body from which the pain originates. As such, there are three classifications of pain, including nociceptive, neuropathic and inflammatory (Woolf *et al.*, 1998; Yam *et al.*, 2018).

1.5.2 Peripheral Sensitisation and the DRG neurons:

In the peripheral nervous system, the cells are comprised of sensory neurons, forming ganglia adjacent to, but outside the spinal cord and the CNS. These bundles of fibres are known as the Dorsal Root Ganglion cells (DRGs) and in many ways, form the link between the peripheral nervous system and the integration of a nociceptive signal to the central nervous system. These sensory neurons innervate target tissue in the periphery, but transport neuronal signals into the CNS via the dorsal horn of the spinal cord (via the substantia gelatinosa.) Here the primary afferent fibres synapse with dorsal horn neurons (known as the second order neurons) and form projections to the brain (Todd, 2010; Zeilhofer *et al.*, 2020).

It is the relationship between sensory neuron input to the dorsal horn and the downstream activation of the second order neurons that determines the excitability of the dorsal horn. For this reason, investigating changes in the excitability of these pseudo-unipolar sensory fibres form the basis of the model outlined later in this project.

Peripheral sensitisation refers to the changes in neuronal excitability and sensitivity that occur often following peripheral nerve injury and/or inflammation. For example, following injury, the threshold for activation of the peripheral nociceptors is reduced, and the sensitivity of

these sensory fibres to stimulation is also increased, often manifesting as primary hyperalgesia (Gold and Gebhart, 2010).

There are several ways in which cells can become sensitised, although at a molecular level there are often transcriptional dependent changes in protein expression (for example, activation of protein kinase A pathway by PGE₂.) One of the ways in which peripheral sensitisation manifests is via up-regulation of receptors on the terminals of the afferent fibres following exposure to inflammatory stimuli such as bradykinin, ATP and prostaglandins (Staud and Smitherman, 2002; Campbell and Meyer, 2006). This translational regulation of receptors on the DRG terminal increases action potential firing of the nociceptors, and induces a state of “pain.”

1.5.3 The switch from acute to chronic pain:

Neuropathic pain arises from a combination of both peripheral sensitisation in the nociceptor terminals, and central sensitisation of nociceptive signalling. The changes in nociceptor signalling manifest as mechanical allodynia and hyperalgesia. As such, central sensitisation is defined as an increased responsiveness in the neurons of the central nervous system (Latremoliere and Woolf, 2009; Louw, Nijs and Puentedura, 2017). The pathophysiology arising from a single nociceptive input can lead to either an increase in excitability, and a reduction in the threshold for activation of a nociceptor. For example, if the nervous tissue is irreversibly damaged a state of mechanical allodynia is induced, and consequently the threshold for a pain response is lowered so that even innocuous stimuli are perceived as painful (von Hehn, Baron and Woolf, 2012). Unlike other forms of algesia, allodynia serves no protective purpose, but is often a co-morbidity underlying conditions such as diabetes, where mechanosensitive receptors in the periphery become irreversibly damaged.

However, the inflammatory response arising from exposure to a nociceptive stimulus is dynamic and protective. Reversible changes in the sensory nervous system may also induce transient hyperactivity of nociceptive neurons known as hyperalgesia. In this condition the nociceptors have sensitised so that the detection of a low-level noxious stimulus, induces overactivation of nociceptors, and a long-lasting pain response. Whilst primary hyperalgesia is said to refer to a state of increased sensitivity at the site of injury, secondary hyperalgesia

is referred pain accompanying the damage to tissues surrounding the site of injury (Latremoliere and Woolf, 2009; Kuner, 2010).

Rodent studies have previously shown differential responses to inflammatory mediators between neonatal and adult DRGs in hyperalgesic priming experiments (Beland and Fitzgerald, 2001). For example, peptidergic DRG fibre terminals have been identified in rodents before birth, but larger, non-peptidergic fibres are not present until post-natal day 5. Furthermore, evidence suggests that the functionality of the sensory circuits is acquired postnatally. For example, in the dorsal horn of newborn rodents, neuronal input predominantly arises from the low threshold A-fibres, where input from nociceptive C-fibres develops later, around post-natal day 10. *In vivo* it was shown that in adult rodents, the exposure of the hindpaw to mustard oil penetrated the skin and produced rapid and long-lasting flexor responses. However, these flexor reflexes to chemical irritants such as mustard oil did not begin to occur until postnatal day 10-11 (Jennings and Fitzgerald, 1998). In the second week of postnatal development it has been demonstrated that there is development of glycinergic inhibitory control of the dorsal horn. This coincides with the emergence of C-fibre maturation, which is most likely responsible for the ability of these neonatal rodents to respond appropriately to chemical and inflammatory irritants. Results have shown that in tissue at P10-14 the selective block of primary afferent C-fibres with Lidocaine and Capsaicin delays the development of glycinergic inhibitory networks, and maintains the dorsal horn in a state of newborn excitability (Koch *et al.*, 2012).

Where newborn animals are particularly sensitive to tactile responses, the maturation and refinement of the networks in the spinal cord coincides with a postnatal pruning of A-fibre input, and strengthening of nociceptive C-fibre connections.

When adult tissue was injected with carrageenan at 2% body weight, maturation of the DRGs showed development of two sub-populations of cells. This hyperalgesic priming is thought to be partially controlled by peptide plasticity in inflammation, especially since many neuropeptides are dependent on NGF, which is upregulated in the periphery during the inflammatory response (Woolf *et al.*, 1994). In neonatal culture, both the CGRP (peptidergic) and IB4 positive (non-peptidergic) cell populations were affected by carrageenan, but only after postnatal day 5. Through development the TrkA receptor diversifies the nociceptive sublineage and is upregulated on peptidergic fibres but downregulated on the non-

peptidergic fibres in favour of the glial derived neurotrophic receptor Ret. These non-peptidergic neurons now bind isolectin B4 (IB4) in two distinct populations of small and medium diameter non-peptidergic neurons. Results have shown that following an injection with 2% carrageenan in adult tissue, only those cells expressing CGRP increased. These CGRP-expressing, peptidergic A δ /C-fibres are affected by inflammation and also express the TrKA receptor for NGF in the mature nervous system.

Of relevance to this work, it was important to consider that tissue was extracted from embryonic mice and may not reflect what was previously observed in adult tissue.

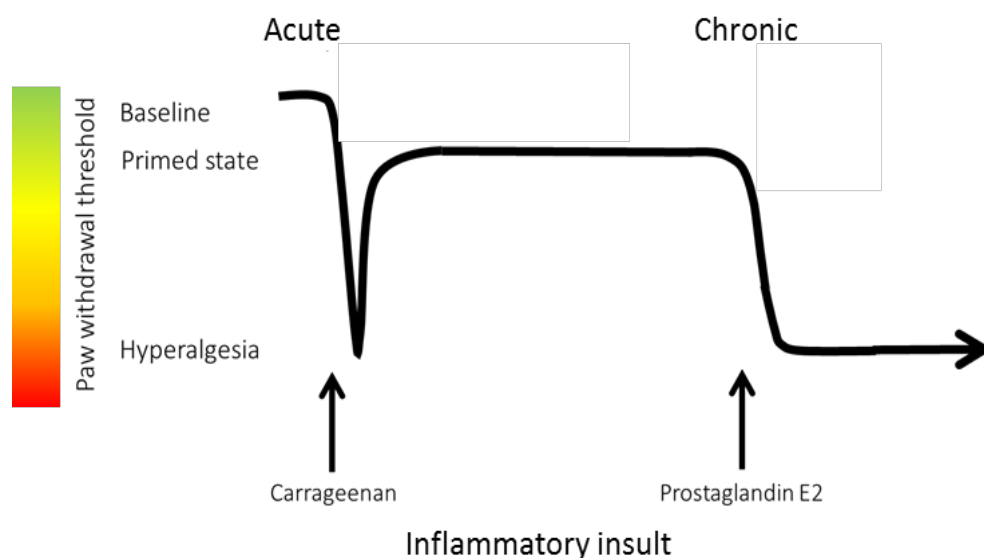


Figure 1.5.1: The changes in paw withdrawal threshold associated with development of peripheral sensitisation and hyperalgesia.

In the model described later in this work, we have focused on the role of inflammatory cells in inducing a change to the excitability of DRG neurons following exposure to an acute stimulus. As such, this model more closely resembles the changes observed *in vivo* arising from primary hyperalgesia. It is important to note that whilst immune cells release inflammatory mediators to modulate neuronal response to a stimulus, the nociceptors in turn release neuropeptides to modulate the immune cell function at the site of injury. This two-way signalling between the neurons and the immune system is not only essential for the initiation and maintenance of a behavioural response to a nociceptive stimulus, but also for the resolution of the inflammatory response to a painful stimulus.

1.6 Neurons of the pain pathways:

There are primarily three types of neurons involved in the transmission and modulation of a nociceptive stimulus. This includes the primary afferent fibres, connective interneurons, and efferent motor neurons. Although the central nervous system is required for higher processing and 'interpretation' of a noxious stimulus, the neurons involved in transmission lie in the peripheral nervous system.

1.6.1 Dorsal Root Ganglion Neurons (DRGs):

The pseudo-unipolar neurons that comprise the bundles of fibres known as the dorsal root ganglion (DRGs) act as first order sensory neurons of the somatosensory system (Chen *et al.*, 2019). With the ganglion located in the dorsal root, the DRG neurons themselves form part of the peripheral nervous system. However, due to their unique morphology, these neurons 'bridge-the-gap' between detection of a sensory stimulus at receptors in the terminals of peripheral nerves, and communicate directly with the neurons of the CNS.

The DRG fibres terminate in the skin, where they form distinct subtypes of low-threshold mechanoreceptors based on the diameter and conduction velocity of the fibres. There is overwhelming evidence for the role of DRGs in processing both proprioceptive (Koerber, Mirnics and Mendell, 2017; Madden *et al.*, 2020) and nociceptive stimuli (Krames, 2015; Emery *et al.*, 2018) and therefore the activity of the DRGs have been extensively studied in culture. Neuronal fibres of the DRG are varied in diameter, and as such function. For example, a cross section of the DRG reveals that small diameter, unmyelinated fibres known as the C-fibres, are primarily involved in integrating noxious stimuli to the CNS. Whereas, larger diameter fibres (such as type II A β fibres) can also respond to light-touch. Although the existence of A β fibres as nociceptors was initially overlooked, evidence has recently suggested that in rodent tissue the proportion of A β fibre nociceptors ranged from 18-65% (Djoughri and Lawson, 2004).

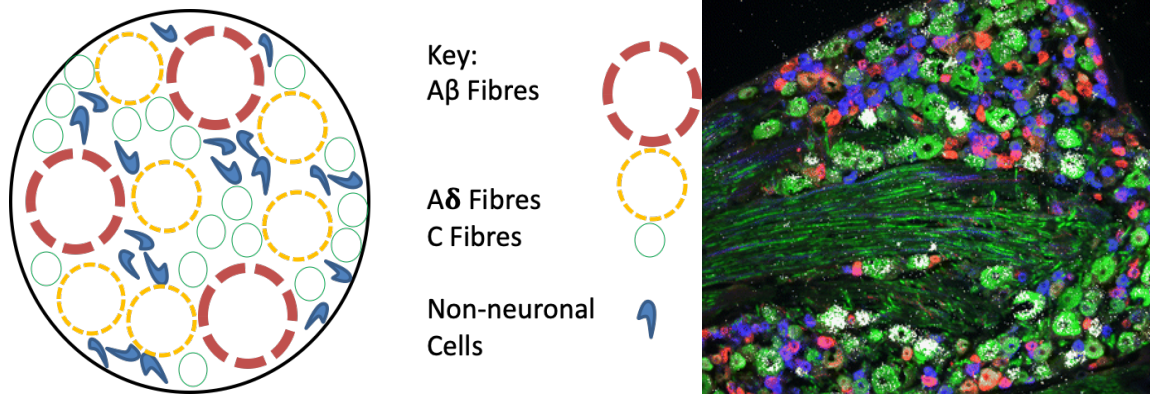


Figure 1.6.1 A) simplified diagram of a cross section of the fibres of the DRG showing relative subpopulations of neuronal fibres.

Thicker dotted lines represent additional layers of myelination between the nodes of Ranvier. B) A transverse section of a rat lumbar dorsal root ganglion stained with fluorescent markers to distinguish sensory neuron subpopulations involved in the pain pathway. (Tsantoulas et al., 2012)

1.6.2 A summary of the activity of fibres within the DRG:

Some of the sensory fibres within the DRG are myelinated and demonstrate saltatory conduction along the axon. These are larger diameter fibres, involved in proprioceptive function rather than solely nociceptive function (Djouhri and Lawson, 2004; Koerber, Mirnics and Mendell, 2017).

The large diameter, myelinated Aβ fibres can be further subdivided into type I and type II mechanoreceptors dependent on the mechanical and thermal threshold of fibre activation. However, the importance of the Aβ (as well as unmyelinated C- and thinly myelinated Aδ fibres) must not be overlooked. As well as being functionally different in adult tissue, the neurogenesis of these fibres appears to emerge sequentially throughout development.

It has been documented that *in vivo* that A-fibres develop between E15-17 and are later followed by C-fibres at E18-20. Therefore, the addition of specific growth factors was optimised to help promote differentiation of a nociceptive culture including Aδ and C-fibres. Manipulation via transgenic overexpression or deletion of receptors has demonstrated the importance of neurotrophin signalling for neuronal survival and differentiation in the DRG fibres. The non-peptidergic C-fibres appear to be dependent upon glial derived neurotrophic factor (GDNF) in early post-natal life, where the receptor for GDNF (Ret) was shown to be

expressed in embryonic rat fibres as early as embryonic day 15.5 (Molliver *et al.*, 1997). The addition of GDNF to the *in vitro* culture of murine DRGs may have helped a sub-population of fibres differentiate to represent IB4 positive C-fibres.

Whereas, the addition of the neurotrophin nerve growth factor (NGF) to the cultures not only promoted neuronal growth but may have promoted the expression of the TrkA receptor found on C- and A δ -fibres. *In vivo* >50% of neurons in the DRG of embryonic mice at E11.5 have been shown to be TrkA+, with IHC demonstrating the presence of TrkA-mRNA detected in 80% of DRG neurons by E13-15. However, in both mice and rats, the proportion of TrkA₊ve cells was shown to decreased to between 40-60% in post-natal development.

In adult rodent tissue around 40% of DRG neurons have been shown to express receptors for NGF (Barker *et al.*, 2020). Furthermore, many of these NGF-responsive neurons also express TRPV1 (Caterina *et al.*, 1997), and treatment with NGF can upregulate TRPV1 expression on the plasma membrane (Xue *et al.*, 2006a). *In vivo*, following peripheral inflammation anti-NGF treatment in the hindpaw of rodents appeared to reduce TRPV1 expression, and also reduced inflammation-induced hyperalgesia (Cheng and Ji, 2008). As such, there is evidence that dysregulation of expression of NGF or it's corresponding receptor may have a role in development of neuropathic pain. There was thought to be potential for anti-NGF treatment in humans although this has not yet been verified (Saldanha *et al.*, 1999; Abdiche, Malashock and Pons, 2008).

	Diameter (μM)	Conduction Velocity (m/s)	Myelin?		
Aβ	6.0-12.0	35.0-75.0	Y	Touch/ Pressure	Mechanoreceptors (<i>with some function in nociceptive signalling</i>)
Aδ	1.0-5.0	5.0-35.0	Y	Fast Pain	Heat Sensitive (Not all Capsaicin Sensitive, only subtype II)
C	0.4-1.2	0.5-2.0	N	Slow Pain	Low pH/ Heat sensitive

Figure 1.6.2: An simplified overview of the fibres of the DRG (Susuki, 2010). There is a wide variability in the range of stimuli that can activate the neurons of the DRG in pain based processing. Whilst the role of C- and A δ fibres in nociceptive

processing is widely explored, there is also evidence for function of the larger diameter A β fibres as both mechanoreceptors and nociceptors.

The A δ nociceptors can be further divided into two subtypes based on their sensitivity to heat and Capsaicin, dependent on how highly the TRPV1 (Transient vanilloid receptor 1) receptor is expressed on the neuron (Chen and Sehdev, 2019). For example, in a rodent model for neuropathic pain, exposure to Resiniferatoxin (RTX) only induced rapid cell death in those axons expressing TRPV1 (Tender, Li and Cui, 2008). RTX is a highly potent agonist of the TRPV1 receptor and induces rapid influx of calcium into the cell via a non-selective cation channel and cell death. However, since TRPV1 is selectively expressed on the C-fibres and the type II A δ -fibres, the type I A δ -fibres remained functional. After this peripheral nerve injury, it was demonstrated that there was a significant increase in paw withdrawal threshold (PWT) suggesting that although these animals were still allodynic, large diameter fibres are also involved in the development of neuropathic pain.

In contrast, **the unmyelinated C-type fibres** form around 70% of the afferents involved in nociceptive signalling. However, as these fibres are unmyelinated action potentials are transmitted much more slowly along the axon relative to the larger diameter A δ fibres. The C-fibres are polymodal, activated by heat, pH and even mechanical stimuli (Dubin and Patapoutian, 2010). However, they can be categorized into two distinct types; peptidergic (expressing CGRP and Substance P) or non-peptidergic fibres, that are highly responsive to GDNF. Whilst expression of NGF is essential for function-related development of the nociceptors in embryos, it has been deemed evident that this molecular 'switch' from NGF sensitivity in the peptidergic fibres, to GDNF sensitivity in the non-peptidergic nociceptors occurs early in post-natal development (Molliver *et al.*, 1997).

Non-peptidergic C-fibres have been demonstrated to be involved in the development of hypersensitivity to a mechanical stimulus via peripheral sensitization in a mouse model (Pinto *et al.*, 2019). These nerves bind Isolectin-B4 (IB4) and may not be involved in low level physiological pain processing. However, ablation of these IB4 sensitive nociceptors led to a reduction in the expression of TRPV1 as well as P2X3 (an ATP-sensitive purinoceptor)

(Burnstock, 2000; Wirkner, Sperlagh and Illes, 2007). Whilst the mechanical threshold for activation of these neurons was not altered, there was inhibition of hypersensitivity to GDNF (glial derived neurotrophic factor) but not NGF (nerve growth factor). The expression of these growth factors, and the corresponding receptors will affect how highly other receptors are expressed on the primary afferent fibres via post-transcriptional regulation, for examples TRP channels and sodium channels. Therefore, the function acquired in post-natal development determines how sensory fibres responds to and overcomes a nociceptive stimulus.

1.7 Receptors expressed on the nociceptors:

Mechanoreceptors found in the superficial laminae of the skin relay somatosensory stimuli via mechanically gated ion channels. Receptors may be either encapsulated or “free” and fall into one of four main categories including Merkel’s disks, Meissner’s corpuscles, Ruffini endings and Pacinian corpuscles (Abraira and Ginty, 2013). As the somatosensory neurons of the DRGs develop in embryonic development, the expression of the A-type fibres emerge first (E9-E11) characterised by the expression of Neurogenin 2 (*Ngn2*) (García-Piqueras *et al.*, 2019). The cutaneous mechanoreceptors detect a wide range of physiological stimuli, from vibration, stretch and noxious pressure depending on which somatosensory fibres are activated. Local depolarisation of ion channels located on these mechanoreceptors induces receptor potentials which can summate to induce the propagation of an action potential.

The sensory fibres of the DRG are a heterogeneous population of neurons that both respond to and detect a diverse range of stimuli. As such, there are a range of proteins expressed on these fibres, ranging from neurotransmitter receptors, to ion sensitive channels. The molecular composition of the DRG fibres enables the detection of very selective stimulus, dependent on the role of the fibre. Of particular interest here are those neurons involved pain signalling, often referred to as the ‘high threshold mechanoreceptor’ neurons (HTMRs) in the epidermis.

These nociceptive fibres express a variety of receptors involved in pain processing of different sensory modalities. In particular, the mechanosensitive responses of the DRG fibres is partly due to the cellular organization of ion channels present on the neuronal terminals, and the

intrinsic gating properties of each receptor. Furthermore, it has been demonstrated that receptors are selectively expressed depending on the function of a fibre. A classic example of this is the selective expression of the TRPV1 receptor to the C-fibre terminals, and the consequent links with nociception. This localised expression of specific proteins provides a molecular profile of which neurons are involved in acute and inflammatory nociceptive signalling. Therefore, when developing an *in vitro* model for changes in cell excitability associated with nociception, studying the expression patterns and intrinsic properties of ion channels and receptors associated with the nociceptive fibres is a good place to start:

1.7.1 Transient receptor potential channels (TRP):

One of the most potent families of receptor involved in nociceptive signalling is undoubtedly the TRP channels. In mammals, there have been 28 TRP channels identified, which can be further subdivided into 6 categories dependent on the shape of the active site of the receptor (Montell, 2005). These calcium permeable channels are highly expressed on the neurons of the peripheral nervous system, specifically the DRGs, and several have been deemed essential in detection of nociceptive stimuli. Real time PCR (polymerase chain reaction) has been used to quantify the expression of the TRP channels on somatosensory neurons, with particular interest to those fibres of the DRGs (Vandewauw, Owsianik and Voets, 2013). Of those channels screened, the data confirmed that 6 TRP channels previously associated with sensing noxious stimuli, were all highly detected in the DRGs, including TRPV, TRPM and TRPA channels. Of note, there was a variable level of mRNA detected for TRPV1 (vanilloid 1, capsaicin sensitive) and TRPM8 (melastatin 8, cold sensitive) dependent on where the ganglia were anatomically isolated from in relation to the spinal cord (Vandewauw, Owsianik and Voets, 2013).

It is important to note, that whilst useful, quantitative levels of mRNA expressed of any one channel do not necessarily correlate to the protein level, or furthermore determine the functional relevance of this channel.

With regards to those channels involved in pain, three subtypes of thermally activated TRP channel have been determined a largely important in nociceptive signalling (Patapoutian,

Tate and Woolf, 2009). These include the TRPA, TRPV and TRPM channels, a summary of which is shown below.

1.7.1.1 TRPV1: Vanilloid-1 receptor, A heat sensitive ion channel and key integrator of nociceptive signals

The TRPV1 receptor is a noxious-heat channel, widely regarded for sensitivity to capsaicin, and is particularly important in nociceptive pathways involved in hyperalgesic priming (Ferrari *et al.*, 2013). Although there are 6 members of the TRPV family, only TRPV1 is sensitive to vanilloid compounds, although the other receptors retain a similarity in the amino acid sequence forming the channel (Rosenbaum Emir, 2017). Physiologically the TRPV1 receptor is best defined as being sensitive to heat greater than 42°C, and is largely expressed on the unmyelinated C-fibres of the DRG (Caterina *et al.*, 1997) although it has also been shown to be expressed on A δ fibres too.

In vivo, the TRPV1 receptor has been identified as early as E12.5 on the terminals of some neurons (Hjerling-Leffler *et al.*, 2007), but in P2 neonatal rat cultures it was demonstrated that TRPV1 expression was already at a similar level to that of an adult culture (Fitzgerald, 2005).

In an early knockout study, it was determined that mice lacking the TRPV1 receptor demonstrated impaired responses to selective nociceptive stimuli. Whilst the VR1-/- genotype mice showed no change when exposed to a noxious stimulus of a mechanical nature, if the stimuli was thermal, and targeted the TRPV1 receptor, the response was impaired (Caterina *et al.*, 2000).

Since this study it has been determined that whilst TRPV1 is more selectively expressed on the C-fibres of the DRG, it is not expressed on all C-fibres. Evidence has also demonstrated that TRPV1 is expressed on the medium diameter A δ fibres, although the role of TRPV1 here may be in response to different threshold temperature or pH. Although it is expressed in several regions of the body, such as the respiratory system (Zhao *et al.*, 2016) and the bladder (Liu *et al.*, 2014), TRPV1 is also prominently expressed in laminae I and II of the superficial dorsal horn in the CNS (Rosenbaum Emir, 2017). These are the terminals of the pseudo-unipolar DRG neurons, terminating in the spinal cord.

1.7.1.2 Inflammation and TRPV1:

Although TRPV1 is a heat-noxious receptor, primarily responsive to temperature $>42^{\circ}\text{C}$, a low pH of the surrounding tissue will dramatically alter the activation threshold of the receptor. A good example of this is during inflammation, when the exogenous pH drops due to the release of inflammatory cells into the periphery (Rajamäki *et al.*, 2013). Immune cells are highly metabolically active, working to reduce inflammation and therefore the glycolysis rate is high, with lactic acid secretion increasing. During inflammation, many cytokines are released by surrounding inflammatory cells, which sensitize nociceptors via peripheral sensitization. These include interleukins, ATP, Substance P and neurotrophins such as NGF (Pinho-Ribeiro, Verri and Chiu, 2016).

Inflammatory pain is often modelled *in vivo* via the injection of Complete Freund's Adjuvant (CFA) to induce changes in the threshold of activation of the nociceptors. This is known as CFA-induced hyperalgesia, as is characterised by factors such as prolonged activation of the nociceptors correlating with an increased amplitude of the pain and the persistence of the pain at the site of inflammation. CFA is an emulsion of oil and water, containing inactivated mycobacterium tuberculosis. By injecting the antigen into the joint or paw of the animal, the corresponding antibodies will be produced and released in the acute immune response. CFA has been demonstrated to contain ligands for toll like receptors (e.g. TLR2, TLR4 and TLR9) and injection inactivation of the mycobacterium present induces a TH1 dominated immune response (Fang *et al.*, 2010). This Th1 response co-ordinates the polarization of immune cells like lymphocytes and macrophages (into an M1-like state,) inducing cell-mediated immunity (Billiau and Matthys, 2001).

An early study conducted in Wistar rats demonstrated that injection of CFA into a hindpaw led to peripheral sensitization and rapid mechanical allodynia of the affected paw (Stein, Millan and Herz, 1988). Inflammation was physiologically evident as a result of changes in increase in paw volume, core body temperature and reduced water consumption over the course of one-month post inoculation with CFA. These results have since been replicated in mice to conclude that injection with CFA induced thermal hyperalgesia and mechanical allodynia (Pitzer, Kuner and Tappe-Theodor, 2016). The effects of injection on stimulus evoked changes in behaviour were investigated using methods such as Von Frey testing, and

CatWalk analysis of gait. Results demonstrated a decrease in body weight correlating with temporary disruption of gait, potentially as an effect of underlying inflammation in the paw. However, it is debated whether the use of gait analysis underlying inflammatory pain is a relevant paradigm, since changes may also occur due to neuronal sensitization caused by development of neuropathic pain (Piesla *et al.*, 2009).

Although TRPV1 has been identified on both medium diameter A-fibres and smaller diameter fibres, it is evident that there is a higher expression of TRPV1 on C-fibres (Michael *et al.*, 2019). Using injection of CFA to the paw, the role of the TRPV1 receptor in the development of thermal hyperalgesia and mechanical allodynia has been further investigated. Evidence has shown that ongoing pain, induced by injection of CFA was likely dependent on input from primary afferents expressing high levels of TRPV1 (Okun *et al.*, 2011).

1.7.2 Other TRP channels and pain:

Temperature is a critical mediator in the activation of many TRP channels involved in nociception (Patapoutian *et al.*, 2003). Where the TRPV1 channels are activated at temperatures higher than 42°C, there are also those channels that are cold-sensitive. TRPM8, also known as the menthol receptor is typically activated at cool temperatures, around 25°C although this temperature is not necessarily considered noxious threshold (Bandell *et al.*, 2004). It was hypothesised that therefore a second population of cold-sensitive TRP receptors must be responsive to noxious cold temperatures. The TRPA1 channel, also known as ANKTM1 (Corey, 2003) has been located on selective populations of the DRG fibres, but is only activated at temperatures of 17°C or below. Whilst some fibres of the DRG solely express TRPV1, or TRPM8 there are some fibres that appear to be polymodal, expressing TRPV1 alongside TRPA1 (Patapoutian *et al.*, 2003; Story *et al.*, 2003). These sensory neurons are therefore activated by noxious heat and noxious cold temperatures, implicating these receptors in acute transduction of nociceptive stimuli.

TRPA1 is an 'itch-sensitive' transduction channel expressed on the sensory fibres of the DRG neurons (Bandell *et al.*, 2004; Schmidt *et al.*, 2009). These TRP channels can be activated by a diverse range of noxious stimuli, particularly cold temperature and selective environmental

irritants. For this reason, TRPA1 is widely regarded as a mediator of acute and inflammatory pain signalling.

TRPA1 expression was quantified using Northern Blot from adult mouse tissue. Receptors were localised to only 3.6% of DRG fibres, 97% of which expressed CGRP, and TRPV1. It was evident that TRPA1 did not co-localise with NF-150kd expression, used as a marker for the large diameter A-fibres. It was determined that TRPA1 was mainly expressed in unmyelinated C-fibres, or lightly myelinated A δ fibres (Story *et al.*, 2003). Although the role of the TRPA1 channel in nociception was first suggested in 2003, it was not until 2006 that this was confirmed using knockout mouse modelling (Kwan *et al.*, 2006). If the *Trpa1* gene was deleted in mice, the removal of the pore loop domain led to a reduction of sensitivity in response to chemical stimuli such as mustard oil. The knockout cohort were normal in viability and appearance but demonstrated no calcium response when stimulated with mustard oil (Bautista *et al.*, 2006). Meanwhile the prevalence of TRPV1 response was the same in the wild type versus the mutant strain, confirming that TRPA1 does not have an impact on heat-sensitive stimulation by TRPV1. However, the *Trpa1*^{-/-} population did demonstrate a loss of sensitivity to cold temperature relative to wild type littermates (Kwan *et al.*, 2006).

TRPM8 has also been implicated in pain since the receptor is saturated at 8°C, which overlaps with the TRPA1 nociceptive range of activation (McKemy, Neuhauser and Julius, 2002). However, selective activation of the TRPM8 receptors has also been implicated in inducing a state of analgesia. Since the TRP family are calcium-sensitive, activation induces flow of calcium (and sodium into the cell) and promotes propagation of the action potential along the nociceptor. Of particular importance is the vast range of stimuli that activate those receptors involved in nociceptive signalling.

1.7.3 Voltage Gated Sodium Channels:

Voltage-gated sodium channels (VGSCs) are important in regulating excitability of the primary afferent fibres. From integrating the generator potential upon stimulation, to propagation of the all-or-nothing action potential along the axon, the voltage-gated nature of the VGSCs determines excitability of the neuron. Although there are many subtypes of VGSC, few have

been identified with specific roles in acute nociception. This includes NaV1.3, NaV1.7, NaV1.8 and NaV1.9, all of which are expressed in adult primary afferent fibres. This selective expression of VGSCs associated with small fibre neuropathy makes them an attractive target for the development of newer, more effective analgesics (He *et al.*, 2010; Chen *et al.*, 2011a).

Hodgkin and Huxley first demonstrated the effect of VGSCs on regulating neuronal excitability, through their work on giant squid axons in 1951 (Hodgkin and Huxley, 1952a). These experiments formed the basis for understanding neuronal excitability today. Voltage-clamp experiments were initially used to confirm that the initial depolarising phase of the action potential was caused by movement of sodium ions (Hodgkin and Huxley, 1952b). By replacing sodium with choline, only the rising phase excitability was affected, whilst the resting potential remained unaffected. Under normal physiological conditions, sodium conductance rises rapidly, then falls exponentially. However, VGSCs associated with pain have shown changes in activity associated with the development of neuropathic pain (Cummins, Sheets and Waxman, 2007; Fischer, Mak and McNaughton, 2014).

In mature primary afferent fibres, selective VGSCs are highly expressed, and associated with changes in excitability of the neurons. In adult primary sensory neurons five subtypes of VGSCs have been shown to be highly expressed, three of which are tetrodotoxin sensitive (TTX-S) (Kim *et al.*, 2002). This includes NaV1.1, 1.6 and 1.7, whilst NaV1.8 and 1.9 are known to be TTX-resistant (Dib-Hajj *et al.*, 1999; Bao, 2015). NaV1.3 is usually constitutively expressed during adulthood, following downregulation associated with functional development of the neuron acquired post-natally (Waxman, Kocsis and Black, 1994; Bao, 2015). However, this subtype of channel can also be re-upregulated following nerve injury and is therefore important in the development of neuropathic pain states. The expression pattern of the VGSCs of interest have been highlighted the table below, summarised from work by Kwong and Carr (Kwong and Carr, 2015).

NaV1.7 has been demonstrated to be abundantly expressed in many regions of the peripheral nervous system. Of interest with regards to nociceptive processing is the expression of NaV1.7 in the primary afferent fibres of the DRG. However, evidence shows higher levels of

expression in peptidergic C-fibres, as well as the free nerve endings, suggesting a role for NaV1.7 in pain processing (Levinson, Luo and Henry, 2012).

Aβ-Fibres	Aδ- Fibres	C-Fibres (IB4+)	C-Fibres (CGRP/ SP+)
NaV1.1	NaV1.1	NaV1.1	NaV1.1
NaV1.6	NaV1.6	NaV1.6	NaV1.6
NaV1.7	NaV1.7	NaV1.7	NaV1.7
NaV1.8	NaV1.8	NaV1.8	NaV1.8
		NaV1.9	

Immunohistochemical studies has demonstrated that isoforms of NaV1.7, 1.8 and 1.9 are localised to excitable cells of the peripheral nervous system, including the DRGs and peripheral sensory ganglia (Cregg *et al.*, 2010). Of particular interest as new therapeutic targets for pain are NaV1.7, from genetic links to development of pathological pain, and NaV1.8 due to selective expression in the axons of the sensory fibres of the DRG (Dib-Hajj *et al.*, 2010).

It is understood that prolonged and repetitive firing from peripheral sensory neurons to the spinal cord is thought to be one of the ways in which central sensitisation is induced. However, the onset of peripheral sensitization also induces up-regulation of nociceptive ion channels such as NaV1.7 on the terminals of the DRG (Staud and Smitherman, 2002; Campbell and Meyer, 2006). Under physiological conditions, the voltage-gated sodium channels (NaV) expressed in the DRG depress this ectopic discharge, and the corresponding pain behaviours (Amir, Michaelis and Devor, 1999). This random, increased firing of sensory fibres can be inhibited by blocking VGSCs, using selective antagonists such as QX-314. This membrane impermeable sodium channel blocker binds to the same target site as Lidocaine, and has been shown to dose-dependently inhibit ectopic firing at the DRGs and dorsal horn (Omana-Zapata *et al.*, 1997).

There is also evidence to suggest that upregulation of TTX-S channels in the primary afferents may contribute to this increased ectopic firing, and ultimately sensitisation of these nerves.

For this reason, those NaV channels that are TTX-Sensitive (such as NaV1.7) are of particular interest, since low doses of TTX have been demonstrated to reduce ectopic firing of the sensory fibres (Lyu *et al.*, 2000). This has been successfully modelled in rats using axotomy of the sensory fibres via segmented spinal nerve ligation (C. H. Kim *et al.*, 2001). In a spinal nerve ligation model for neuropathic pain the mRNA expression of NaV1.7 was reduced by 40% up to 5 days post-operatively (Kim *et al.*, 2002).

1.7.4 Potassium Channels:

Whilst the role of the voltage gated sodium channels is well-elucidated in the rising phase of the action potential, the role of potassium channels, especially voltage-gated channels, is known to regulate re-polarisation of the membrane (Hodgkin and Huxley, 1952b). Potassium ion current, referred to from here-on as I_k was first assumed to be linearly proportional to ' $V-E_K$,' where V is membrane potential and E_K represents the Nernst potential. However, this assumption has since been disproven where I_k shows non-linear dependence on $(V-E_K)$ under physiological conditions. Simply put, the relationship between I_k and V_m can be well characterised by the Goldman-Hogkin-Katz (GHK) equation (Goldman, 1943; Hodgkin and Katz, 1949).

For this reason, evidence has suggested that changes in the expression, or gating kinetics of these potassium channels, may alter the way in which action potentials are propagated. This hyperexcitability of sensory neurons is considered essential for the generation of a chronic pain state, whereby the nociceptors become sensitised to nociceptive stimuli (Tsantoulas and McMahon, 2014).

Aside from being the most diverse family of ion channels expressed in human neurons (Ocaña *et al.*, 2004) it is also noticeable that there is a selective expression of multiple potassium channels on the DRG neurons. With 78 genes in humans expressing potassium channels, it is unsurprising that there are multiple subclasses of ion channel identified (Ocaña *et al.*, 2004). Potassium channels can be subdivided into four distinct groups, of which the largest superfamily is the voltage-gated potassium channels (Kv) (Johnston, Forsythe and Kopp-Scheinflug, 2010). This Kv superfamily is further subdivided dependent on the ability of the

capacity of the alpha subunit to form a pore subunit. Only members of the K_v1 - K_v4 , K_v7 and K_v10 - K_v12 are pore-forming subunits. However, as figure 8 demonstrates there appears to be selective expression of K_v1 subtype receptors at the juxta-paranodal regions in nociceptive fibres. Figure 1.7.1 below is a comprehensive overview of where K_v subtypes are found in the nociceptors:

However, we cannot disregard the importance of background “leak” channels in maintaining resting membrane potential. Although these channels are largely voltage independent, the KCNK family of proteins is key in re-setting the membrane potential after action potential propagation. Leak channels are driven both by electrical potential and the conductance of permeating ions across the neuronal membrane. The rectification of the membrane potential is driven by the concentration gradient of ions moving across these leak channels, a phenomenon that can also be attributed to the GHK equation (Goldman, 1943; Huang, Hong and De Schutter, 2015). Figure 1.7.1 shows how these channels are also expressed throughout the fibres of the DRGs, localised mainly to the C-fibres, but having shown expression patterns in both the somal and axonal regions.

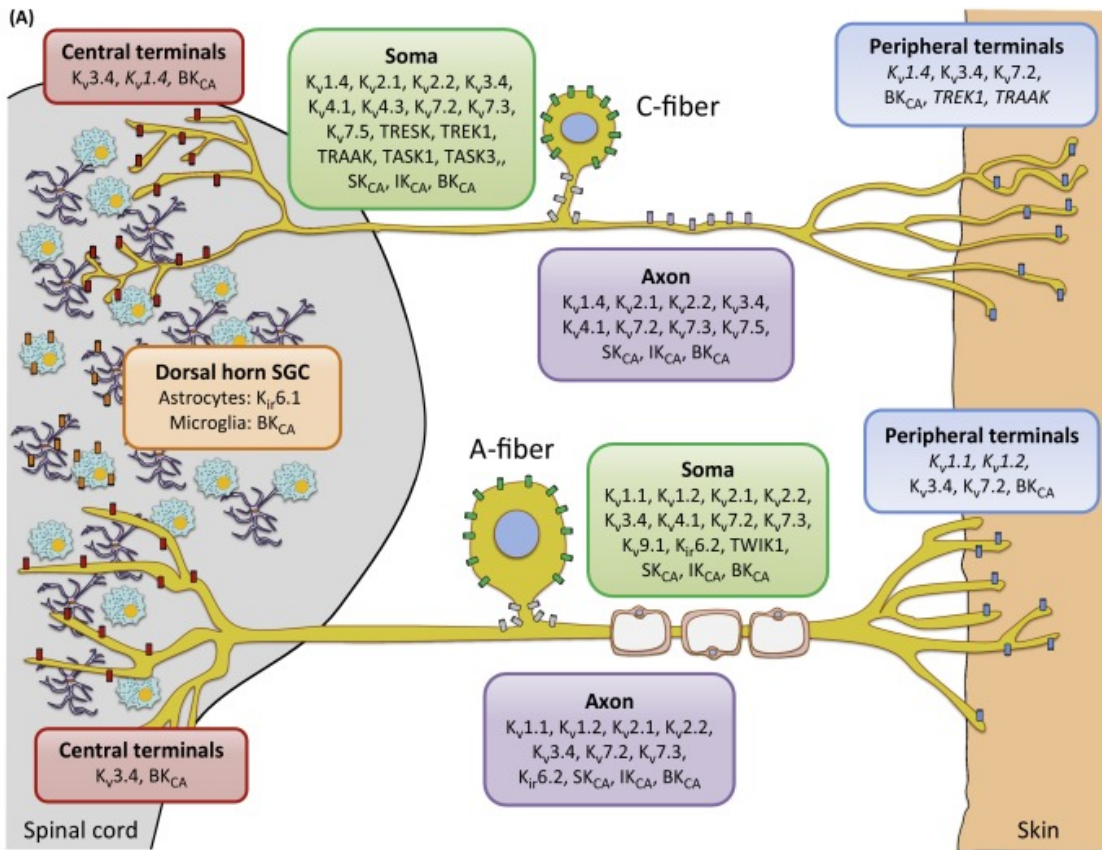


Figure 1.7.1: A) Subcellular localization of potassium channels in murine DRG neuron (Tsantoulas and McMahon, 2014).

The pattern shown is not absolute, but reflective of data reported in the literature. Expression patterns may vary between organisms or species.

1.8 Role of non-neuronal cells in nociception:

1.8.1 Non-Neuronal Cells:

With regards to excitability and nociception, the full extent of the role of myelinating cells in neuropathic pain still remains poorly understood compared to the neurons. However, sciatic nerve injury models (SNI) have shown that Schwann cells have the ability to change phenotype following damage to the axon (Scheib and Höke, 2013). Schwann cells adopt a 'repair' cell phenotype and regain capacity for proliferation and release of growth factors such as NGF and GDNF (R. R. Ji, Chamessian and Zhang, 2016; Jessen and Arthur-Farraj, 2019). With several subtypes of P2X receptors identified on Schwann cells, these cells clearly also have a role in ATP signalling (Su *et al.*, 2019). Of course, ATP is well characterised as a key modulator of both peripheral and central sensitisation of neurons (Tsuda, Tozaki-Saitoh and Inoue, 2010)

and therefore the high expression of P2X-R on Schwann cells led to the conclusion that these non-neuronal cells must play a role in the development of neuropathic pain (Burnstock, 2000; Su *et al.*, 2019). Although overexpression of P2X4 did not induce increased states of hyperalgesia (Su *et al.*, 2019) it was demonstrated that administration of broad-spectrum P2 receptor antagonist pyridoxal phosphate-6-azophenyl-2',4'-disulfonic acid (PPADS) following nerve injury reduced tactile allodynia and thermal hyperalgesia, and reduced the levels of secreted IL-6 and IL-1 β (Martucci *et al.*, 2008). Furthermore, it has been demonstrated that following CCI, the expression levels of pro-inflammatory cytokines (TNF α , IL-1 β and IL-6) are upregulated in the DRG fibres and sciatic nerve (Jančálek *et al.*, 2010; Austin *et al.*, 2015). These chemokines are not only released from infiltrating macrophages, but also from non-neuronal cells surrounding the damaged tissue. Activated Schwann cells are hypothesised to be an additional source of TNF α production in the early hours following SNI (Wagner and Myers, 1996; Campana, 2007). TNF α is detectable 6H post injury in high concentrations, and has been shown to induce the release of further pro-inflammatory cytokines such as IL-6 by infiltrating macrophages. Further evidence has shown that COX-2 and MCP-1 (both potent inflammatory mediators involved in sensitising neurons) are expressed by Schwann cells following nerve injury in rats (Toews, Barrett and Morell, 1998; Takahashi *et al.*, 2004).

1.8.2 Macrophages:

Macrophages are highly motile mononucleolar cells derived from hematopoietic tissue. They are widely distributed throughout the body, and due to their phagocytic nature are highly involved in mediating innate and adaptive inflammatory processes (Bailey *et al.*, 2020). The morphology of macrophages is highly dynamic and dependent on the surrounding microenvironment (Mulay *et al.*, 2016). Throughout embryonic development macrophages arise from yolk-sac progenitor cells and persist throughout adulthood as self-renewing populations of inflammatory cells. However, after birth, macrophages derived from bone-marrow monocytes are also recruited, to replenish tissue resident macrophages in states of inflammation or infection (Gordon and Martinez-Pomares, 2017). Since these blood derived monocytes are highly heterogeneous, there is still a wide debate about whether specific populations of monocytes migrate to specific tissues in inflammatory processes (Nahrendorf *et al.*, 2007). However, in mice it has been demonstrated that the first bone marrow derived

monocytes have an innate inflammatory phenotype (Passlick, Flieger and Loms Ziegler-Heitbrock, 1989) and rapidly develop into mature tissue macrophages or dendritic cells (Randolph *et al.*, 1999).

The plasticity of macrophages refers to the process by which macrophages are polarized to differentiate to specific phenotypes, each with a specific biological function. On a simplistic level, macrophages are polarized either to an M1 (classically activated, pro-inflammatory) phenotype, or an M2 (alternatively activated, anti-inflammatory) phenotypes (Murray, 2017). However, the M2 phenotype has rapidly evolved to encompass all those macrophages that don't exhibit a pro-inflammatory phenotype (Martinez *et al.*, 2008). At the centre of this M1/M2 axis is arginine metabolism (Thomas and Mattila, 2014) but in line with the way cells are polarized, three roles for macrophages have been defined including, wound healing, host defence and immune regulation (Edwards *et al.*, 2006). Following the innate response of M1-like or M2-like macrophages, these polarized cells induce T-helper lymphocytes to further amplify the macrophage polarization, and promote continuation of the immune response where appropriate (Rath *et al.*, 2014a).

Classically activated macrophages typically refers to pro-inflammatory macrophages induced by cell mediated immune responses. This includes the stimulation by cytokines such as IFN γ or TNF α inducing a tumoricidal phenotype and increased secretion of pro-inflammatory cytokines and nitric oxide synthase (Wager and Wormley, 2014). Nitric oxide is a particularly important marker of the innate tumoricidal nature of these pro-inflammatory cells. Nitric oxide itself is cytotoxic (Li *et al.*, 2004), but will also induce downstream release of metabolites to remove pathogens. Since the adaptive immune response is much slower, the rapid innate response of these macrophages is required to remove and reduce inflammation (Mills, 2012). Other notable markers for the M1 phenotype include CXCL9, CXCL10, CXCL11, IL-12 and suppressor of cytokine signalling 3 (SOCS3) (Mosser and Edwards, 2008). Of particular interest here is the presence of SOCS3, which restricts cell responsiveness to IL-4, a typical promoter of the anti-inflammatory phenotypes (Arnold *et al.*, 2014). On the other hand, alternatively activated macrophages are induced by cytokines such as IL-4, IL-10 and IL-13, and characteristically resemble the anti-inflammatory phenotype of macrophages. In these cells, the expression of arginase metabolises arginine to ornithine and urea (Briken and Mosser,

2011; Rath *et al.*, 2014a). However, it is uncommon to see either an M1 or an M2 population, but rather a mixed population with a preference for either a pro- or anti-inflammatory phenotype dependent on the stimulation and surrounding microenvironment. Studies have indicated that these characterizations are more indicative of interlaced signalling pathways, and the range of phenotypes that can be induced following stimulation (Atri, Guerfali and Laouini, 2018). In line with the classification of cells defined above, it is understandable as to why there is potential overlap between phenotypes. Recent evidence has suggested that as opposed to discrete populations, macrophages polarize in a spectrum based on their function (Mosser and Edwards, 2008).

In fact, it has been suggested that the first cells to infiltrate a lesioned area following peripheral nerve injury are macrophages, neutrophils and Schwann cells (Stoll G *et al.*, 1989; Lindborg, Mack and Zigmond, 2017). However, the changes in the periphery are also rapidly followed by those in the CNS, although these are less involved in the initiation of a pain response. For example, microglia (the resident immune cells of the CNS) are also important in modulating the neuronal response to nociceptive stimuli (Moalem and Tracey, 2006b).

Although acute inflammatory and neuropathic pain are deemed as separate clinical pathologies, evidence has suggested that pro-inflammatory cytokines released from infiltrating inflammatory cells are prominent in the development of peripheral sensitization and also chronic pain (Miller *et al.*, 2009). In sciatic nerve transection, murine modelling showed that upon injury there was a 3-fold increase in infiltrating macrophages relative to resident immune cells (Mueller *et al.*, 2003). In models such as Wallerian degeneration, following the distal nerve crush there has been shown to be a rapid influx of cytokine production induced by infiltrating macrophages derived from the bone marrow (Mueller *et al.*, 2003; Fregnan *et al.*, 2012). *In vivo*, following axotomy of the DRG neuron, an accumulation of infiltrating macrophages has been observed 4-days post injury, and high levels of these infiltrating inflammatory cells remained present up to 32-days post injury (Lu and Richardson, 1993; Kwon *et al.*, 2015). Immunohistological tissue analysis has shown that infiltrating macrophages form 'rings' around larger diameter fibres of the DRG neurons, with fewer cells migrating towards undamaged tissue or smaller diameter fibres (Vega-Avelaira, Géranton and Fitzgerald, 2009). In this study it was shown that reactive macrophages, most likely M1-like phenotype, appeared to cluster around larger diameter DRG neuron cell bodies

in a model of neuropathic pain. Since these neurons were highly sensitised following spared nerve injury, this implicated a strong correlation between the regulation of the peripheral nervous system, the peripheral immune system and the development of neuropathic pain.

Whilst *in vitro* culture of bone derived monocytes is useful in the context of flexibility and tissue availability, the response seen in these cells may not be translatable to other forms of cultures. The L-conditioned media from L929 cells contains high concentrations of mCSF (colony stimulating factor) and as such is used to sustain a population of healthy monocytes. However, evidence has shown that the presence of mCSF in the culture may cause cells to favour an M2 like phenotype, prior to stimulation.

1.8.3 Microglial cells:

Microglial cells are the resident macrophages of the CNS, accounting for up to 15% of the glial cells expressed in the brain and spinal cord. First described by Rio-Hortega in the early 20th century (Del Rio-Hortega, 1919), the origin of microglial cells has been widely debated, where they were first described as “non-neuronal elements deriving from oligodendrocytes and astrocytes”. However, unlike bone marrow derived macrophages, it has since been demonstrated that microglial cells originate from the yolk sac early in gestation (Ginhoux *et al.*, 2010). Rodent studies have shown that progenitor cells colonize the cerebrum as early as the 4th week of development, maturing into microglial cells throughout the CNS (Menassa and Gomez-Nicola, 2018; Wang *et al.*, 2019). Two key functions are thought to define the function of microglial cells in the CNS including homeostasis of the CNS and immune regulation and defence (Ginhoux and Prinz, 2015).

Microglial cells develop from the mesodermal layer in development and have many common features with other myeloid cells such as macrophages. Although each cell develops differently, both macrophages and microglial cells are essential in the innate immune response, by maintaining homeostasis and actively scanning the surrounding environment for invading pathogens. As such, both cells types have the ability to adapt to changes in the surrounding environment and polarize accordingly. Upon detection of invading pathogens or chemokines released from damaged surrounding tissue, microglial cells undergo physiological changes to help resolve injury, promote repair of damaged tissue and resolve inflammation

(Goldmann and Prinz, 2013). In a similar way to that observed in peripheral macrophages, the microglial cells of the CNS can also be stimulated to exhibit a pro-inflammatory M1-like or a more regenerative M2-like phenotype (Michelucci *et al.*, 2009). However, in spinal cord tissue extracted from disease models, where inflammation is increased (such as murine modelling *in vivo* for ALS) the microenvironment of the microglia is far more complex. Characteristically, upon detection of invading pathogens, the CNS microglia undergo a switch from a ramified resting state, to an amoeboid morphology (Davalos *et al.*, 2005).

Phenotypic similarities were first reported in immunohistochemical studies where it was demonstrated that microglial cells also expressed several markers that are highly expressed on macrophage cells (Perry, Hume and Gordon, 1985). In mice and humans this first included the presence of the surface glycoprotein F4/80, CSF-1 receptor, as well as integrin CD11b (Akiyama and McGeer, 1990). Additional markers that have since been identified include the presence of the fractalkine receptor (CX3CR1) and the calcium binding protein Iba-1 (Prinz and Mildner, 2011; Amici, Dong and Guerau-de-Arellano, 2017). Whilst there are many similarities between macrophages and microglial cells, it has also been shown that microglia have a unique transcriptomic 'signature' that distinguishes them from other inflammatory cells (Butovsky *et al.*, 2012). Using flow cytometry and RNA sequencing of microglia isolated from the spinal cord tissue of mice, in a single study 29 genes were identified that distinguished peripheral monocytes from CNS microglial cells (Chiu *et al.*, 2013).

In early post-natal rodent tissue (P10) the dorsal horn response to nerve injury was demonstrated to be weak where there was low activation of the neuroimmune response in these animals (Moss *et al.*, 2007). Although in early life the dorsal horn was shown to be insensitive to pro-inflammatory cytokines, it has been demonstrated that neuropathic injury in neonates primes microglia to become reactive in later life (Vega-Avelaira, Géranton and Fitzgerald, 2009). Using neonatal microglia it was recently demonstrated that the phenotype of the cells changed dependent on how long they were kept in culture (Caldeira *et al.*, 2014). In a 'quiescent' state, microglia appear to exhibit a more ramified phenotype, with shorter processes extending from the cell body. However, it is important to note that even when quiescent, microglia are still actively sensing changes in the surrounding cellular environment. Upon inflammation, it has been demonstrated that the cell structure changes to a more amoeboid morphology, where cells are more phagocytic (Leong and Ling, 1992; Kozłowski and

Weimer, 2012). It was demonstrated that the longer cells were left in an *in vitro* culture, the more they favoured a ramified morphology closer to that of an M0-M2 like cell (DiV16.) The cells isolated from murine spinal cord here were cultured for a minimum for 14-days prior to use in any downstream experiments, and this time period may have affected the morphology of the cells.

Scattered throughout the CNS, microglia come into close contact with neurons, mediating synaptic pruning and neuronal cell signalling (Kim and De Vellis, 2005). In particular there is evidence for the role of chemokines such as fractalkine (CX3CL1) in mediating release of trophic factors from microglial cells in neurodevelopment. Binding of fractalkine to receptors on the surface of spinal cord derived microglia induces activation of the MAPK pathway and promotes the release of pro-inflammatory cytokines from the cell, as well as the transcription and upregulation of membrane bound receptors such as P2X4 for ATP (Ji and Strichartz, 2004; Kazuhide and Makoto, 2009). The P2X4 receptor for ATP is solely expressed on microglia in the spinal cord, and evidence has shown that knockdown of P2X4 can partially reverse mechanical and thermal hyperalgesia evoked by spinal nerve transection (Tsuda *et al.*, 2003, 2009). In a separate murine model deficient in CX3CR1, neurons in cortical layer V showed decreased post-natal survival. This correlated with reduced secretion of insulin-like growth factor secretion from microglial cells surrounding the neurons, demonstrating the role for microglial cells in mediating neuronal survival as well as modulating the inflammatory response to changes in DRG excitability (Ueno *et al.*, 2013).

1.9 Protein turnover and local translation in the nervous system:

In the mature nervous system, it is estimated that each excitatory neuron synapses with up to 100,000 other neurons. To regulate and maintain function and plasticity of the nervous system, protein turnover is essential. Although action potentials are only propagated in one direction along the axon, the cytoskeleton of the neuron also acts as scaffolding for bidirectional transport of protein or mRNA (Sotelo-Silveira *et al.*, 2006). The specialised function of each part of the neuron means that proteins must be selectively regulated. Recent works have provided evidence that translation of mRNA is not only temporally regulated but

also spatially regulated. This dynamic turnover of protein in the cell is resultant from a process known as local translation (Di Liegro, Schiera and Di Liegro, 2014). Local translation of proteins refers to post-transcriptional regulation of mRNA in subcellular compartments. Undoubtedly in highly polarized cells like neurons this is essential for dynamic regulation of efficient cell-to-cell signalling, where regular turnover of proteins is necessary to adapt to changes in the microenvironment of the cell (Jung, Yoon and Holt, 2012). Classic examples of local translation in the neuron include turnover of proteins the growth cone, and synaptic plasticity. The fastest rate of protein transport in human axons has been recorded at 1 μ M/second. However, since the longest axons of the body can be up to 1 metre long, without local translation it could take up to 11.6 days to transport proteins from the soma to the distal part of an axon (Maday *et al.*, 2014). Therefore, on-site synthesis of proteins in neurons has evolved as an essential component in effective cell signalling and synaptic plasticity.

Local protein synthesis was first observed by the detection of amino acids being incorporated into the axon of the neuron, although at the time a lack of evidence meant that the theory of local protein translation in neurons was not widely acknowledged (Giuditta, Dettbarn and Brzin, 1968; Sotelo-Silveira *et al.*, 2006). It was first hypothesised that local protein translation did not occur in mature axons, and ribosomal RNA observed in the axoplasm was most likely RNA transfer from the mitochondria of the neuron. However, this study used polyacrylamide gel electrophoresis to visualise the RNA and as such, the low sensitivity of the technique meant that only low levels of ribosomal RNA were detected in the axoplasm of the squid giant axon (Lasek, Dabrowski and Nordlander, 1973). Initial evidence subsequently suggested that although present, local protein synthesis in the axon only occurred during development of the cell since electron dense polysomes were only detected in the proximal axonal segments, but not in the distal compartment (Steward and Ribak, 1986). However, as biochemical detection methods have become more sensitive (e.g. the development of microarrays, qPCR and electron microscopy) ribosomal RNA has been observed from both cortical and sensory neuron axons (Bassell *et al.*, 1998). Compelling evidence came in 2009 when axons of cultured peripheral sensory neurons showed metabolically labelled, newly synthesized proteins being trafficked to the cell membrane (Merianda *et al.*, 2009). Synaptic plasticity is one of the earliest acknowledged examples of local translation, where connections are formed based on neuronal firing and metabolic requirements of the cell. This process of protein turnover at

the synapse requires new RNA, and protein synthesis (Davis and Squire, 1984; Sutton and Schuman, 2006). It has been demonstrated that neuronal proteins quantified *in vitro* had a short half-life of up to 6 days (Dörrbaum *et al.*, 2018) whilst *in vivo* protein turnover appears occur every 10 days (Fornasiero *et al.*, 2018). In particular those proteins that demonstrated highest levels of turnover included proteins found in the growth cone, like MAP2 (Garner, Tucker and Matus, 1988) and proteins involved in synaptic transmission such as Camk2A (Burgin *et al.*, 1990). Several techniques have been used to identify proteins (or polysomal RNA) in the distal portion of the axon. In-situ hybridization was one of the first methods that made it possible to identify proteins in the distal compartment of the cell, although initially low-sensitivity of the detection meant that few transcripts were identified, two of which were Camk2A and Map2. However, more recent developments including qPCR of rodent sensory neurons have led to the identification of hundreds of transcripts located in the distal compartment of the axon, not having been translocated from the soma (Zheng *et al.*, 2001). Furthermore, the purification of excitatory synaptosomes led to the identification of more than 400 transcripts selectively expressed in the active zone of the synaptic terminal (Hafner *et al.*, 2019).

Nowadays it is widely accepted that mRNAs are 1. locally translated within the cell. 2. Are transported via the microtubules of the axon, and 3. That the 3' and 5' untranslated regions of an mRNA are key in the regulation and localization of a protein (Eom *et al.*, 2003; Tushev *et al.*, 2018). RNA interference (or RNAi) refers to the cellular mechanisms of post-transcriptional regulation of protein expression, whereby protein synthesis may be inhibited. Small changes in the sequence of the UTRs affect downstream binding and subsequent translation of a protein. Furthermore, it is clear that there is a large scale of diversity in the 3'UTR of neuronal mRNAs especially, since these cells must constantly react and adapt to incoming cell signals and adjust protein expression accordingly. Genes transcribing proteins in the nucleus are usually transcribed by RNA polymerase II. The primary transcript is processed by splicing to form mRNA and is exported into the cytoplasm where ribosomes catalyze translation of mRNA to mature polypeptide chains. However, this translation can be regulated by small sequences of double stranded RNA molecules involved in translational repression. Both siRNA (short interfering) and miRNA (micro) are short double-stranded RNA molecules involved in RNAi. The key difference is that siRNA binds with full complementation

to one mRNA of interest, which is then degraded. Whereas, miRNAs only bind to mRNA at the seed sequence in the 3'UTR; meaning that one microRNA sequence can potentially bind to and inhibit the translation of multiple mRNA sequences. Therefore, alternative regulation of neuronal mRNAs via the UTRs most likely arises as a consequence of the presence, or absence of several microRNA sequences (Lin and Holt, 2008; Tushev *et al.*, 2018).

1.10 MicroRNA:

MicroRNAs are an endogenous family of small, non-coding RNA roughly 21-25 nucleotides in length. First discovered in *C.Elegans* in 1993, Lin-4 was initially thought to be an isolated regulatory sequence (Lee, Feinbaum and Ambros, 1993). However by 2000, the conserved and temporal expression of the Let-7 family of microRNA had been first reported (Pasquinelli *et al.*, 2000). To date around 2000 microRNA have been identified in the human genome, although sequencing shows that many are conserved between species such as rat and mouse (De Rie *et al.*, 2017; Alles *et al.*, 2019).

1.10.1 MicroRNAs as regulators of translation in the nervous system:

It is well established that these short non-coding sequences are involved in regulating protein turnover, by targeting mRNA degradation and facilitating translational repression. In particular, the role of microRNA in local protein translation has been investigated with relevance here to the subcellular expression in polarised cells such as neurons (Siegel *et al.*, 2009). For example, it has been elucidated that the expression of specific microRNA in the axonal “compartment” of a neuron can repress translation of proteins, thereby acting as regulators of translation (Wang *et al.*, 2015; Zhang *et al.*, 2015). Of course, given the dynamic metabolic requirements of neurons, it is unsurprising that these cells can rapidly regulate protein turnover at a subcellular level, where the soma and the axon often have different metabolic requirements with respect to the surrounding microenvironment. Given the distinct subcellular expression of select mRNAs in the axons of neurons, recent works have also identified roles for microRNA in axonal outgrowth as well as maintaining neuronal viability (Baudet *et al.*, 2012). In a screen of several microRNAs, it was demonstrated here that the specific loss of miR-124 induced a synchronised “loss of function” in growth cone pathway-finding. This finding was most likely induced by the delayed onset of Semaphorin-3

sensitivity in these neurons by inhibition of miR-124 expression in the axon (Baudet *et al.*, 2012).

Work has been ongoing in the Dajas-Bailador lab for many years to characterise the function of specific microRNAs in neuronal development and connectivity. In an earlier study it was shown that miR-9 had roles in regulating axonal extension of cortical neurons, by regulating expression of Map1b and subsequent microtubule stability (Dajas-Bailador *et al.*, 2012). Results showed that microRNA-9 was detected as early as embryonic day 17 (E17) in culture, but the addition of a locked nucleic acid inhibitor (LNAi) for miR-9 showed reduced axonal extensions in cortical outgrowths. Furthermore, the role of miR-9 as a target for signalling pathways controlling neuronal extension was elucidated. The expression of miR-9 was identified as being linked to expression of the chemoattractant brain derived neurotrophic factor (BDNF) in a biphasic manner, thus linking the microRNA of interest to a protein target in a signalling pathway of interest. Short stimulation of the axons with BDNF induced an increase in axonal length, although this response was reversed if miR-9 was overexpressed. Critically, in this study neurons were cultured using compartmentalised microfluidic devices, where the change in miR-9 expression correlating with increase in axonal length, was only observed when BDNF was locally applied to the axons. Consequently, this work has helped to pave the way for further studies in compartmentalised devices, investigating the role of microRNA in local translation of mRNA in neurons.

Following this, the role of miR-26a was elucidated in early stage development of mouse cortical neurons using microfluidic devices (Lucci *et al.*, 2020). MiR-26a was shown to modulate neuronal growth and polarity in primary neuron cultures via the activity of GSK-3 β . Functionally GSK-3 β was detected in both the somal and axonal compartments of the microfluidic devices, and a molecular mechanism was demonstrated whereby the local translation of GSK-3 β is quiescently repressed by miR-26a, and allows elongation of cortical axons. However, upon targeted inhibition of the expression of miR-26a in the axon, translational repression of GSK-3 β is removed, and protein turnover is increased. This increase in GSK-3 β has been further implicated in neurodegeneration, with implications in the development of Alzheimer's and Parkinson's disease models (Jacobs *et al.*, 2012; Golpich *et al.*, 2015).

There is increasing evidence for the role of microRNA and translational repression in disease pathology. For example, the extracellular expression of specific microRNAs have been facilitated as potential biomarkers for the onset of disease (Reid, Kirschner and van Zandwijk, 2011). It is evident that the aberrant expression of microRNA often underlies the pathologies of diseases; such as cancer where the dysregulation of microRNA expression is key to the disease pathology (Tüfekci *et al.*, 2014). There is compelling evidence for microRNAs acting as either tumour suppressors or oncogenes, depending on the endogenous expression of the microRNA. One of the most well-known examples of this, is the role of miR15a and miR16-1 in leukemia. In a mouse model it was demonstrated that mice that developed chronic lymphocytic leukemia (CLL) had a much lower expression of these miRs endogenously. Physiologically these miRs act as tumour suppressors by inducing apoptosis, but ablation of the mature miR sequence led to development of a cancer phenotype (Esquela-Kerscher and Slack, 2006).

MicroRNAs have also been demonstrated to affect pathologies of the nervous system, including nociception (Andersen, Duroux and Gazerani, 2014; Sakai and Suzuki, 2014). Pain is highly dependent on the sensory nerves, but dysregulation of protein expression, specifically receptors or ion channels may induce hypersensitivity of these neurons.

There are multiple stages at which the regulation of microRNA could be endogenously affected. In order to understand how microRNA expression affects disease pathologies, the process of miRNA biogenesis must be further examined.

1.10.2 Biogenesis of microRNA:

There are still new microRNAs being discovered, although the majority of miRNA biogenesis follows a similar pathway. MicroRNA is transcribed from the DNA sequence into a primary miRNA sequence (pri-miRNA). From here, pri-miRNA is processed into a precursor sequence and eventually a mature microRNA (O'Brien *et al.*, 2018). It is widely reported that these mature microRNA sequences interact with the 3' untranslated region (UTR) of mRNA to regulate translational repression of protein (Ha and Kim, 2014). However, there have been

examples where the miR target is the 5'UTR or even the gene promoter sequence (Lytle, Yario and Steitz, 2007).

The majority of microRNAs are generated via the canonical biogenesis pathway (O'Brien *et al.*, 2018) as shown below in figure 1.10.1:

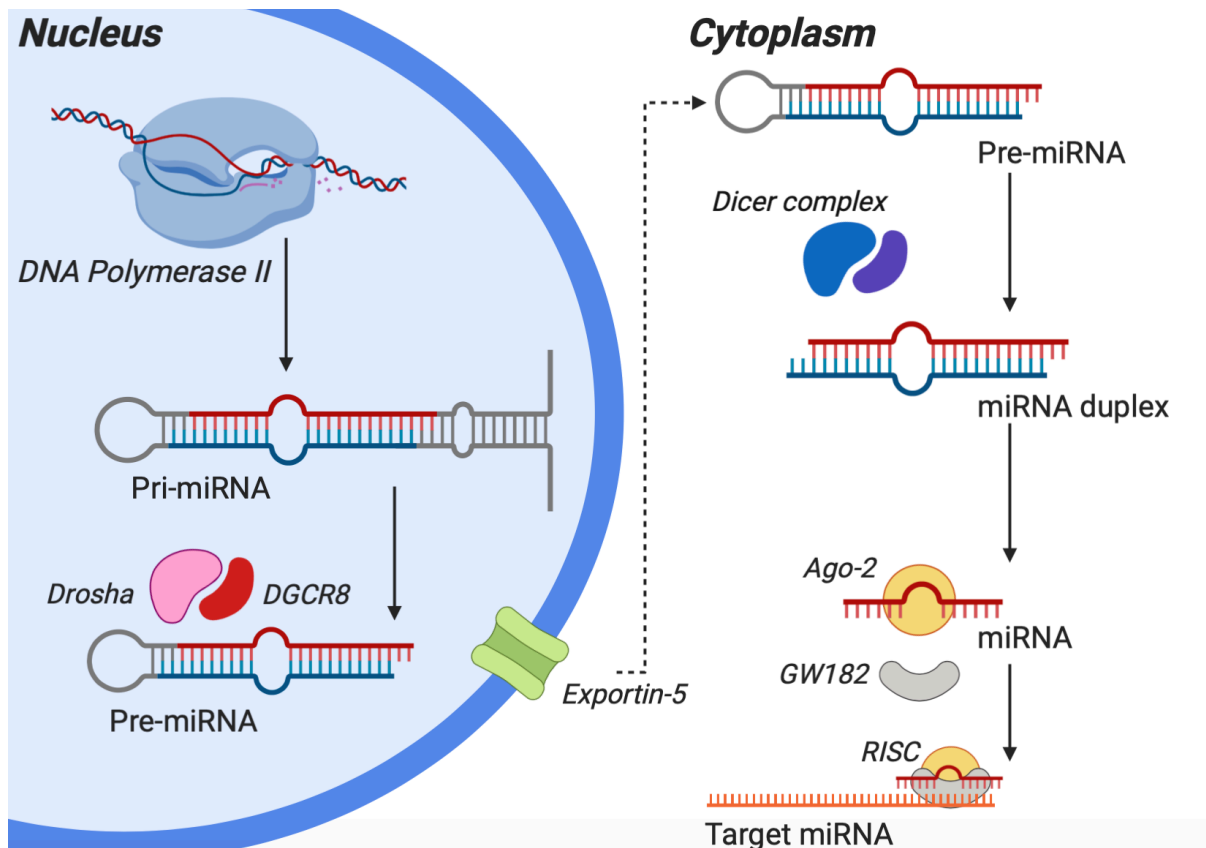


Figure 1.10.1: An overview of the canonical pathway of microRNA biogenesis, made using Biorender

The canonical pathway begins by transcription of DNA by Polymerase II, into the pri-miRNA stem-loop sequence. From here, flanking sequences on the pri-miRNA are cleaved by ribonuclease III enzyme Drosha and the associated RNA binding protein DGCR8 (Denli *et al.*, 2004). The pri-miRNA is processed into a smaller pre-miRNA molecule with a 2 nucleotide overhang at the 3' end of the stem loop (Han *et al.*, 2004).

The pre-miRNA is then exported to the cytoplasm where it is processed by the double stranded RNA-specific RNase III endonuclease, Dicer (Lee *et al.*, 2003; Bartel, 2004). Dicer

cleaves phosphodiester bonds in the RNA sequence to form small dsRNAs, including (but not limited to) microRNAs. Pre-miRNA is cut by removing the loop and terminal base pairs, whilst leaving a short sequence, including the 5' phosphate and 2 nucleotide overhang at the 3' end that is characteristic of RNase III digestion.

There is some evidence to suggest that different at different stages of the canonical pathway, microRNAs are selectively expressed at different regions of the neuron. Where neurons are polarized cells, the metabolic requirements of the axon versus the soma are different but also dynamic. For example, it has been shown that pri-miRNAs are localised only to post-synaptic densities (Lugli *et al.*, 2012). However, PCR reactions from the distal portion of DRG neurons detected amplicons for precursor microRNAs such as pre-miR-138-1 in the somal RNA only, but not in the dendritic RNA fragments (Natera-Naranjo *et al.*, 2010; Kim *et al.*, 2015). In contrast, mature miR-138 has been localised to the soma, axons and dendrites of cultured DRG neurons using fluorescence *in situ* hybridization (Siegel *et al.*, 2009; Kim, H. H., Kim, P., Phay, M., and Yoo, 2015). As such, the evidence provided here demonstrates that the expression of microRNA may change dependent on the microenvironment of the cell, and consequently the translational repression activity of the microRNA is dependent on the biogenesis of mature microRNA.

1.10.3 Association with the RNA Induced Silencing Complex:

The RNA induced silencing complex (RISC) is a protein complex that can actively promote mRNA degeneration or inhibit translation of RNA. In the canonical pathway for miRNA biogenesis this RISC is comprised of Argonaute (AGO) and the guide strand of the pre-miRNA molecule. The miRISC binds to a complementary sequence on target mRNA known as a microRNA response element (MRE.) The degree of complement binding between the miRNA duplex and miRISC determines the mechanism of post-transcriptional regulation of mRNA. If the target sequence of the MRE is fully complementary to the miRISC, then mRNA is immediately cleaved by AGO2 endonuclease activity (Ipsaro and Joshua-Tor, 2015; Jo *et al.*, 2015).

However, the majority of MREs do not show complete complementation to the miRISC (Jonas and Izaurralde, 2015). If cleavage by AGO alone is not possible, the RISC is also comprised of additional elements. In humans, this RISC is comprised of an AGO2 component, as well as glycine-tryptophan (GW182) and other proteins like helicases (Krol, Loedige and Filipowicz, 2010). Interestingly it has been demonstrated that whilst important, the miRNA:mRNA binding is not essential for translational repression. Artificial tethering of either the Ago (Pillai, Artus and Filipowicz, 2004) or GW182 (Eulalio *et al.*, 2009) components of miRISC at the 3'UTR of target mRNA demonstrated a positive effect on gene silencing in a luciferase reporter format (Bos *et al.*, 2016).

Although either strand of the miRNA duplex can associate with the miRISC, it is widely acknowledged that most microRNAs have a dominant guide strand. For example, miR-138-5p recognises the 5' dominant strand in the precursor (Ambros *et al.*, 2003). When the dominant strand of the miR duplex associates with miRISC, the other strand of miRNA is degraded. From here, microRNA associated with AGO2 and GW182 induces downstream translational repression of target mRNA (Kim, Han and Siomi, 2009; Galagali and Kim, 2018).

There also appears to be a developmental effect of miRISC association and the effect on gene silencing. For example, it has been demonstrated that in early development, miRISC activity induces translational repression by shortening the poly-A tail of the transcript, but critically does not reduce transcript stability (Bazzini, Lee and Giraldez, 2012; Subtelny *et al.*, 2014).

1.10.4 Other pathways for microRNA Biogenesis:

Multiple non-canonical methods of microRNA biogenesis have been hypothesised to date, proposing alternate combinations of proteins involved in canonical biogenesis. Of particular interest are Drosha, Dicer, Exportin activity and Ago in the RISC. For this reason, non-canonical biogenesis can be categorised into Drosha-independent and Dicer-independent pathways (O'Brien *et al.*, 2018). For example, pre-miRNA generated with a 7-methylguanosine cap in the Drosha-independent pathway, resembles a Dicer substrate (Xie *et al.*, 2013). The m7G cap

at the 5'UTR are directly exported from the nucleus, without the need for Dicer cleavage (Yang and Lai, 2011; Xie and Steitz, 2014)

The resultant effect of miRNA association with the RISC is variable with respect to expression of target mRNA. There is evidence for both translational repression and RNA degradation inducing gene silencing (Bartel, 2009) but the environmental factors governing how this is determined have not yet been fully elucidated.

1.10.5 Utilising the miRNA seed sequence for target recognition in a signalling pathway:

A prominent method of target interaction with microRNA is the utilisation and cross-referencing of bioinformatic databases. As previously stated, microRNA duplexes bind to the miRISC. It has become evident that since microRNA conforms to Watson-Crick base pairing, the MRE sequence of the mRNA is complementary to the 'seed sequence' of the microRNA. This seed sequence, usually 6 nucleotides long near the 5'UTR, is the only section of the microRNA that must be entirely complementary to the target mRNA (Lewis *et al.*, 2003), in order for a microRNA to potentially target a protein of interest. Other factors, such as low GC composition or length of the 3'UTR (Grimson *et al.*, 2007) have been demonstrated as additional factors that may affect seed binding to a target. However, the basis of most binding prediction algorithms first investigates the complementation of the seed sequence to the mRNA of interest (Paraskevopoulou *et al.*, 2013a; Kozomara and Griffiths-Jones, 2014; Peterson *et al.*, 2014; Agarwal *et al.*, 2015).

Although it is evident that seed sequence complementation to the MRE is important, the inaccuracy of prediction algorithms often leads to false predictions (Liu and Wang, 2019). This is most likely due to the effect of interactions between the miRNA and mRNA that are independent of complementary seed sequence binding. As such, there is often a need for experimental validation of microRNA, following bioinformatic identification of a protein target of interest. Chapter 2.4 describes the use of the dual luciferase reporter system for target validation, a technique that is later used and discussed in Chapter 5.

1.11 Summary and aims of this thesis:

Of particular interest to this project was the use of microfluidic culture for modelling complex multi-cellular signalling pathways, such as those involved in nociception. Until recently the study of nociception *in vitro* has often been limited by the method of culture, and failure to replicate the complex cell signalling pathways and cell morphologies involved in pain-based signalling. However, the development of microfluidic culture has been previously demonstrated to provide a useful tool for modelling the complexity of neuronal signalling *in vitro* (Taylor *et al.*, 2005).

The primary objective of this project was to develop a microfluidic model that could be used to investigate induced changes in neuronal excitability, in the context of pain-based signalling. This included healthy and reproducible culture of DRG neurons *in vitro* that replicated the unique pseudounipolar morphology of these cells observed *in vivo*.

The following aims were outlined during the initial stages of this project:

- To replicate the complex microenvironment of the pseudounipolar DRG neurons by using microfluidically isolated cultures. This included, but was not limited to the additional culture and characterisation of non-neuronal cells that interact with and induce changes in DRG neurons at the neuronal terminals.
- To use the microfluidic model developed in this project to investigate changes in neuronal excitability as a proxy for pain.
- Neurons are highly polarised cells, and it was hypothesised that protein expression is locally regulated in the cell. By exploiting the microfluidic nature of the model, we also aimed to investigate the effect of local protein translation on DRG excitability. This work also included the investigation into a microRNA of interest and the potential role in regulating excitability in pain-based signalling.

Additional objectives have been elaborated on and discussed within the results section of this Thesis.

2 Materials and Methods

Standard protocols are not repeated (i.e DRG dissection and microfluidic seeding). Suppliers for all reagents have been named in the first citing.

2.1.1 Animals

Mice (C57/BL6) were housed, bred and treated in compliance with the ethics and animal welfare in place in the University, in accordance with the *Animal (Scientific Procedures) Act 1986*. Animals were sacrificed and tissue collected in accordance with UK home office regulations and procedures under Schedule 1 of ASPA 1986.

2.1.2 Cell culture:

As an NC3Rs project, this thesis describes the use of multiple cell types. Per dissection, up to 3 cell subtypes were potentially extracted from one pregnant female adult mouse, and the additional embryonic tissue in the case of DRG neuron culture.

2.2 Cell Culture based protocols:

All tissue dissections used sterile instruments and cell culture was undertaken in a sterile environment using a class II cabinet. All reagents used in the sterile culture environment were sprayed with 70% ethanol before use.

2.2.1 Coating of plates, dishes and coverslips

Dishes or coverslips (if non-sterile) were soaked thoroughly in 70% ethanol and air-dried in a class II cabinet.

Poly-L-Lysine (PLL, Sigma) was diluted in sterile water to a final concentration of 0.02mg/ml and added so that the coating covered the base of the dishes. The coating was left soaking on the dishes for one hour in a class II cabinet. PLL was removed from coated Nuncs/ coverslips,

at which point they were washed twice with sterile water and left to dry completely overnight.

On the day of dissection, laminin (Sigma) was diluted in DMEM (D6546) to a final concentration of 20µg/ml. In microfluidic devices a minimum of 100µl per channel was added. Or if using coverslips for dissociated plate culture, a 50µl drop was added to the centre of a culture dish. Plates were incubated for one hour at 37°C in an incubator whilst neurons were dissected. Laminin was removed and plates were washed with DMEM prior to seeding of cells.

2.2.2 In vitro culture of bone marrow derived macrophages:

In order that the cell culture medium is consistent throughout the model, this protocol describes the culture of macrophages with Dulbecco's modified eagle medium (high glucose DMEM, D6546 Sigma) from an adapted form of the culture method by (Massier *et al.*, 2015).

2.2.2.1 Preparation of L-conditioned media (LCM)

L929 cells (Sigma) were kindly provided by the Martinez laboratory and thawed in a water bath at 37°C. LCM media stock was made by combining DMEM with 10% (v/v) HI FBS, 1% (v/v) PS, 1% (v/v) GM in a 500ml bottle.

1ml of defrosted cells was added to a sterile falcon tube, with 17.5ml LCM media stock added drop-by-drop. Media was not added vigorously to avoid damaging the cells. Cells were centrifuged at 250xg for 5-minutes at +4°C to form a dense pellet and remove DMSO from suspension. The supernatant was removed, and the pellet resuspended in the small volume remaining by tapping the falcon tube gently. From here the cell pellet was completely re-suspended in 3ml of the LCM media stock and added to a T-75cm² with 15ml additional LCM media to cover the base of the flask. After 2-days in culture, the flask was passaged into 4-T-75cm² flasks, and after a further 2 days the T-75cm² were sub-cultured into 10 x 225cm² petri dishes. When the cells began to touch each other in culture on day 8, the time elapsed was counted for a further 10-days. On the 10th day the supernatant was filtrated and frozen at -20°C in 15ml aliquots until required.

2.2.2.2 Preparation of media for culture of macrophages in vitro:

The initial stock was made by combining DMEM with 10% (v/v) HI FBS, 1% (v/v) PS, 1% (v/v) GM in a 50ml tube. At which point, 7.5ml of the “stock” was removed, and replaced with 7.5 ml of the defrosted LCM.

In order that the macrophage media could be tested in live imaging protocols, a protocol for making a stock without phenol red present was also prepared. In this case, all reagents were the same but high glucose DMEM without phenol red (Gibco, 31053028)

2.2.2.3 Culturing cells in macrophage media:

Bone marrow was usually isolated from fresh tissue since the viability of cells appeared increased: the long bones from a pregnant adult female were cut, and excess muscle surrounding the bones was removed. Using a 25G needle and 20ml PBS (without calcium and magnesium, Sigma) the bone marrow was flushed from within the bones, into a sterile 50ml falcon.

Cells were centrifuged at 250xg for 5 minutes at 4°C. By quickly discarding the supernatant into the waste pot, this process forms a dense pellet of cells at the bottom of the falcon. Cells were partially re-suspended by gently flicking the end of the falcon, before 5-10ml pre-prepared DMEM macrophage media was added drop-by-drop to completely re-suspend the cells.

25ml of ‘macrophage media’ was added onto a 140mm **non-tissue culture treated** petri dish (Fisher, 501V) prior to the addition of the cell-suspension. Cells were incubated at 37°C, 5% CO₂ for 3-5 days before changing the media. Although undifferentiated, a healthy macrophage culture appeared between 70-90% confluent, where cells were morphologically rounded or elongated with a ‘halo.’

At day 7 *in vitro* (DiV7) cells were washed twice with PBS (without calcium and magnesium) each time incubating on ice for between 2 to 10 minutes. By adding PBS-EDTA at 10mM (pH 8.0) for up to 20 minutes on ice, cells were detached easily from the cell plate.

If cells were re-plated into a 6-well plate, 2ml/well of cells was pipetted and the plate re-incubated at 37°C, 5% CO₂ until ready to be used. If used for immunofluorescence, cells were re-plated into a 6-well plate onto a glass coverslip and cultured until used. Cells could also be cryopreserved in resuspension 10% (v/v) DMSO with 90% (v/v) FBS.

2.2.2.4 Polarizing cells in vitro:

Culture of mature macrophages in media supplemented with cytokines of interest has been shown to demonstrate changes in the phenotype of cells. In this protocol, from DiV7 onwards, macrophage cells were re-plated and grown in macrophage media supplemented with inflammatory stimuli to promote cell polarisation.

Exposure to cytokines was required for a minimum of 24 hours, with literature suggesting that this period was optimized between 24-48 hours. Phenotypic changes were observed between cells cultured in the presence of lipopolysaccharide (LPS) with interferon- γ (IFN- γ , Miltyni Biotech) as compared to those cultured with interleukin-4 (IL-4, Miltyni Biotech) only. As a control, following re-plating, murine macrophage colony stimulating factor (m-CSF, Fisher) was used to maintain a population of cells in the M \emptyset condition.

Cells from one confluent 140mm petri dish were divided and plated onto three 90mm bacterial-grade petri dishes (Sarstedt.) At this point, once cells had adhered to the plastic, the following protocol for cell polarization was used, based on the literature on classical activation of macrophages (Murray *et al.*, 2014; Massier *et al.*, 2015.)

The concentrations of the cytokines used to promote differentiation of each culture were as follows:

M1-like culture: 100ng/ml IFN- γ + 100ng/ml LPS

M2-like culture: 20ng/ml IL-4

M \emptyset - like control culture: 100ng/ml mCSF

Media from polarized cells was collected and frozen in aliquots at -20°C to be used in downstream co-culture or live cell imaging techniques. The protocol was optimised for use so that cells were exposed to polarizing stimuli for 24-hours, then the media replaced for 2-hours prior to collection. In this way the frozen stocks of 'polarized media' contained cytokines released from polarized cells, but low levels of polarizing stimuli.

Based on the stimuli used, the polarized macrophages produced most closely resembled an M1a-like and M2a-like phenotype, as described by (Melton *et al.*, 2015). For use in imaging

protocols, all polarized media generated was phenol red free to avoid cross-reaction at 470nm excitation wavelength.

2.2.2.5 Cytokine array:

The cytokine array was purchased from Abcam (ab133999) for use with media extracted from polarized macrophage cells (see 2.2.2.4.) The cytokine array permitted semi-quantitative analysis of 40 targets in one experiment rather than the quantification of selected targets of interest. Rather than being a plate-based assay, media was added to a membrane, followed by a biotinylated detector antibody, as well as horseradish peroxidase (HRP.)

Using ImageJ the results of the array were analysed using dot-blot densitometry. The background was removed from each image, using a rolling ball radius set to 25 pixels as standard. Only after correcting to the background does the integrated density for the empty wells equal 0 (or close to.) The scan of the membrane shown has been converted to an 8-bit binary image and inverted. Only those cytokines detected at levels higher than the negative control are now quantified. Densitometry was used for a semi-quantitative analysis of the fold change in the most highly expressed cytokines present in different media subtypes. N=2, error bars representing the standard deviation of the fold change. The results provided a 'snapshot' of inflammatory cell profiles, although the results observed in mice may not directly reflect that observed in human tissue.

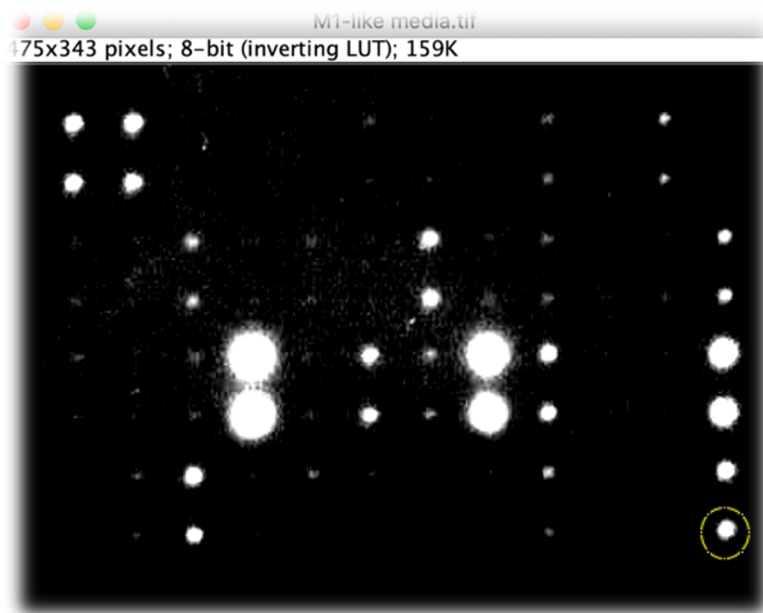


Figure 2.2.1: Example scan of cytokine array membrane exposed to M1-like media for 10-minutes.

Figure 2.2.1 shows an example of a membrane exposed to M1-like media after a 10-minute exposure. A circle was drawn around D6 for both media subtypes, since this point was considered to be the largest spot recorded on the membrane. The integrated density was calculated using Fiji. The area analysed was left the same for every point on the membrane, and the result for wells 1C-2D were subtracted, since these points are “blank” controls. In this way, the background on the membrane was removed from the result, and the data was then normalised to the endogenous positive control.

See below the plate map for the 40-target cytokine array:

	A	B	C	D	E	F	G	H	I	J	K	L
1	Pos	Pos	Neg	Neg	BLANK	BLC	CD30 L	Eotaxin	Eotaxin-2	Fas-L	Fractalkine	GCSF
2	Pos	Pos	Neg	Neg	BLANK	BLC	CD30 L	Eotaxin	Eotaxin-2	Fas-L	Fractalkine	GCSF
3	GM-CSF	IFN γ	IL-1 α	IL-1 β	IL-2	IL-7	IL-4	IL-6	IL-9	IL-10	IL-12 p40/p70	IL-12 p70
4	GM-CSF	IFN γ	IL-1 α	IL-1 β	IL-2	IL-7	IL-4	IL-6	IL-9	IL-10	IL-12 p40/p70	IL-12 p70
5	IL-13	IL-17	I-TAC	KC	Leptin	LIX	Lymphotactin	MCP-1	MCSF	MIG	MIP-1 α	MIP-1 γ
6	IL-13	IL-17	I-TAC	KC	Leptin	LIX	Lymphotactin	MCP-1	MCSF	MIG	MIP-1 α	MIP-1 γ
7	RANTES	SDF-1	TCA-3	TECK	TIMP-1	TIMP-2	TNF α	sTNF RI	STNF R II	BLANK	BLANK	Pos
8	RANTES	SDF-1	TCA-3	TECK	TIMP-1	TIMP-2	TNF α	sTNF RI	STNF R II	BLANK	BLANK	Pos

2.2.3 Microglial Culture in vitro:

Using the spinal cords isolated from E16.5 tissue, a mixed glial population was cultured from which the microglia were isolated as required.

Microglial seeding media= High glucose DMEM, no Ca^{2+} (Gibco 21068028) supplemented with 10% (v/v) HI FBS, 1% (v/v) PS and 1% (v/v) GM

Microglial replating media= High glucose DMEM, no Ca^{2+} (Gibco 21068028) supplemented with 10% (v/v) HI Horse serum (Gibco), 1% (v/v) PS and 1% (v/v) GM

Spinal cords were removed during embryonic dissection and placed in 5ml Leibovitz's L-15 media (Gibco) on ice. The tissue was then transferred to a sterile 50ml tube, and the volume of media was topped up to a minimum of 10ml before the spinal cords were homogenized by pipetting. The suspension was then centrifuged at 2500xg for 5 minutes at 4°C, and the supernatant aspirated from the pellet. Cells were gently re-suspended in 10ml L-15 using a 10ml serological pipette, and the suspension passed through a 100 μM cell strainer (Corning) to remove cell debris.

The cell suspension was re-spun at 2500xg for 5 minutes at 4°C, and the pellet re-suspended in 6ml microglial seeding media. Cells were transferred to T-25cm² flasks, were incubated at 37°C, 5% CO₂ and the media changed on day 5, then every 48-72 hours until cells were confluent.

Upon reaching confluency (usually between DiV10-14) cells were placed on an orbital shaker at 150rpm for between 2-4 hours (maximum) at 37°C, 5% CO₂ to lift the microglial layer from the astrocytes. The flask was checked every hour to ensure only the microglial cells were removed. These cells were resuspended in microglial re-plating media, on pre-coated PLL dishes or coverslips (see Chapter 2.2.1,) using 100 μl droplet per coverslip, and topping up media after 24 hours.

2.2.3.1 Microglial polarization:

Culture of mature microglia in media supplemented with cytokines of interest also demonstrated changes in the phenotype of cells. For continuity, the same protocol was used

for the microglial polarization as the macrophage culture (section 2.2.2.4), although IFN γ was not used to prime the development of the M1-like cells.

2.2.3.2 Microglial Phagocytosis assay:

(see Bioprotocols (Lian, Roy and Zheng, 2016))

After microglia were attached to pre-coated PLL coverslips (0.1mg/ml, see section 2.2.1) polarization was promoted for between 24-48H using the protocol described in section 2.2.2.4.

Latex fluorescent beads (diameter 1 μ M, Sigma L1030) were pre-opsonized in HI FBS for 1 hour at 37°C, then diluted into high glucose DMEM (D6546) for a final concentration of beads to FBS in DMEM at 0.01% (v/v) and 0.05% (v/v) respectively.

Cell media was replaced with microglial media containing the latex beads and cells re-incubated for a minimum of 1 hour at 37°C. Cells were washed thoroughly with PBS and then fixed with 4% PFA. Downstream immunofluorescence protocols (section 2.5) were used to quantify microglial phagocytosis with relevance to cell phenotype.

2.2.4 In vitro culture of dorsal root ganglion:

Embryonic DRG (E16.5) were extracted from pregnant adult C57-BL6 mice and placed in Leibowitz-15 (L15, Fisher) medium on ice. From here DRGs were treated for 10 minutes with 0.025% (w/v) trypsin (Sigma) in calcium and magnesium free PBS followed by 15-20 minutes digestion with 0.2% (w/v) collagenase-II (Gibco) at 37°C. The cell pellet was removed from the collagenase and transferred to 1ml high glucose DMEM (D6546 Sigma) supplemented with 10% FBS (Fisher) and gently dissociated.

Cell suspension was centrifuged for 5 minutes at 100xg (4000rpm) in a tabletop minicentrifuge and the resulting cell pellet suspended in the appropriate volume of DRG growth media (DMEM, 2% (v/v) B27 (Invitrogen), 1% (v/v) PS (Sigma), 2mM GM (Fisher), 50ng/ml Glial-Derived Neurotrophic factor (GDNF, Sigma), 50ng/ml Nerve Growth Factor (NGF 2.5S, Invitrogen) and 4 μ M Aphidocolin (Aph, Sigma). The anti-mitotic Aphidocolin was

included within the DRG growth media in order to restrict excessive growth of non-neuronal cells.

2.2.4.1 Microfluidic seeding:

Top-down view

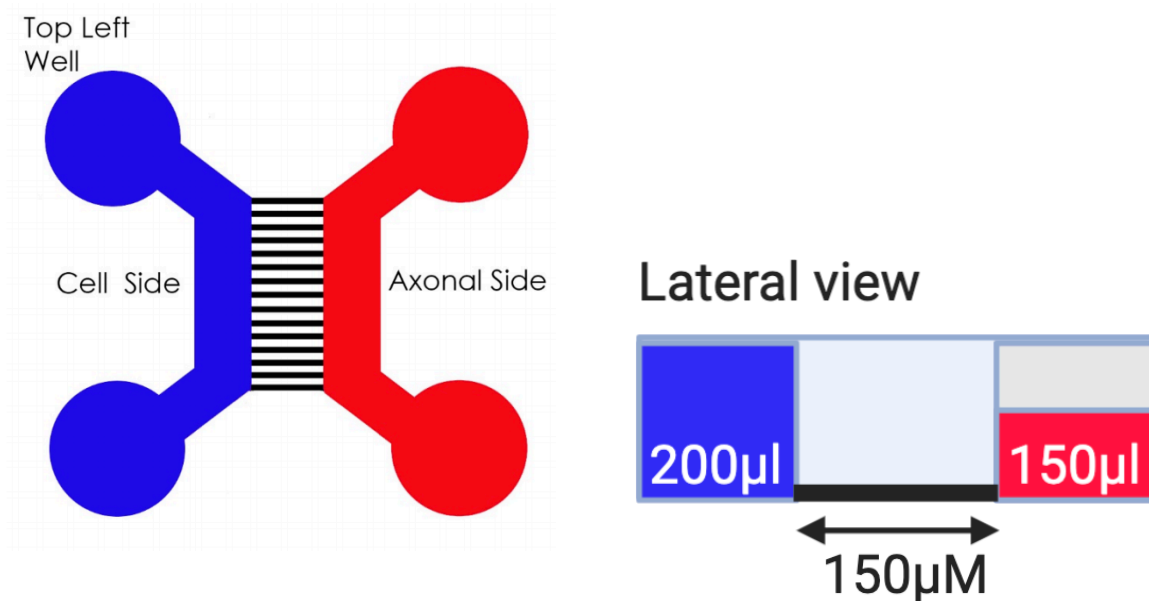


Figure 2.2.2: Schematic showing the design of a two channel microfluidic device with microgroove length 150µM separating the microfluidically isolated compartments, image taken from Xona microfluidics.

Preparation of the microfluidic devices SND150 (Xona) was completed as described by Garcez *et al.*, (2016.) Dissociated cultures were seeded in microfluidic chambers on plates pre-coated with PLL and Laminin as described in 2.2.1. A maximum 10µl cell suspension was slowly added drop-by-drop to each well in the somal compartment, with each of the axonal compartments being filled with 150µl DRG growth media.

After 4 to 6 hours the culture was supplemented with 200µl additional growth media for culture on the somal side. Cultures were maintained at 37°C, 5% CO₂ in a high humidity incubator with an average of 8-12 DRGs dissociated to a cell concentration of 5x10⁶ cells/ml in each 2-channel microfluidic chamber (Xona, SND150.)

Hydrostatic pressure was used to ensure that media entered but did not pass through the microgrooves. This was achieved by ensuring that the volume of media was higher in the somal compartment than the axonal compartment of the chamber at all times (see figure

2.2.2.) Wells on the axonal side of the chamber were filled with 150µl each of DRG growth media compared to 200µl per well on the somal side.

2.2.4.2 Dissociated plate-based culture of DRGs:

Laminin (Sigma) in DMEM was applied to the centre of a PLL-coated Nunclon (35x10mm) cell culture dish at least one hour prior to cell seeding. Laminin solution was removed, and 30µl of DRG cell suspension containing 3-5 dissociated ganglia was applied to the centre of the dish in a droplet. Cells were left to adhere overnight, and 1-2ml of DRG growth media was added to the cells the following morning. Media was gently replaced every 3-4 days of culture, ensuring not to lift the cell suspension from the plate when re-adding new media.

2.2.4.3 Culture of DRG on porous membranes:

Cell culture inserts (Corning) with a porous PET membrane (1.0µm diameter pores) were placed into a tissue culture grade 6-well plate. The culture method was derived from works described by Unsain *et al.*, (2014) regarding the culture of sensory neurons using porous filters. When the insert was placed into the 6-well plate, two compartments were formed as shown by chapter 5, figure 5.3.1.

All cultures using these inserts were pre-coated with 1mg/ml PLL for 1 hour (on both sides of the insert) before exposure to laminin (20µg/ml) for 1 hour at 37°C on the day of culture. The “axonal compartment” of these inserts sits in a minimum of 2ml DRG growth media, which contains growth factors, whilst the cell pellet is seeded in 100µl of DRG growth media without NGF and GDNF onto the membrane, and topped up to 1ml after 24 hours, after the cells have attached to the membrane. Media was exchanged every 3 days of culture.

2.3 Functional studies with DRG in microfluidic chambers:

2.3.1 Calcium Imaging:

Standard imaging buffer was prepared fresh every two to four weeks in autoclaved sterile water containing 135mM NaCl, 3mM KCl, 10mM HEPES, 15mM glucose (all Sigma), pH 7.4. To each 10ml of complete buffer used 1mM MgSO₄ and 2mM CaCl₂ was added on the day of use.

Changes in fluorescence were recorded by quantifying the increase in Fluo-5F (AM) signal following stimulation of a cell. Fluo-5F AM (ThermoFisher) is a single wavelength, labelled calcium indicator, with similar properties to other indicators such as Fluo-3 (Thomas *et al.*, 2000). However, unlike other analogs of calcium indicators used in epifluorescent signalling experiments, Fluo-5F has a lower binding affinity for calcium within the cell, making small changes in intracellular calcium (1μM-1mM) more easily detectable without saturation of the response of the fluorescent ligand (Paredes *et al.*, 2008, 2009). A lower affinity calcium indicator dye was selected as most suitable for this assay, where the concentration of calcium in the endoplasmic reticulum ranges between 0.1 and 1mM (Raffaello *et al.*, 2016).

Cell permeable Fluo-5 AM (ThermoFisher, 11544786) was diluted into 454μl Pluronic F127 20% solution in DMSO (Sigma, 10767854) in order to create a 10mM stock of Fluo-5, aliquoted to 10μl aliquots and stored at -20°C until use. The aliquots were protected from white light at all times (foil wrapped vessels etc.)

This protocol has been optimised for live cell imaging of DRG cultures seeded into two-channel microfluidic chambers, although can also be carried out for dissociated cell cultures seeded onto coverslips.

2.3.1.1 Cell loading and de-esterification:

The media was removed gently from the somal compartment of the chamber, and the cells gently washed twice with complete imaging buffer. From this point onward, the entire protocol was completed in the dark, to avoid bleaching of the Fluo-5 signal.

Fluo5 (in pluronic) stock was diluted in complete imaging buffer to a final concentration of 100nM, and 100μl applied to the somal compartment of each microfluidic device.

Fluo-5 was then removed from the somal compartment of the chamber after a loading period of 30 minutes, and replaced with 100µl imaging buffer, at which point the cells were left to completely de-esterify for a minimum of 30 minutes.

2.3.1.2 Technical notes on dye loading and extrusion:

Loading of the calcium indicator dye was highly efficient, but there was potential for extrusion of the molecule from the cell body during longer imaging protocols, especially if the cell was continuously exposed to light. When exposed to light at a specific wavelength, 470nm the increase in “free” calcium in the cell was recorded as an increase in fluorescence where calcium binds to fluo-5 and light is emitted. However, if exposed for long periods of time, or to high intensities of light (such as ambient light) the fluorophore becomes unstable and the signal will photobleach, rendering the fluorophore unable to fluoresce and inducing high levels of background fluorescence. Whilst the acetoxymethyl ester group attached to fluo-5 was essential for making the dye cell permeable, once inside the cell, the de-esterification period was required to completely hydrolyse this AM ester bond before recording (Lock, Parker and Smith, 2015). Since Fluo-5 is a fluorescent molecule, complete removal of the attached ester was required to reduce background fluorescence when quantifying changes in fluorescence to a stimulus.

The phenomenon referred to as “bleaching” of the signal, is one of the disadvantages of using non-ratiometric calcium indicators, such as Fluo-5. Calcium indicator dyes have been engineered in several forms, including salts, dextrans and hydrophobic acetoxymethyl (AM) ester forms. With a lower binding affinity, and a cell permeable nature, the most appealing form for this experimental design was the AM ester form (Paredes *et al.*, 2009; Lock *et al.*, 2015). However, without complete de-esterification of the indicator loaded into the cell, the background signal would fluctuate where there was a mixture of free and calcium-bound indicator dye trapped within the cell whilst imaging. For this reason, it was important to time the de-esterification period of the cells for a minimum of 30 minutes.

2.3.1.3 Imaging:

An Olympus IX70 Inverted tissue culture microscope coupled to a CCD camera (photometrics CoolSnap MYO, global shutter) was used and data acquired in micromanager (Tsuchida *et al.*, 2014). Using multi-acquisition in Fiji an image stack was recorded in line with cell stimulation. An exemplar recording measured 480 frames, one every 250ms, with a total run time of 2 minutes. Appropriate imaging settings were selected on micromanager (Tsuchida *et al.*, 2014). Usually this was set for 50ms exposure in the 470nm wavelength filter and 2x2 image binning. However, if doing longer read times reducing the binning to 4x4 reduced the size of the file. For analysis purposes, the images were saved as a stack file to allow multiple analyses of the same cell.

Once the cells were completely loaded imaging buffer was removed from the chamber and placed on the platform. Using 10X magnification the cells were brought into focus (using eyepieces and green light illumination, 470nm). Once the cells were in focus the eye piece was switched to camera and the image re-focused before stopping live imaging.

All cultures were recorded for up to 20 seconds prior to stimulation, in order to determine an initial level of excitability. Since pseudounipolar sensory neurons do not fire spontaneously (unlike cortical neurons) this provided a stable baseline Fluo-5 signal, for which the post-stimulation response would be normalised to.

By starting the acquisition sequence, the shutter opened and closed every 250ms until the sequence was complete. Watching the timer on the screen, after a maximum of 10 seconds, the first stimulus was added (e.g., 30µl KCl 25mM) to the axonal compartment of the chamber, then if required the second stimuli was added at 2 minutes and 20 seconds. Different stimuli were selected according to which fibres of the DRG were being targeted.

Although cell viability was not an issue during this time period, the background signal from Fluo-5 would begin to saturate the image if the cells were continuously exposed at 470nm for prolonged periods of time. All time-course analyses have been adapted to show a total time-course of 60 seconds, including 10 seconds baseline prior to stimulation.

2.3.1.4 Image Analysis for Ca²⁺ signalling experiments:

All image analysis was completed using the ImageJ software from Fiji (Schindelin *et al.*, 2012). Using ImageJ, the stack file was opened and navigated to find excitation of the cells in response to a stimulus. Cells were manually selected, and added to the ROI manager tab. Once a minimum of 10 cells were selected, the multi-measure feature calculated the area (μM) as well as the mean fluorescence intensity (ΔF) of each cell per image taken. Data was exported to an excel template and manually analysed to plot a time-course analysis. All data was normalised to the baseline fluorescence intensity.

Each chamber was only imaged once, starting with stimulation of the axonal compartment, at which point it was removed from the stage, washed with imaging buffer and the stimuli usually then added directly to the somal compartment.

In order to normalise the intensity of the Fluo-5 signal, an average value for the baseline fluorescence (F_0) was calculated before stimulation. The stimulus-response was calibrated by removing this background from the maximum fluorescence at every time point (F_t) on the image stack.

The change in fluorescence over time was plotted using the equation $((\Delta F = F_t - F_0) / F_0)$. In this equation F_t represents fluorescence at a given time point, where F_0 is equal to the 'resting fluorescence' of a cell.

Values were primarily plotted as a time-course analysis (XY curve) to visualise the change in fluorescence as a measure of excitability in response to a specific stimulus. The percentage increase in fluorescence following stimulation could be extracted from the data, by calculating the difference between maximum and minimum $\Delta F / F$.

2.3.1.5 Statistical analysis of Ca^{2+} imaging:

For the purposes of the data shown in this thesis the following definitions are important:

Biological replicates (N): Each chamber was only imaged once, with different conditions tested across multiple preparations. Given that each biological replicate was taken from a separate embryonic litter, each microfluidic device (or dissociated plate) was assumed to be a biological replicate.

Technical replicates: it is important to acknowledge that the tissue used here was taken from dissociated embryonic tissue, with tissue from multiple embryos used when seeding multiple plates. In the case of the microfluidics we refer to the individual cells within each channel as the technical replicates of each condition.

Data represents the mean \pm SEM of 3 (or more) independent biological replicates/repeats of an experimental condition. The N number chosen was dependent on the type of test condition, in line with necessary power calculations and the principles of the 3Rs. Where possible, conditions were tested using tissue from more than one animal to allow for tissue variability, but without wasting tissue. The significance level for statistical analysis was assumed to be 5%.

In line with the principles of the 3Rs a power calculation was performed to ask;

- a) What was the smallest effect that could have biological relevance?
- b) What was the largest effect of a treatment compared to a control?

For example, when comparing stimulation of dissociated plates versus microfluidics, a post-hoc power calculation estimated that a minimum N=6 would determine statistical significance, and the P values have been highlighted on the figures. The power calculation was estimated using the peak excitability (ΔF) for three biological repeats, where no appropriate published data was available to perform the calculation before starting the experiment. Estimates were calculated using a low and high estimate of the signal to noise ratio:

	Mean 1	Mean 2	Std Dev.	S/N Ratio	N number at 80% confidence
N=3	2.5	1.8	0.2	3.5	3
			0.4	1.8	6

This estimation assumes $P=0.05$ is significant and used a two-sided format.

In each repeat (N) a minimum of 10 cells (replicate values) were analysed, although this was dependent on the field of view and normally approximately 20 cells were selected. Using GraphPad Prism 9.0 peak fluorescence data was analysed to show a Gaussian population for downstream statistical analysis purposes.

With three or more groups for comparison, a one-way ANOVA (analysis of variance) was used to determine significant differences between data sets. For multiple comparisons of data sets,

an additional Dunnett's comparison. Tests was used. Degrees of freedom (F) was calculated within groups and between groups and was reported as F(Df1, Df2).

If comparing significance between two groups, a parametric (usually unpaired) t-test was used. Where descriptive statistics deemed the standard deviations of data sets were different then a post-hoc Welch's analysis was also applied (as stated in the figure legends.) A Grubbs' analysis was performed and a maximum of one outlier was removed where $\alpha=0.05$.

Values of $P<0.05$ were considered to be statistically significant.

2.4 MicroRNA functional analysis tools:

2.4.1 MicroRNA 'power' inhibitors;

A cell permeable miRNA power inhibitor control (Negative Control A, TAACACGTCTATACGCCCA, ID Y100199006-DDA) and the miRCURY LNA miR-138-5p Power inhibitor (MIMAT0000150: 5'AGCUGGUGUUGUGAAUCAGGCCG, ID Y104102106) were obtained from Qiagen.

At DiV5 the media was changed in the microfluidic device, and the miR-138-5p inhibitor (or non-targeting control probe) was added at a concentration of 100nM for 24-hours. The schematic in each figure indicates where the inhibitor was added.

2.4.2 Small interfering RNA (siRNA):

Accell smartpool siRNA for Mouse Kcna2 (Horizon, E-058746-00-0010, 10nmol) and a non-targeting siRNA control (Horizon, D-001910-10-20, 20nmol) were purchased from Horizon discoveries. Pellets were resuspended to a working concentration of 100 μ M in 1X siRNA buffer and stored at -20°C until required.

At DiV5 the media was changed in the microfluidic device, and the smartpool siRNA for Kv1.2 (smartpool negative control siRNA) was added to the axonal compartment at a final concentration of 100nM for 24-hours.

2.4.3 Target prediction using Bioinformatics:

Target searching for interactions with the 3'UTR of miR-138-5p is described in-depth in Chapter 5, part B. It is important to be aware that prior to use of siRNA, targets of interest were identified and validated. When identifying potential candidate targets a range of bioinformatic searching tools were used. This included, Diana Tools microT-CDS (Paraskevopoulou *et al.*, 2013a) Tarbase (Karagkouni *et al.*, 2018) TargetScan v7.2 (Agarwal *et al.*, 2015) and miRTarBase (Hsu *et al.*, 2011).

2.4.4 Target validation using Luciferase assay:

The dual-luciferase reporter assay is relatively low throughput, but can be easily manipulated to provide a semi-quantitative output regarding changes in protein expression dependent on a microRNA of interest (Jin *et al.*, 2013). First the protein of interest is expressed in a vector such as pmiRGlo (Guo *et al.*, 2013). Once the insert has been successfully sequenced to contain the seed sequence of the microRNA of interest, an immortalised cell line is transfected with the protein. A microRNA mimic is co-transfected alongside the luciferase reporter construct and the microRNA mimic binds to the target site identified in the construct, protein translation is subsequently repressed.

By inserting miRNA target sites downstream of the primary reporter gene (FLuc) a reduced FLuc expression is observed. This indicates binding of miRNA mimic to cloned miRNA sequence inserted into the pmiR vector. Where reduction in FLuc expression is used to monitor miRNA regulation, the RLuc site acts as a control reporter sequence. In this way, by remaining stable, the RLuc site normalizes the signal of the dual luciferase assay between samples in transfected cell lines.

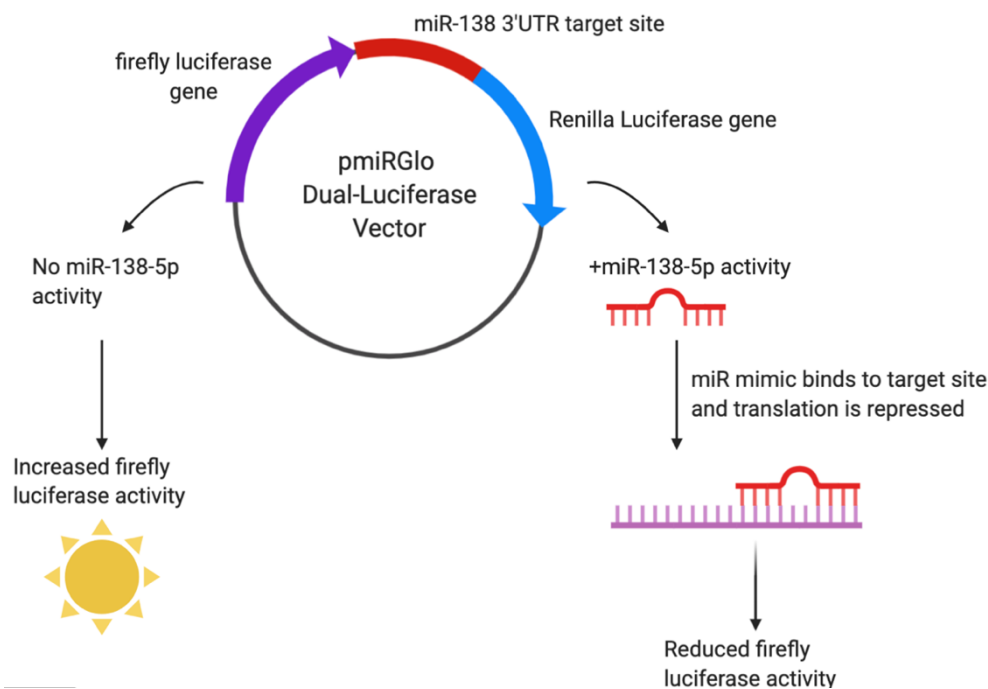


Figure 2.4.1 The dual luciferase reporter system using pmirGlo and expression of firefly luciferase (FLuc) to quantify miR-mimic binding to a protein sequence of interest in vector

2.4.4.1 Luciferase cloning:

Forward and reverse oligonucleotides were designed for 4 protein targets of interest, encompassing a total of 9 potential target sites to be tested where proteins such as KCNA2 (also known as Kv1.2) contained 5 potential target sites for miR-138-5p. The oligonucleotides were all 51 bp in length and were designed so that when annealed they contained the potential 3'UTR target sequence in 3' – 5' direction.

Only the desired miRNA target region was inserted into the pmirGLO Dual-Luciferase miRNA Target Expression Vector (Promega), as opposed to the entire 3'UTR. Restriction sites were included on either end (*NheI* and *Sall*) so that overhangs created by oligonucleotide annealing

were complementary to those generated by restriction enzyme digestion of the pmirGLO Vector's multiple cloning site. Primers were also phosphorylated at the 5' end of the oligonucleotides for ease of insertion into the pmirGLO vector. An internal *NotI* restriction site was also added to oligonucleotides for downstream clone confirmation. This addition creates a ~125bp insert when digested with *NotI* because of a *NotI* site at position 93 in the vector.

miR138-5p complement: 3' cggccugauucacaac**ACCAGC**u 5'

Seed sequence 3' to 5' **uggucg** (search complement **accagc**). Seed sequence in bold.

	Forward Sequence (<i>NheI</i> / <i>NotI</i> / <i>Sall</i>)	BP	%GC	Tm
KCNA2 Site 1	CTAGCATGCGGCCGGAATGTATCTTTGGGGAGGGGGC ACCAGC TTACACG	51	61	87
KCNA2 Site 2	CTAGCATGCGGCCGGAATGTACACATGCAAAATGCAC ACCAGC CTACACG	51	55	85
KCNA2 Site 3	CTAGCATGCGGCCGGAATGTATCATCTGCTAGTATT ACCAGC TTACACG	51	51	81
KCNA2 Site 4	CTAGCATGCGGCCGGAATGTACTTGGCCCTTATTGAG ACCAGC ATACACG	51	55	83
KCNA2 Site 5	CTAGCATGCGGCCGGAATGTATCATGAAAATTTAGAC ACCAGC TTACACG	51	47	79
KCNB1 Site 1	CTAGCATGCGGCCGGAATGTAGTGCCGGTACGTGC ACCAGC GTACACG	51	65	89
KCNB1 Site 2	CTAGCATGCGGCCGGAATGTAGGCCATCCAGAAGGC ACCAGC GTACACG	51	63	88
KCNG1 Site 1	CTAGCATGCGGCCGGAATGTACCTGTTCAGACCTCCC ACCAGC CTACACG	51	61	86
KCNG1 Site 2	CTAGCATGCGGCCGGAATGTAGCTCTGTCCCTGCAGG ACCAGC CTACACG	51	63	88
KCNK10 Site 1	CTAGCATGCGGCCGGAATGTAGGCAGCTTTCCCTTAG ACCAGC CTACACG	51	59	85
KCNK10 Site 2	CTAGCATGCGGCCGGAATGTAGAGTCTCCTTTCCCA ACCAGC CTACACG	51	59	85
KCNK10 Site 3	CTAGCATGCGGCCGGAATGTAGTATGTCTGGCAAAGA ACCAGC CTACACG	51	55	83
KCNK10 Site 4	CTAGCATGCGGCCGGAATGTATGGTAGATCACATGAC ACCAGC TTACACG	51	53	82
	Reverse Sequence	BP	%GC	Tm
KCNA2 Site 1	TCGACGTGTAA GCTGGT GCCCCCTCCCCAAAGATACATTGCGGCCGCATG	51	61	87
KCNA2 Site 2	TCGACGTGTAG GCTGGT GTGCATTTTGCATGTGTACATTGCGGCCGCATG	51	55	85
KCNA2 Site 3	TCGACGTGTAA GCTGGT AATACTAGCAGGATGATACATTGCGGCCGCATG	51	51	81

KCNA2 Site 4	TCGACGTGTATGCTGGTCTCAATAAGGGCCAAGTACATTGCGGCCGCATG	51	55	84
KCNA2 Site 5	TCGACGTGTAAAGCTGGTGTCTAAATTTTCATGATACATTGCGGCCGCATG	51	47	80
KCNB1 Site 1	TCGACGTGTACGCTGGTGCACGTGACCCGGCACTACATTGCGGCCGCATG	51	65	89
KCNB1 Site 2	TCGACGTGTACGCTGGTGCCTTCTGGGATGGCCTACATTGCGGCCGCATG	51	63	88
KCNG1 Site 1	TCGACGTGTAGGCTGGTGGGAGGTCTGAACAGGTACATTGCGGCCGCATG	51	61	86
KCNG1 Site 2	TCGACGTGTAGGCTGGTCCTGCAGGGACAGAGCTACATTGCGGCCGCATG	51	63	88
KCNK10 Site 1	TCGACGTGTAGGCTGGTCTAAGGGAAAGCTGCCTACATTGCGGCCGCATG	51	59	86
KCNK10 Site 2	TCGACGTGTAGGCTGGTTGGGGAAAGGAGACTCTACATTGCGGCCGCATG	51	59	86
KCNK10 Site 3	TCGACGTGTAGGCTGGTTCTTTGCCAGACATACTACATTGCGGCCGCATG	51	55	84
KCNK10 Site 4	TCGACGTGTAAAGCTGGTGTTCATGTGATCTACCATACATTGCGGCCGCATG	51	53	83

Table 2.1 Oligonucleotides designed for protein target sites for use in the luciferase assay. Complementary oligonucleotides were designed for the potential targets of KCNA2, KCNB1, KCNG1 and KCNK10, they contained *NheI* and *Sall* ends to incorporate into the pmirGLO vector and an internal *NotI* site (sites indicated in different colours). The site of the seed sequence for miR138-5p is also highlighted in yellow.

The pmirGLO vector (500ng/ μ l) was digested with 20u of both *NheI*-HF (NEB) and *Sall*-HF (NEB) for 15 minutes at 37°C as per the manufacturers instructions, before being treated with 1u alkaline phosphatase (NEB) for 60-minutes at 37°C, to dephosphorylate the oligonucleotides and prevent re-ligation of the linearized plasmid DNA. Samples were purified by running the digested vector on a 1% (w/v) agarose gel using Tris-Acetate-EDTA buffer (40 mM Tris, 20 mM acetic acid, 1mM EDTA), excising the DNA band and then gel extracting the DNA using the QIAquick Gel extraction kit as per manufacturer's instructions (Qiagen).

Oligonucleotides were delivered in a lyophilised state (Integrated DNA technologies) and suspended in hyclone water to a concentration of 1 μ g/ μ l prior to annealing.

Forward and reverse primer were combined with oligonucleotide annealing buffer (10mM Tris pH7.5, 50mM NaCl and 1mM EDTA), and heated to 90°C for 3 minutes, then to 37°C for 15 minutes to anneal the complementary pairs.

4ng of annealed oligos were ligated into 50ug of the linearized pmirGLO dual luciferase vector overnight at 16°C using T4 DNA ligase (NEB) as per manufacturer’s instructions. The resulting plasmid was transformed into XL10 gold high-efficiency competent cells. In brief, 5ul of the ligation reaction was incubated with 100ul of XL10 competent bacterial cells for 30 minutes on ice, then heat shocked at 42°C in a pre-heated waterbath for 40 seconds, before being incubated immediately on ice and re-suspended in 900µl LB broth. After 1-hour shaking at 200rpm and 37°C the ligation mixture was cultured on an LB agar plate with selectivity for Ampicillin (Sigma) overnight at 37°C.

Colonies were picked and cultured for miniprep (Qiagen) extraction of the plasmid using distilled water following manufacturer’s instructions. Efficient cloning was confirmed through *NotI* (NEB) digestion of plasmid followed by agarose gel visualisation of resulting fragment bands.

Successful insertion of the annealed oligonucleotides was then confirmed through Sanger sequencing (DeepSeq Lab, University of Nottingham). Upon optimisation of this protocol, it was evident that insert would only be detected at concentrations higher than 500ng/µl.

2.4.4.2 Site directed Mutagenesis:

Primers were re-designed for those sequences successfully cloned into the pmirGlo vector. This time a mutant version of the inserted sequence was generated via PCR, where four nucleotides in the target seed sequence were mutated. In each mutation, the site represented the 2nd to the 6th nucleotides of the microRNA seed sequence.

The primers for site-directed mutagenesis were designed in-house and are shown in Table 2.2 below:

	Forward Primer SDM (Seed mutation ACCAGC to AAACAC)	BP	%GC	Tm
KCNA2 Site 1	GTATCTTTGGGGAGGGGGCAAAACACTTACACGTCGACCTGCAGG	44	57	80.4
KCNA2 Site 4	GTACTTGGCCCTTATTGAGAAACACATACACGTCGACCTGCAGGC	45	51	78.5
KCNA2 Site 5	GTATCATGAAAATTTAGACAAACACTTACACGTCGACCTGCAGGCATGC	49	43	77.2
KCNK10 Site 1	GTAGGCAGCTTTCCTTAGAAACACTTACACGTCGACCTGCAGG	44	59	81.2
	Reverse Primer SDM (Seed mutation GCTGGT to GTGTTT)	BP	%GC	Tm
KCNA2 Site 1	CCTGCAGCTCGACGTGTAA GTGTTT GCCCCTCCCAAAGATAC	44	57	80.4

KCNA2 Site 4	GCCTGCAGGTCGACGTGTATGTGTTTCTCAATAAGGGCCAAGTAC	45	51	78.5
KCNA2 Site 5	GTACGCCTGCAGGTCGACGTGTAAAGTGTGTCTAAATTTTCATGATAC	49	43	77.2
KCNK10 Site 1	CCTGCAGGTCGACGTGTAGGTGTTTCTAAGGGAAAGCTGCCTAC	44	59	81.2

Table 2.2 Primer sequences used for SDM

The PCR reaction for mutant strand synthesis is shown here:

1 cycle 95°C 30 seconds

18 cycles 95°C 30 seconds

 55°C 1 minute

 68°C 9 minutes

hold at 4°C.

The product was digested using 20u DpnI (NEB) at 37°C for 1-hour as per the manufacturer's instructions, to remove the parental dsDNA strand prior to transformation into XL10 cells as described above. Confirmation of mutagenesis was achieved using Sanger sequencing.

2.4.4.2.1 Treatment of pmirGLO with miRNA mimic and transfection into HEK cells:

HEK-293T cells were seeded into a 24-well plate at a seeding density of 0.8×10^5 cells/ml in high glucose DMEM with 10% (v/v) FBS and 1% (v/v) PS. After 24-hours incubation at 37°C and 5% CO₂ cells were transfected with the pmirGLO vector containing the DNA insert.

The DNA was diluted to 200ng/μl, with each condition to be tested run in triplicate for both the miRNA mimic and the LNA control sequence.

Transfection mixture was assembled as follows (per well):

- 0.5μl Lipofectamine2000 mixed with 100μl Opti-Mem and incubated for 20 minutes at room temperature.
- 50μl Opti-mem + 1μl DNA (insert in pmirGLO at 200ng) + 2.5μl 20μM mimic/ LNA mimic control. Mix was incubated for 5 minutes at room temperature.
- Solutions were combined and incubated at room temperature for 30 minutes, then added dropwise to cells without removing the media. Cells were then incubated at 37°C and 5% CO₂ for 48 hours with the transfection mix.

Following transfection, media was removed from cells and they were washed with ice-cold PBS prior to lysis in 100µl passive lysis buffer (per well.) Cells were rocked for 30-minutes at room temperature, making sure to cover the plate to protect the light sensitive reagents. When lysis was complete, the contents of each well were collected in separate lo-bind DNA tubes before use in the dual luciferase assay. The protocol could also be stopped here, with DNA frozen at -80°C until required.

2.4.4.2.2 Dual Luciferase assay:

This assay required the use of a GloMax® Navigator microplate luminometer (Promega), as well as the Promega Dual-Luciferase® reporter assay kit.

The reagents luciferase assay reagent II (LARII) and Stop and Glo® were prepared as per manufacturer's instructions.

In triplicate 10µl of each sample was pipetted into a well of a white 96 well plate. A slightly modified method from that of the manufacturer was used; 25µl of each of the luciferase assay reagent II (LAR II) and Stop & Glo® was used per well.

An additional 700µl of each reagent was also required to prime the lines of the Glomax plate reader.

2.4.4.2.3 Analysis of Luminescence:

Luminescence emission was recorded in relative light units (RLU) in counts per second (CPS) by the GloMax Luminometer plate reader. Results were exported to excel, and the relative result for FLuc was divided by the control response for the RLuc response of the same sample. The changes in the FLuc/RLuc ratio are indicative of direct inhibition of the FLuc reporter gene. Therefore, this FLuc/RLuc ratio was used as a reflective change in target modulation, arising as a result of miR target binding to the introduced mimic and results were expressed as percentage change from the control samples. Whilst this dual-luciferase assay is ratiometric by design, there were some limitations to the assay.

2.5 TRizol extraction of RNA:

This is a standard protocol used in the Dajas-Bailador lab for RNA extraction from neuronal cultures (Garcez, Guillemot and Dajas-Bailador, 2017). However, when extraction RNA was

extracted from microfluidic chambers RNA is pooled to increase the concentration, particularly from the axonal compartments.

Samples were lysed using 1ml TRIzol reagent (Invitrogen) per condition and incubated at room temperature for 5 minutes to allow dissociation of ribonucleoprotein complexes. One fifth volume of chloroform (ThermoFisher) was added to each of the samples and vortexed, before being incubated for up to five minutes at room temperature. Each sample was then centrifuged at 12,000x g for 15 minutes, in a centrifuge pre-cooled to 4°C.

Following centrifugation, three layers become visible; the clear aqueous phase, the interphase, and the organic layer (phenol-red chloroform phase.) The upper, known as the aqueous layer, contains the RNA required. Without disturbing the layers below, as much of the aqueous phase as possible was collected and transferred to a new Lo-bind tube (Eppendorf.)

One half volume of isopropanol (i.e. 500µl for every 1ml TRIzol used for lysis, ThermoFisher) was added to the aqueous phase and the samples incubated at room temperature for 10 minutes. If extracting RNA from only the axonal compartment, the concentration is often very low. To make the downstream pellet more visible, 0.66µl Glycoblue (ThermoFisher) was added into the aqueous phase per 0.5ml isopropanol. Each sample was centrifuged again at 12000x g, this time for 10 minutes at 4°C.

The supernatant was gently removed from each of the RNA pellets and the RNA was washed in one volume of 75% ethanol in Hyclone RNase and DNase free water (GE healthcare.) Each sample was briefly vortexed before one final centrifugation for 5 minutes at 7500xg, at 4°C. The RNA pellet was allowed to air dry before resuspension in maximum 30µl Hyclone, and to aid RNA resuspension, each sample was incubated for up to 10 minutes at 55-60°C.

RNA concentration and purity was then determined using a 2000c UV/IV Spectrophotometer (Nanodrop, ThermoFisher Scientific) before storage at -80°C. Partially dissolved RNA showed a 260/280 ratio of less than 1.6, although a good yield from the axonal compartment was considered anything between 30-50ng/ml.

2.5.1 Extraction of RNA fractions from porous trans-well inserts:

After culturing DRGs in Twiss-chambers (Corning) for a minimum of 5 days *in vitro*, and once the axons have crossed through the channel to the axonal side, the chamber was washed with PBS, whilst the cells remained attached to the insert.

Media was aspirated gently from the cultures, usually following exposure of the “axonal compartment” to polarised media (or control media) for 8 hours, and the cells were washed gently twice with sterile PBS. To increase the yield of RNA collected, when washing the inserts with TRIzol, the cells were also gently scraped to promote cell lifting. The procedure for RNA extraction was followed as described in 2.5 above.

2.5.2 Quantitative polymerase chain reaction (qPCR):

qPCR was carried out to determine the levels of select miRNAs within extracted RNA samples and uses SYBR green that binds to double stranded DNA and subsequently fluoresces. The emitted fluorescence during the PCR is directly proportional to the amount of DNA amplified product detected in every cycle.

2.5.3 cDNA Synthesis:

cDNA was synthesised from mature miRNAs using the miRCURY LNA™ Universal cDNA synthesis kit (Qiagen, UK), which uses a poly-T primer. This method uses ExiLENT SYBR Green master mix dye (Qiagen) that binds to double stranded DNA and subsequently fluoresces. The emitted fluorescence during the PCR is directly proportional to the amount of DNA amplified product detected in every cycle.

2.5.4 qPCR using SYBR green:

qPCR was undertaken using the ExiLENT SYBR® Green master mix kit (Qiagen, UK), and the Applied Biosystems Step One Plus thermocycler was used in standard mode using cycling parameters recommended by Qiagen:

Polymerase Activation/Denaturation; 95°C for 10 min

Amplification cycles; 40 cycles at 95°C for 10s, then 60°C, for 1 min. The ramp-rate was set to 1.6°C/s, with an optional melt-curve analysis.

Data was acquired using Applied Biosystems SDS2.3 programme and Ct values were analysed for relative miRNA quantification using the comparative $\Delta\Delta\text{Ct}$ method (Livak and Schmittgen, 2001; Nolan, Hands and Bustin, 2006; Rao *et al.*, 2013). Biological repeat samples were run across multiple mouse dissections, using miRCURY LNA™ primers (Qiagen, UK). Per plate each biological repeat was run with two technical replicate wells. See section 2.5.4.3 below for a technical note on the exclusion of CT values for housekeeper miR133b, which was only consistently detected in 3 out of 5 biological repeat samples.

microRNA of interest: miR-138-5p primers used were the hsa-miR-138-5p LNA PCR primer set (Qiagen) which have been reported to be compatible with samples from mice (as well as rat.)

2.5.4.1 Internal Controls for normalization of fold change expression in qPCR:

ROX™ (Fisher Scientific - UK Ltd) was used as a passive reference for normalising for non-PCR related fluorescence variations, and was incorporated by SDS2.3 to calculate Ct values. A non-template control (NTC) of water was also included for each primer to confirm absence of background signal and lack of contamination. Spike in samples containing Sp6 were used as inter-plate calibrators (IPCs) to confirm PCR efficiency and added at the cDNA synthesis stage. If possible, an IPC was run for one sample and one control sample per plate (in minimum duplicate.) In most cases, the DRG media control (or the MØ control) were used as the IPC samples between plates. Average IPC Ct values between plates that were within $\leq 5\%$ of each other were deemed acceptable to use.

2.5.4.2 Housekeeper genes for reference fold change expression in qPCR:

A range of housekeepers were used, having first been identified in a hyperalgesic priming study by J. Spalton, in collaboration with Dr Alex Rathbone and Professor Victoria Chapman. Since this study involved the effect of inflammation on RNA, it was anticipated that most housekeepers would change dependent on the inflammatory condition that they were exposed to. A housekeeper was deemed suitable if the change in Ct value was less than 2-

fold overtime and between pooled control and treated samples and when the same trend of the Ct value was seen between housekeepers and miRNAs of interest in control samples when serial diluted (Livak and Schmittgen, 2001).

Housekeepers used were miR-133b, miR-134-5p and SNORD33

Primers for SNORD33 were designed in-house for rat using Primer3 software by Clare Martin, but have been demonstrated to be compatible with mice:

SNORD33_F: 5'AGCTTGTGATGAGGATGTCTCC

SNORD33_R: 5'TGGTAGTGCATGTAGAGTCGTC

miR-133b and miR-134-5p primers were LNA PCR primer set (Qiagen), details in Table 2.3

	Sequence	ID	Conserved in Mouse
mmu-miR-133b	5'UUUGGUCCCCUUAACCAGCUA	MIMAT0000770	Y
hsa-miR-134	5'UGUGACUGGUUGACCAGAGGGG	MIMAT0000447	Y
hsa-miR-138-5p	5'AGCUGGUGUUGUGAAUCAGGCCG	<u>MIMAT0000430</u>	Y

Table 2.3 Details of LNA Primers (Qiagen, UK)

2.5.4.3 Analysis of qPCR:

Using the SDS2.3 software thresholds were standardised for each miRNA and remained consistent between plates. The Ct values were analysed using relative quantification and the comparative Ct method ($2^{-\Delta\Delta Ct}$); the geometric mean of the housekeepers miR-134-5p, miR-133b, and SNO33 was used as the endogenous control and the 24-hour time point exposure to DRG media as the calibrator. Results were expressed as fold change in expression. GraphPad Prism was then used to plot the fold change data with error bars showing SEM. **Individual housekeeper values for miR133b of 34.8 and 39.9 were excluded prior to calculation of the geomean, where the average dCT value was 24-29.**

2.6 Immunofluorescent staining of primary cells:

Cells were washed in PBS before being fixed with 4% (w/v) Paraformaldehyde (PFA) in PBS containing 2.7% (w/v) sucrose at room temperature for 30 minutes. Following which samples were washed twice in PBS with 10mM glycine (PBS/glycine), before being permeabilised by

incubation for half an hour in PBS/glycine with 0.2% (v/v) triton. After washing cell samples twice for 2 minutes in PBS with 0.1% (v/v) Triton (PBS/Triton), cells were blocked in 3% (w/v) BSA in PBS for 30 minutes. The primary antibody was diluted in 3% (w/v) BSA, 50µl was added per coverslip and samples left overnight at 4°C in a humidified chamber.

Cells were washed three times in PBS/Triton. At this point the secondary antibody was added after dilution in 3% (w/v) BSA (e.g. 1µl alexa fluor 488 for βIII-tubulin in 300µl 3% BSA was a typical stain for the axons of the neuronal cultures). Coverslips were left at room temperature for up to two hours, and then washed again once with PBS/Triton before being mounted on slides with up to 20µl hard set VectaShield (Vector Laboratories). If required, DAPI was also added to the stain in the presence of the secondary antibody, at final concentration of 300nM.

Antibodies	Working dilution	Manufacturer details
Anti-Acetylated tubulin	1:300	Cat no. T7451; Sigma-Aldrich
Anti-βIII tubulin	1:100	Cat no. ab18207; Abcam
Rabbit polyclonal to liver Arginase	1:300-1:500	ab91279, Abcam
Mouse monoclonal [NOS-IN] to iNOS	1:300-1:500	ab49999, Abcam
Kv1.2 trial size antibody	1:300	Alamone labs, APC-010

Table 2.6.1: List of antibodies, dilutions and suppliers used in this Thesis

2.6.1 Quantifying relative expression of protein markers using immunofluorescence:

2.6.1.1 Acquisition:

Unless stated otherwise phase contrast/brightfield images were acquired using a 20X objective of a widefield fluorescence microscope (Zeiss 200M, Axiovert) couple to a CCD camera (CoolSnap MYO). All images were acquired using Micro-manager software v2.0 (Edelstein *et al.*, 2014) and analysed using ImageJ (FIJI). All images in this assay were acquired at 20X magnification, 100-milliSecond exposure and using a triple channel stain (including DAPI for nuclear localisation) where appropriate.

2.6.1.2 Plot profile analysis:

Upon analysis the image stack was opened in ImageJ and converted to an 8-bit colour image, in this way all images were comparable where the pixel intensity always ranged from 0-255. (In a binary image format, zero represents an area of black, whilst 255 is white, although over exposure can lead to a value of 256, indicating greyscale.) By splitting the channels (FITC, Arginase-1 in green /TRITC, iNOS in red) it was possible to view the relative intensity of each stain. The image was converted to binary, and the whole area selected. Using ImageJ built in analysis, the Plot profile plugin tool was used to a 2-dimensional representation of the relative pixel intensity along a line within the image. Of course, this selection also included background regions, where little to no stain was present within a cell. For this reason, 5 areas of background were selected from each image and an average intensity was calculated. This background value was subtracted from every value in the plot-profile range, and subsequently an average “marker-intensity” value was calculated for each channel.

3 *In Vitro* modelling of nociceptive cellular connectivity using compartmentalised microfluidic culture systems

3.1 Introduction

International guidelines for the study of nociception *in vivo* require that all animal studies are carried out under strict ethical guidelines. The framework of these guidelines are based on the principles of the 3Rs incorporating the Reduction, Replacement and Refinement of animals in research (McGrath *et al.*, 2010). Complete replacement of animals in pain-based research is difficult due to the nature of behavioural testing, where pain can be inferred *in vivo* from the development of pain-like behaviours. For example, rats and mice can be assessed or their willingness to move and behaviour such as paw withdrawal can be quantified following exposure to inflammatory mediators such as carrageenan in the hindpaw (Larson, Wilcox and Fairbanks, 2019). Especially with regards to drug development (e.g. analgesics) it is important to monitor changes in pain in a living animal for reasons such as efficacy and safety. Although useful for studying behavioural changes, there are also clear limitations to *in vivo* modelling. For example, monitoring changes in cellular excitability at a molecular level enables the study of subtle changes in protein regulation and neuronal signalling, which cannot be detected from an *in vivo* behavioural model (Sandkühler, 2009). Furthermore, models involving scoring such as the use of the facial grimace scale analyses have the potential for human bias, where it is down to the investigator to determine the level of 'pain' that the animal is feeling (Hirst *et al.*, 2014; Deuis, Dvorakova and Vetter, 2017). Therefore, there is a clear need for the development of biologically relevant *in vitro* models of nociception that reduce the use of animal tissue, and enable the study of the molecular changes underlying development of pain pathologies.

At a cellular level, the formation of precise axonal connections between the peripheral and central nervous system is particularly important for complex multi-cellular processes such as

pain. Until recently, it has not been possible to model the cellular interactions in nociceptive circuits *in vitro*, with cell culture experiments often failing to replicate the complex pseudo-unipolar nature of the dorsal root ganglia (DRG) neurons (Djouhri and Lawson, 2004; Krames, 2014; Fenstermacher, Pazyra-Murphy and Segal, 2015; Emery *et al.*, 2018). *In vitro* modelling using **microfluidic compartmentalised cell cultures** has previously been used to demonstrate the capability of DRG neurons to locally respond to a nociceptive signals (Tsantoulas *et al.*, 2013). However, despite the response of the peripheral and central nervous systems being critical in promoting a painful response to an inflammatory mediator, non-neuronal cells are also essential in the resolution (R.-R. Ji, Chamesian and Zhang, 2016). *In vivo* this includes cells such as the keratinocytes in the skin, microglial (see chapter 1.8.3) and astrocytic cells of the CNS, as well as peripheral macrophages; the resident cells of the innate immune system (Katz and Rosenbloom, 2015). With respect to understanding the inflammatory response to a nociceptive stimulus, the response of peripheral inflammatory cells like macrophages is key (see chapter 1.8.)

This chapter describes the development and optimisation of an *in vitro* microfluidic model, (including the culture of DRG neurons) that permits the replication of some of the diverse environments these cells encounter *in vivo* in the context of inflammatory responses and nociception.

3.1.1 Peripheral Sensitization of DRG neurons

In states of inflammation, primary afferents of the DRG become sensitized (Gold and Gebhart, 2010). This sensitisation refers to the change in the threshold for activation of these sensory neurons, which is potentially accompanied by a change in the magnitude of response of the peripheral terminals to stimulation, and consequently a downstream change in the physiological response (see Chapters 1.5.2 regarding peripheral sensitisation and 1.7 for receptors on the nociceptors). For example, one of the key components of sensitization is that the painful sensation outlasts the presence of the noxious stimulus at the nociceptor terminals (Sandkühler, 2009). This phenomenon occurs in response to the prolonged activation of sensory afferents and the chemical mediators released by surrounding non-neuronal cells (e.g. macrophages etc.).

There are a wide range of receptors present on the surface of the peripheral terminals of these neurons, although intra-cellular secondary messenger systems are also important (R. R. Ji, Chamesian and Zhang, 2016). The diagram in figure 3.1.1 shows an example of the range of signalling molecules that have been studied as key modulators of the DRGs and pain, although there are undoubtedly more.

There are also a wide range of signalling molecules involved in the development and mediation of peripheral sensitization, including ATP, prostaglandins (PGE₂) and neurotrophins such as NGF. The role of NGF in peripheral sensitization is well documented, with long standing evidence to support the role of NGF as a peripherally produced mediator of inflammatory pain states (Aloe and Levi-Montalcini, 1977). NGF has been demonstrated to have a complex role in inflammatory pain as well as chronic pain states, where endogenous levels of NGF can be elevated (Sarchielli *et al.*, 2007). NGF is synthesised and released from inflammatory cells such as mast cells, macrophages and Schwann cells upon tissue injury or inflammation, and binds to high affinity tropomyosin kinase A receptors (TrkA) selectively expressed on the terminals of subpopulations of DRG neurons. NGF is also known to bind p75 receptors although the role of p75 is not discussed here. Upon trkA receptor binding, the NGF/TrkA complex is retrogradely transported to the DRG where the cell bodies of the primary afferent fibres are located. This leads to transcription and upregulation of neuropeptides (e.g. substance P), ion channels, and receptors as well as anterograde transport of neurotransmitters (Mantyh *et al.*, 2011). The modulation of these proteins (such as ion channels) sensitizes the primary afferent fibres by changing the excitability of the neuron. Where NGF signalling occurs via retrograde transport, there is a delay (hours to days) before the onset of hypersensitivity of the neurons is observed. One particularly important mechanism of NGF-TrkA binding is the sensitisation of the heat-sensitive TRPV1 channel expressed on smaller diameter peptidergic fibres via phosphorylation. The mechanisms by which TRPV1 is phosphorylated have been debated, including evidence to support the role of mitogen activated pathway kinase (MAPK) signalling and phosphatidylinositol-3-kinase (PI3K.) (Bonnington and McNaughton, 2003). However, it is evident that even the direct binding of NGF to the TrkA receptor induces phosphorylation of TRPV1. This sensitisation of the TRPV1 channel lowers the threshold for thermal activation of these channels, and

consequently lowers the temperature of the sensory neurons for detection of noxious heat (Galoyan, Petruska and Mendell, 2003).

Underlying the onset of peripheral sensitisation, it is likely that receptors other than TRPV1 present on the terminals of the DRG neurons are also upregulated and sensitized. For example, an influx of neutrophils migrate to an area of damaged tissue and the release of pro-inflammatory cytokines induces changes in neuronal excitability (Cunha *et al.*, 2008). For example, in studies of neuropathic pain, the release of chemokines such as CCL2 from nociceptors has been shown to regulate the production of inflammatory cytokines from polarized macrophages via TLR signalling pathways (Zhang *et al.*, 2013; Liu *et al.*, 2016).

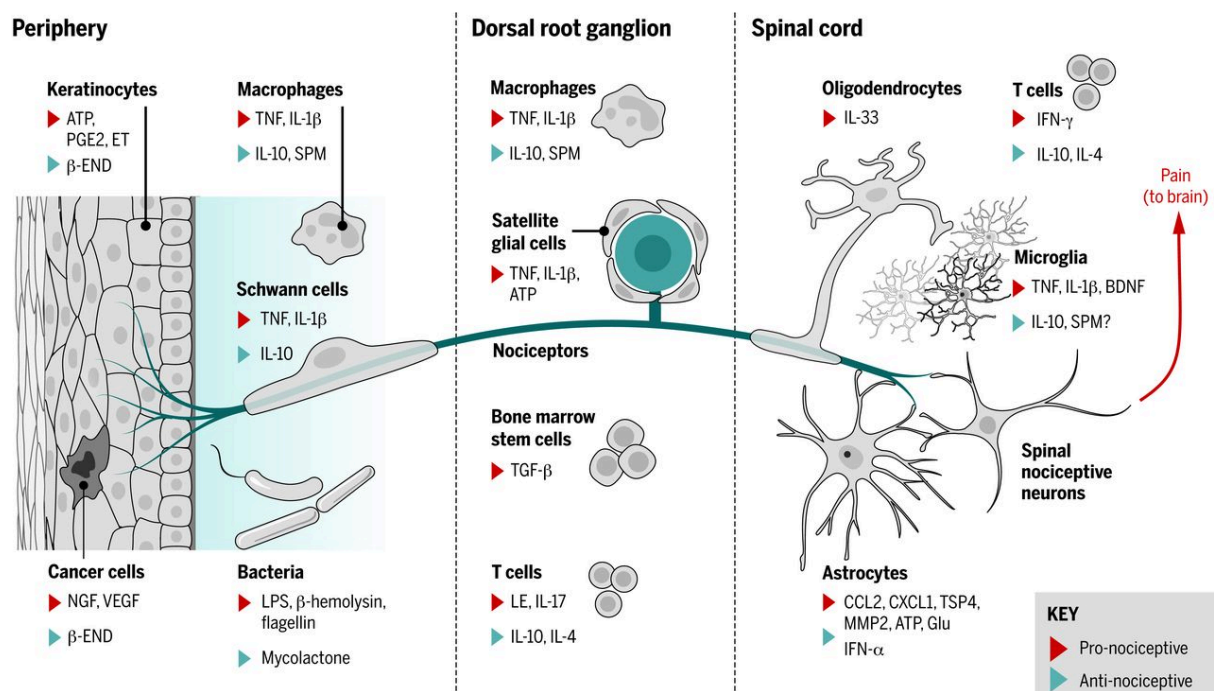


Figure 3.1.1: Interactions between distinct parts of a nociceptor with different types of non-neuronal cells, (R. R. Ji, Chamesian and Zhang, 2016)

3.1.2 Hyperalgesic priming and the transition from acute to chronic pain

It is essential for survival that animals are able to sense and avoid hazardous situations that may cause physical harm. Although acute pain is defined as a protective and evolutionary response, the onset of chronic pain is not deemed to have any physiological benefits.

First developed by Levine in 2003 (Parada *et al.*, 2003; Reichling and Levine, 2009; Ferrari *et al.*, 2013) the *in vivo* models of hyperalgesic priming have become very useful for investigating the cellular and molecular processes involved in the transition from acute to chronic pain (see chapter 1.5.3, hyperalgesic priming and central sensitiation.). Levine (Reichling and Levine, 2009) showed that a short-lived exposure of a rat hind paw to an inflammagen such as carrageenan led to an acute inflammatory response (see figure 1.5.1.) The initial exposure to this inflammatory mediator (e.g. carrageenan) was then followed a reduction in mechanical pain threshold, as measured by the change in paw withdrawal threshold using Von Frey filament recording. This model provides an insight into the mechanism by which the development of acute and chronic pain can be investigated. The nervous system was said to have been “primed” for a hyperalgesic response. For example, a second exposure to prostaglandin-E₂ (PGE₂) now evoked a prolonged decrease in paw withdrawal threshold lasting at least 24 hours (Reichling and Levine, 2009).

3.1.3 Modelling Nociceptive networks in vitro:

In order to model the complexity of the nociceptive circuit *in vitro*, we used microfluidic culture devices to attempt to closely replicate the complex and dynamic cell signalling pathways between the peripheral nervous system and the central nervous system. The pseudounipolar DRG neurons are characterised as the neurons that “bridge the gap” between detection of an inflammatory stimulus at the periphery, and integration to the higher processing centres of the CNS via the dorsal horn of the spinal cord.

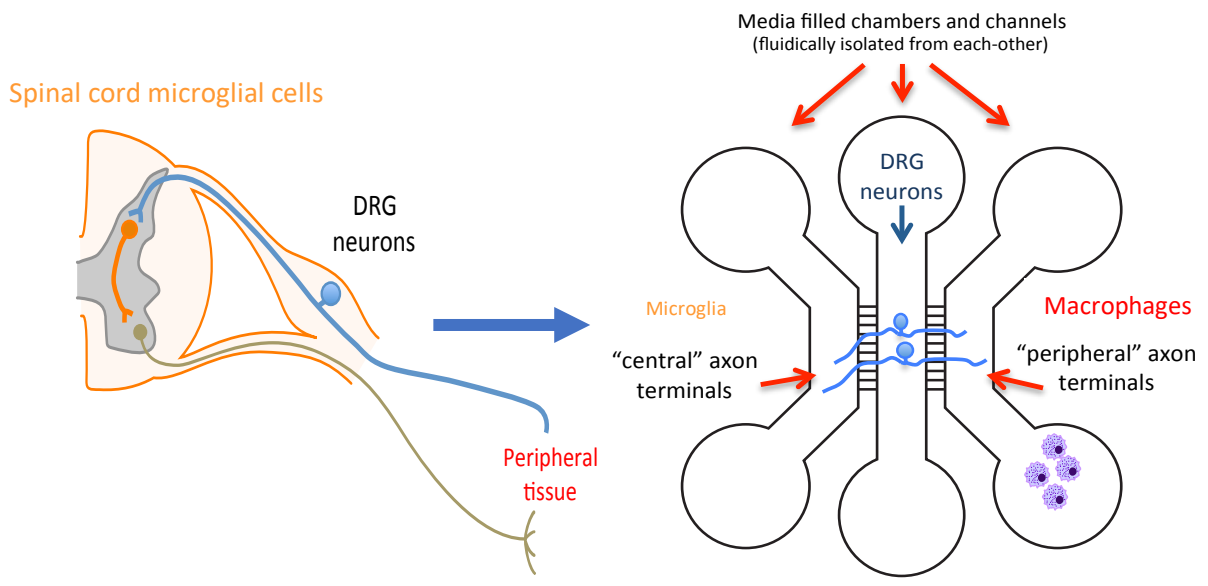


Figure 3.1.2: Modelling the reflex arc in vitro using compartmentalised microfluidic models

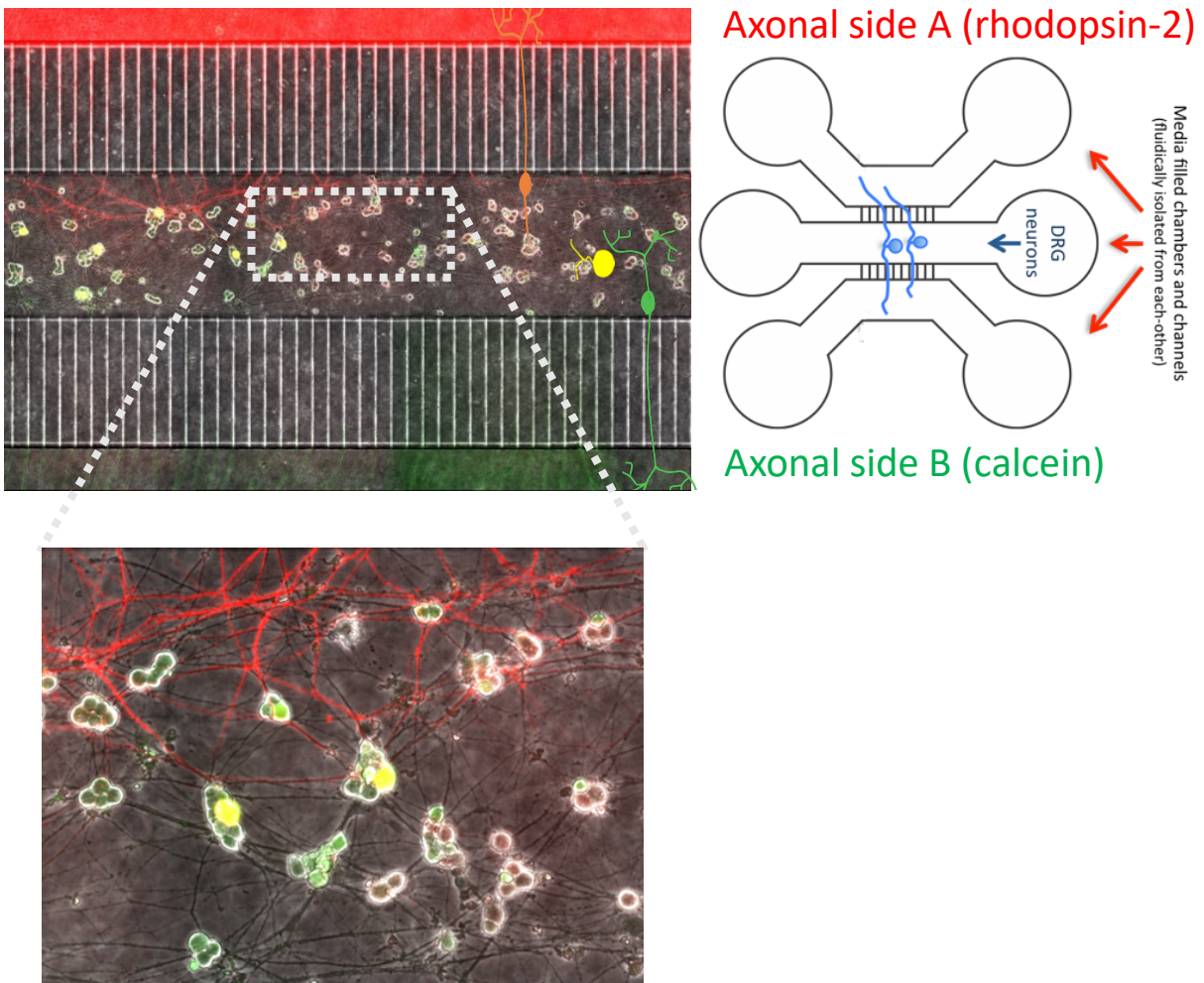


Figure 3.1.3: The pseudounipolar nature of the DRG neurons was highlighted using triple channel microfluidic devices. The uptake of fluorescent dyes into the soma was used to determine if the axon had developed through the microgrooves using changes in Calcium signalling.

The image shown in figure 3.1.3 is taken from Clara Patricio of the Dajas-Bailador lab using E18 rat tissue cultures in a triple channel microfluidic device. This preliminary data helped to show functional characterization of the DRGs in microfluidic chambers, where the soma and the axons were fluidically isolated. The pseudounipolar nature of these cells has also been highlighted here using dual-staining immunofluorescence.

A red dye (Rhodopsin-2) and a green dye (Calcein) were applied to opposite lateral compartments of a triple channel microfluidic device, as shown in the schematic in figure 3.1.3 above. Only some of the cells in the device have taken up both rhodopsin-2 and calcein resulting in these cells being labelled yellow. This indicated that they had axons crossing into both lateral compartments of the microfluidic device. Figure 3.1.3 demonstrates that where a significant number of neurons developed axons that extended into both lateral compartments, the pseudounipolar nature of the DRG neurons was replicated *in vitro* using the compartmentalised microfluidic devices. Since the DRG neurons develop this unique pseudounipolar morphology, it was hypothesised that the axonal terminals would polarize based on what the axon was exposed to in the microfluidic device.

A recent work published after our original findings, confirmed our original findings, showing that in triple channel microfluidic devices from rat cultures, on average $18\pm 7\%$ of DRG soma extended bilaterally, with both axons responding to stimulation. In this model, the DRG neurons from embryonic rats were co-cultured with mixed populations of dorsal horn neurons from the ascending pain pathway in an attempt to model the cell-to-cell signalling between the peripheral and central nervous systems (Vysokov, McMahon and Raouf, 2019). The regulation of excitability of the second order interneurons in the dorsal horn is directly related to input from the DRG neurons, and affects the modulation of pain (section 1.5.2.)

In contrast, we developed a step-by-step approach, beginning the investigation studying cell signalling at the peripheral terminals of the DRG neurons rather than the level of the spinal cord (or the CNS.) Two-channel microfluidic devices were used to reduce materials and time course of *in vitro* culture of primary cells in line with the 3Rs. In our model, the dual-channel microfluidic devices (Xona, SND150) were used to demonstrate changes in the excitability of the DRG neurons.

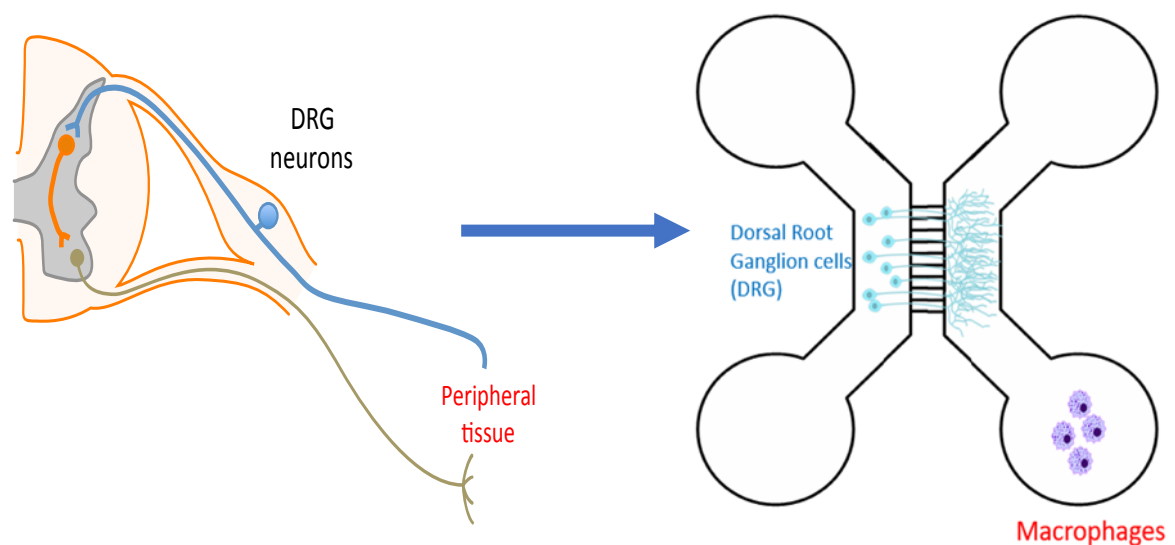


Figure 3.1.4: A schematic showing the development of a simplified version of the NC3Rs model. This model focused on the investigation of cell signalling between the peripheral inflammatory cells and the dorsal root ganglion

In vivo, the exposure of the peripheral terminals of the nociceptor to inflammatory mediators reduces the threshold of activation (see chapter 1.5-1.7.) The molecular processes underlying hyperalgesic priming also include translational regulation of ion channels on the neuron terminals. In our model, investigating the bi-directional signalling between peripheral macrophages and DRG neurons has been deemed to most closely resemble the development of hyperalgesia following peripheral sensitisation.

One of the advantages of these microfluidic cultures was the flexibility of the model for culture and analysis. The hydrostatic pressure in the device created two microfluidically isolated chambers as described in 2.2.4.1. As shown in this work, immunofluorescence and brightfield imaging provided a useful tool for visualising and quantifying changes in cellular markers following treatments. Furthermore, the unique microfluidically isolated nature of the

devices led to the development of stimuli that were more biologically relevant in the study of nociception.

In this model, there were several further techniques that could be applied downstream of the cell culture to quantify changes in protein expression or neuronal signalling. This included the capacity to functionally investigate changes in the excitability of the DRG cultures via calcium signalling assays, such as those described by Tsantoulas *et al.*, (2013.). This microfluidic model also provided the ability to selectively record information being relayed from the axon to the soma. This included both retrograde transport of proteins, and the propagation of the action potential along the axon of the DRG.

We also included direct comparison to standard plated-based culture (colloquially referred to as 'dissociated plates'). In these cultures, a stimulus was applied to the whole culture, and therefore could not be solely ascribed to an axonal receptor or channel response. Additionally, it was possible to isolate axonal versus 'somal' RNA from the microfluidic devices. This technique is commonly used in the Dajas-Bailador laboratory to investigate changes in local protein translation following treatment of the axonal compartment (Garcez, Guillemot and Dajas-Bailador, 2017; Lucci *et al.*, 2020).

In some experiments the direct culture of inflammatory cells that could potentially migrate through the microgrooves was excluded. Instead, media extracted from polarized cells, such as bone marrow derived macrophages, was used to induce a change in neuronal signalling. As shown in the schematic in figure 3.1.4, the culture of spinal cord microglia was removed, with this simplified microfluidic model focusing on how peripheral inflammatory cells induced changes in neuronal excitability. (See chapter 1.8.3 for discussion on the role of microglial cells as inflammatory mediators in the CNS.)

The use of smaller two-channel microfluidics provided the flexibility to characterise functional changes in each cell type more quickly, and as such the development of the model of hyperalgesic priming was accelerated. Whilst the microglial cells were removed from cell-to-cell signalling experiments involving microfluidic culture, a protocol was devised for maintaining an embryonic culture and characterising polarised cells.

3.1.3.1 Objectives of the NC3Rs:

This work was funded by the national centre for reduction, replacement and refinement of the use of animal tissue in scientific research (NC3Rs.) This project was categorised as a **reduction** project, and as such when developing the model, it was imperative that while we gained knowledge on nociceptive mechanisms, we did so by meeting the NC3Rs objectives.

3.1.3.2 Reducing the number of animals required:

In order to maximise the tissue taken per animal, as well as the viability of the cultures seeded, cell culture protocols were adapted accordingly in line with the principles of the 3Rs. Theoretically, microfluidic modelling has the potential to reduce the number of mice required by 90%.

Based on previous studies from the Hathway and Chapman laboratories, it was estimated that an *in vivo* model for hyperalgesic priming would require around 300 animals to screen 15 compounds of interest (at a minimum N=3.) In comparison, only 30 mice embryos would be required to seed up to 75 dual channel microfluidic chambers for *in vitro* testing of DRG neuronal excitability. Furthermore, in contrast to standard *in vitro* models that have limited capacity to model the complexity of neuronal cell signalling in nociception, the microfluidic model replicates the pseudounipolar nature of the cells observed *in vivo*. Therefore, this model provides flexibility to investigate both how localised axonal exposure to specific compounds can affect DRG neuron excitability in live cell signalling, and also quantify changes in local protein expression using standard molecular biology techniques such as qPCR.

One litter from a pregnant C57/BL6 at E16.5 served up to 6 people per preparation, with the additional potential for culture of multiple cell types extracted from animal. Theoretically this could include astrocytes, cortical neurons, bone marrow derived macrophages, DRG neurons, with the possibility for development of other cell preparations if desired. The methods used in this chapter have been described in full detail in chapter 2.

3.1.4 Experimental aims of the chapter:

- **In line with the proposed NC3Rs model, develop experimental models for 3 cell types involved in primary afferent function.**

- **Compare the use of microfluidic culture of DRG neurons to the traditional culture of dissociated DRG neurons in normal culture plates**
- **Investigate phenotypic changes of those cells involved in inflammatory responses, to model what would typically be observed *in vivo* when these cells responded to an inflammatory stimulus**

3.2 Results and Discussion:

3.2.1 Culture of DRG neurons in compartmentalised microfluidic chambers:

As a first attempt to model hyperalgesic priming *in vitro*, work focused on the use of neonatal cultures from rats, which have been previously used in an *in vivo* study in the Hathway lab (James Spalton PhD thesis). Rodent models of nociception commonly involve the use of both rats and mice, where both species can be inexpensively housed, are easily to handle and mature quickly (Larson, Wilcox and Fairbanks, 2019). Over time, several stimulus-evoked methods have been developed to model nociceptive behaviours *in vivo*, including Von Frey stimulation (Görlitz and Frey, 1972; Deuis, Dvorakova and Vetter, 2017) and the Randall-Selitto test as a measure of mechanical hyperalgesia (Randall and Selitto, 1957). Although the genomes of mice and rats are largely similar, evidence has suggested that some fragments in the genome of the rat are closer to that of humans (Zhao *et al.*, 2004). However, 99% of the human genome is conserved in mice, making either species a suitable candidate for modelling nociception *in vitro* (Commission, 2010).

To reduce the use of tissue in line with the 3Rs, this study was developed to incorporate the use of a pre-existing colony of rats, isolating cells from neonatal tissue at P2. Neonates were chosen as they more closely reflect the functional phenotype of nociceptive neurons observed in adult rodents, than the partial development of nociceptive function observed in embryonic tissue. Furthermore, neonates have been shown to display pain-like behaviours such as hyperalgesia *in vivo* (Vega-Avelaira, Ballesteros and López-García, 2013). The use of multiple pups versus one adult yielded increased capacity for microfluidic device cell culture per prep.

However, preliminary results demonstrated that non-neuronal cells extracted in the dissection of DRGs from P2 rats were capable of active migration through the microgrooves despite the narrow width (1-2 μ M (Taylor *et al.*, 2005)). The localisation of a DAPI nuclear stain was present in both the somal and the axonal compartment, where the NeuN neuronal cell marker was only shown in the soma (see figures 3.2.1 below.) This migration of non-neuronal cells between compartments removed the properties of compartmentalisation from the device and rendered these cultures of P2 rat neurons impractical for modelling localised changes in central and peripheral connectivity. In particular the presence of a high number of non-neuronal cells present in the P2 culture was deemed responsible for the migration of cells through the microgrooves.

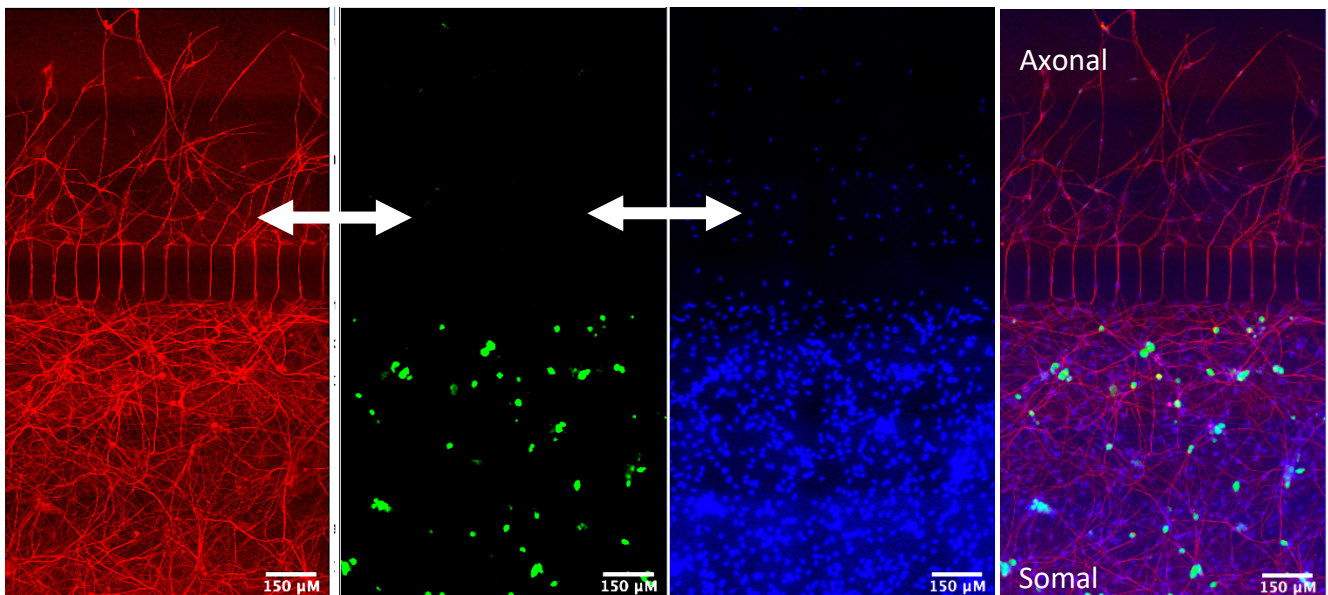


Figure 3.2.1: Separating channels to demonstrate migration of those cells stained with DAPI nuclear stain through the microgrooves of a two-channel microfluidic device. Where DAPI nuclear staining was localised to both the axonal and the somal compartment of these devices, the microfluidic isolation was lost, rendering them useless.

Image was taken from a P2 neonatal rat culture around DiV5 using Zeiss 200M. (Red=acetylated tubulin staining for axons, Blue= DAPI nuclear stain, Green= NeuN staining for neuronal cells only. Composite image on the far right shows all channels combined at 20X magnification.)

3.2.1.1 Troubleshooting cell migration in P2 rat DRG cultures:

Initially the concentration of GDNF was halved from 50ng/ml to 25ng/ml to attempt to reduce non-neuronal cell proliferation. Following culture in adjusted media for 5 days *in vitro*, cells

were fixed and stained. Figure 7.1.1 (appendix 1) showed that the reduction of GDNF concentration did not stop the movement of cells through the microgrooves.

Following the observation that halving the concentration of GDNF in the media did not prevent cell migration, anti-mitotics were introduced to the culture (see figure 3.2.2.) When using P2-derived cells this included testing increased concentrations of Aphidicolin, as well as the introduction of 5'-fluorodeoxyuridine (FDU). FDU has been shown to reduce the dividing of non-neuronal cells in culture of primary cells (Rieske and Kreutzberg, 1977). By co-staining with DAPI and NeuN it was possible to distinguish between neurons and non-neuronal cells, such as satellite glia. Since non-neuronal cells will only express DAPI, an estimated number of cells in each section of the chamber was calculated, and used to quantify cell migration.

Figure 3.2.2 shows that even higher concentrations (40 μ M FDU, fig. 3.2.2C) anti-mitotics did not completely prevent migration of non-neuronal cells, as was demonstrated by the presence of the DAPI stain in the axonal compartment (see figure 3.2.2D). Furthermore, as the concentration of anti-mitotics was increased the number of neurons stained with NeuN that appeared viable at DiV5 was reduced from 54.8 \pm 9.2 cells per chamber to 23 \pm 5.6 cells with 40 μ M FDU. FDU has previously been shown to be preferable for use in culture compared to anti-mitotics such as Ara'C (cytosine arabinoside) where Ara'C was shown to reduce neuronal viability overtime where 99% of proliferating cells were removed in a cortical culture (Hui, Zhang and Herrup, 2016).

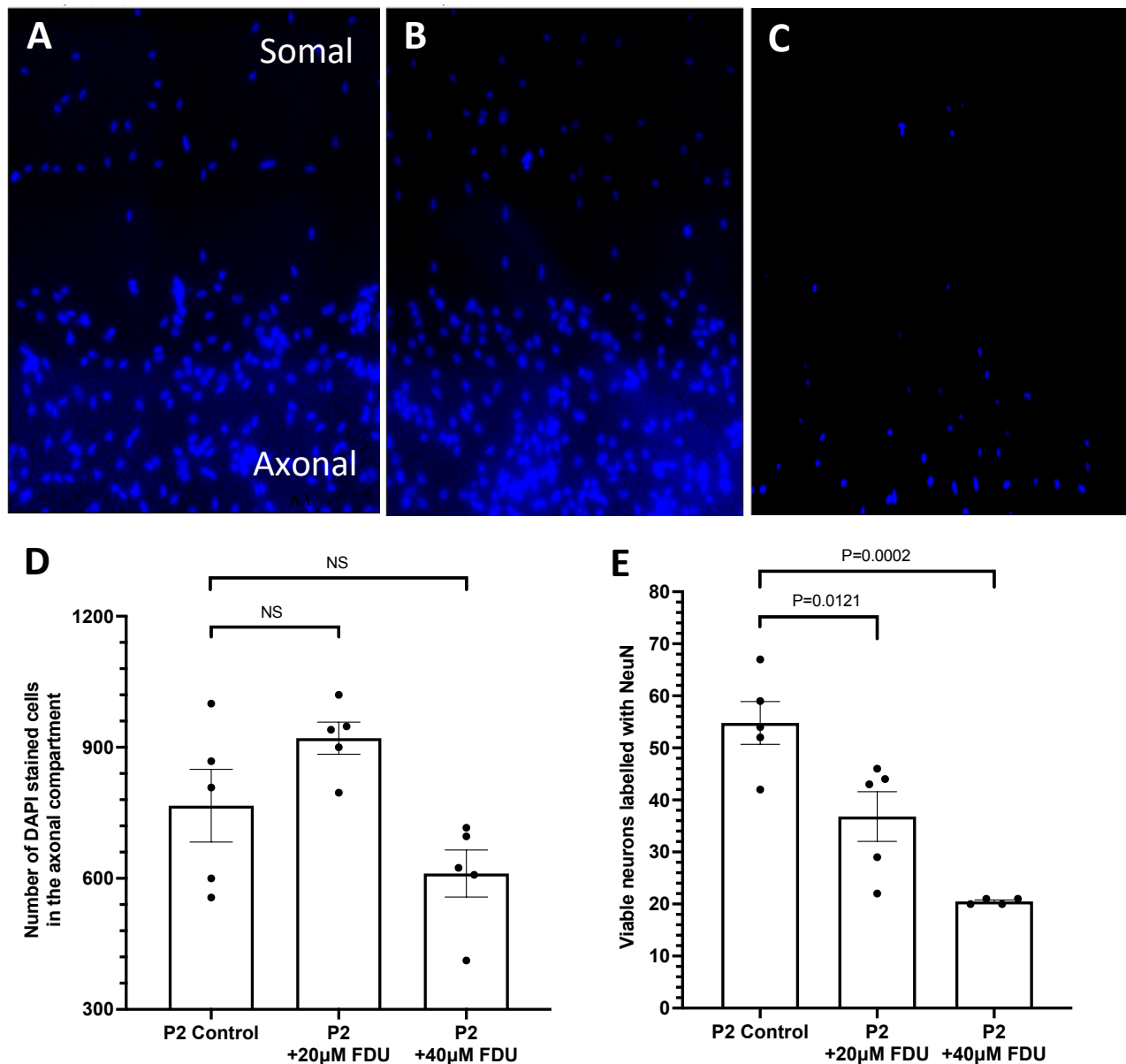


Figure 3.2.2: Attempting to optimise neonatal rat culture in microfluidic devices. Addition of DAPI nuclear stain showed migration of non-neuronal cells through the microgrooves, meaning microfluidic isolation of these cultures was lost. Anti-mitotics were added to attempt to reduce the ratio of non-neuronal cells in culture;

A) Rat P2 cells (Control) in DRG media. B) P2 Rat cells in DRG media supplemented with 20µM FDU only. C) P2 rat cells in DRG media supplemented with 40µM FDU with Aph. D) Counting the number of cells stained with DAPI in the axonal compartment. Results of a one-way ANOVA with multiple comparisons to the P2-control, Degrees of freedom (F)= 6.431 (2, 12), P=0.012. N=5 biological replicate chambers. Bars showing Mean ± SEM, P<0.05 significance threshold. Post-hoc Dunnett's multiple comparisons (df=12) showing P-values of 0.17 (NS) and 0.16 (NS) respectively. E) Counting the number of cells marked with NeuN in the somal compartment. Results of a one-way ANOVA with multiple comparison to the P2-control. F(2, 11)= 18.27 where P=0.0003. Mean ± SEM, P<0.05 significance threshold, N=5 vs N=4 biological replicates with one statistical outlier removed using Grubbs' analysis for P2 +40µM FDU. Post-hoc Dunnett's multiple comparison test (df=11) showing P values 0.0121 and 0.0002 respectively.

3.2.1.2 Culturing embryonic murine DRG cultures in vitro:

As an alternative approach, from here-on we used E16.5 mouse cultures, where the ratio of non-neuronal cells surrounding DRG neurons is intrinsically lower due to the age-related development of nociceptive neurons (Herculano-Houzel, Mota and Lent, 2006; Bandeira, Lent and Herculano-Houzel, 2009). Effectively, embryonic cultures had fewer non-neuronal cells to migrate to the somal compartment, and the chamber showed retained microfluidic isolation and functional compartmentalisation when sealed to the plate. No migration of cells through the microgrooves was observed in these cultures (figure 3.2.3.)

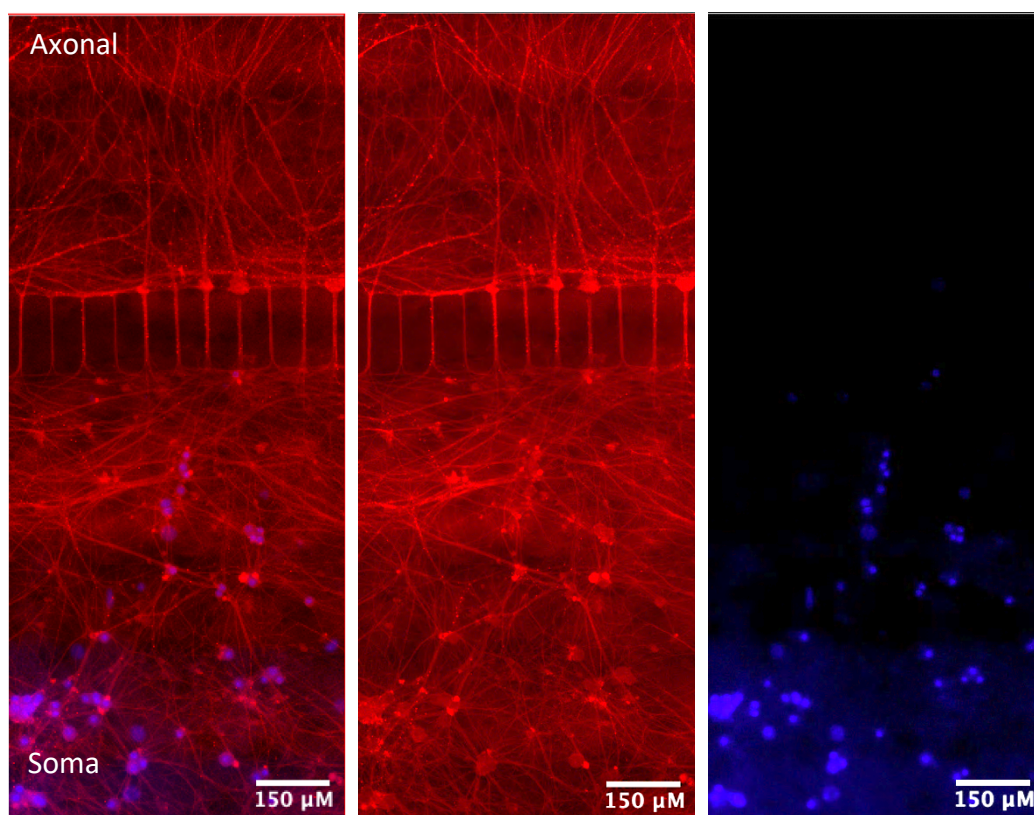


Figure 3.2.3: Dual-staining of DRG neurons cultured from E16.5 murine tissue in a two-channel microfluidic device. No migration of cells through the microgrooves was observed, the DAPI nuclear stain (blue) remained localised to the somal compartment. 20X magnification. Red= Acetylated Tubulin, Blue= DAPI

By maintaining a fluid gradient between the compartments and retaining fluidic isolation (as described in chapter 2.2.4.1,) it was possible to spatially isolate the axon from the cell body (Taylor *et al.*, 2005). The development of a microfluidic model for the culture of DRG neurons often required comparison to standard 'dissociated' plate cultures. The immunofluorescent

staining depicted in figure 3.2.4 shows DAPI (blue) with β III-Tubulin marking the axons of the neurons (green in the microfluidic device, and red in the dissociated plate culture.)

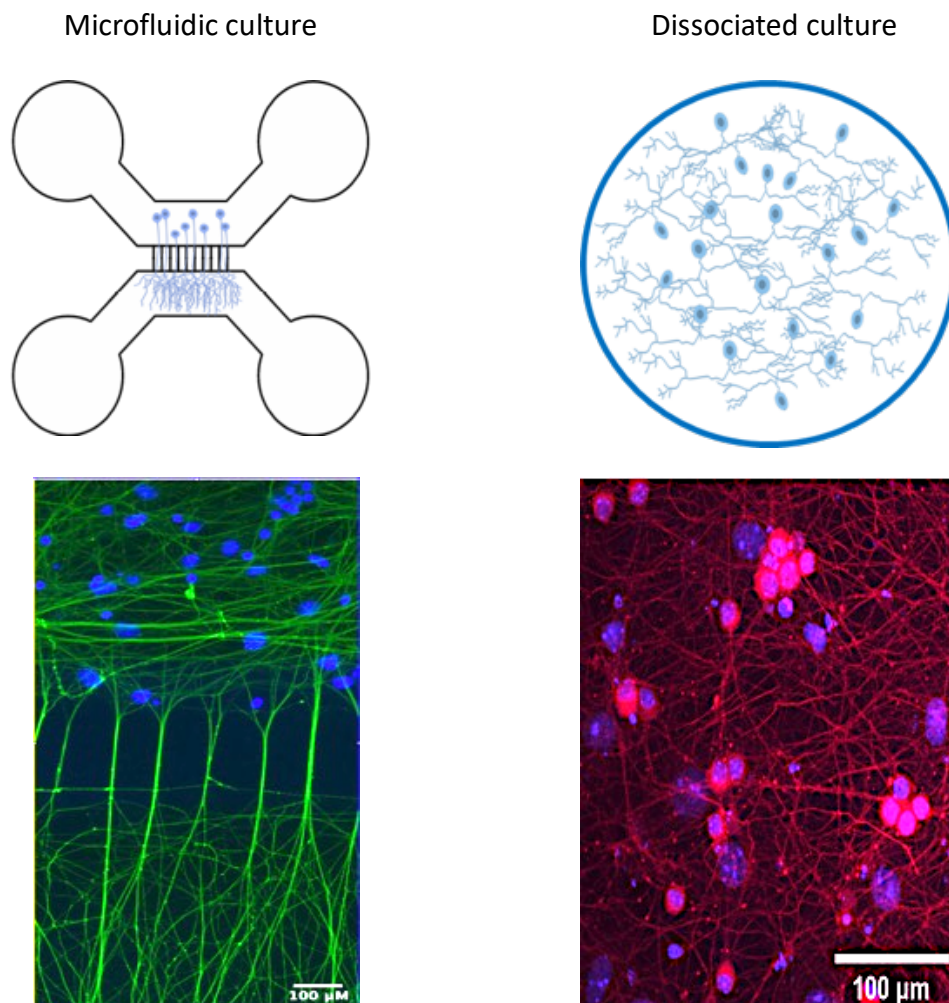


Figure 3.2.4: Immunofluorescent staining of E16.5 mouse DRG neurons at Div5 in culture to compare methods of culture.

Images taken at 20X magnification using Zeiss 200M axiovert microscope. (DAPI nuclear stain= blue, β -tubulin axonal marker=green in microfluidic culture, red in dissociated plate culture)

It is important to note that in the microfluidic devices used for testing, the DAPI (nuclear) stain was only localised to the somal compartment, into which the dissociated cells were seeded. However, not all cells that were stained with DAPI were also labelled with β -Tubulin, which most likely identifies them as non-neuronal cells. The addition of an anti-mitotic (Aphidicolin, see Chapter 2.2.4) to the cultures helped to reduce the population of non-neuronal cells, but crucially did not eliminate them.

In the peripheral nervous system, the Schwann cells are the most abundant form of glial cells, and can be myelinating or non-myelinating- although both phenotypes originate from neural crest tissue. Where satellite cells surround the somata of the DRGs, the myelinating Schwann cells ensheath the larger diameter axons of the DRG fibres in a one-to-one ratio for trophic support (R. R. Ji, Chamessian and Zhang, 2016; Chen *et al.*, 2018). Therefore, for viability of the neurons *in vitro* it was important that they were surrounded by non-neuronal cells such as these perineuronal Schwann cells.

3.2.1.3 Discussion and conclusions from the development of *in vitro* culture of DRG neurons:

Initial extraction of DRG neurons from postnatal rat tissue was not deemed successful, but healthy cultures of neurons were isolated from E16.5 murine tissue and retained microfluidic isolation.

The switch from P2 to E16.5 tissue was necessary to reduce the migration of non-neuronal cells through the microgrooves of the microfluidic devices. However, these myelinating non-neuronal cells are essential for viability of the culture, and were not completely removed. Whilst non-neuronal cells provide essential trophic support to neurons, there is compelling evidence to support a role in modulating excitability in pathologies such as neuropathic pain. *In vivo*, the production of cytokines from non-neuronal cells has been linked to nerve damage and the infiltration of inflammatory cells such as macrophages. For example, the infiltration of pro-inflammatory macrophages was observed after only 2 hours following CCI in a model of peripheral nerve injury, and was shown to exacerbate muscle atrophy in the model of pain described (Shimada *et al.*, 2020).

In vivo models of nociception generally focus on the responses of A δ and C fibres (see chapter 1.6 regarding the structure of the DRG fibres) the morphological diversity of neurons in the DRG does not fully arise until postnatal development (de Moraes, Kushmerick and Naves, 2017). In adults, the neurons of the DRGs have distinct action potentials based on the amplitude of response and duration of cell signalling. This reflects the development of mature DRG neurons in adult cells, and the downstream effect of this on protein expression and subsequent threshold activation of nociceptors (Lawson, 2002; Koerber, Druzinsky and

Mendell, 2017). When developing an embryonic model *in vitro* it was important to acknowledge that the results may not directly replicate the results observed from adult tissue, since there are many differences between the transcriptomes of adult and embryonic tissue (Gumy *et al.*, 2011).

It has been demonstrated that the subtypes of fibres involved in nociceptive signalling develop in waves (E12.5, E15.5) during embryonic development, and often only acquire full functionality post-natally. Evidence has shown that by E15.5 *in vivo*, only 80% of the neurons in the DRG have acquired sensory diversity (Lechner *et al.*, 2009). However, the remaining 20% do not reach maturity until P0-P1 post-natally (where often this response requires mechanosensitive priming, for example by NGF.) A good example of this phased development includes the TRP (transient receptor potential) receptors involved in a range of nociceptive signalling. Although the TRPV1 channel (heat sensitive,) is present by E15.5 *in vivo*, the TRPM8 receptor (cold-sensitive) does not appear until postnatal development (Hjerling-Leffler *et al.*, 2007). Despite this meaning that the suitability for these embryonic *in vitro* cultures in a pain-based study must be approached with caution, the layered development of the nociceptive pathways also gives rise to the ability to stimulate selective neuronal subtypes.

The following sections describe the development and optimisation of culture methods for non-neuronal subtypes which are involved in bi-directional signalling with the DRG neurons. Cell signalling between the primary afferents and inflammatory cells at the peripheral terminals induce changes in DRG signalling, and as a consequence inflammatory cells such as microglia in the CNS respond accordingly to modulate a pain-based response.

3.3 Culture of inflammatory macrophage cells:

The inherent sensitivity of bone marrow derived cells to inflammatory cytokines and chemokines make them highly useful as tools for *in vitro* modelling of inflammation and macrophage biology, although there are still clear limitations to this (Bailey *et al.*, 2020). Cell heterogeneity is a common limitation of *in vitro* culture of macrophage tissue (Murray *et al.*, 2014a), where inflammatory mediators and culture conditions affect the endogenous morphology and motility of the cells. Not only are macrophages highly motile, of particular interest is the ability of these cells to adapt to their surrounding environment, and become transiently ‘polarized.’ The role of macrophages as inflammatory mediators has been discussed in Chapter 1.8.2.

One full set of adult female long bones were flushed per prep to culture bone marrow derived macrophages as inflammatory mediators of the peripheral immune system. By 7 days *in vitro*, cells formed a mature population of monocytes. Cells were re-plated and polarized in accordance with protocols described for classical versus alternative “activation,” (Classen, Lloberas and Celada, 2009; Rath *et al.*, 2014a). Chapter 2.2.3 describes in detail the protocol used for isolation and *in vitro* culture of BMDMs. A healthy culture of macrophages showed adherence and elongation of cell processes at DiV7 as shown in figure 3.3.1.

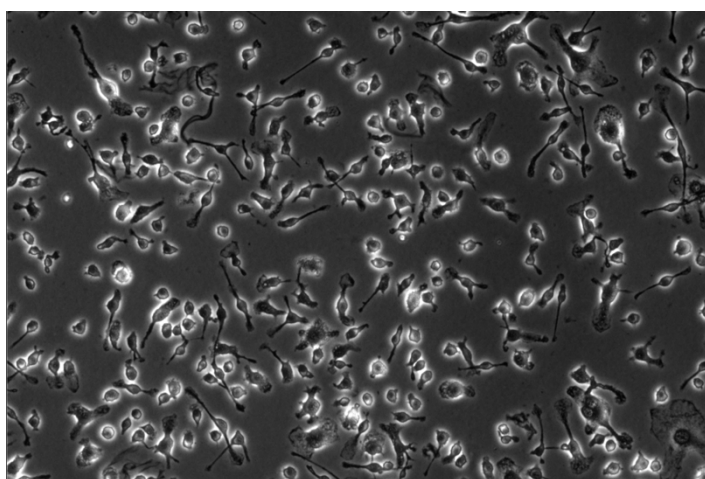


Figure 3.3.1: Bright-field imaging at 20X of a healthy culture of monocytes isolated from bone marrow of adult mouse femur tissue. Imaged at DiV7. Cells have attached to the plastic and showed an elongated phenotype

3.3.1 Culture of Macrophages in microfluidics:

One of the main objectives of this model was to attempt co-culture of 2 types of primary cell types in a 2-channel microfluidic device, in order to accurately reproduce the bi-directional signalling between peripheral inflammatory cells and the axonal terminals of the sensory primary afferents.

Having previously demonstrated the ability to culture E16.5 neurons in the 2-channel microfluidic device (see section 3.2.1.3) the direct co-culture with bone marrow derived macrophages in one compartment of the microfluidic device was attempted.

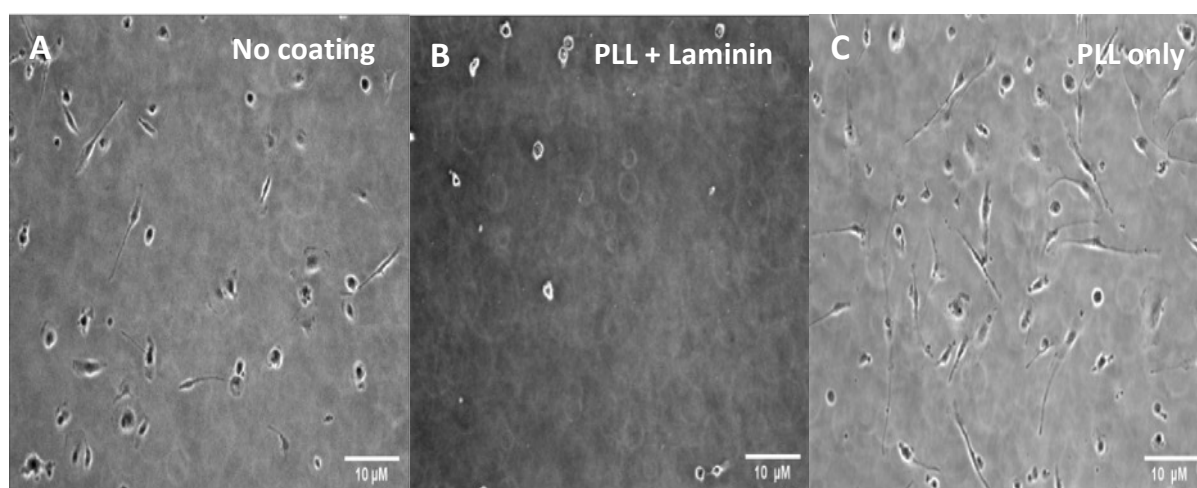


Figure 3.3.2: Multiple methods of coating for culturing bone derived monocytes in the lateral compartment of microfluidic devices were investigated to ensure cell adhesion without migration through the microgrooves:

A) No coating; whilst few cells adhered and elongated, most cells died and developed a rounded morphology once they detached from the chamber. B) PLL+ Laminin; few cells made it past the well, those that did, did not adhere and died within the channel. C) PLL only; A greater yield of cells passed from the reservoir into the channel and adhered within 24H hours. There was also evidence of cellular elongation that would be typically observed in a mature population of BMDMs.

Upon lifting the monocyte layer from bacterial grade plastic at DiV7, cells were re-plated into two-channel microfluidic devices. A range of coating was used to demonstrate what, if any preparation would be required to seed macrophage cells into microfluidic upon downstream co-culture with DRG neurons. The results demonstrated that unsurprisingly cells did not adhere to laminin, a class of protein extracted from the basement membrane of viable cells that forms an extracellular scaffold for cellular support, adhesion and migration of cells (Yurchenco, 2011).

Whilst some cells adhered to cell-culture grade plastic (without coating, figure 3.3.2A) there was still some evidence of low cell viability, or cells self-polarizing towards the M1_{like} phenotype, with a “fried egg” like morphology (see Chapter 1.8.2.)

To achieve co-culture of macrophages with DRG neurons, macrophages must adhere to PLL (20 µg/ml) and Laminin (20 µg/ml), as this coating was required to support DRG culture in microfluidics (see Chapter 2.2.1), and therefore this combination was also tested. When macrophage-like cells did not adhere to the coating, they died within the chamber, exhibiting a rounded morphology (figure 3.3.2B.)

It was evident that most cells adhered to PLL only. Cells that survived seeding into the microfluidics quickly elongated (figure 3.3.2C.) All cultures were seeded at 1×10^6 cells/ml. However, the representative images in figure 3.3.2 show that not all the cells made it past the reservoir in the chambers.

For this reason, the model was altered to fulfil the original requirements for “co-culture” of primary cells in one microfluidic device. It was decided to instead utilise the unique nature of the microfluidic devices, and expose only the axonal compartment to media extracted from polarized macrophages. Following polarization, the media collected from polarized macrophages should contain high and changing levels of inflammatory cytokines.

3.3.2 Polarization of macrophages in vitro:

In vivo there are two types of macrophages, resident cells and infiltrating cells (Griffin, George and Ho, 1993).. For example, it has been well characterised that following nerve injury, high levels of chemo-attractive peptide C-C motif ligand 2 (CCL2 formerly called MCP-1) induce migration of monocytes to the inflamed area (Zigmond and Echevarria, 2019).

Macrophages have been shown to continuously adapt to cues in the surrounding microenvironment, and can even express both M1 and M2 markers in response to surrounding pathological conditions (Bazzan *et al.*, 2017; Lee *et al.*, 2018). It has also been demonstrated that *in vitro* macrophages demonstrate cellular plasticity and switch phenotype in response to surrounding stimulus, making BMDMs a suitable candidate for this project (Khallou-Laschet *et al.*, 2010). Following axotomy, it has been shown that

accumulation of polarized macrophages can be detected as early as 4-days after injury, and continues to be detectable up to 32-days post-injury. These infiltrating polarised cells have been shown to form rings around larger diameter neurons, with macrophages contributing to the innate inflammatory response (Vega-Avelaira, Géranton and Fitzgerald, 2009).

There are varying models of macrophage biology *in vitro*, where peritoneal cells mature *in vivo* prior to culture (see Chapter 1.8.2.) Furthermore, it has been suggested that the *ex vivo* nature of differentiating the BMDMs may induce functional differences to those acquired by cells *in vivo*. Of particular interest to this study was the capacity of BMDMs to polarize towards different phenotypes. It has been demonstrated that exposure to polarizing stimuli induces BMDMs to upregulate chemokine and cytokine expression, as well as releasing more cytokines, therefore making them a useful tool for this model (Zajd *et al.*, 2020).

Cells were polarized using appropriate stimuli for classical (Celada *et al.*, 1984) and alternative (Stein *et al.*, 1992) activation of cells (Zhang, Goncalves and Mosser, 2008) as discussed in Chapters 1.8.2. Based on the literature (Mosser and Zhang, 2008) it was hypothesised that a minimum period of 24-hours was required to induce a change in the phenotype of inflammatory cells. To promote development of a classically activated cell (M1a,) macrophages were exposed to LPS and IFN γ or to IL-4 to promote development of a population of alternatively activated (M2a) cells (see Chapter 2.2.2.4.) Following stimulation and incubation for 24-hours, most cells had polarized either towards an M1a or M2a phenotype (Huang *et al.*, 2018). Since macrophages are inflammatory cells, they respond dynamically to the cues in the surrounding microenvironment, which in many ways makes a perfect candidate for use in a microfluidic culture system of hyperalgesic priming.

However, since inflammatory cells continually respond to these changes, it would be inappropriate to refer to these cells as solely “pro” or “anti” inflammatory, while a better reflection of the cellular process should consider that polarization always generates a mixed population of cells depending on how much a cell was exposed to a cytokine in culture. Therefore, from now on, inflammatory cell populations are referred to as M1-like or M2-like, dependent on the stimulus used to trigger the eventual shift in the population.

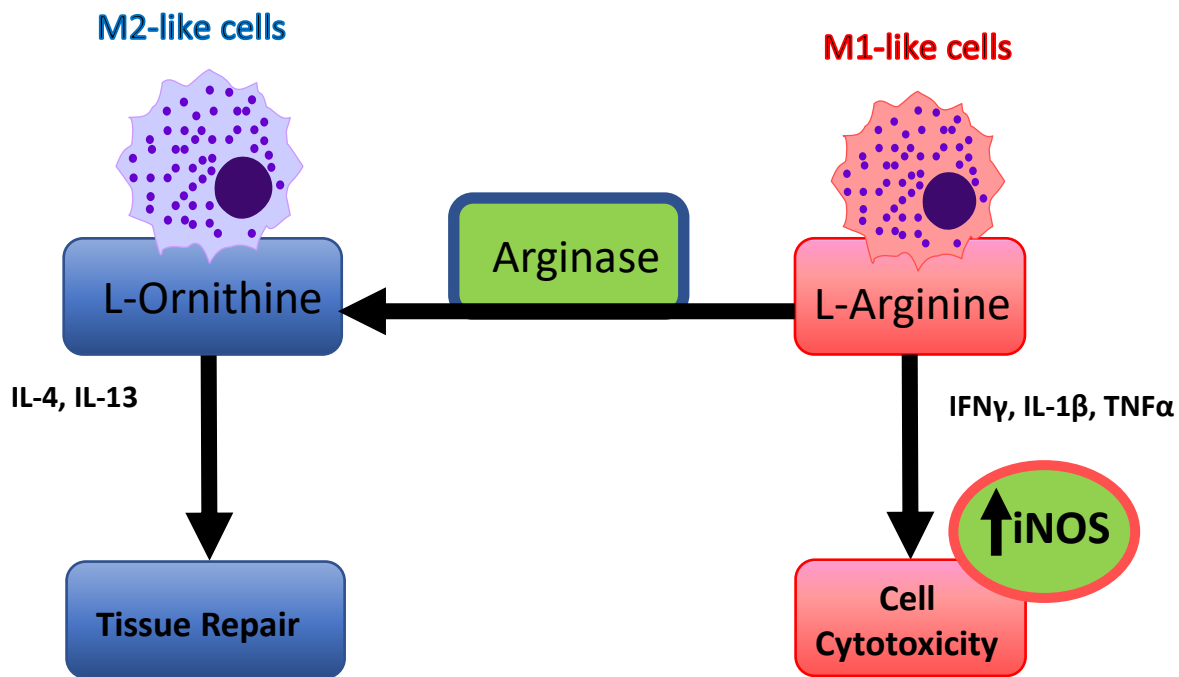


Figure 3.3.3: Overview for the role of the metabolism of L-arginine in characterising the phenotype of macrophages. In vivo, this switch between arginine and ornithine metabolism can be used to characterise the phenotype of inflammatory cells (See Mosser and Zhang., 2008)

The route of macrophage polarization can at least partly be classified by the route of arginine metabolism induced by an inflammatory stimulus (Thomas and Mattila, 2014). The diagram in Figure 3.3.3, based on that by Yang and Ming, (2014) demonstrates how specific proteins surrounding the conversion from L-Arginine to L-Ornithine can be used as cell markers of polarization. Using immunofluorescence for markers of inflammation, there was a quantifiable shift between arginase-1 (Arg-1) and inducible nitric oxide synthase (iNOS) as shown in figure 3.3.4A.

Arginase-1 was higher in cells exposed to IL-4 for 24H, where these cells were stimulated to polarize more towards an M2_like, anti-inflammatory phenotype. Whereas, those cells exposed to IFN γ and LPS for 24 hours, polarized towards an M1_like (pro-inflammatory) cell type, shown by the higher levels of the classical M1 marker iNOS. It was unsurprising that the results of polarizing cells did not show a complete shift towards only one phenotype. Figure 3.3.4B demonstrates how it was possible to quantify the shift towards an inflammatory phenotype, based on the changes in expression of cellular markers iNOS and Arg1. Exposure

with pro-inflammatory mediators demonstrated a $62.4 \pm 3.3\%$ expression of iNOS in M1_like macrophages (N=3, Mean \pm SD), relative to a $20.4 \pm 7.2\%$ expression of iNOS in an M2_like population (N=3, Mean \pm SD).

An important step in understanding the process mediating the potential changes in neuronal excitability after macrophage polarisation is the investigation of the cytokine composition present in the media. This was important to determine since the polarized inflammatory cells would be required for the model of hyperalgesic priming, to induce changes in neuronal excitability. To determine the presence of multiple populations of cells, the chosen subtype of conditioned media was tested using a semi-quantitative cytokine array, to ascertain the concentration of 40 selected inflammatory targets (as described in Chapter 2.2.2.5). The results of this array are shown and discussed in further detail in appendix 1, figure 7.2.1.

As shown in figure 7.2.1 the array was used to primarily to determine if there were obvious differences in the cytokine profiles of the M1-like media and M2-like media. The array provided some interesting insight in the composition of the media, but the semi-quantitative nature of the assay meant that it did not have the capacity to provide absolute quantification of the concentration of selected cytokines present. In order to confirm the results of the assay, future work would include the use of media extracted fresh from cells, as well as lysis of the polarized cells in the plate to also calculate the total concentration of protein within each population of cells.

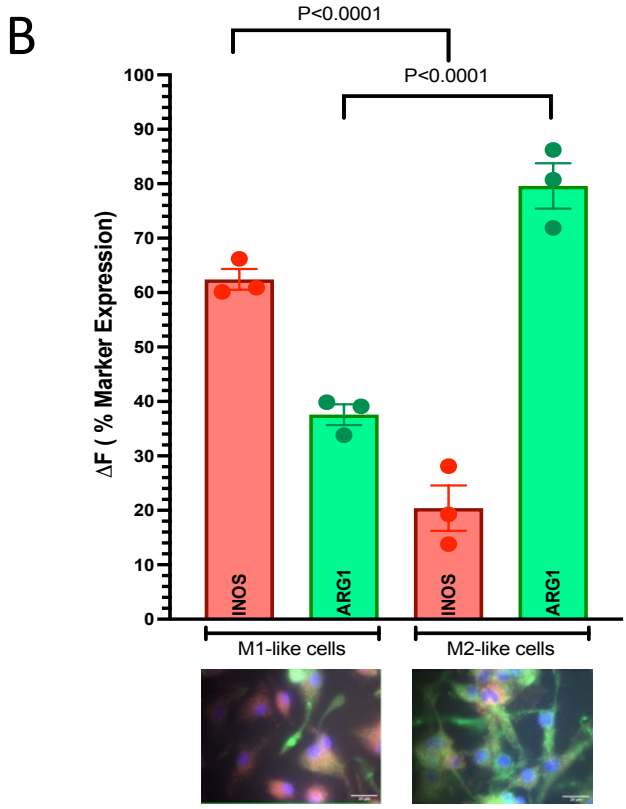
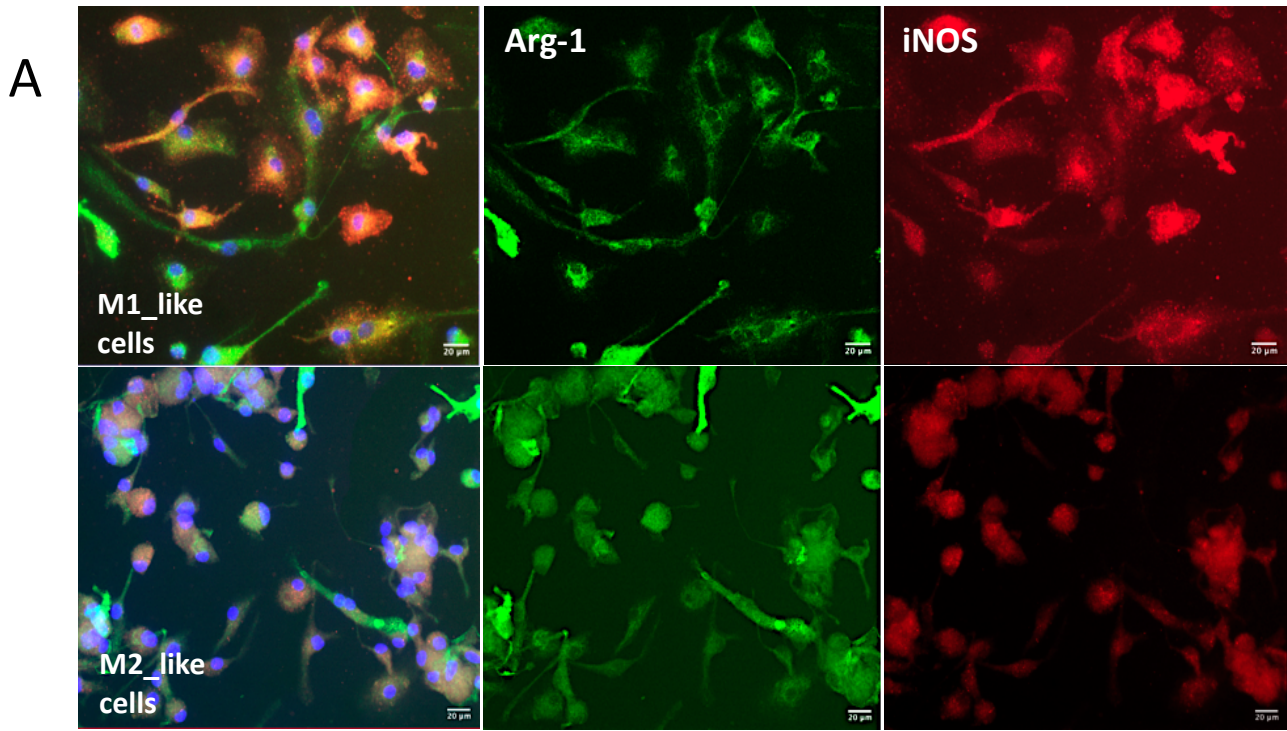


Figure 3.3.4: Exposure to inflammatory stimuli for 24H induced a quantifiable change in macrophage phenotype:

A) Triple channel immunofluorescence to directly compare the expression of markers of activation. (FITC= iNOS, TRITC= ARG-1, +DAPI nuclear marker. Both channels were exposed at 100mS for direct comparison. Background fluorescence has been removed during statistical analysis.

Legend continued overleaf...

- B) Quantifying marker expression in a region of interest using densitometry of the split channel immunofluorescence images. Data represents N=3 stainings from different dates, with 5 replicate images taken from each coverslip. All images were taken at 20X magnification using the Zeiss 200M. Results of a one-way ANOVA with statistical threshold at $P < 0.05$. $F(3, 8) = 65.18$ where $P < 0.0001$. Post-hoc Sidak's test for multiple pairwise comparisons showed $P < 0.0001$ and $P < 0.0001$ as shown.

3.3.3 Discussion and conclusions from the culture and polarization of macrophages *in vitro*:

Bone marrow was isolated from adult murine tissue and cultured on bacterial grade plastic to produce healthy populations of BMDMs. When optimising the culture of macrophages in microfluidic devices it was shown that coating was particularly important in the development of a healthy culture.

In vitro it has previously been demonstrated that macrophages will not adhere solely to laminin (20 μ g/ml) without the addition of phorbol myristate acetate (PMA, 50ng/ml) which resulted in rapid adhesion (Mercurio and Shaw, 1988). Although the basement membrane is formed from multiple protein subtypes such as laminins, fibronectins and collagens, the composition varies dependent on the tissue (Guldager Kring Rasmussen and Karsdal, 2016). Critically, it has been demonstrated that adherence of immune cells (such as monocytes and macrophages) to the basement membrane can induce specific immune functions of these cells. For example, the expression of laminins-111, 411 and 511 *in vivo*, induce the adherence on monocytes, followed by production of pro-inflammatory cytokines such as TNF α , IL-6 and IL1 β , and increased phagocytic cellular activity (Simon and Bromberg, 2017). For this reason, although cells did not adhere to culture plates in the presence of laminin alone, the use of this protein to coat the lateral compartment of the chamber was not appropriate, as it would potentially induce pro-inflammatory phagocytosis.

The unique requirements for optimal culture of macrophages did not meet the culture conditions previously optimised for the culture of E16.5 murine DRGs in two-channel microfluidic devices. It was hypothesised that the cytokines in the media collected from polarized macrophages could induce sensitisation of axonal terminals without the need for

direct cell co-culture. In addition, only changing media in the device would help to maintain optimal conditions for neuronal growth and give flexibility to the model.

By quantifying the expression of Arg1 or iNOS as markers for polarized cells, it was shown to be possible to induce populations of macrophages similar to either an M1-like or an M2-like phenotype *in vitro*. Upon extracting media from polarized cells, it was also determined that each cell population had a unique cytokine profile. Although the use of iNOS and Arginase-1 as markers for polarized cells is highly documented, it may have been more conclusive to use 4 cell markers. This would have helped reduced the cross talk between cell types, since both proteins are expressed in both cellular phenotypes. Other useful markers may include mannose receptor (CD206, normally downregulated by exposure to IFN γ) or changes in the IL-12 axis. Of course, there is little evidence reported in embryonic tissue, and therefore this novel model cannot necessarily be directly compared to neonatal or adult studies.

It is important to note that the media tested here was extracted from polarized cells relatively early in relation to the development of an anti-inflammatory phenotype. M2 macrophages are often hallmarked by the presence of IL-10 and other key anti-inflammatory cytokines. However, it is also true that M2-like cells may secrete cytokines associated with M1-cell activation (Roszer, 2015). Of particular interest from this array (figure 7.1.2) was the presence of high levels of IL-12, CCL5 and CCL2. Although the inactive form (p40 subunit) of IL-12 was detected at a high concentration in the M2-cell population, it was noticeable that the IL-12 p70 (active subunit) was only detected from M1-like cells. This data supported the evidence for IL12 as a pro-inflammatory cytokine, but also demonstrated the plasticity of macrophages, whereby the stimulation with IL-4 induced release of IL-12 from an M2-cell culture. However, it is essential to acknowledge that the signatures of macrophages observed *in vivo* and those cultured *in vitro* will not be identical since they are dynamic inflammatory cells, highly respondent to the surrounding environment.

The classical versus alternative activation axis was first established as a binary dichotomy by (Mills *et al.*, 2000), but this simplified explanation of the M1/M2 paradigm has since become outdated. It has been established that M1/M2 polarization is largely dependent on the stimuli used, where polarized cells form a spectrum, and the M1 and M2 phenotype sit at either end

(Mantovani *et al.*, 2004). Physiologically, a “cocktail” of inflammatory mediators regulates macrophage polarization, although here a fixed concentration of only one cytokine was used to induce a specific phenotype. Therefore, it was difficult to anticipate how downstream inflammatory targets would respond. Although the upregulation of Arginase-1 was more prominent in the M2-like macrophage populations, it has been demonstrated that M1-like macrophages stimulated by TLRs also express this marker (El Kasmi *et al.*, 2008). The endogenous phenotype of macrophages is most likely regulated by multiple cell signalling pathways, for example the SOCS (suppressor of cytokine signalling) proteins (Briken and Mosser, 2011; Davis *et al.*, 2013). It has been observed, specifically in M2-like macrophages, that SOCS1 (but not SOCS3) can lead to rapid downstream induction of the M2-like phenotype after treatment of IL-4 *in vitro* (Dickensheets *et al.*, 2007). Therefore, although Arginase-1 is a well characterised marker for M2-like macrophages, caution should be exercised when considering the change in phenotype of the cells, since there are likely other cellular processes involved in the regulation of these markers.

Although cells were stimulated with cytokines aimed to evoke M1a and M2a cells, our results support the now overwhelming evidence suggesting that this “switch” between pro and anti-inflammatory cells is not as binary as once thought. In fact, in *in vitro* studies it is possible to distinguish between phenotypes based on the stimulus used to induce the molecular change. In this case the cells would therefore be referred to as M[LPS+IFN γ] or M[IL-4]. This is because multiple stimuli can be used to polarize cells towards an M2-like phenotype, but not all M2-like cells show the same molecular profile (Murray *et al.*, 2014b). The regulation of macrophage phenotype is a dynamic process, where concentrations of surrounding cytokines can rapidly induce changes to the cellular activity and morphology. Whilst M1-like cells release cytokines to inhibit proliferation of surrounding cells, the M2-like phenotype is more involved in the resolution phase of inflammation. For this reason, M2-like cells release cytokines more involved in tissue regeneration and repair. Polarizing these cells *in vivo* is tightly regulated by surrounding signalling pathways and post-transcriptional regulation. However, it is not as simple as to suggest that the molecular switch between phenotypes is an “all or nothing” response. Crucially there is also evidence to support the hypothesis that some cytokines may mediate the regulation of both pro-inflammatory and anti-inflammatory

phenotypes (Martinez and Gordon, 2014). The role of a select cytokine appears to be dependent on 3 distinct parameters (Shachar and Karin, 2013):

1. Local concentration of the cytokine surrounding an area of inflammation
2. The stage of injury in disease pathology
3. The combination with other cytokines

Bone marrow derived macrophages have a unique cytokine profile compared to other inflammatory cells such as peritoneal macrophages. If this study were continued or optimised further, the use of additional antibodies such as CD68 or CD11b would have been useful to create a panel of markers for cell specific antigen detection to distinguish macrophages from other hematopoietic cells. It would theoretically have also been possible to use techniques such as flow cytometry to identify the inflammatory 'profile' of the different phenotypes of bone marrow derived macrophages grown in our cultures.

3.4 In vitro culture of spinal cord microglia as a model for inflammatory cells in the CNS:

In addition to modelling the inflammatory cells that can affect the peripheral nervous system, a protocol was developed to culture spinal cord derived microglial cells. *In vivo* the microglia modulate the inflammation in the CNS to further promote inflammation and hyperexcitability of neurons, or to resolve injury and hyperalgesia (see Chapter 1.8.3.) In a similar way to peripheral macrophages, CNS microglia respond dynamically to cytokines in the microenvironment, which is critical in resolution of sensitisation. It was hypothesised that the media extracted from polarized microglia would either potentiate the hyperexcitability induced by pro-inflammatory macrophages, or reduce nociceptor sensitisation. Other potential cellular candidates included second-order dorsal horn neurons isolated from the spinal cord, to which the DRG neurons might synapse *in vivo*.

To determine the purity of the microglial culture we used a dual-staining IF model with Iba-1 (microglial cell marker) and GFAP (astrocytic cell marker), as shown in figure 3.4.1 below. Since the cells were isolated from embryonic spinal cord, the GFAP signal represents

progenitor cells for CNS astrocytes. A higher level of expression of Iba-1 versus GFAP in culture (see Chapter 1.8) suggested that the culture method of the cells favoured the development of microglial like cells. Shown here is the quantification of Iba-1 relative to GFAP in a culture of quiescent microglial cells extracted from the spinal cord. In a mixed population of cells Iba-1 was detected at $80.58 \pm 8.1\%$ (mean \pm standard deviation) relative to $19.42 \pm 8.1\%$ GFAP. These results suggested the presence of a microglial-rich population of non-neuronal cells isolated from the spinal cord of embryonic mice.

A

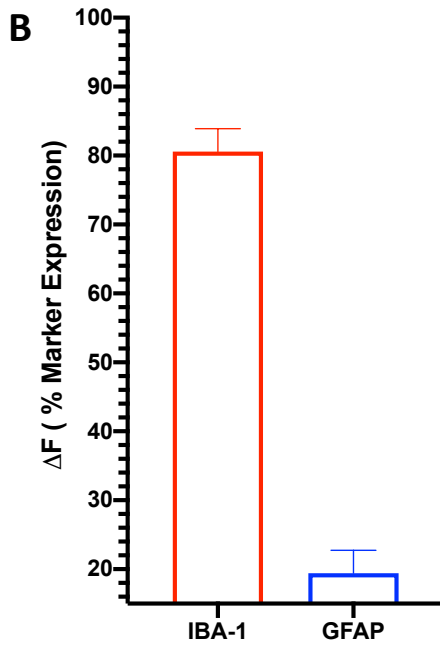
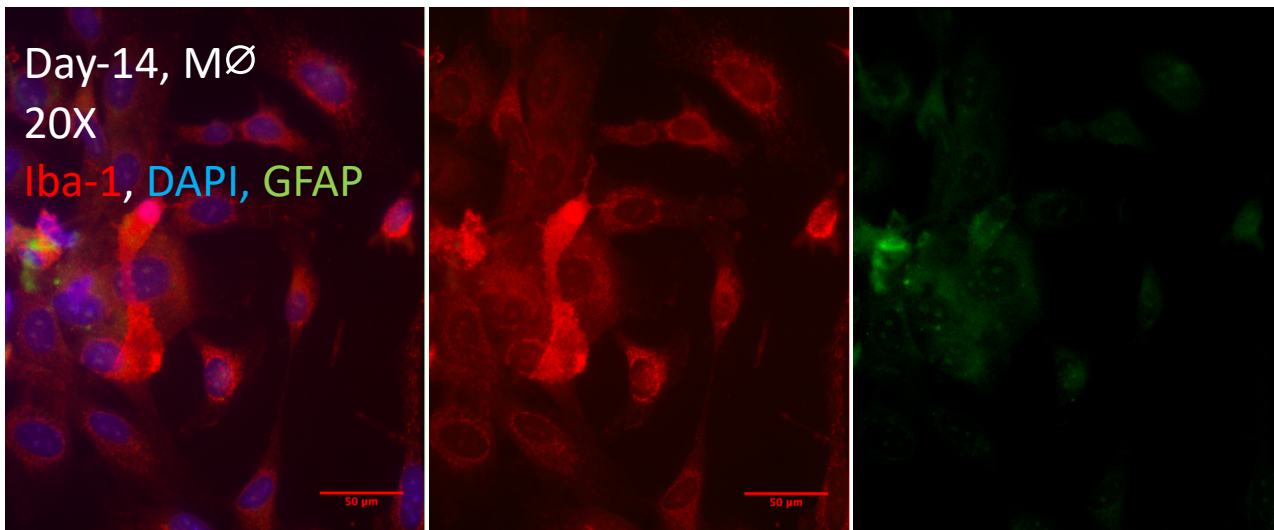


Figure 3.4.1: Determination of the purity of a microglial culture isolated from embryonic spinal cord tissue.

A) An exemplar image of M0 microglial cells at 20X magnification, showing dual-staining with iba1 (microglial marker) versus GFAP (astrocytic cell marker.) Shown on the left is the triple-channel image including DAPI nuclear stain, iba-1 (TRITC) and GFAP (FITC). The FITC and TRITC channels have been separated to show a lower expression of the GFAP marker respectively.

B) Quantification of the purity of a mixed glial cell population, using %-expression IBA-1 vs. GFAP in M0 population of cells. Data represents an N=3 coverslips from 3 separate cell preparations, with n=5 ROI analysed per coverslip. (Error bars \pm standard error of the mean.)

3.4.1 Polarizing microglial cells in vitro

It has been demonstrated that microglial cells polarize to favour different phenotypes in a very similar way to peripheral macrophages (Michelucci *et al.*, 2009). Although the transcriptional profiles of monocytes and microglial cells are similar, they are not identical (as discussed in Chapter 1.8.3.) One of the defining factors of microglial cells is the innate cellular response to inflammation. Unlike macrophages which are stimulated to polarize, the microglial cells become activated and differentiate from a resting quiescent state to either a ramified or an ameboid morphology, dependent on the surrounding microenvironment. The morphological change in the cell also coincides with upregulation of surface markers such as CD206 or CD86 (Heneka, Kummer and Latz, 2014). The classifications of polarized microglia are often compared to the classically activated M1-like macrophages and alternatively activated M2-like macrophages (Goldmann and Prinz, 2013; Zanier *et al.*, 2015; Amici, Dong and Guerau-de-Arellano, 2017). However, given that these cells are quiescently ramified rather than resting, and *in vivo* studies have failed to demonstrate the presence of morphological regulators in isolation, there is some debate about the application of the M1/M2 dichotomy to microglial cells in general (Ransohoff, 2016).

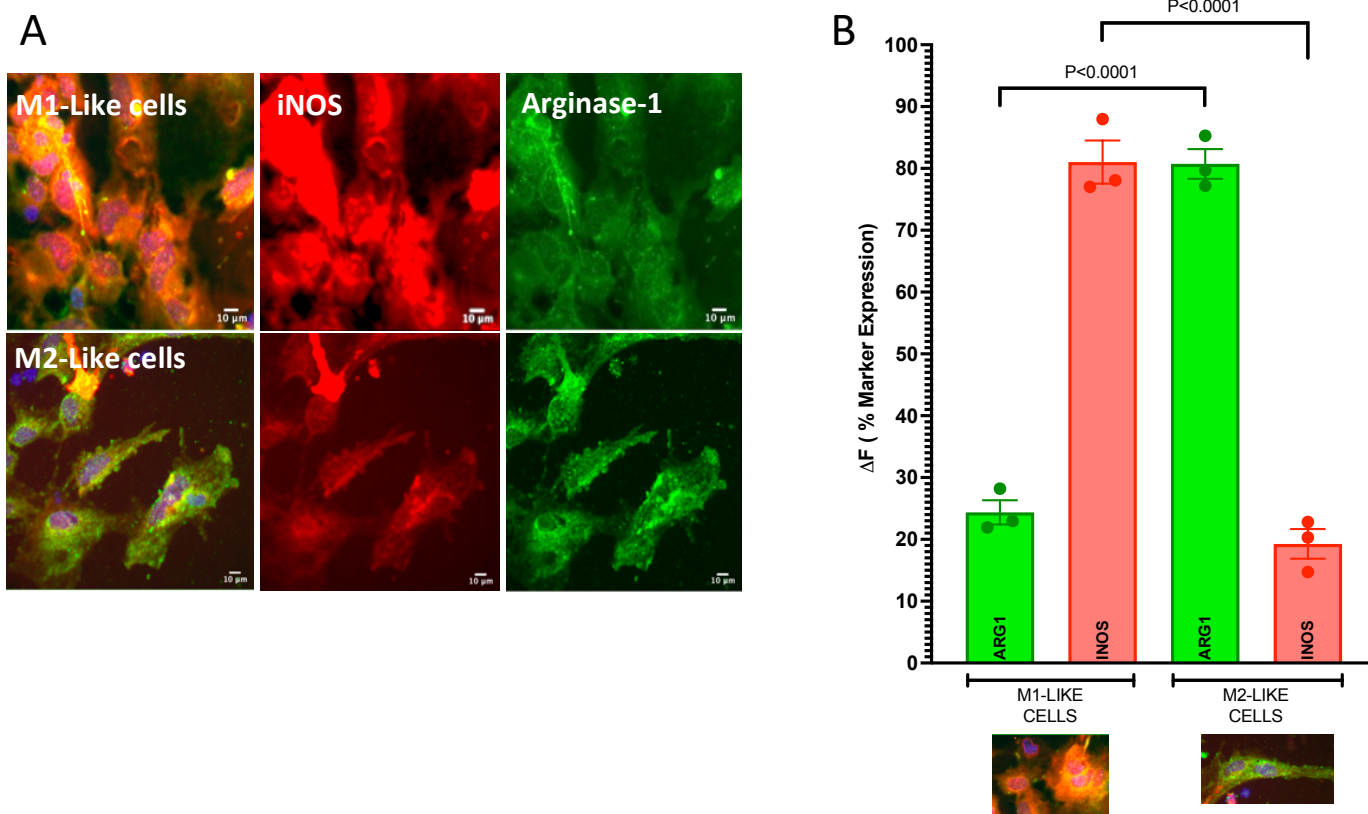


Figure 3.4.2: Exposure to inflammatory mediators induced significant changes in the phenotype of spinal cord derived microglial cells.

A) Triple-channel immunofluorescence using DAPI, iNOS (FITC) and Arg1 (TRITC) as markers for inflammation. All channels were exposed for 100ms to enable direct comparison. M1-like microglia demonstrated a more amoeboid phenotype compared to a ramified phenotype in the M2-like populations of cells.

B) Converting detection of a marker to a % expression to quantify the effect of polarizing stimuli on the phenotype of cells. Results of a one-way ANOVA with selected pairs of comparisons. $P < 0.05$ Significance threshold, $F(3, 8) = 170.4$. Post-hoc Sidaks test showed $P < 0.0001$ and $P < 0.0001$ respectively as shown. $df = 8$

$N = 3$ coverslips from 3 separate animal preparations. Error bars represent the SEM. Background fluorescence has been removed during statistical analysis.

Assuming that microglial cells can be induced to demonstrate changed morphologies based on exposure to inflammatory stimuli, we attempted to quantify the presence of “M1-like” (activated, amoeboid) and “M2-like” (activated, ramified) microglial cells following stimulation.

Once again it was noticeable that cells did not fully shift towards a specific phenotype, supporting the evidence for a spectrum of inflammatory cells. In fact, it was observed that there was a $81.3 \pm 6.0\%$ expression of iNOS in the M1-like population versus an $80.7 \pm 4.1\%$ shift

towards Arg-1 in the M2-like cells (and $19.27 \pm 2.4\%$ iNOS expression relatively.) Figures 3.4.2B represents an N=3 independent stainings (biological replicates,) with a minimum of 3 representative areas (technical replicates) imaged per coverslip (mean \pm standard error of the mean%).) The threshold for each immunofluorescent image was set the same before the image was taken, so that the stainings were directly comparable.

It was noticeable that unlike the M2-like macrophages, the M2-like microglia did not demonstrate a large shift towards the M2 phenotype given 24-hours exposure to IL-4 only. However, a quantifiable shift in morphology suggested that the cells had undergone translational regulation and were secreting different profiles of inflammatory cytokines (see appendix, figure 7.1.3 and table 7.1.4.1.) Therefore, exposure of the DRG terminals to the media extracted from these cells would theoretically either potentiate a state of hyperalgesia, or reduce excitability of the cell.

3.4.2 Discussion and conclusions from the development of in vitro culture method of spinal cord derived microglial cells:

Immunofluorescent staining successfully validated the extraction of embryonic spinal cord for the selective culture of microglia, although it did not help to determine the functional differences of the cell phenotypes. As resident immune cells of the CNS, *in vivo* microglial cells act as first-line defense cells against invading pathogens (Zhou *et al.*, 2017). However, there may be a difference in the phenotype of microglia derived from the spinal cord versus the brain. It is understood that microglia localised to the brain are more involved in regulating cognitive function, whereas microglia found in the spinal cord are more relevant in the control of sensory-motor neuron mediated functions (Xuan *et al.*, 2019) Usually *in vitro models* use immortalised cell lines such as cortical BV2 murine cells, where these cells are easily maintained in culture, and readily proliferate, reducing the need of fresh tissue (Timmerman, Burm and Bajramovic, 2018).

It has also been suggested that *in vitro* culture of microglia leads to the development of a different phenotype than *in vivo*. Of particular interest was the length of time cells were kept in culture. Cells kept for over 14-days *in vitro* appeared to lose their ameboid shape and prefer

a more ramified, quiescent morphology. However, *in vivo* this shift towards M0-M2-like cells does not occur until the cells become “aged.”

The physiology of microglial cells dynamically changes in response to secretions of pro- and anti-inflammatory cytokines into the surrounding microenvironment (Helmut *et al.*, 2011). Having ascertained it was possible to change the phenotype of the cells in response to a select stimulus, it was also important to investigate the capacity of the microglia to phagocytose foreign bodies (see figure 7.3, appendix 1). A number of functional assays were implemented in order to help further define polarisation states of the microglia in line with published literature. The results of a phagocytosis assay and a Feret’s diameter calculation are shown in appendix 1.

The results of a phagocytosis assay supported the evidence that pro-inflammatory cells have a more active role in phagocytosis, whilst also demonstrating that the M2-like (anti-inflammatory) phenotype displays some phagocytic behaviour. In order to improve the dynamic range of this experiment it would have been preferable to increase the number of biological repeats, or test other polarizing stimuli to induce the polarized microglial cell populations.

A Feret’s analysis is often also used in statistical analysis of inflammatory cells. Feret’s (maximum) diameter is a measure of cell length and is useful where some cells change morphology dependent on their activity (Zanier *et al.*, 2015). A good example of this is inflammatory cells like macrophages and microglial cells, which switch from an elongated morphology in quiescent or M2-like cells to a more rounded morphology in the M1-like cells as the phagocytic activity of the cell is increased (Caldeira *et al.*, 2014). The results have then been combined as shown in table 7.1.4.1 to calculate an average diameter (μM). As expected, the analysis showed a larger value output for those cells deemed to be M2-like phenotype, where the cell area of cells in an M1-like phenotype was consistently lower as these cells were more amoeboid following exposure to LPS, and activation of phagocytosis.

These results helped to support the evidence that we had successfully isolated microglia from the spinal cord of embryonic tissue, and used inflammatory stimuli to induce different populations of inflammatory cells based on morphology and phagocytic activity. The characterisation of changes in CNS microglia was useful for potential addition to the microfluidic model of hyperalgesic priming.

3.5 Chapter conclusions:

The main objectives of this chapter were to develop protocols for the culture and characterisation of multiple cell types involved in nociceptive signalling. Due to the pseudounipolar nature of the DRG neurons, and the flexibility of microfluidic modelling, it would also be possible to model nociceptive signalling between the PNS and the CNS, by exposing the DRG axons to either macrophages or microglial cells.

The characterisation of development of DRG neurons in the triple-channel microfluidic was previously carried out by Clara Patricio of the Dajas-Bailador lab. In the initial stages of this project, the microfluidic model in this project was simplified to a 2-cell model and the use of macrophages as peripheral cells changing the excitability of the axon of the DRG was further investigated.

Reasonable efforts were made here to co-culture more than one cell type within a microfluidic with the DRG neurons. However, in order to optimise the environment required for *in vitro* culture of DRGs, it was decided to avoid changes in culture media that would be required for physical co-culture of primary cells. Although the cell types were easily cultured individually, each cell has its own timeline for development, ranging from 5-days *in vitro* for DRG neurons, to 7-days *in vitro* for macrophages, and longest of all 14-days minimum for a microglial rich culture (see chapter 2, section 2.2.3). It was also evident that each cell type required specific culture conditions, where macrophages were preferential to a bacterial grade plastic, but DRG neurons require tissue culture grade sterile plastic, coated with PLL (20 µg/ml) and laminin (20 µg/ml.)

The following conclusions can be drawn from the work shown in this chapter:

1. DRG neurons can be isolated from E16.5 mice and cultured in microfluidic compartmentalised devices for the study of neuronal excitability in culture.
2. It was possible to extract and maintain a healthy culture of bone marrow derived macrophages from an adult female mouse. Cells were polarised and used to investigate the effect on neuronal function.
3. Using classical stimuli such as IFN γ versus IL-4 it was possible to generate two populations of macrophages, with distinctive cytokine signatures of polarization.

4. It was also possible to isolate microglial cells on demand from the embryonic spinal cord tissue
5. Similarly to macrophages, microglial cells could be polarised towards different phenotypes, changing the morphology and apparent phagocytic nature of the cell.
(This metric would require further investigation to improve robustness of data.)

The efforts of this project largely focus on the interaction between the periphery (where a stimulus would be applied *in vivo*) and the downstream effect on DRG excitability following infiltration of inflammatory cells. For this reason, more work was completed on characterising changes in bone marrow derived macrophages. Media from polarized cells was extracted at an optimised time-point, and frozen until required, meaning the model only required consistent culture of DRG neurons and improving the flexibility of experiments. The next step in development was to determine what, if any effect the inflammatory mediators released from macrophage cells would have on the excitability of DRG neurons at the peripheral terminals. Microfluidic modelling provides a useful tool for this setup, where media can be locally applied to the axonal compartment, and if an increase in free intracellular calcium is recorded at the soma, it must be dependent on propagation of action potentials to the somal compartment.

4 Investigation of changes in DRG excitability using a compartmentalised microfluidic model

4.1 Introduction:

As part of a model of changes in neuronal excitability as a proxy for pain, we were interested in utilising the microfluidic model to quantify changes in excitability of DRG neurons (see Chapter 1.5 and 1.6). Due to the compartmentalised nature of the microfluidic device, it was highly suitable for monitoring localised changes in calcium transients (Ca^{2+}) at the soma, in response to axonal stimulation.

The excitability of DRG neurons is dependent on stimulation of the neuronal terminals and membrane depolarization inducing the propagation of an action potential. When the action potential reaches the soma, the change in membrane potential elicits a response. This includes, but is not limited to the activation of voltage-gated Ca^{2+} sensitive channels and evoked release of Ca^{2+} transients from intracellular stores such as the endoplasmic reticulum (Berridge, Bootman and Roderick, 2003). Elevated concentrations of free, active Ca^{2+} is therefore dependent on propagation of the action potential along the axon, and can be assumed to be proportional to changes in excitability of the neuron.

4.1.1 Using evoked Ca^{2+} transients as a reporter for changes in neuronal excitability:

In excitable cells like neurons, changes in intracellular Ca^{2+} are essential for synaptic function (Stevens and Wesseling, 1998; Neher and Sakaba, 2008) as well as the activation of signalling pathways within the cell (Hagenston and Baing, 2011; Burgoyne and Haynes, 2015). In neurons, the cytosolic Ca^{2+} concentration is determined by an equilibrium between the influx and efflux of Ca^{2+} ions in the cell, where Ca^{2+} binding proteins (e.g. Parvalbumin in cortical interneurons) buffer the concentration of metabolically active free Ca^{2+} in the cytosol (Rink

and Merritt, 1990; Schwaller, 2010). Therefore, quantifying dynamic changes of intracellular Ca^{2+} within the cell was used here as a measure of cellular excitability.

A rise in intracellular Ca^{2+} activates potassium channels to induce re-polarization of the membrane and trigger neurotransmitter release (Jow *et al.*, 2004; Iosub *et al.*, 2015). However, it has been demonstrated that the efficacy of Ca^{2+} as signalling molecule, is not only due to the concentration gradient maintained between extra and intracellular compartments of the cell, but also due to the physical distance of a Ca^{2+} sensor (e.g. VGCC) from a stimulus (Heine *et al.*, 2019). To restrict Ca^{2+} fluctuations without physical stimulation, cells such as the neurons of the DRG regulate the level of free Ca^{2+} in the cytoplasm. Ca^{2+} is compartmentalized within the cell so that a small change in the intracellular concentration can potentiate downstream signalling, and modulate excitability of the neuron (Grienberger and Konnerth, 2012a). It has been estimated that at rest most cells of the nervous system have an cytosolic Ca^{2+} concentration of between 50-100nM (Berridge, Lipp and Bootman, 2000). Depolarization of the membrane and propagation of an action potential stimulate the release of Ca^{2+} in the neuron (e.g. from the endoplasmic reticulum,).

It is possible to quantify changes in cytosolic Ca^{2+} transients *in vitro* by loading cells using cell permeable, hydrophobic fluorescent indicator dyes. In this way, Ca^{2+} acts as a reporter for changes in neuronal excitability, where evoked Ca^{2+} transients at the soma can be quantified as a proxy for a change in cellular excitability. Following stimulation, when 'free' Ca^{2+} binds to the dye within the cell, a fluorescent signal is emitted (see Chapter 2.3.1). The change in fluorescence recorded can be assumed directly proportional to the fluctuations of Ca^{2+} within the cell. However, it is important to note that the indicator dye will only bind to Ca^{2+} that is freely diffusing through the cytosol following stimulation, whilst most intracellular Ca^{2+} remains sequestered to stores such as the endoplasmic reticulum.

The efficiency of Ca^{2+} as a modulator of cell excitability is due to the capacity of a cell to maintain a concentration gradient of up to 20,000x fold difference between intracellular and extracellular stores of Ca^{2+} (Clapham, 2007). There is ongoing evidence for the use of evoked Ca^{2+} transients as a measure of cell excitability from *in vivo* models. Critically these *in vivo* setups monitor whole ganglia rather than Ca^{2+} transients in the soma corresponding with axonal stimulation. Recent advances have also led to the use of two-photon imaging of DRG neurons in awake animals. It was shown that hyperexcitability of DRG neurons induced by

plantar formalin injection correlated with ongoing pain behaviour in the animal across 5-weeks of live recordings (Chen *et al.*, 2019).

This change in intracellular Ca^{2+} is also a validated method for monitoring neuronal function and changes in excitability *in vitro* (Grienberger and Konnerth, 2012b). Using neonatal rat cultures this technique has also been applied to neurons grown in microfluidic cultures, to quantify changes in neuronal excitability (Tsantoulas *et al.*, 2013). In this setup, it was demonstrated that stimulation of the axonal compartment induced propagation of action potentials towards the somal compartment. It was hypothesised that these action potentials triggered the opening of voltage-gated Ca^{2+} channels upon reaching the soma (Tsantoulas *et al.*, 2012, 2013).

4.1.2 The effect of inflammation on neuron excitability and calcium transients in neurons:

Inflammation is often associated with changes in excitability of the primary afferent fibres. The onset of inflammation often precedes changes in neuronal excitability including action potential conductance, propagation and neurotransmitter release (Ma, Greenquist and LaMotte, 2006; Wang *et al.*, 2007). All of these factors contribute towards sensitization of the peripheral fibres (Hamilton and McMahon, 2000; Raddant and Russo, 2011). However, at a cellular level the onset of inflammation is critically associated with changes in the concentration of intracellular free Ca^{2+} . Specifically an increased resting concentration of intracellular Ca^{2+} in the neuron, as well as an increase in the magnitude of evoked Ca^{2+} release upon stimulation (Lu and Gold, 2008). Several prominent findings from *in vivo* studies have helped develop an understanding of how inflammation affects Ca^{2+} transients of the DRGs through the use of fluorescence dyes (Chen *et al.*, 2019). In these models the increase in fluorescence observed upon evoked release of Ca^{2+} transients at the soma is proportional to changes in the neuronal excitability. Electroporation of the L4/L5 ganglia *in vivo* also included direct stimulation of voltage-gated channels on the soma as well as membrane depolarization at the axonal terminals (Chen and Huang, 2017). Upon stimulation of the axons, the propagation of the action potential induces release of Ca^{2+} from intracellular stores and the opening of voltage-gated Ca^{2+} channels, both of which contribute to the fluctuation in Ca^{2+} transients recorded in the soma.

In a transient nerve injury model it was shown that there was a decrease in voltage-gated calcium channel density following the onset of nerve injury and inflammation (Baccei and Kocsis, 2000; Hogan *et al.*, 2000). Axotomy of the DRG fibres also induced a reduction in intracellular Ca^{2+} in rats (Duncan *et al.*, 2013) and reduced fluctuations of free Ca^{2+} recorded following stimulation of the axotomized fibres (Fuchs, Rigaud and Hogan, 2007). These findings were consistently observed in small and medium fibre subtypes of the DRG only, or those fibres involved in nociceptive signalling (Lu *et al.*, 2010). I have discussed the implications of this in Chapter 5.

4.1.3 Modelling in vitro responses to an acutely applied stimulus

In a physiological environment, the peripheral terminals of the sensory neurons are exposed to an array of inflammatory cytokines and chemokines, especially upon invasion of a polarized macrophage. In chapter 3 the development of culture methods for both DRG neurons in microfluidic devices, as well as the culture and polarization of BMDMs was discussed. In the following chapter, a model was developed to investigate the effects of inflammatory mediators released from these polarized macrophages on neuronal excitability.

Initial experiments involved acute stimulation with either a depolarising agent (KCl 25mM) or polarized macrophage media, whilst further development of the protocol included pre-incubation of cells in polarized macrophage media to attempt to sensitize the axons before acute stimulation with KCl (25mM.)

The method described in chapter 2.5.1 for a Ca^{2+} indicator assay gives an in-depth overview of how the assay was performed. In response to a stimulus (e.g. KCl) membrane depolarisation lead to a rapid and acute increased concentration of cytosolic Ca^{2+} . Free Ca^{2+} ions were bound by Fluo-5F in the cytosol (Thomas *et al.*, 2000; Paredes *et al.*, 2008) and the corresponding emission of fluorescence at a single wavelength of light was recorded.

The increase Ca^{2+} transients were recorded as a change in fluorescence, and used as a proxy for neuronal excitability. It was hypothesised that stimulation of the neuronal culture would induce local depolarization of the membrane. If suprathreshold the action potential would propagate, whereby Ca^{2+} is released via opening of voltage gated sensitive channels, and intracellular mechanisms such as calcium induced calcium release involving secondary

messenger systems. The detectable increase in free intracellular Ca^{2+} was recorded as a transient change in fluorescence recorded.

In order to quantify the increase in calcium fluorescence following stimulation of a population of cells the following formula was applied: $\Delta\text{Ca}^{2+} = \Delta\text{F}/\text{F} = (\text{F} - \text{F}_{\text{rest}})/\text{F}_{\text{rest}}$

4.1.4 Experimental aims and objectives of the chapter:

Part A:

- **Demonstrate the advantages of compartmentalised microfluidic models in the investigation of neuronal excitability**

Part B:

- **Utilise compartmentalised microfluidic devices to model intrinsic and extrinsic cell processes in primary afferent nociception, by combining DRG neurons and bone marrow derived macrophages**
- **Investigate the effect of inflammatory stimuli on neuronal excitability using compartmentalised microfluidic cultures**
- **Compare the effect of acute versus prolonged inflammatory stimulation on neuronal excitability**

4.2 Part A: Axonal stimulation of embryonic DRG cultures in microfluidic devices evokes rapid Ca^{2+} transients and changes in cell excitability:

Chapter 3.4 described the optimisation of culture of dissociated DRG neurons isolated from embryonic murine tissue in compartmentalised microfluidic devices. This model was used here to functionally test the stimulation of the axons for efficient transmission of an action potential. In order to quantify the result of stimulation, evoked Ca^{2+} transients in the soma were recorded as a change in fluorescence. This section describes the use of a Ca^{2+} signalling assay, to validate the use of embryonic microfluidic culture in the study of nociception *in vitro*. Following acute stimulation, a rapid and transient change in intracellular Ca^{2+} was recorded via change in fluorescence emitted. Initially a stimulus was added acutely to the axonal compartment to evoke a change in excitability of the cell soma.

4.2.1 Stimulation of the axons with potassium chloride in a compartmentalised microfluidic device evoked Ca^{2+} transients in the soma:

In the experiments discussed here, the fluctuation in Ca^{2+} transients at the soma were recorded as a proxy for the change in cell excitability induced by stimulation of the cell culture. Figure 4.2.1 below shows that microfluidic stimulation only records the somal response of those axons that have crossed to the lateral compartment of the device. Whereas, the responses labelled “dissociated cultures” recorded a summation of direct and indirect somal stimulation.

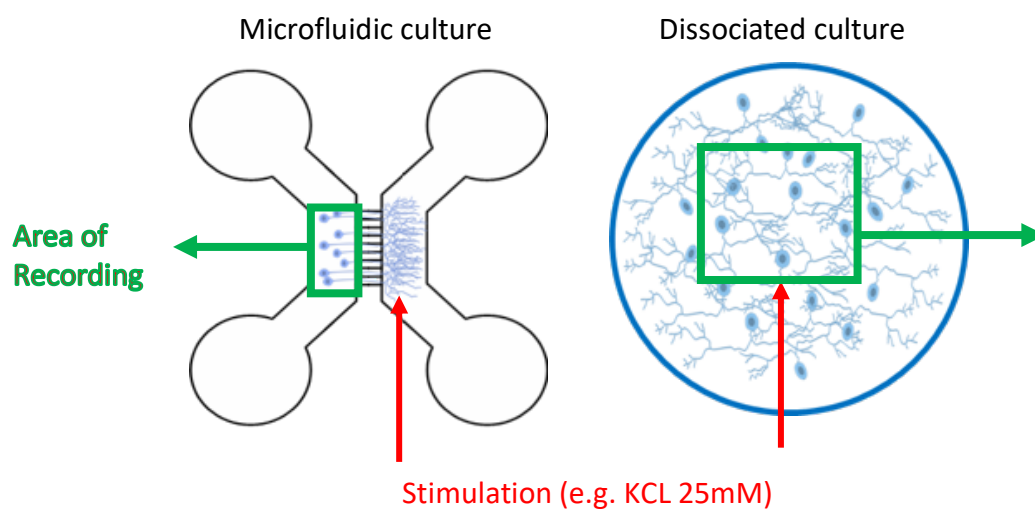


Figure 4.2.1: Schematic representation of the differences between stimulating the axons in compartmentalised microfluidic culture versus the whole cell population in a standard dissociated plate culture.

Potassium chloride (KCL) is as a powerful depolarising agent of all subtypes of sensory neurons, and all neuronal cultures were only stimulated with KCL at a saturating concentration of 25mM. Figure 4.2.2 shows a comparison between the effects of acute application of KCL to a standard plate-based dissociated culture, versus the effects on localised axonal stimulation of a microfluidic culture.

Stimulation of dissociated cultures with KCL evoked a higher amplitude and longer duration response with comparison to axonal stimulation of microfluidic devices (see figure 4.2.2A.)

This was likely reflection of the fact that this stimulation adds direct somal and axonal stimulation mechanisms. The response seen in neurons cultured in a microfluidic culture only reflected the Ca^{2+} transients evoked by stimulation of the axon and transmission of the action potential to soma of the DRG, following membrane depolarization. The direct comparison of peak excitability in figure 4.2.2B demonstrates that the method of culture did not significantly affect the response recorded.

However, the AUC calculation in figure 4.2.2C demonstrated that the duration of the response was significantly increased in dissociated plate cultures, where Ca^{2+} mobilising processes being stimulated were present on the soma as well as the axon. This suggested the presence of longer duration excitation and ongoing cytosolic Ca^{2+} that outlasted the application of an acute stimulus. Where Fluo-5 binds free Ca^{2+} moving through the cell, the prolonged response suggests either Ca^{2+} stores are being replenished, or there is a background signal intensity that must be taken into account.

Figure 4.2.2D shows that the Ca^{2+} signal recorded in microfluidic chambers stimulated with KCL recovered on average by 77.7% from the peak ΔF recorded in the 50-seconds following stimulation. Analysis of individual stimulations demonstrated that 5 out of 6 of the recordings in microfluidic culture showed 100% recovery to baseline fluorescence. In contrast, the average recovery of fluorescence in dissociated plate cultures was only 36.1% by the end of a 60-second recording. The increased recovery towards baseline fluorescence in microfluidic cultures served as further identification of rapid but transient Ca^{2+} responses recorded because of action potential propagation in compartmentalised and fluidically isolated cultures.

This significant increase in cytosolic Ca^{2+} following axonal stimulation in a microfluidic culture was dependent on the following conditions:

- a) Crossing of the axons through the microgrooves whilst retaining microfluidic isolation in the device.
- b) Addition of a stimulus increasing the extracellular positive charge and inducing membrane depolarization via activation of voltage-gated ion channels either at the axonal terminal or on the axons

- c) Subsequent propagation of the action potential to the cell body, where the change in excitability was recorded as a change in fluorescence evoked by the increase in cytosolic free Ca^{2+} within the cell body.

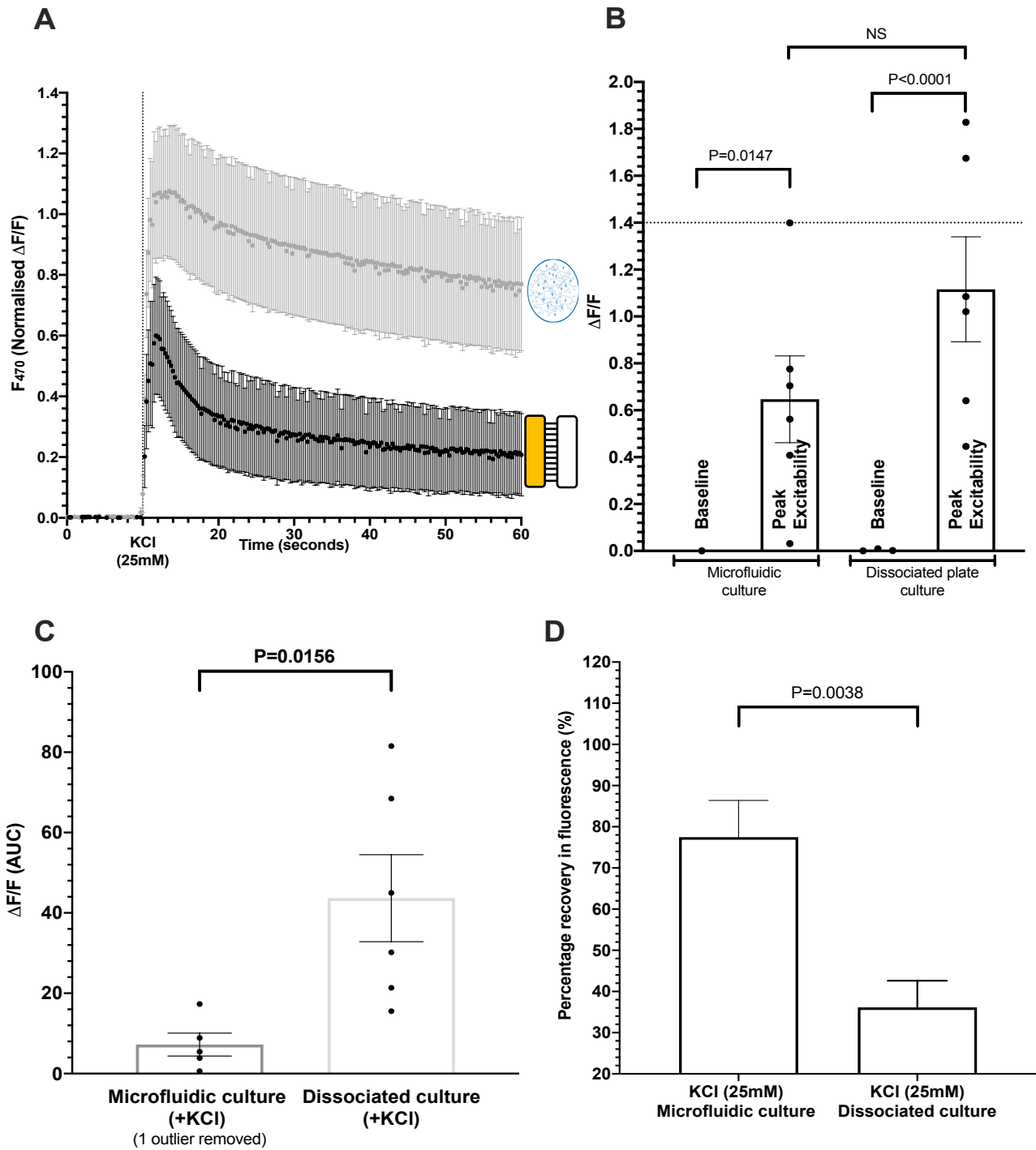


Figure 4.2.2: By measuring change in fluorescence as a proxy for cell excitability, the effects of KCl stimulation on evoked Ca^{2+} transients was quantified in two different DRG neuron culture systems:

- A) Stimulation with KCl evoked rapid Ca^{2+} transients in normal and microfluidic culture. The increase in cell excitability in microfluidic cultures showed a lower amplitude and faster recovery due to local application of the stimulus to the axons. (Legend continued overleaf...)

Figure 4.2.2 *continued*: By measuring change in fluorescence as a proxy for cell excitability, the effects of KCL stimulation on evoked Ca^{2+} transients was quantified in two different DRG neuron culture systems:

- B) Quantification of the peak Ca^{2+} transients showed a statistically significant increase from baseline fluorescence was recorded irrespective of the method of culture. Results of a one-way ANOVA showed $P < 0.0001$ where $F(3, 20) = 14.03$. Post-hoc Sidak's test for multiple comparisons showed a significant increase in cellular excitability irrespective of the method of culture. As shown, $P = 0.0147$ for stimulation with KCL in microfluidic culture and $P < 0.0001$ in dissociated plate cultures. The peak amplitudes recorded between cultures were not significantly different. $P < 0.05$ significant threshold. $N = 6$ biological replicates.
- C) The AUC showed a significant difference in neuronal excitability following stimulation of cultures with KCL, where the AUC of dissociated cultures was increased due to the sustained duration of the Ca^{2+} transient response recorded at the soma. ($P = 0.0156$) Unpaired t-test, $\pm \text{SEM}$, $P < 0.05$ significance threshold, 1 outlier removed via Grubbs' analysis.
- D) Recovery of cellular excitability following stimulation with KCL was represented as %-recovery in fluorescence. Cells cultured in microfluidic devices showed higher %-recovery in fluorescence in a 60-second recording ($P = 0.0038$.) Unpaired t-test, $\pm \text{SEM}$, $P < 0.05$.

4.2.2 Capsaicin evokes increase in neuronal excitability by stimulation of C-like fibres in vitro:

Identifying an appropriate stimulus was dependent on what the model was trying to demonstrate. KCL was used as a general depolarising agent, where subtypes of potassium channels are found on all fibres of the DRG. However, the activation of fibres specifically involved in nociceptive signalling ($A\delta$ and C fibres) required a more selective stimulus. Figure 4.2.3 (shown below) demonstrates a significant increase in the excitability of embryonic cultures when stimulated with Capsaicin, a stimulus that is known to activate TRPV1, a sodium/calcium sensitive ion channel receptor expressed on small diameter nociceptors (Caterina *et al.*, 1997; Yang and Zheng, 2017). Activation of the TRPV1 receptor has a key role in detecting thermal and chemical stimuli and is expressed on both the small-diameter unmyelinated C-fibres, as well as the myelinated $A\delta$ -fibres in the adult (Morgan *et al.*, 2019). However, in rodent behavioural studies investigating ablation of the TRPV1 receptor, it is often hard to distinguish between the behavioural responses mediated solely by fast-conducting $A\delta$ fibres. For that reason, behavioural studies often focus on thermal pain responses associated with TRPV1 activation in unmyelinated, slow conducting C-fibers (Mitchell *et al.*, 2014). However, it is important to note that TRPV1 is expressed on both

myelinated and unmyelinated nociceptors. As discussed in Chapter 1.6 and 1.7 both the A δ and the C-fibre subtypes have been demonstrated to be involved in nociception.

In experimental models a stimulus such as KCL has the potential to depolarize any of the axons within the neuronal population. The time-courses plotted in figure 4.2.3A were used to visualise the change in fluorescence following stimulation of cultures with Capsaicin. In a similar manner to the depolarisation induced by exposure to the axonal terminals to KCL, the evoked increase in Ca²⁺ transients following stimulation by Capsaicin showed higher amplitude and longer duration in a plate-based culture. The smaller amplitude of the response to stimulation with Capsaicin suggested the involvement of TRPV1 receptors on the soma of the embryonic neurons as well as the axons.

Previous evidence by Tsantoulas et al., (2013) has shown that there is a dose-dependent response of neonatal DRG neurons to capsaicin stimulation. For example, it was demonstrated that in neonatal experiments, the EC₅₀ for capsaicin stimulation was 94 μ M from 3 independent axonal stimulations and 135 μ M from 3 independent somal stimulations. In these experiments, 72% of cells responded to a “low” concentration of capsaicin (100nM) whilst 92% of cells were shown to respond to stimulation with a “high” concentration of capsaicin (500nM) (Tsantoulas and McMahon, 2014). The concentration used in this setup was 200nM, based on previous evidence from the Hathway laboratory.

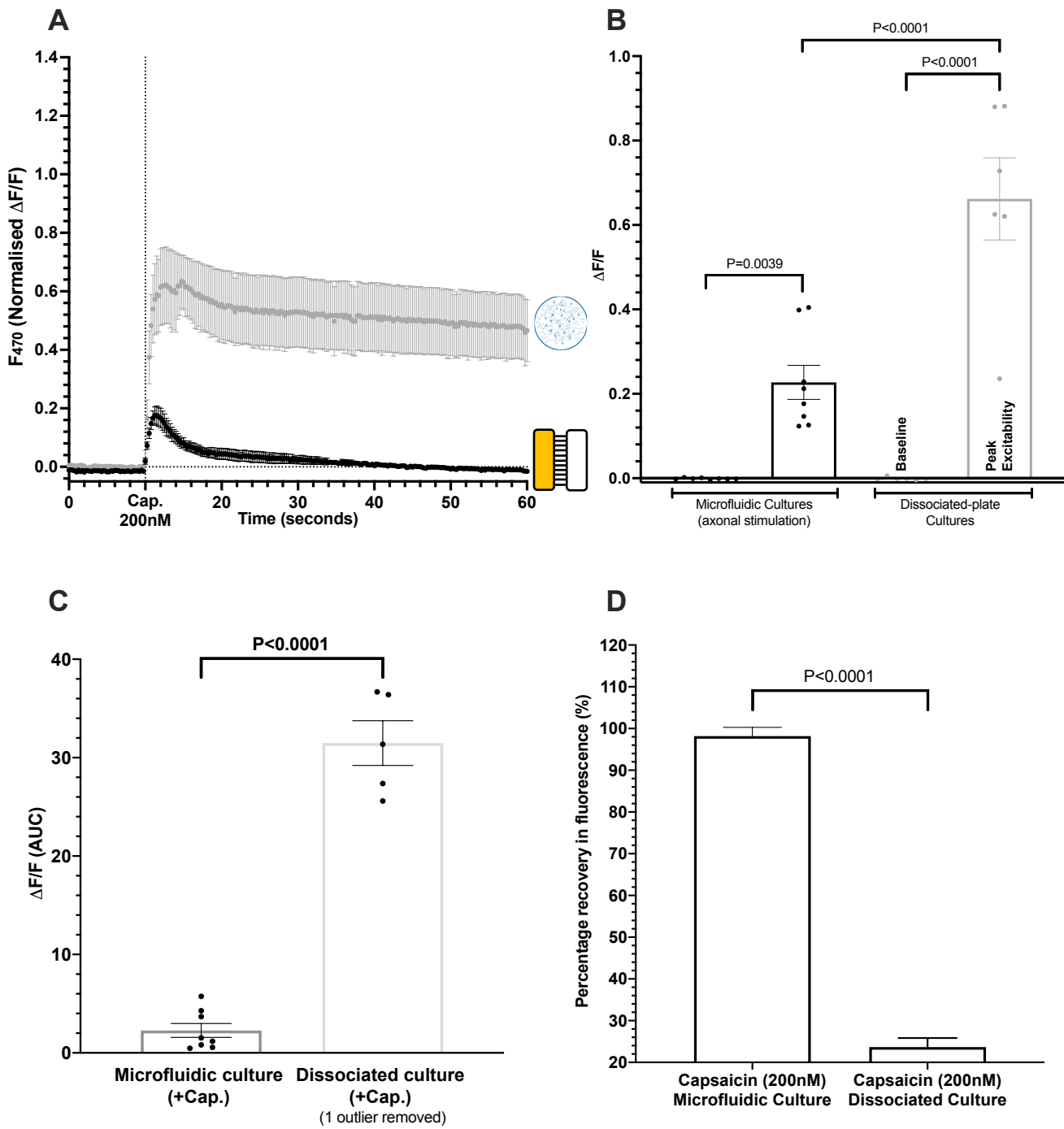


Figure 4.2.3: Stimulation with Capsaicin evoked Ca^{2+} transients in subpopulations of DRG neurons in culture, recorded as an increase in fluorescence:

- A) Stimulation of microfluidic devices vs. dissociated plate cultures. The amplitude and duration of response observed in the dissociated plates was higher due to direct somal stimulation

Figure 4.2.3: Stimulation with Capsaicin evoked Ca^{2+} transients in subpopulations of DRG neurons in culture, recorded as an increase in fluorescence:

- B) Quantification of the peak Ca^{2+} transients showed a statistically significant increase from baseline fluorescence was recorded dependent on the method of culture. Results of a one-way ANOVA with pre-selected pairs of comparisons showed $P < 0.0001$ where $F(3, 24) = 46.08$. Post-hoc Sidak's test for multiple comparisons showed a significant increase in cellular excitability irrespective of the method of culture. As shown, $P = 0.0036$ for stimulation with capsaicin in microfluidic culture and $P < 0.0001$ in dissociated plate cultures. The peak amplitudes recorded between cultures were also significantly different at $P < 0.0001$. $P < 0.05$ significant threshold. $N = 6-8$ biological replicates.
- C) The AUC showed a significant difference in neuronal excitability following stimulation of cultures with Capsaicin, where the AUC of dissociated cultures was increased due to the sustained duration of the Ca^{2+} transient response recorded at the soma. Unpaired t-test, \pm SEM, $P < 0.05$ significance threshold, 1 outlier removed via Grubbs' analysis.
- D) Recovery of cellular excitability following stimulation with Capsaicin was represented as %-recovery in fluorescence. Cells cultured in microfluidic devices showed higher %-recovery in fluorescence in a 60-second recording. Unpaired t-test, \pm SEM, $P < 0.05$ significance threshold.

As shown in figure 4.2.3B, there was a significant difference recorded between the peak excitability of the culture subtypes in response to stimulation with Capsaicin, where the peak excitability recorded from microfluidic cultures was significantly lower than that observed in dissociated plate-based cultures.

The AUC for stimulation of microfluidic devices with Capsaicin was significantly smaller than the AUC for stimulation of dissociated plates (figure 4.2.3C.) Whereas, the recovery to baseline fluorescence was higher in microfluidic culture, where the duration and amplitude of the responses were lower. Following acute stimulation with capsaicin (200nM) in microfluidic devices, the average recovery was 100%, ranging from 87.9% to 100%. In contrast the average recovery of cells in dissociated cultures was only 23.66%, ranging from 19.3% to 117%.

It could be hypothesised that these results suggested that the TRPV1 receptors may not be uniformly expressed on the DRG neurons cultured from E16.5 tissue. The lower amplitude response from stimulation of microfluidics was dependent on propagation of the action potential. However, a larger amplitude response was observed following direct activation of TRPV1 on the soma in dissociated plates.

4.2.3 The peak excitability of a cell was affected by the cross-sectional cell area of the DRG neuron:

Cell size is one of the earliest criteria used to differentiate the diverse populations of DRG neurons (Tandrup, 2004). Using electrophysiological recordings of whole cell DRGs, it has been demonstrated *in vivo* that the cross-sectional area of L4/L5 rat DRG neurons show normally-distributed populations of cells, with overlapping receptive fields (Lawson, Fang and Djouhri, 2019). As previously discussed in Chapter 1.6.2, the neurons of the DRG fibres have different roles in neuronal signalling, largely defined by the fibre size and threshold for activation. Larger diameter fibres, known as A β -fibres are involved in proprioception, whilst smaller diameter fibres (A δ /C) with lower thresholds for mechanical and heat-sensitive stimulation are involved in nociception (Lawson, 2002). This functional dependence on cell size can be extrapolated to an *in vitro* model and used to determine what kind of stimulus might induce a response in the cells. However, one of the common problems with *in vitro* modelling is the limited capacity to recapitulate the myelination of whole nerve fibres observed *in vivo* (Thomson *et al.*, 2008; Zuchero, 2014). In this experiment, we have used the observed cross-sectional area of the somata as an indication for the neuronal subtype. This measurement has previously been used in studies of the nociceptive function of selective DRG neurons via *in situ* hybridisation (Wang and Wessendorf, 2001; Xiuli *et al.*, 2013) and whole DRG Ca²⁺ studies in L4/L5 ganglia of rats *in vivo* (Lawson, Fang and Djouhri, 2019).

The results from figures 4.2.2 and 4.2.3 demonstrated that microfluidic culture was a useful and appropriate method of culture for *in vitro* investigation of neuronal excitability in an embryonic model of nociception. However, it was also important to ascertain what subset of DRG neurons was most likely prevalent in the embryonic culture, as well as eliminate the question of unintentional bias when selecting cells for analysis. Therefore, the results of axonal stimulations were used to statistically determine which subset of DRG fibres was most likely being stimulated in both embryonic and for comparison, in adult cultures of dissociated DRG neurons.

The cross-sectional area of 100 cells was compared to the peak excitability induced in each cell following axonal stimulation of the microfluidic device. Figure 4.2.4A (embryonic data only) shows the prevalence of each cell size dependent on the stimulus used. This data represents the cross-sectional area at the nucleus in μM^2 but the diameter of the cell body is estimated to be between 10-50 μM , as suggested by (Lawson, Fang and Djouhri, 2019). No small cells were detected for either stimuli between 0-200 μM^2 or between 700-900 μM^2 if a culture was stimulated with KCL (25mM).

The axonal stimulation of microfluidic devices with KCL was repeated with cells cultured from adult mice to compare the effects of tissue development on excitability. Figures 4.2.4B and 4.2.4C show a comparison between embryonic and adult cell culture. When directly comparing embryonic to adult cultures, there was no statistical significance difference between amplitude of the peak excitability of each culture. The duration of the response was longer in embryonic cultures, where fluorescence did not return to baseline within 60-seconds of recording, although neuronal excitability was stable at the end of the recording. The adult neurons also failed to return entirely to true baseline fluorescence, although there was a larger standard error of the data where embryonic cultures had not yet fully differentiated to express all subsets of receptors. *In vitro* studies have previously shown that electrical excitability of mouse DRG neurons evolves in waves. The emergence of mechano-transducers emerged at E11.5 and nociceptive function emerging between E12.5 to E14.5 in gestation. However, the duration and amplitude of APs recorded did not resemble that of an adult population of neurons until P0-P1 (Stucky and Lewin, 1999; Lechner *et al.*, 2009)

Having determined that it was possible to perform the same Ca^{2+} experiment using dissociated adult DRGs in microfluidic devices, figure 4.2.4D shows the %-number of cells selected from each culture, dependent on the cross-sectional area of the cell. This figure showed that neither the adult nor the embryonic cultures showed the presence of small diameter DRGs with a cross-section of between 0-200 μm^2 . Only the adult population appeared to have cells larger than 1000 μm^2 , which have previously been suggested to be mechanosensitive or involved in proprioception in whole cell DRG Ca^{2+} imaging studies taken from adult rat tissue *in vivo* (Lawson, Fang and Djouhri, 2019). In fact, this figure demonstrated that 100% of the cells selected in the embryonic culture were less than 900 μm^2

in cross-section. It could be hypothesised that these most likely more closely resembled the *in vivo* development of A δ or C-fibres involved in nociceptive signalling.

There is significant evidence using this measurement as a proxy for fibre subtype from *in situ* hybridisation data in adult rodents (Holmes *et al.*, 2000; Fang *et al.*, 2006; Lawson, Fang and Djouhri, 2019). The evidence from *in vitro* culture is more limited. However, it has been demonstrated using dissociated E14.5 cultures of murine DRGs that the cross-sectional area of cells detected was normally distributed, with an average perikaryal area of $658 \pm 7.9\mu\text{M}$ (Hall *et al.*, 1997). The results here also showed a normal distribution in the cross sectional area of cells detected, although the average area was smaller, which could reflect the development of nociceptive neurons by E16.5 (Lechner *et al.*, 2009). It is worth noting of course that dissociated cultures of DRG neurons *in vitro* may not directly replicate the morphology acquired *in vivo*.

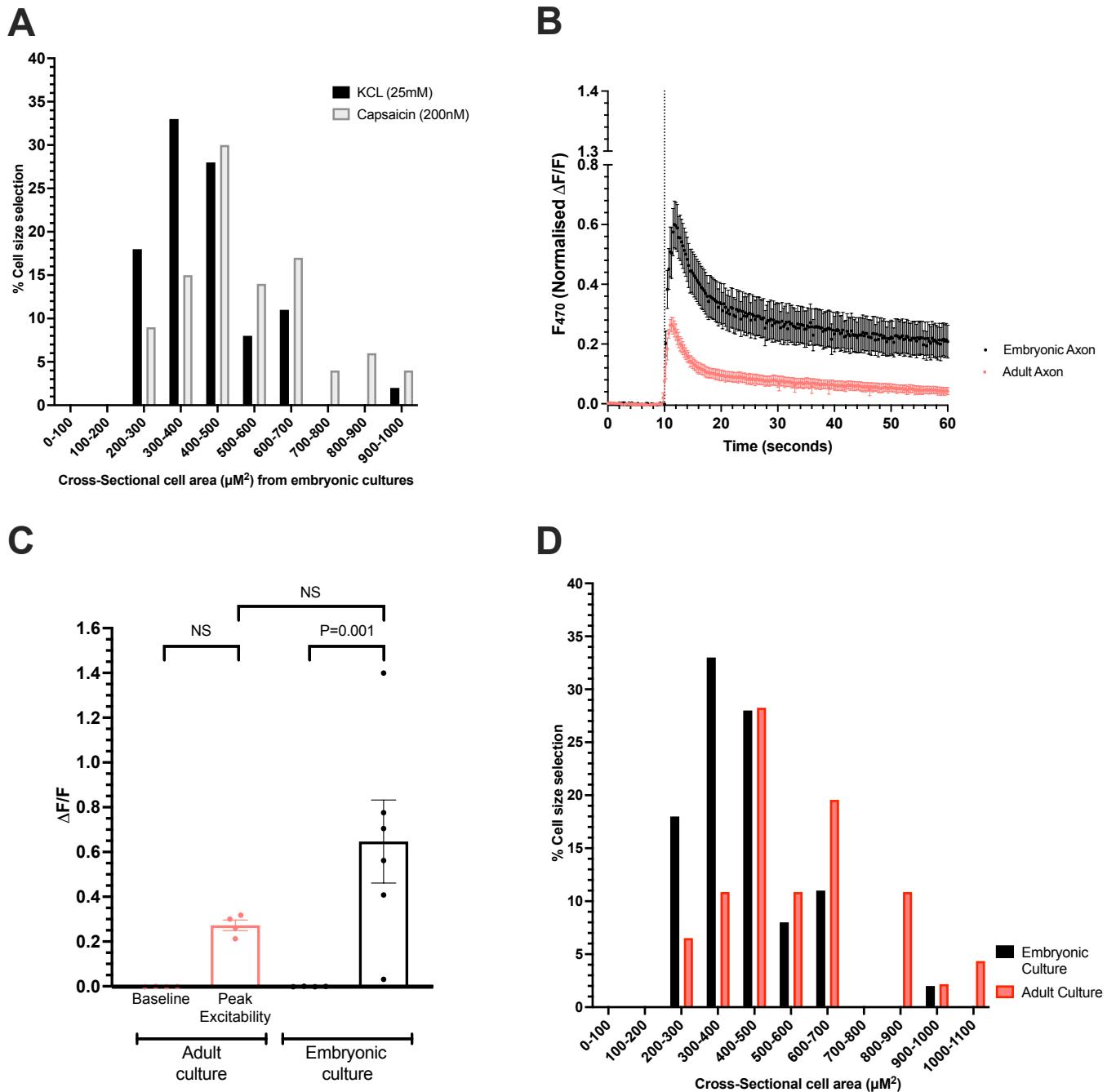


Figure 4.2.4: A comparison of cellular response to stimulation based on cell size and age of tissue:

- A) Cross-sectional area demonstrated development of multiple subtypes of sensory neurons in embryonic cultures. Embryonic cultures showed a higher proportion of neurons with a larger cross-sectional area.
- B) The peak amplitude of axonal stimulation was higher in embryonic culture (N=6) relative to adult DRG neurons (N=4.) The duration of the response in adult cells was shorter and returned rapidly to baseline, whereas stimulation of embryonic cultures only demonstrated partial recovery of excitability.
- C) The peak amplitude of evoked Ca²⁺ transients in embryonic cultures was not significantly different to the amplitude of adult culture (P=0.1.) Results of a one-way ANOVA with post-hoc Sidak's test F(3, 16)=8.15. Significance threshold at (P<0.05). Error bars represent mean ± SEM. Only the embryonic stimulation showed a significant increase in fluorescence following stimulation (P=0.001.)
- D) The culture of DRG neurons from adult mouse tissue demonstrated the development of larger diameter somata that were not present in the embryonic cultures.

4.3 Part B: Macrophage dependent changes in neuronal excitability and Ca²⁺ transients:

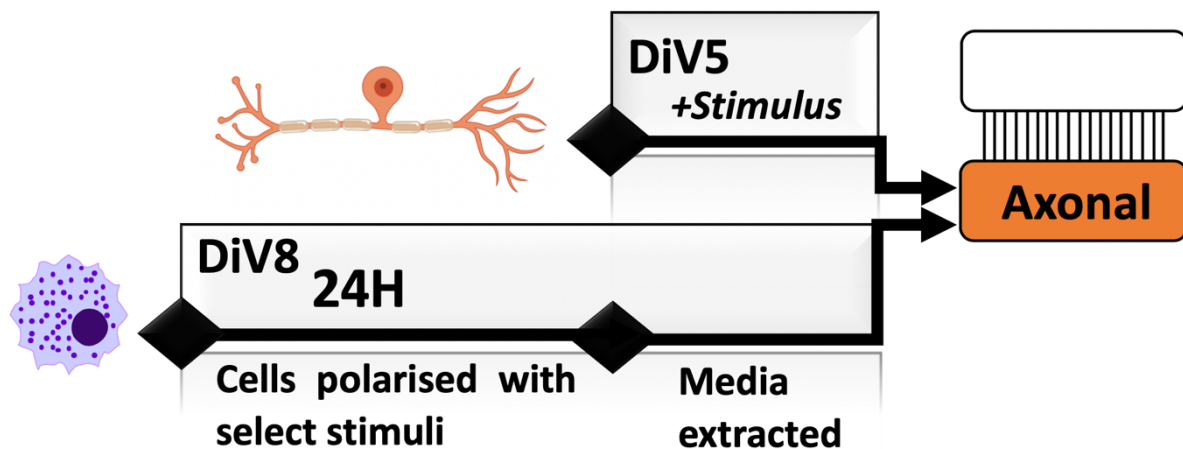


Figure 4.3: The optimised time-course of parallel culture for DRG neurons and macrophages *in vitro*. Once the DRGs reach DiV5, a stock of polarized macrophage media was extracted and used to stimulate the axons in Ca²⁺ imaging.

Chapter 1.8 discussed the role of non-neuronal cells in the onset and development of neuronal hyperexcitability in pain. At the peripheral terminals of the nociceptors *in vivo* this includes, but is not limited to the influx of polarised macrophages in response to an inflammatory insult (Baral, Udit and Chiu, 2019). The release of cytokines and chemokines from polarised cells induces peripheral sensitisation via multiple mechanisms such as lowering the threshold for activation of receptors such as TRPV1 expressed on the terminals on the nociceptor (Pinho-Ribeiro, Verri and Chiu, 2016) (see Chapter 1.5-1.7.)

The results shown in chapter 3 demonstrated the *in vitro* culture and polarisation of macrophages derived from bone marrow monocytes extracted from mice. The direct use of co-culture was complicated due to the extensive optimisation of culture conditions required for primary cells *in vitro*. Figure 7.1.2 showed that the extraction of media from polarised cells demonstrated quantifiable and unique signatures of inflammatory mediators released from different populations of inflammatory cells.

A protocol was devised in order to be able to expose DRG axons to cytokines released from polarized macrophages, without the need for direct co-culture in the microfluidic devices. The schematic in figure 4.3 shows the timings of how macrophage cells and DRG cells were cultured in parallel.

The effect of inflammatory cytokines on neuronal excitability was quantified following localised exposure of the axonal compartment to media extracted from polarized cells.

4.3.1 Acute axonal addition of polarized macrophage media evoked changes in DRG neuronal excitability:

A model was devised to investigate the effect of acute exposure to polarized macrophage media on DRG neuron excitability. Polarized media was generated using the protocol described in full in Chapter 2.2. All data shown here used phenol red free DMEM (NPR) to reduce cross-reaction fluorescence from excitation of Fluo-5 at 470nM.

In the experiments described here “acute exposure” refers to neurons stimulated between DiV5-6, where the stimulus of interest was applied after a minimum of 10 second baseline recording, and images collected for a further 1-2 minutes. Tests are all comparable to the preliminary data recorded for “acute” exposure to KCL (25mM) and Capsaicin (200nM) described in part A (figures 4.2.2 and 4.2.3.)

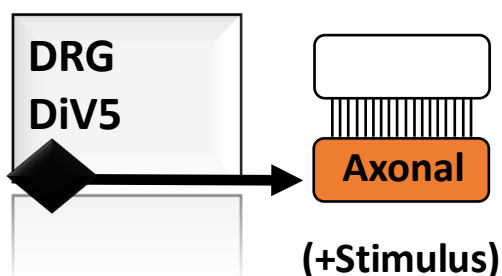


Figure 4.3.1: Schematic showing acute addition of polarized macrophage media to the axons of DRG cultured in microfluidic devices

Acute stimulation with polarized macrophage media in the axonal compartment demonstrated significantly lower amplitude responses compared to a depolarising stimulus such as KCL. The time-course analyses in figure 4.3.2A below demonstrated that the addition of polarized media induced a negligible increase in fluorescence, with a 0.095 ΔF increase following M2-like media, and 0.077 ΔF max following M1-like media.

(For reference, figure 4.3.2B includes the peak excitability following stimulation with KCL (0.65 ΔF) as seen in figure 4.2.2.)

The increase in excitability from baseline was calculated for each stimulation. Figure 4.3.2B shows a comparison of the increase in fluorescence induced following stimulation with either M1-like or M2-like media. Using stimulation with KCL to compare the results for acute M1/M2-like stimulation, it was evident that the macrophage media induced little to no response at the axonal terminals of the DRGs in culture. Overall, and despite a very small transient increase, the acute addition of media extracted from polarized macrophages did not produce statistically significant changes in Ca^{2+} transients when applied to the axon.

In vivo the cytokines released from inflammatory cells such as macrophages sensitize the axons of the DRG neurons over the course of hours, and therefore this model of ‘acute addition’ to the axons of the DRGs may not have induced results considered to be biologically meaningful in this setup.

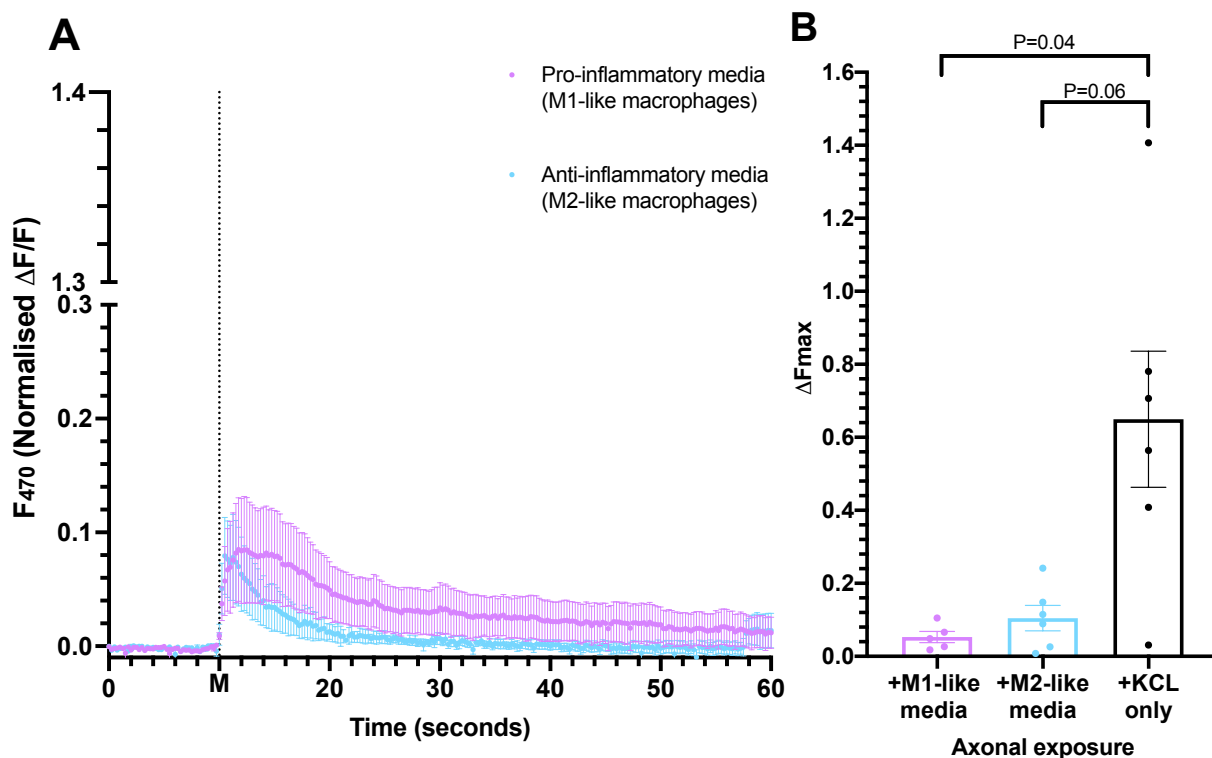


Figure 4.3.2: Addition of polarized macrophage media to the DRG axons demonstrated negligible changes in cell excitability relative to the stimulation with KCL

A) Neuronal populations cultured in microfluidics were stimulated with polarized media. The time-course analysis shows the change in excitability, recorded as change in fluorescence. Y-axis shown used the same scale as stimulation with KCL for direct comparison.

B) The increase in excitability (as shown by ΔF_{max}) was significantly reduced when cells were stimulated with M1-like media in particular ($P=0.04$). The data shown for M1/M2 like stimulation is plotted next to the results from figure 4.2.2 (stimulation with KCL) for direct comparison. One-way ANOVA with Dunnett’s multiple comparisons. \pm SEM, $P < 0.05$. $F(3, 18)=1.319$

4.3.2 Acute stimulation with macrophage media induced changes in the amplitude of a subsequent stimulation with KCL :

This model was also useful for determining if exposure to an inflammatory stimulus (such as media extracted from a polarized macrophage) would affect the amplitude of a subsequent response of the DRG neurons. *In vivo*, a phenomenon like this is referred to as “priming,” and is a key characteristic of peripheral sensitisation in nociceptive neurons (Fischer, Mak and McNaughton, 2014). A second acute stimulation of the axons with KCL was used here as a control for viable neuronal signalling.

In this model, after 2 minutes exposure to macrophage media, the cells were re-stimulated with 25mM KCL to quantify what, if any, effect the cytokines secreted by polarized macrophages had on cell excitability and resting membrane potential. Only the first 50 seconds following each stimulation have been shown, as by this point the fluorescence had returned to a baseline level of excitability.

Figure 4.3.3A shows that the amplitudes of a primary stimulation to macrophage media and the secondary stimulation to KCL were not statistically significantly different. The primary stimulation of the cells with macrophage media reduced the concentration of unbound fluo-5 in the cell, and therefore it was hypothesised that this might reduce the amplitude of a second stimulation such as KCL. However, given that the amplitude of the primary stimulation with macrophage media was so low, it was possible that the second stimulation with KCL would evoke a higher amplitude response (similar to that observed in figure 4.2.2.) Given that the amplitude of both the primary stimulation with macrophage media and the subsequent stimulation with KCL were negligible, it was possible that the macrophage media (or the cytokines within) had ‘desensitised’ the axons to a second stimulation.

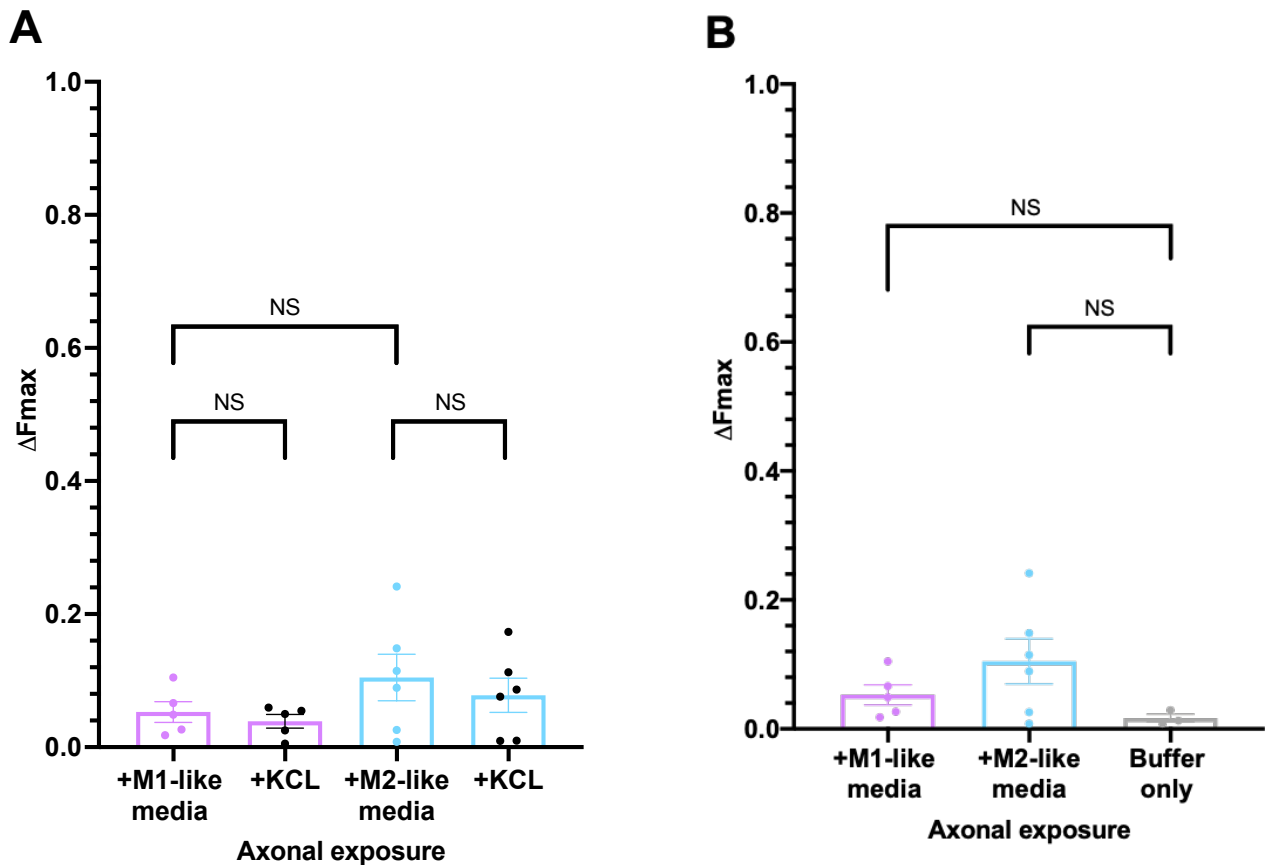


Figure 4.3.3: The acute stimulation of the axons with inflammatory media induced no significant change in cell excitability, but the subsequent axonal response to KCL was significantly reduced following a stimulation with inflammatory macrophage media:

- A) There was no significant difference in cell excitability following axonal stimulation with macrophage media and a downstream stimulation with KCL. One-way ANOVA showed no statistically significant difference between the ΔF_{max} following axonal stimulation with macrophage media versus subsequent axonal stimulation with KCL, $F(3,18)=1.319$, $P=0.29$. A post-hoc Sidak's test for selected multiple comparisons also demonstrated no significance was observed comparing the peak excitability of M1-like and M2-like stimulations. $N=5$ microfluidic chambers imaged for M1/KCL, $N=6$ microfluidic chambers for M2/KCL. Error \pm SEM, $P<0.05$ significance threshold.
- B) Stimulation of the axons with just imaging buffer showed a lower amplitude response than stimulation with inflammatory media. A one-way ANOVA, with post-hoc Dunnett's multiple comparison test (using buffer only exposure as the control comparison) determined that the amplitude of response to M1/M2 media ($N=5/6$) was not significantly greater than just buffer alone ($N=3$.) All data was deemed to be normally distributed. M1-like data is plotted at $N=5$, where one biological replicate was removed by the Grubb's outlier test. Bars represent mean \pm SEM, where $P<0.05$ was deemed significant. $F(2.000, 6.979)= 3.399$.

The results of these experiments can be interpreted in multiple ways:

- 1) Evoked Ca^{2+} transients in DRGs were lower in response to inflammatory media than by stimulation with KCL. The acute exposure to macrophage media potentially reduced the excitability of the cells.
- 2) One potential limitation of only leaving 2-minutes between stimulations was that the Ca^{2+} stores in the cell may not have replenished by the second stimulation. Acute stimulation of axons with inflammatory macrophage media partially depleted the available stores of fluo-5 in the soma. Therefore, the reduced secondary response to KCL stimulation was likely partially because of reduced starting concentration of fluo-5 in the cell.
- 3) Given that the low amplitude of the response observed was similar over multiple cell preparations it was unlikely that the results observed were an artefact of low cell viability. Figure 4.3.3B also included a comparison with N=3 stimulations using just imaging buffer. The amplitude of these responses were lower than the responses to inflammatory media. Although not significant, this suggested that the response to acute stimulation with macrophage media was a 'real' response, and not the artefact of mechanical stimulation of the axons.
- 4) The results in figures 4.3.2 and 4.3.3 showed a significant change in the amplitude of the response to KCL, if the axons were stimulated first with macrophage media. It could be hypothesised that the macrophage media (and cytokines within) had an inhibitory effect on the neuronal response to stimulation with KCL. Stimulation with KCL prior to the macrophage stimulation would help to confirm points 3 and 4.

To confirm whether the contents of polarized media could affect neuronal excitability without reducing viability, the next step was to culture the axons in polarized media for a prolonged period of time prior to stimulation.

4.3.3 Prolonged exposure of the axon terminals to polarised macrophage media induced quantifiable changes in neuronal excitability

As a model derived for the purpose of investigating the effects of inflammatory mediators on peripheral nociceptors, a timeline was devised to mimic “long-term” exposure of the DRG terminals to sensitising agents. A protocol was devised to quantify the effects of longer-term effects of axonal exposure to inflammatory cytokines on neuronal excitability.

The diagram shown here represents a simplified version of the timeline used for these *in vitro* “priming” experiments.

Once the axons covered the axonal compartment of the chamber (usually DiV5-6) the axons were exposed to polarized macrophage media for a period of 8 hours prior to stimulation with KCL (25mM) over a period of two minutes. It has previously been shown that intraganglionic injection with 8-bromo cAMP (transcription factor activator) induced hyperalgesic priming by a minimum of 6-12 hours. Although if injected to the hindpaw (i.e at the terminals) then 72-hours was required to observe a change in cell excitability (Araldi, Ferrari and Levine, 2015).

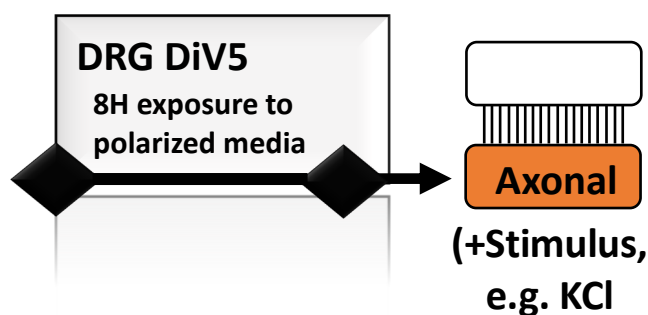


Figure 4.3.3.1: A schematic showing the setup for prolonged exposure of the axonal compartment to polarized macrophage media prior to stimulation of the axons with KCL.

Following an 8-hour incubation of the axonal compartment in polarized macrophage media, an increase in fluorescence was still observed when axons were stimulated with KCL (figure 4.3.4A.) The change in fluorescence following stimulation was used again as an indirect

measure of the change in cell excitability. The amplitude of the response for cells exposed to M1-like media was higher than if the axons were exposed to M2-like media for 8-hours. However, the amplitude of the responses in figure 4.3.4A were much lower than stimulation of naïve microfluidic cultures with KCL (as shown in figure 4.2.2, $\Delta F=0.65$.)

The comparison of the peak excitability induced by Ca^{2+} transients in the soma, did not show a significant difference between prolonged incubation of axons in M1-like media or M2-like media prior to stimulation with KCL (figure 4.3.4B.)

In figure 4.3.4C the maximum change in fluorescence (as a proxy for cell excitability) for each condition has been directly compared to the result observed for cells cultured in DRG media and stimulated acutely with KCL. The amplitude of the response to stimulation with KCL was consistently lowered when axons were exposed to inflammatory media for 8-hours. Although incubation in both subtypes of inflammatory media demonstrated a reduction in cell excitability relative to stimulation of naïve microfluidic cultures with KCL, the viability of axons was not reduced. (i.e. Upon visual inspection, alongside the continual uptake of Fluo-5, it was determined that the prolonged exposure of the cells for 8-hours was not detrimental to cell viability.) It could be hypothesised that the terminals of the peripheral nociceptors had been 'desensitised' by prolonged exposure to inflammatory media (and the cytokines within,) and were less excitable.

In conclusion, it was determined that culture of the axonal compartment in macrophage media, prior to stimulation, was not detrimental to cell viability. The prolonged exposure for 8-hours in culture appeared to reduce the evoked Ca^{2+} transients recorded following axonal stimulation with KCL. This data supported the results seen in figure 4.3.3 and suggested that exposure to macrophage media induced a reduction in axonal excitability. Figure 4.3.4D has been added to show a direct comparison of the results shown in figure 4.3.4C and figure 4.3.3A. The stimulation of axons exposed to M1-like media for 8-hours with KCL was significantly different to those cells acutely stimulated with both M1-like media followed by KCL. However, there was no significant difference in the evoked Ca^{2+} transients recorded following prolonged exposure to M2-like media relative to acute stimulation with M2-like

media (and KCL.) These results indicated that there was potential for this model to be further developed, where the time-period for incubation with polarized media could be optimised.

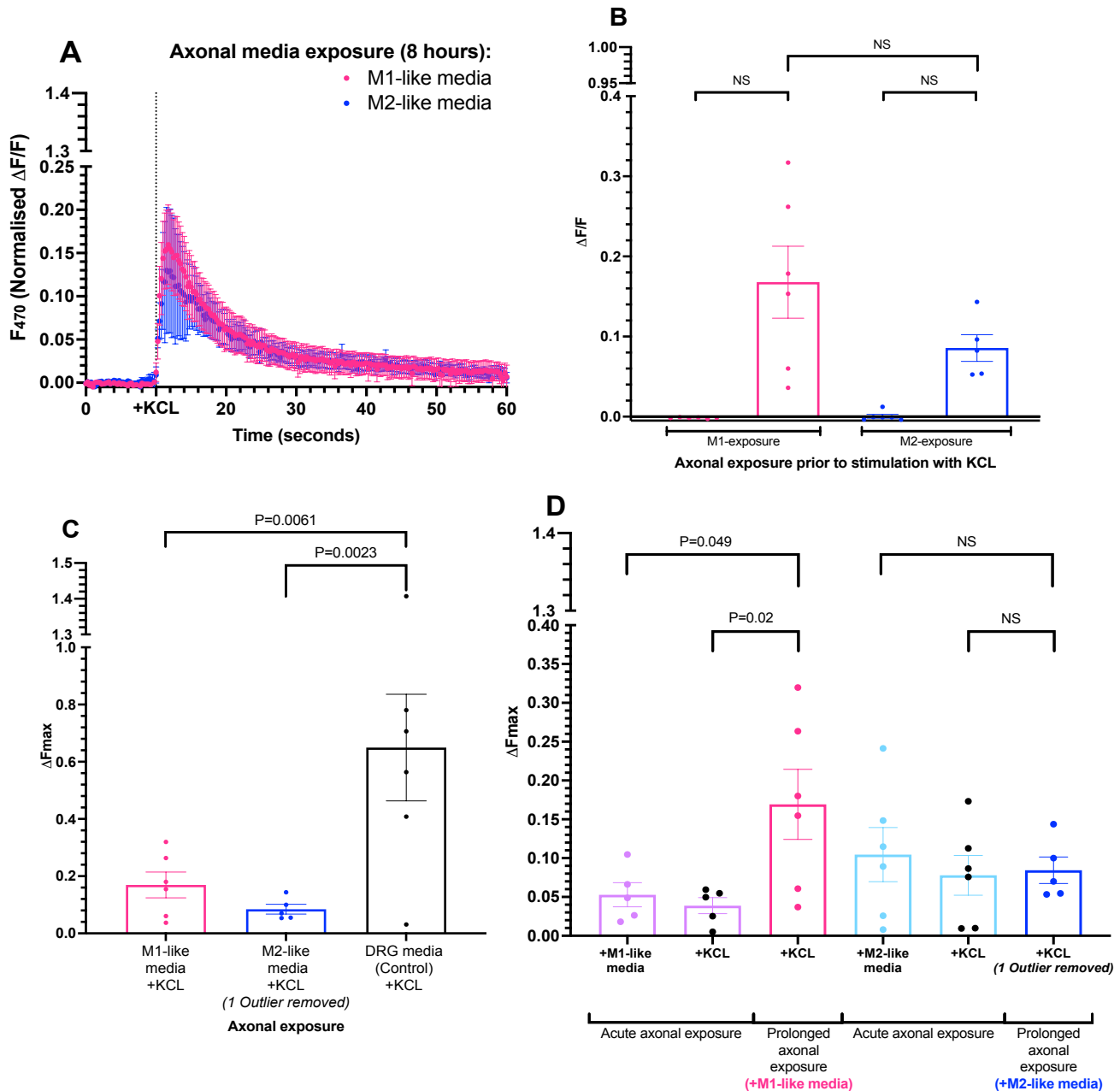


Figure 4.3.4: Prolonged exposure of the axonal compartment to polarized macrophage media exerted a significant reduction in neuronal excitability compared to stimulation of naïve cultures with KCL.

A) A time course analysis showing the effect of axonal stimulation with KCl (25mM) following 8-hours incubation of the axonal compartment in either M1-like or M2-like media. The amplitudes of responses was not significantly different between treatments.

B). Exposure to inflammatory media exerted a reduction in excitability. However, the increase from baseline fluorescence in both conditions was deemed to be significant. Results of a one-way ANOVA with post-hoc Sidak's multiple comparisons test, where $P < 0.05$ was significant. Error \pm SEM. $F(5, 28) = 9.699$

Legend continued overleaf.

C) The maximum fluorescence demonstrated no significant difference between M1-like and M2-like exposure prior to KCL stimulation. However, both treatments demonstrated a significant reduction in excitability relative to a negative control. One-way ANOVA with Dunnett's multiple comparison's test, \pm SEM, $P < 0.05$ significance threshold. $F(3, 21) = 6.45$

D) Directly comparing the evoked Ca^{2+} transients recorded following acute stimulation with M-like media and KCL versus prolonged axonal incubation in macrophage media followed by stimulation with KCL. Only the prolonged incubation with M1-like media induced a significant difference in cell excitability compared to relevant acute stimulations. Results of a one-way ANOVA with Sidak's multiple comparisons tests, mean \pm SEM, $P < 0.05$ significance threshold. $F(5, 27) = 2.489$

4.4 Discussion and chapter conclusions:

In recent years the use of compartmentalised microfluidic devices (such as those developed by Xona) has proved an invaluable tool in the study of primary cell cultures, including neuronal and glial cell populations ((Taylor *et al.*, 2005; Park *et al.*, 2006; Dajas-Bailador *et al.*, 2012)). The fluidic isolation of the soma from the axons has led to in-depth study of compartmentalised changes in biochemistry of the cell (Taylor *et al.*, 2005; Dinh *et al.*, 2013; Neto *et al.*, 2016; Garcez, Guillemot and Dajas-Bailador, 2017). Furthermore, microfluidics provide a flexible cell-culture platform to quantify changes in cellular excitability using live-cell imaging formats, as well as downstream quantification of changes in biomarker expression arising from localised addition of a treatment.

Unlike cortical neurons of the central nervous system the DRGs show limited spontaneous activity in normal physiological conditions. (Esposito, et al., 2019). However, following nerve injury or exposure to an inflammatory stimuli (e.g. polarized macrophage media,) the DRGs may become hyperexcitable, since they are involved in maintaining chronic pain states (Weng *et al.*, 2012). In line with the objectives for this chapter, I have shown here how the compartmentalised microfluidic nature of the 2-channel device has the potential to model changes in excitability of DRG neurons. In order to do this, live-cell imaging was used to quantify changes in cytosolic Ca^{2+} transients in the somal compartment of a device, following localised stimulation at the axonal compartment.

This model demonstrated the rapid and dynamic response of the pseudo-unipolar DRGs when stimulated at the peripheral terminals. To ensure reproducibility of results, each chamber was only imaged once, and replicate data was taken from separate embryo dissections.

One of the advantages of compartmentalised microfluidic modelling is the flexible nature and capacity for development of reproducible and adaptable protocols. Multiple stimuli (such as KCL and Capsaicin) were used to induce quantifiable changes in neuronal excitability, as well as the use of polarized macrophage media as a more biologically relevant stimulus for modelling changes in excitability. Not only was there a significant difference in evoked Ca^{2+} transients dependent on the stimuli used, but there was a reduced amplitude of response in cells stimulated selectively in the axonal compartment of a microfluidic device (compared to a standard dissociated culture.)

In microfluidic devices, the evoked change in fluorescence quickly returned to a stable baseline, usually within 30 seconds of the stimulus being added. In these cultures, the action potential arriving at the soma had triggered the release of Ca^{2+} from intracellular stores such as the endoplasmic reticulum or via activation of voltage-gated Ca^{2+} channels. Consequently, the response was rapid, but short lived where the source of free calcium diffusing through the cell was sequestered rapidly. However, in dissociated plate culture the addition of a stimulus such as KCL or Capsaicin (a potent TRPV1 agonist) also opened voltage-gated ion channels on the soma, and induced further influx of Ca^{2+} ions into the cell. In these cultures, the fluorescence had not returned to true baseline by 60-seconds. Fluorescence was no longer increasing, but had not returned to the original baseline fluorescence observed prior to stimulation. The additional direct stimulation of the soma in dissociated plate cultures induced a larger amplitude and duration of response, where more cytosolic Ca^{2+} was available to interact with fluo-5 at the time of recording.

Chapter 1.7.1.1 introduced the TRPV1 channel, for which Capsaicin is a potent agonist. The TRPV1 channel is Ca^{2+} permeable (Samways *et al.*, 2016) and therefore evoked larger Ca^{2+} transients in the somal compartment, where propagation of the action potential was not always necessary. The somal compartment of the microfluidic device is also comprised of an axonal network connecting the soma, so it is likely that some of the response recorded was dependent on activation of TRPV1 receptors on the axons. However, the distance required

for the action potential to be propagated to the soma was clearly much less if the axons in the somal compartment were stimulated.

Alternatively, activation of the TRPV1 channels located directly on the DRG soma induced a rapid influx of Ca^{2+} , which was recorded by the increase in fluorescence following stimulation. TRPV1 receptors are only localised to selective fibres of the DRG, and although it has been demonstrated they are expressed throughout the sensory fibres (Andresen, 2019) the results shown here suggested a more dense expression of TRPV1 receptors in the somal compartment (most likely on the soma,) from cells extracted at E16.5.

The peak amplitude of response to capsaicin was also consistently lower than that of KCL in neuronal cultures from E16.5 tissue. This could be attributed to a higher prevalence of potassium sensitive ion channels expressed axonally and on the soma. Of particular relevance is the potential for selective protein expression at this early stage of development. These results suggested that stimulation of the axon by TRPV1 agonism was less effective at depolarising the membrane of the neuronal terminals (and subsequently generating an action potential) than the addition of a positive charge such as KCL to the extracellular space.

It was concluded that not only are the microfluidic devices a useful tool for isolating the axonal and somal responses to a stimulus, but that the response of a cell *in vitro* is also dependent on age related functionality acquired *in vivo* (Lechner *et al.*, 2009). The evidence for *in vitro* cultures of dissociated embryonic DRG cells is limited, but recent work has suggested that by E18.5 in development, a deficiency in Ret protein (tyrosine kinase) demonstrated a shift towards a cell distribution of smaller cells only, with limited development of mechanoreceptive DRG neurons (Honma *et al.*, 2010). There is more supporting literature for a similar protocol performed from whole cell DRGs extracted from adult rodents. Chronic constriction models of injury conducted in adult mice identified three 'ranges' in somal cell area (Ruscheweyh *et al.*, 2007). Small DRGs ($<300 \mu\text{m}^2$) medium-sized cells ($300\text{--}700 \mu\text{m}^2$) and large cells (defined as $>700 \mu\text{m}^2$). However, what this study did not discern, was how the subtypes of A- and C-fibres can be subcategorised within these sizes.

The results of the *in vitro* model shown here suggested a high percentage of small to medium size DRG neurons dissociated in culture, which would suggest the presence of cells with a similar function to C and $\text{A}\delta$ nociceptive fibres. *In vitro* differences in cell body size did not

appear to be directly correlated with neuronal type. All dissociated neurons had the capacity to be depolarised by the addition of KCL at the neuronal terminals, but there was also a significant overlap in the responses of small diameter to cells to also be depolarised to selective stimuli such as Capsaicin.

These results were particularly important in later experiments when identifying a protein target of interest downstream of a microRNA that was locally expressed in the axons or terminals of the DRG neurons.

As well as utilising the microfluidic model to show differences in the evoked responses recorded between KCL and Capsaicin, we attempted to model peripheral sensitisation of the nociceptors. There is extensive research on the bi-directional signalling processes between inflammatory cells such as macrophages and sensory neuron fibres of the DRGs (R. R. Ji, Chamesian and Zhang, 2016). A common limitation of standard *in vitro* modelling is the limited capacity of most models to selectively record changes in excitability arising from direct axonal stimulation. This microfluidic model was also used to demonstrate how cytokines released by infiltrating polarized macrophages can induce rapid changes to DRG neuron excitability, with particular relevance to nociceptive function. Although it could be argued that further work would be required on development of the inflammatory stimuli used, the model shown was useful for inferring the link between addition of an inflammatory cytokine to the tissue and correlating downstream changes in excitability of the neurons.

Whilst immune cells release cytokines and growth factors that act at the peripheral nerve terminals, the nociceptors in-turn release neuropeptides from the terminals to modulate this immune response (Baral, Udit and Chiu, 2019). However, it is not only polarized macrophages that release inflammatory mediators to modulate nociceptor activity. Where macrophages have been characterised in the release of cytokines such as TNF α , IL-6 and IL-1 β , there are other inflammatory cell types involved in the regulation of nociceptive function. These include mast cells, neutrophil cells, TH-17 cells (Pinho-Ribeiro, Verri and Chiu, 2016) as well as cell shuttling from the satellite glial cells surrounding the nociceptor fibre. Taken as a whole, it would therefore be very difficult to replicate the complexity of this bi-directional signalling *in vitro* using only two cell subtypes.

The resultant sensitisation of the peripheral nerve fibres that arises from release of cytokines from circulating inflammatory cells is implicated in several neuropathies and pain pathways (Coutaux *et al.*, 2005; Burnstock *et al.*, 2009; Reichling and Levine, 2009). In physiological conditions there are multiple mechanisms by which the nociceptors become sensitised, since many types of immune receptors are found on the terminals of the DRGs in close contact with inflammatory cells (Thacker *et al.*, 2007). These include (but are not limited to) cytokine and chemokine receptors such as those found to be upregulated in the media of polarized macrophages. For example, following chronic constriction injury to the sciatic nerve, the concentration of both TNF α and IL-1 β have been shown to increase 10-fold up to 1-hour after injury (Ueceyler, Tschärke and Sommer, 2007; Sacerdote *et al.*, 2008). Both of these cytokines are pro-inflammatory and produced in high concentrations by M1-like macrophages (Lu *et al.*, 2018). Furthermore, the release of these cytokines induces the cascade of further inflammatory cytokine production such as IL-6, and the increased activation of inflammatory signalling cascades.

The mechanisms by which pro-inflammatory mediators modulate DRG neuronal excitability is also dependent on the nature of the inflammagen (Scholz and Woolf, 2007; Sandkühler, 2009; von Hehn, Baron and Woolf, 2012). For example, TNF α is released from M1-like cells and has been shown to be important in the maintenance of neuropathic pain via sensitisation of the NaV channels (Jin and Gereau IV, 2006). Both TNF and the TNF-receptors have been shown to be upregulated post-injury in rodent models of pain (Schäfers *et al.*, 2003). *In vivo* modelling has shown that following upregulation, TNF targets voltage-gated sodium channels, specifically the TTX-resistant NaV channels found on nociceptor terminals (Chen *et al.*, 2011b; Leo *et al.*, 2015). The direct application of TNF α to DRG neurons in culture has also been shown to transiently sensitize nociceptive firing in hairy skin isolated from the rat hindpaw (Bretag, 1969; Oprée and Kress, 2000) correlating with an induced upregulation in TRPV1 expression in dissociated ganglia from adult mice (Jin and Gereau IV, 2006). The increased activity of rat nociceptors to noxious heat was short lived, and none of the pro-inflammatory cytokines tested (IL-6, IL-1 β and TNF α) evoked a release of CGRP from larger diameter nociceptors at an innocuous temperature. In a similar mechanism to IL-1 β , TNF phosphorylates NaV1.8 to facilitate channel opening (Jin and Gereau IV, 2006). This increase in activity of the sodium channels induces a neuropathic pain state by making nociceptors

hyperexcitable. However, there is also evidence that some cytokines target nociceptors indirectly, via glial cell shuttling.

There is also evidence that pleiotropic anti-inflammatory cytokines have roles in neuroprotection and the resolution of neuro-inflammation (Amici, Dong and Guerau-de-Arellano, 2017). One important example is the role of IL-4 (and M2-like macrophages) in ameliorating pain induced by increased circulation of pro-inflammatory cytokines. The application of IL-4 to nerve terminals in a mouse model of nerve injury, induced upregulation of anti-inflammatory macrophages (Brundu S, 2015). These M2-like cells synthesise opioid peptides (Met-enkephalin and β -endorphin) and induce reduction in nerve hypersensitivity downstream of the acute treatment with IL-4 (Celik *et al.*, 2020). Other important examples include IL-10, a key cytokine involved in endogenous resolution of pain and released in high quantities from M2-like cells. It has been shown that intrathecal administration of cytokines like IL-10 can reduce neuropathic pain (Milligan *et al.*, 2006) whilst injection of IL-10 neutralising antibodies has been shown to prolong transient inflammatory pain in mice (Krukowski *et al.*, 2016).

Localised application of cytokine-rich macrophage media to axons of the DRG neurons was used to induce changes in excitability. Although circulating levels of cytokines *in vivo* are dynamic (Pettersen *et al.*, 2011) it has also been demonstrated that endogenous M2-like macrophages will re-polarize to an M \emptyset regulatory phenotype after around 6 days (Tarique *et al.*, 2015). One of the advantages of polarized media was that the cytokines released by the cells would not deplete over time. In addition, the protocol used was optimised to ensure that the stimuli used to trigger the changes in the phenotypes of the cells were no longer circulating in the media, and wouldn't produce a depolarization of the axon terminals.

Neither acute stimulation nor prolonged exposure to polarized macrophage media increased the excitability of the DRG neurons in microfluidic culture. However, the use of the polarized media in the microfluidic device produced a significant reduction in neuronal excitability, compared with the evoked Ca²⁺ transients recorded following stimulation with KCL only. Of particular interest, the amplitude of the response to KCL following prolonged exposure to macrophage media was lower, and could potentially suggest that this subset of polarized

media desensitised the neuronal terminals to stimulation. These preliminary results with inflammatory media showed limited differences between the peak excitability induced following incubation of axons in proinflammatory media versus anti-inflammatory media. However, exposure to inflammatory media was not deemed to reduce viability of cells. There is evidence to suggest that there is temporal secretion of cytokines from macrophages, dependent on the state of polarization (Melton *et al.*, 2015). It could be suggested that for the application of prolonged exposure to inflammatory media the set up would require either a) automated perfusion of media over extended periods of time, or b) live-cell imaging in a controlled atmosphere, regulating parameters such as CO₂ and temperature. In this way, images could be taken for hours without observing loss in neuronal viability. Since fluorescent dyes such as Fluo-5 cannot be followed for hours without photobleaching, development of this model in this way would require the use of transiently expressed Ca²⁺ sensitive molecules.

The following conclusions were drawn from this Chapter:

- Two-channel compartmentalised devices were very effective at modelling functional changes in neuronal excitability.
- The peak amplitude of response to capsaicin was also consistently lower than that of KCL in neuronal cultures from E16.5 tissue
- In order to model hyperalgesic priming the stimulus used would require further optimisation, however we were clearly able to show that exposure of the axons to a cytokine rich media acutely changed the excitability of the DRG neurons.
- Significant differences in the evoked Ca²⁺ transients were also observed dependent on whether a stimulus was applied to the axon or directly to the soma. This unique feature of the compartmentalised devices helped to demonstrate that protein expression is not equally distributed throughout the terminals, axons and soma of the pseudounipolar DRG neurons.

5 miR-138-5p regulates DRG excitability

5.1 Introduction:

MicroRNAs (miRNA) are small, non-coding sequences between 21-25 nucleotides that are involved in processes such as mRNA degradation, or more commonly in neurons repression of translation by targeting mRNA. Since their discovery in *C.elegans* in 1993 (Lee, Feinbaum and Ambros, 1993; Wightman, Ha and Ruvkun, 1993) over 2500 conserved miRNA sequences have been identified for humans (Kozomara and Griffiths-Jones, 2014). The role of microRNAs as regulators of translation in the nervous system has been discussed in Chapter 1.8.1. In this model we used the microfluidic nature of the devices to investigate the role of these small non-coding RNAs in local translation in the axon, and regulation of neuronal excitability in the context of those observed in nociceptive signalling.

The role of neuronal plasticity in regulation of cell excitability has been more extensively studied in recent years. It has been demonstrated that local translation of mRNA in the axon is an important process for efficient regulation of neuronal plasticity. One such example of pathways known to be of importance, are the mTOR-dependent (mammalian target of Rapamycin) pathways, where mTOR-dependent local translation of mRNA has been shown to regulate excitability in a subpopulation of nociceptive neurons *in vivo* (Piper and Holt, 2004). Immunohistochemical staining showed that the mTOR machinery was present in subsets of primary afferent fibers, although most likely the A-fibres since phospho-mTOR labelling did not extend to the epidermal layer where the C-fibre terminals are located (Jiménez-Díaz *et al.*, 2008). Subcutaneous injection of rapamycin into the hindpaw of rats also significantly increased the threshold temperature for paw-withdrawal evoked by A-fibres. In contrast, rapamycin did not appear to affect the C-fibre dependent activity. Furthermore, the injection of anisomycin (a global protein synthesis inhibitor) also reduced thermal sensitivity after fast-heat ramps targeting A-fibre nociceptors (Jiménez-Díaz *et al.*, 2008). Behavioural assessment using Von Frey filaments also showed that pre-treatment with Rapamycin significantly attenuated secondary mechanical hyperalgesia (Obara, Géranton and Hunt, 2012). These results showed that the local administration of rapamycin potentially affected the excitability

of subpopulations of sensory neurons, via inhibition of mTOR mediated local mRNA translation. This mTOR dependent local translation is just one example of how and why local translation in the neuron is important and essential for regulating neuronal excitability.

5.1.1 microRNA and pain:

With roles in translational repression, microRNAs (miRs) have also been identified as useful biomarkers for disease pathologies such as chronic pain, and are an important area of interest in upcoming clinical trials. The pleiotropic nature of this class of non-coding RNAs makes them particularly useful for treatment of multifactorial origins. Therefore, as well as interest in understanding their physiological role, much of the research surrounding miRNA investigates their potential role as therapeutic targets (van Rooij and Kauppinen, 2014). The first evidence for the role of miRs in mechanisms of pain were shown by screening miR expression in different *in vivo* models of chronic pain (Andersen, Duroux and Gazerani, 2014). For example, CFA injection into the hindpaw of adult rats showed downregulation of 10-selective microRNA by RT-qPCR (Bai *et al.*, 2007). This downregulation of mature microRNA correlated with the development of allodynia, and supported the evidence that miRs are involved in regulation of an appropriate response to an inflammatory stimulus.

In work by Zhao *et al.*, (2010) it was proven that reduced production of miRs in the sensory DRG neurons resulted in inflammatory pain attenuation (Zhao, M.-C. Lee, *et al.*, 2010). This model used deletion of the Dicer gene in nociceptive neurons of the DRG that express NaV1.8 to reduce production of miRs in these neurons. The NaV1.8⁺ neurons are small fibre, and known to have a role in detection of inflammatory pain-based signalling (Hameed, 2019). Whilst the behavioural response to painful stimuli was normal in Dicer knockout mice (apart from a deficit in cold-sensitivity) the response to inflammatory stimuli was dramatically different. The absence of Dicer correlated with lowered levels of expression of several proteins such as P2X3, NaV1.8 and NaV1.9, all of which have important roles in inflammatory pain signalling (Abrahamsen *et al.*, 2008). Dicer-null mice did not show changes in threshold for activation in response to carrageenan or CFA, and at a cellular level no increased excitability was recorded in response to inflammatory stimuli such as bradykinin or PGE₂ (Zhao, M. C. Lee, *et al.*, 2010).

The overwhelming evidence from models of chronic pain have undoubtedly highlighted the importance of miRs in regulation of pain responses. It is clear that knockout of mature microRNA leads to downregulation of proteins of interest, and subsequently the response of the DRGs to a painful stimulus is inappropriately modulated. In the transition from acute to chronic pain, it is evident that there is upregulation of proteins at the terminals of the nociceptors. Ferrari *et al.*, (2013) tested the hypothesis that transient inhibition of translation in the peripheral terminals of the nociceptors could reverse hyperalgesic priming. The injection of translation inhibitors (e.g. cordycepin) to the peripheral terminals of the neurons in adult male rats showed reversal of hyperalgesic priming (Ferrari *et al.*, 2013). The downregulation of mRNA translation corresponded with a reduced decrease in mechanical paw withdrawal threshold upon exposure to PGE₂. Critically, the reversal of priming was shown to outlast the duration of the action of the translation inhibitors (Cordycepin and Rapamycin) used to prevent development of priming.

At a cellular level it has been demonstrated that miRNAs modulate pain via post-transcriptional regulation of proteins involved in nociception (Bartel, 2009). Therefore, combined with the evidence from Ferrari *et al.*, (2013) that inhibition of local translation in the axon can reverse hyperalgesic priming, of particular interest to this project was the role of miRs in regulating local translation of proteins in the axon.

5.1.2 miR-138-5p and pain:

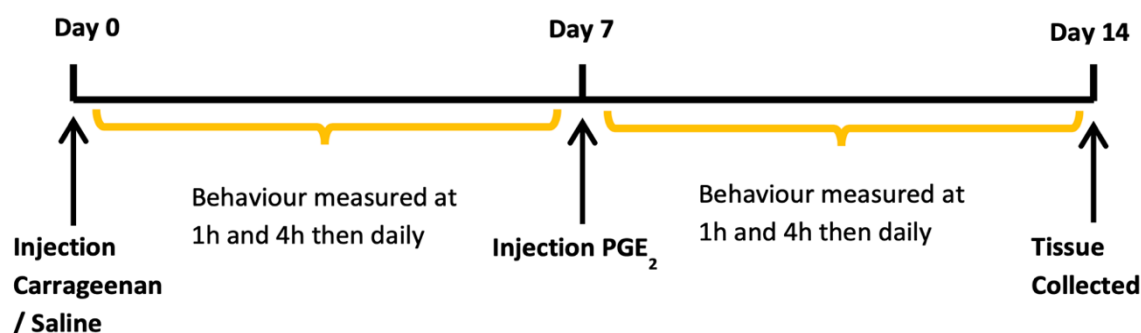


Figure 5.1.1: An overview of a hyperalgesic priming model *in vivo*, as used previously by members of the Dajas-Bailador laboratory.

Hyperalgesic priming experiments in the Hathway and Dajas-Bailador labs have previously demonstrated that out of 726 miRNA tested, only 4% (32 miRNA) showed an increase following hyperalgesic priming, including miR-138-5p. Data from the thesis of Clare Martin (submitted to the University of Nottingham for a doctorate of philosophy in 2018) showed the results of a preliminary microarray using tissue from the hyperalgesic priming model described above. L4, L5 and L6 DRGs (with nerve roots intact) were collected from primed and unprimed tissue 7-days post PGE2 treatment. Levels of microRNA were quantified by microRNA microarray using TORAY 3D gene (see figure 5.1.2.)

All *in vivo* work was completed in Wistar rats using the paw withdrawal threshold as a measure of hyperalgesia. Of those microRNAs that were shown to be upregulated at day-14 of the hyperalgesic priming model, miR-138-5p demonstrated a 2.4 log₂fold change. As shown in Chapter 1.5.3 by day 14, the paw withdrawal threshold of primed animals remains low following removal of the inflammatory stimulus. In these animals the DRG neurons had become more excitable even in the absence of the inflammatory modulator. In line with published data demonstrating a role for miR-138-5p in neuropathic pain and peripheral nerve injury (Liu *et al.*, 2013; Zhou *et al.*, 2016), the results of this microarray pointed towards miR-138-5p being a relevant candidate for further study of peripheral mechanisms regulating inflammatory pain via local translation.

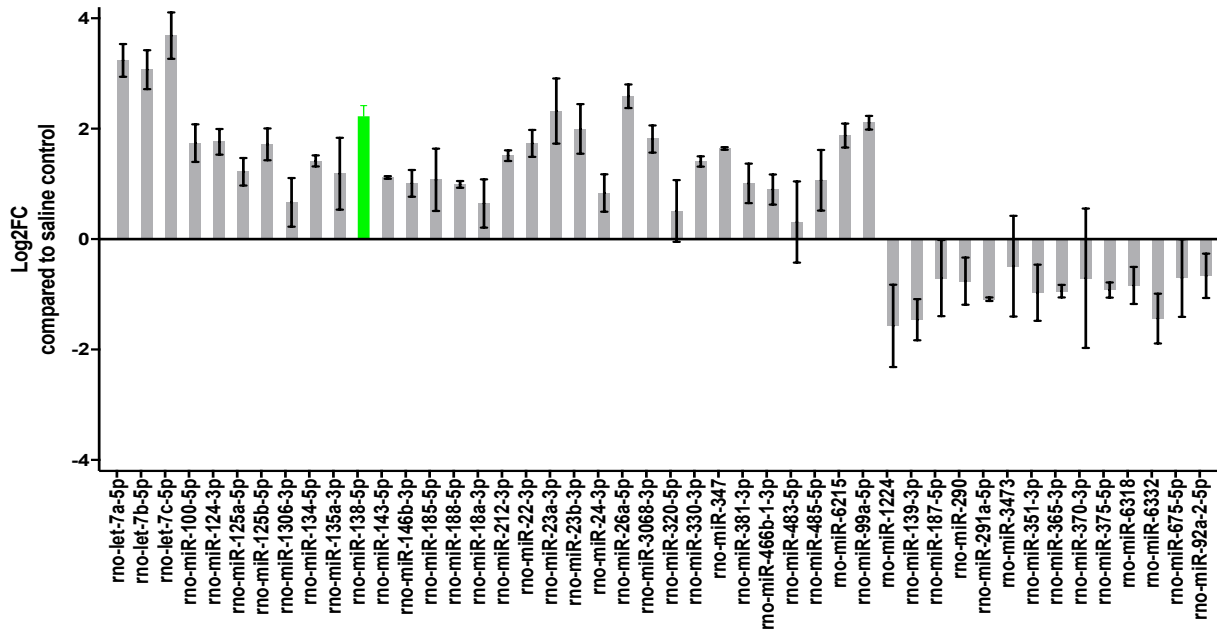


Figure 5.1.2: The results of a preliminary microarray showing upregulation of miR-138-5p in tissue extracted from adult rat primed tissue in the chronic phase of hyperalgesia (Clare Martin, 2016). Saline control N=1, Carrageenan primed tissue N=2.

For example, miR-138 upregulation can be induced by exposure to proinflammatory cytokines, such as those which are released upon tissue damage to stimulate polarization of macrophages in the neuropathic pain response including LPS (Zhou *et al.*, 2016).

5.2 Materials:

Cell culture consumables including media and culture dishes were obtained from ThermoFisher Ltd (UK) and Sigma, as listed in Chapter 2. All microfluidic devices used in this study obtained from Xona Microfluidics were 2-channel chambers (SND150) with a microgroove length of 150µM. Full details of the methods used here have been described in Chapter 2.

In order to investigate microRNAs functional mechanism, and specifically miR-138-5p with regards to regulation of neuronal excitability, I used commercially available miRNA mimics and inhibitors (miRCURY LNA miRNA Mimics and Inhibitors, Qiagen), a tool widely used in the field and in our laboratory (Dajas-Bailador *et al.*, 2012; Lucci *et al.*, 2020)

5.2.1 LNA technology:

Locked nucleic acid (LNA) technology incorporates high affinity RNA analogs where the ribose ring is “locked,” with an extra bridge connecting the 2’oxygen and 4’ carbon. This rigid binding forms the ideal conformation for Watson-Crick base pairing, and increases the thermal stability of the LNA oligonucleotide when hybridized to complimentary RNA or DNA (Stein *et al.*, 2009). This increased melting temperature (T_m) is especially important when oligonucleotides are used to detect short sequences, or those with increased GC% such as microRNAs.

5.2.1.1 MicroRNA mimics:

miRNA mimics are designed to simulate the endogenous activity of a miRNA upon addition to a cell culture, by increasing the proportion of the RISC (RNA-induced silencing complex) containing the guide strand miRNA. The unique design of Qiagen LNA oligonucleotides are characterised by three RNA-LNA strands, rather than the traditional two. This includes an unmodified RNA strand with a complimentary sequence to miRNA of interest, and two LNA-enhanced passenger strands. Since the passenger strand is divided into two, this helps to ensure that only the miRNA guide strand is loaded onto the RISC (Bramsen *et al.*, 2007). This chapter describes the use of a dual-luciferase reporter assay, where a miR-138-5p mimic was transfected into HEK cells with a target of interest (see chapter 2.4.4.2.1.)

5.2.1.2 MicroRNA ‘power’ inhibitors:

miRNA silencing was induced using a miRNA power inhibitor for miR-138-5p. The miRNA inhibitor is an antisense oligonucleotide with a complimentary sequence to the mature sequence of miR-138-5p. Therefore, upon introduction into the cell the miRNA of interest is sequestered by the inhibitor, blocking normal translational repression by miR-138-5p. I have described the use of a cell-permeable miRNA inhibitors that carry phosphorothioate modifications on the LNA backbone. This improves stability in culture and enables transfection-free incorporation into the cell, which is useful for working with cells such as DRG neurons (Griffiths-Jones, 2004). Increased stability of the power inhibitor means it can be added directly to the culture media and up-taken by the cell via gymnosis (Soifer *et al.*, 2012). The efficiency of inhibition is dependent here on several factors including cell density, length of incubation period and the concentration of inhibitor added.

Both the miRNA power inhibitor control and the miRCURY miR-138-5p LNA miRNA Power inhibitor were obtained from Qiagen.

5.2.1.3 Small interfering RNA (siRNA):

Also known as silencing RNA, siRNAs are short double-stranded RNA sequences that function as RNA interference molecules upon binding to complementary target transcripts. In many ways, siRNA and miRNAs are similar. Both molecules decrease protein translation by binding to the RISC complex, however, the downstream mechanism of siRNA is different to that of miRNA. Unlike miRNA which can cause translation repression and degradation of multiple proteins via selective binding of the seed sequence, siRNA only targets a single sequence in mRNA. The RISC proteins unwind the double stranded siRNA molecule, whereupon the antisense siRNA strand binds to the select sequence on mRNA. Slicer protein subsequently cuts the mRNA in the binding region, and the mRNA is degraded by the cell (Kim, 2005).

5.3 Part A: Investigation of miR-138-5p in modulating the excitability of small fibre DRG neurons

This chapter investigates the functional role of miR-138-5p in the control and regulation of neuronal cell excitability. Using established techniques such as qPCR, the relative expression of miR-138 was quantified, with regards to the state of inflammation that the microenvironment of the axon was exposed to. However, regulatory control of microRNAs in the cell is dynamic, much like the processes surrounding inflammation in the cell. Whilst miRNA expression has been investigated in neuronal function, and implicated in processes such as pain, the involvement of miRNA in the development and resolution of inflammation has not yet been fully elucidated.

Previous works from the Dajas-Bailador and Hathway labs showed upregulation of miR-138-5p in a model of hyperalgesic priming. Based on these results it was hypothesised that expression of miR-138-5p would change following exposure to inflammatory mediators such as pro-inflammatory cytokines and chemokines. To investigate this, the axon terminals of DRG neurons were once again exposed to inflammatory media extracted from polarised macrophage media.

5.3.1 Part A objectives:

- Investigate localised changes in miR-138-5p in the modulation of DRG neurons cultured in microfluidic devices
- Study the effect of inflammatory signals on miR-138-5p regulation of axonal propagation of action potentials DRG

5.3.2 Exposure of axons to inflammatory media demonstrated upregulation of miR-138-5p in the soma:

In this experiment DRG neurons were cultured on culture inserts (known as Twiss chambers, see figure 5.3.1) for up to 7 days *in vitro*. Unlike Xona microfluidic devices, these inserts do not provide complete fluidic isolation of the different compartments.

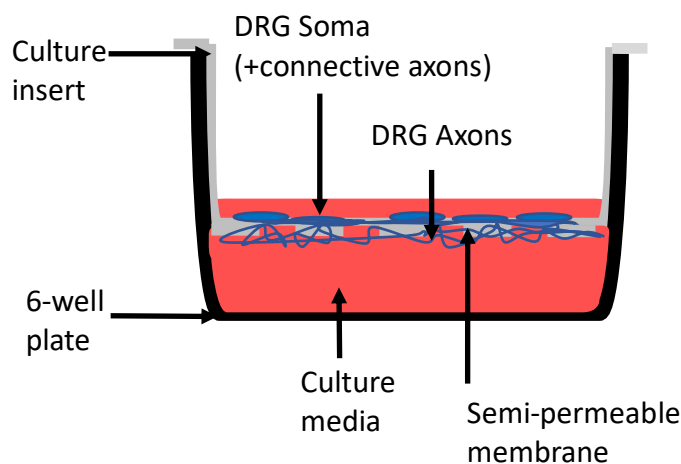


Figure 5.3.1: Culturing cells in semi-permeable "Twiss" inserts for RNA extraction

The diagram in figure 5.3.1 shows a schematic of how cells were cultured using these Twiss chambers. For experiments involving RNA extraction and qPCR, the Twiss inserts were utilised to increase the potential concentration of RNA isolated from each culture. If required for PCR between 20-30 DRGs were dissociated per chamber. Cells were dissociated and seeded into the upper compartment of the insert. On top of the mesh insert, a network of axons (and soma) develop, whilst axons would also pass through the pores in the insert and form an "axonal-rich" layer underneath the mesh. A much higher number of DRGs were dissociated per insert, especially when attempting to isolate RNA from the 'axonal compartment.' At DiV5-6 the DRG neurons showed >80% coverage of the mesh insert. From here, the insert was removed, and cells were extracted via gentle scraping and washing with TriZol (See Chapter 2.5 for complete methods.)

The Twiss model was designed to replicate the layout of the Xona microfluidics used in the Calcium assay, and mirror what might be observed *in vivo* where the axonal terminals of DRG neurons become exposed to a cocktail of inflammatory mediators upon priming by a nociceptive stimulus.

At DiV7, the media on the underneath of the insert (representative of the axonal compartment) was changed for 24 hours prior to RNA extraction. In order to quantify the effect of inflammation on miR-138-5p expression in the DRGs, the media in the axonal compartment was substituted for media extracted from polarized macrophages (see Chapter 2.2.2.4) The "somal" compartment was always cultured in DRG media.

The axonal RNA yield of the chamber was very low from the cells seeded. In un-pooled samples, the CT values were too high to be consistently detected for axons exposed to M1-like media. The pooled samples in the supplementary data show how there was no significant fold change in the expression of miR-138 when cells were exposed to M1-like media. The upregulation of miR-138-5p was more easily detected when axons were exposed to anti-inflammatory media.

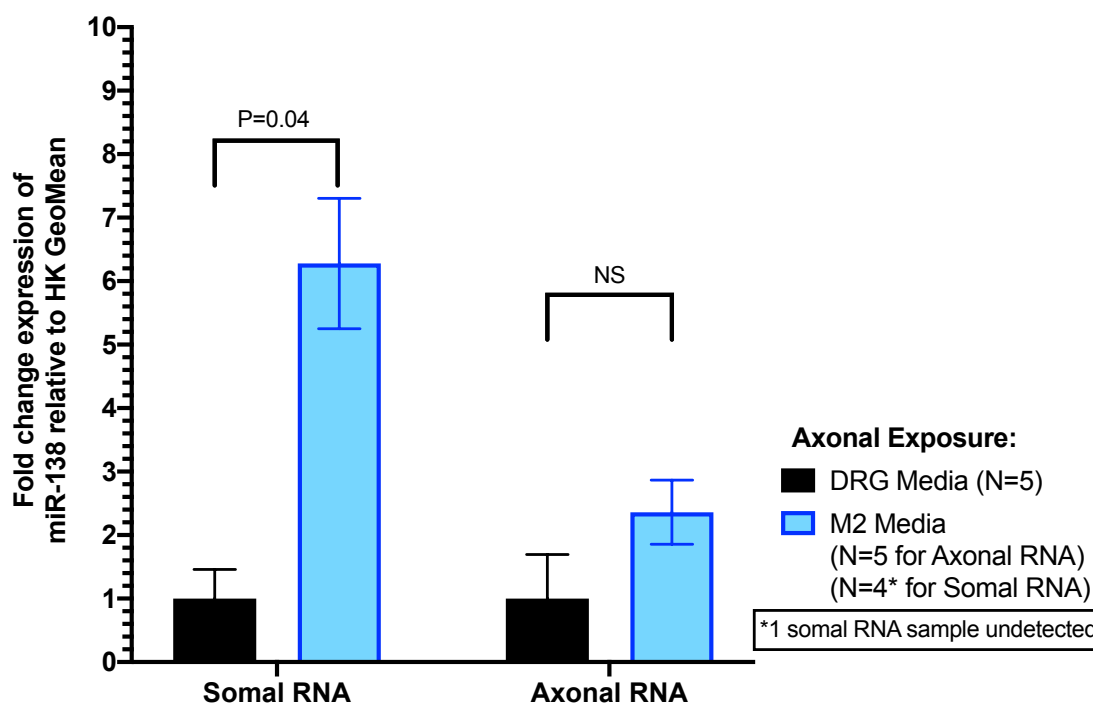


Figure 5.3.2: Exposure of axons to inflammatory media significantly increased the expression of miR-138-5p in the soma

A direct comparison between axonal and somal fragments at N=5 independent RNA extractions. One somal sample was undetected following axonal exposure to M2-like media, and therefore this bar represents N=4. Bars represent mean fold change \pm SEM using the ddCT method. Housekeeper values for miR133b of CT=34.8 and 39.9 were removed from analysis prior to calculation of the fold change where the average CT was 24-29. Figure shows results of a one-way ANOVA from grouped data where $F(3, 15) = 2.334$.

A post-hoc Holm-Sidak's multiple comparisons test was also used to compare exposure to DRG media or M2-like media. $P < 0.05$ was deemed significant. Soma expression of miR-138-5p increased 6.3x on average, if the corresponding axons were exposed to M2-like media ($P=0.03$, DRG exposure N=5, M2-like exposure N=4.)

The effect of anti-inflammatory media on upregulating miR-138-5p was further investigated. Figure 5.3.2 refers to 5-independent RNA extractions, from 5 embryo preparations, where

each Twiss insert utilised one dissociated embryo. In one biological repeat miR-138-5p was not detected in the somal compartment following axonal exposure to M2-like media (N=4.)

Results showed that there was a quantifiable and significant increase in somal miR-138-5p if axons were exposed to M2-like media (figure 5.3.2, results of a one-way ANOVA with multiple comparisons.) This *in vitro* model of inflammation was used to demonstrate that the exposure of axons to anti-inflammatory mediators induced upregulation in somal miR-138-5p expression.

5.3.3 Functional analysis of the dual effect of inflammatory mediators and miR-138-5p on neuronal excitability:

Having shown that inflammatory mediators could change localised expression of miR-138-5p, we investigated the effect of the inhibition of miR-138-5p on neuronal excitability. *In vivo* modelling has shown that miRs are involved in the regulation of inflammatory pain-based signalling by the translational inhibition of protein on the neuronal terminals (Zhao, M.-C. Lee, *et al.*, 2010). *In vivo* models of hyperalgesic priming have also shown that translational inhibition (e.g. treatment with either cordycepin or rapamycin) targeted at the peripheral terminals can reduce sensitisation of the nociceptors (Ferrari *et al.*, 2013). In this study it was also shown that injection with anisomycin (protein translation inhibitor) prevented induction of hyperalgesic priming, suggesting that ongoing local peripheral translation is essential in both the development and maintenance of chronic pain. The capacity to investigate these localised changes *in vitro* has been limited until recently due to the nature of standard dissociated cultures. In this experiment, compartmentalised microfluidic cultures were exposed to inflammatory macrophage media at the same time as the miR-138-5p inhibitor. It was hypothesised that the incubation of peripheral terminals with inflammatory media in conjunction with axonal inhibition of miR-138-5p could promote an increase in excitability of the neurons.

The schematic in figure 5.3.3 shows how the miR-138 power inhibitor was applied to microfluidic devices in which the axonal compartment was also exposed to polarized macrophage media (and the cytokines within) for 24 hours prior to stimulation.

If we refer back to Chapter 4 (figure 4.3.4) it was shown that prolonged incubation of the axons in polarized media reduced the overall excitability of neurons upon stimulation with KCL. The time-course in figure 5.3.3A shows that neuronal excitability was higher in cells incubated with the non-targeting probe (control) than the miR-138-5p inhibitor. The decrease in the amplitude of the response when the axons were incubated with the miR-138-5p inhibitor and M2-like media was not deemed to be statistically significant (figure 5.3.3C, $P=0.3557$ as shown by a one-way ANOVA with post-hoc Sidak's multiple comparison's test.)

Figure 5.3.3B shows a time-course analysis for axons incubated with either the non-targeting probe (control) or a miR-138 inhibitor in the presence of M1-like media. In this setup, those cells incubated with the miR-138 inhibitor were more excitable than the control. This increase in excitability was also not deemed to be statistically significant (also shown in figure 5.3.3C, results of a one-way ANOVA with post-hoc Sidak's test for correction of multiple comparisons, where $P=0.1672$)

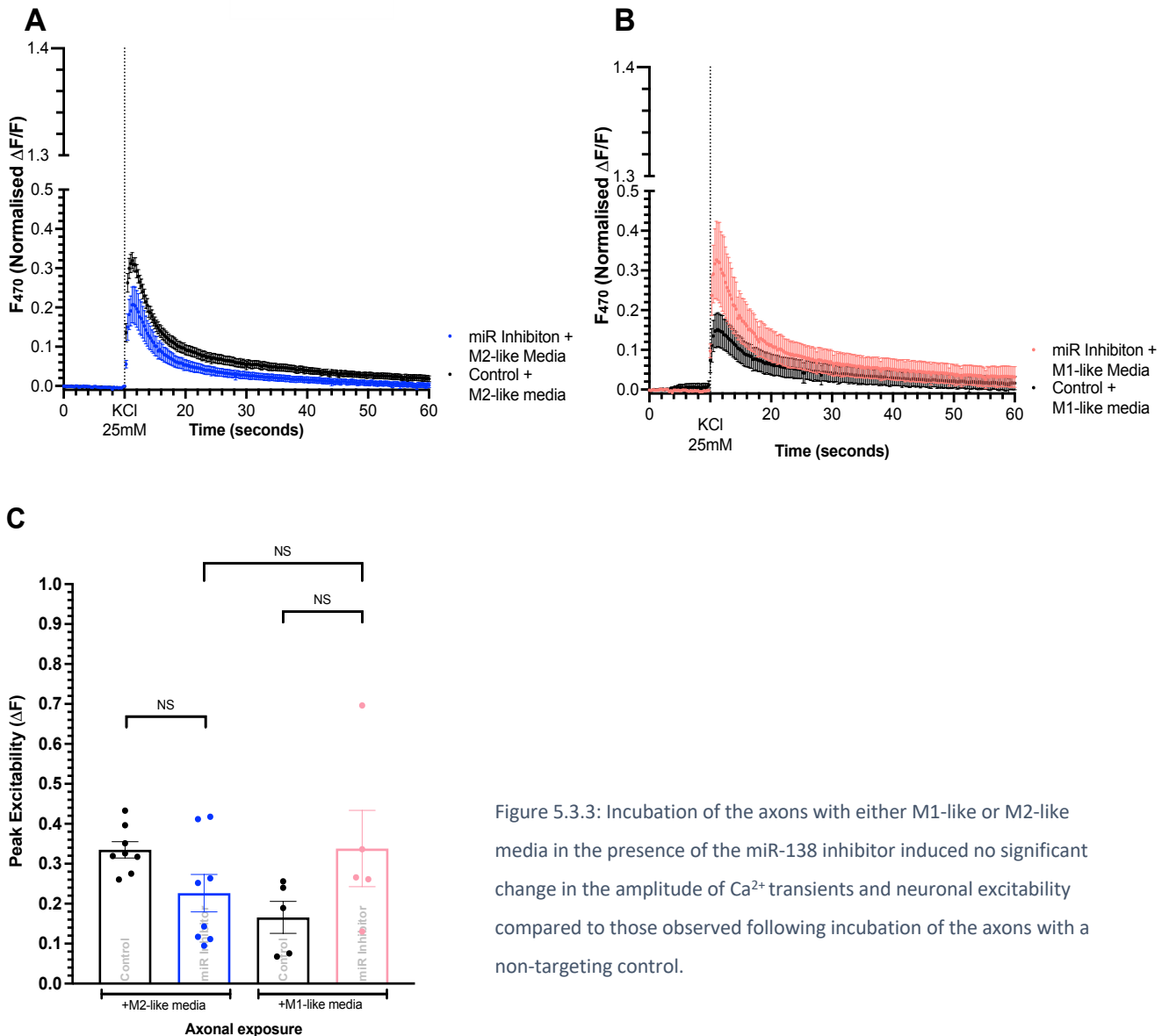
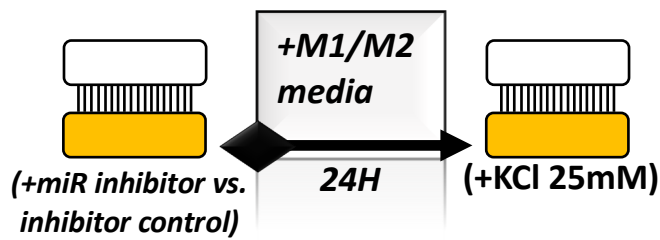


Figure 5.3.3: Incubation of the axons with either M1-like or M2-like media in the presence of the miR-138 inhibitor induced no significant change in the amplitude of Ca^{2+} transients and neuronal excitability compared to those observed following incubation of the axons with a non-targeting control.

- A) The effects of M2-like media and miR-138 inhibition in the axon on the modulation of DRG excitability as observed over a time-course of 60-seconds. Stimulation of the axonal compartment with KCL is shown at 10-seconds.
- B) The effects of M1-like media and miR-138 inhibition in the axon on the modulation of DRG excitability as observed over a time-course of 60-seconds. Stimulation of the axonal compartment with KCL is shown at 10-seconds.
- C) Results of a one-way ANOVA with post-hoc Sidak's correction for multiple comparisons showed no statistically significant difference between peak excitability of cultures incubated with inflammatory macrophage media and a non-targeting control probe, or the miR-138 inhibitor. $F(3, 22) = 2.573$, $N=5$ (M1-like exposure) and $N=8$ (M2-like exposure) biological replicates.

The peak excitability of neurons incubated with miR-138 inhibitor in the presence of macrophage media was also compared to the results previously observed when neurons were pre-cultured in macrophage media prior to stimulation with KCL (data extracted from figure 4.3.4.)

The average peak excitabilities have been compared in table 5.3.1 shown below:

Axonal exposure	miR Inhibitor (Peak Excitability (ΔF))	Inhibitor Control (Peak Excitability (ΔF))	Absolute Control (Peak Excitability (ΔF))
M1-like Media	0.33	0.16	0.17
M2-like Media	0.22	0.33	0.085

Table 5.3.1: Comparing average peak amplitude of evoked Ca^{2+} recorded dependent on axonal culture conditions. All axons were stimulated with KCL. Inhibitor control refers to a non-targeting control probe.

If the DRG media in the axonal compartment was changed for media extracted from pro-inflammatory cells (M1-like phenotype) then the peak excitability was unchanged between addition of the inhibitor control or the absolute control.

However, the amplitude of evoked Ca^{2+} transients recorded following incubation with the miR-138 inhibitor was increased. Co-incubation of miR-138 inhibitor and M1-like media in the axonal compartment increased excitability of the neurons.

In comparison, if the axonal compartment was exposed to M2-like media and the inhibitor control, the average peak excitability was increased relative to the absolute control. The amplitude of the response following incubation with the miR-138 inhibitor was also higher than the absolute control, but was lower than incubation with the inhibitor control. Co-incubation of miR-138 inhibitor and M2-like media in the axonal compartment changed the excitability of the neurons.

In line with the objectives for this chapter, the following conclusions can be drawn from this:

1. The expression of miR-138-5p in the soma was increased when the axons were exposed to M2-like media as demonstrated by the qPCR in figure 5.3.2

2. The excitability of DRG neurons was increased if the axonal compartment was cultured in M2-like media and either an miR-138-5p cell permeable inhibitor or the inhibitor control.
3. The excitability of DRG neurons was only increased if the axonal compartment was cultured in M1-like media and the miR-138-5p cell permeable inhibitor.

It could be hypothesised that the induced increase in miR-138-5p from exposure to M2-like media was counteracted by the addition of the miR-138 inhibitor. This could explain why the excitability of the cells cultured in M2-like media was reduced when incubated with the miR-138-5p inhibitor compared to the non-targeting control probe.

To continue this investigation into the effects of inflammatory mediators and sensitisation, it would have been interesting to determine the effects of miR-138 inhibition in the somal compartment of microfluidic devices where the axons are exposed to polarized macrophage media.

This study showed that inflammatory mediators changed the expression of miR-138-5p in the soma. This increased expression of miR-138-5p was also shown to affect neuronal excitability. The next step was to investigate mechanisms by which changes in miR-138-5p expression could regulate excitability of the neurons using compartmentalised microfluidic devices.

5.4 Part B: Molecular and cellular analysis of the mechanisms underlying the effect of miR-138-5p on sensitization of peripheral neurons:

In Chapter 4 it was demonstrated that axonal stimulation of untreated microfluidic cultures stimulated with KCL induced an increase in evoked Ca^{2+} transients recorded at the soma. In Chapter 5, part A it was shown that inhibition of miR-138-5p affected neuronal excitability. The increase in fluorescence observed was representative of an increase in free cytosolic Ca^{2+} . The delay following axonal stimulation of a microfluidic device likely reflected the time taken for action potentials to propagate from the nerve terminals and induce a Ca^{2+} response.

In this study the role of miR-138-5p in local protein translation and modulation of neuronal cell excitability was further investigated. Microfluidic chambers were cultured until axons extended through the microgrooves and covered the axonal compartment >50%. Previous work from the Dajas-Bailador lab suggested that optimal time for use of microfluidic devices was between DiV5-8 dependent on the nature of the study (Lucci *et al.*, 2020). In this model the media was removed and replaced with media supplemented with a cell permeable protein inhibitor for miR-138, at a final assay concentration of 100nM. Due to the compartmentalised microfluidic nature of the devices the inhibitor was either applied localised to the axons, or the soma and the downstream effect on neuronal excitability was quantified.

5.4.1 Part B objectives:

- **Use local application of a miR-138-5p inhibitor in a microfluidic model to investigate a) the effect of miR-138-5p expression on neuronal excitability and b) the mechanism of action by which miR-138-5p induces changes in neuronal signalling.**
- **Identify and isolate potential downstream targets of interest for miR-138-5p**
- **Validate targets based on seed sequence expression in the 3'UTR and interaction with miR-138-5p.**
- **Investigate the effects of target protein expression on cell excitability using siRNA**

5.4.2 Inhibition of miR-138-5p expression in the axonal compartment of compartmentalised microfluidic devices reduced evoked Ca²⁺ transients and changes in neuronal excitability:

The schematic in figure 5.4.1 below shows an overview of the experimental setup where only the axons were stimulated with KCL. Figure 5.4.1A shows a visual representation of how the amplitude of neuronal response to stimulation was reduced where a miR-138-5p inhibitor was added to the axons (relative to the control chambers where a non-targeting miRNA probe control was added.)

To quantify this reduction in excitability, an unpaired t-test was used to compare the KCL-evoked peak excitability between cultures. Figure 5.4.1B shows that there was a significant decrease in peak excitability in neurons where the miR-138 inhibitor was added to the axonal compartment. (A comparison including the baseline has also been included in the supplementary data, using a one-way ANOVA to compare the baseline fluorescence to the peak fluorescence recorded.)

Both treatments showed a rapid increase in fluorescence upon stimulation, but the duration of the responses returned to near baseline by the end of the 60-second recording. The decreased excitability in those axons incubated with the miR-138-5p inhibitor was reflected in the reduced AUC relative to the control (figure 5.4.1C.)

Results also showed that unlike untreated populations of DRGs stimulated with KCL, both the treatments with the power inhibitor control or the miR-138 inhibitor reduced the overall amplitude of the Ca²⁺ response. This effect was observed across multiple cell preparations and was deemed to not be an artefact of specific tissue showing reduced excitability in the presence of KCL. These results demonstrated that the effect of miR-138 inhibition on reducing cellular excitability was not resultant from manual addition of a substrate to the cell, but reflected a “true” decrease in excitability when miR-138 activity was blocked in the axonal compartment. (Average peak amplitude (\pm SD) of an absolute control was $0.64 \pm 0.45\Delta F$ at N=6

biological repeats, see chapter 4 section 4.2.1. In comparison the peak amplitude following addition of miRNA non-targeting control probe was $0.35 \pm 0.18 \Delta F$ at N=12.)

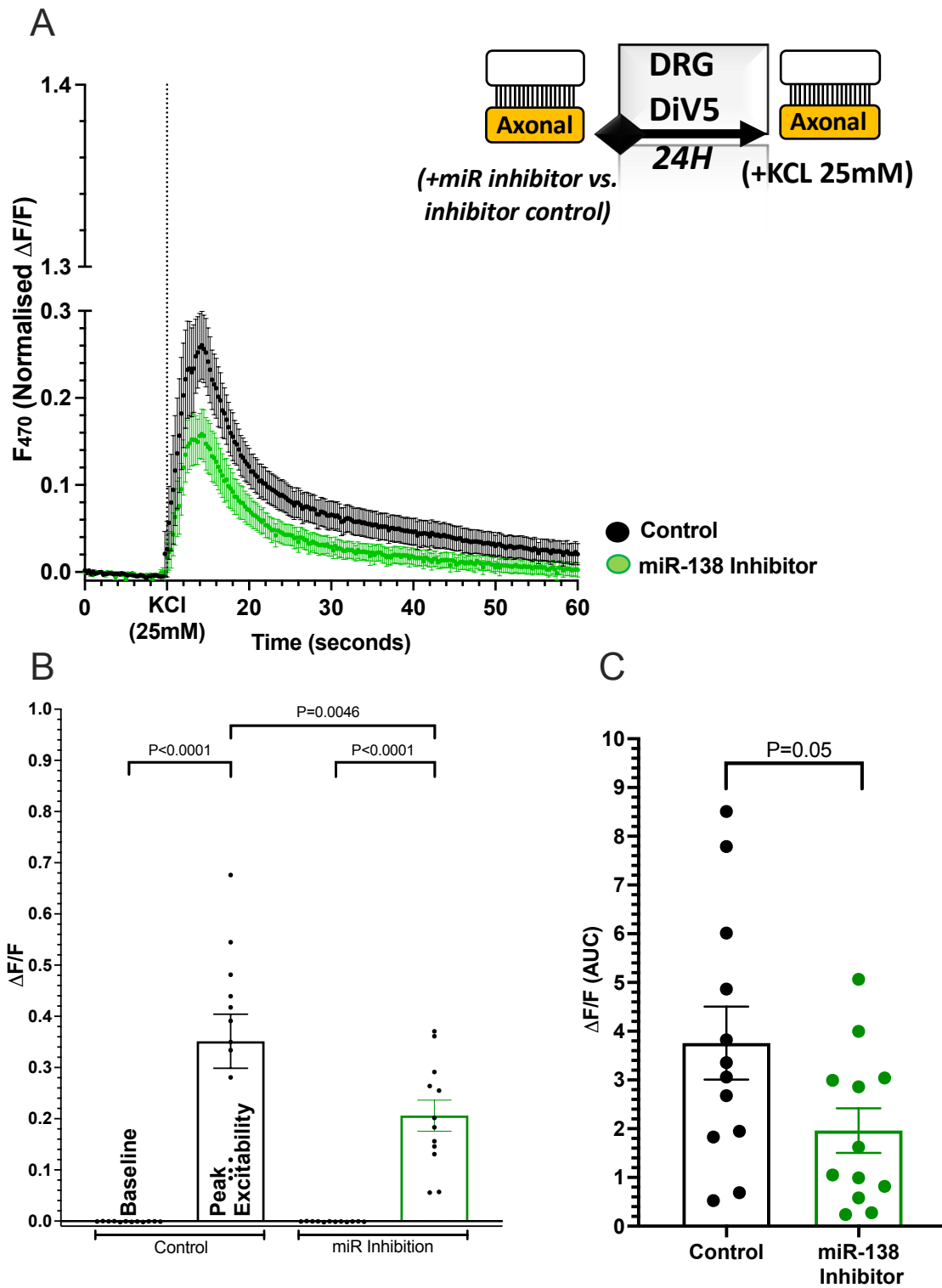


Figure 5.4.1: miR-138 inhibition in the axonal compartment induced a significant decrease in Ca^{2+} transients in the soma following axonal stimulation with KCL (25mM): Legend continued overleaf...

- A) Time-course analysis with stimulation by KCL shows that amplitude in response of cells incubated with a miR inhibitor was reduced relative to the control population.
- B) Increase in fluorescence (following stimulation) was statistically reduced following incubation with a miR-inhibitor. One-way ANOVA with multiple comparisons showed a statistically significant reduction in the excitability of those cultures incubated with a miR-138 inhibitor in the axonal compartment ($P=0.0046$). Significance threshold $P<0.05$, showing representative data from $N=12$ independent biological repeats. $F(3,44)=31.9$ for comparison between treatments. Post-hoc Holm's-Sidak test for multiple comparisons also demonstrated significant increase from baseline excitability irrespective of the axonal treatment.
- C) The AUC also showed a significant decrease in neuronal excitability following stimulation with KCL of cultures incubated with a cell permeable miR-138 inhibitor. Unpaired t-test with Welch's correction showing $P=0.05$. Error showing mean \pm SEM where significance threshold was $P<0.05$. Comparison of variance showed $F(11, 11)= 2.662$ where $P=0.119$.

The same protocol was subsequently repeated using stimulation of the axonal compartment with Capsaicin (200nM) to selectively stimulate TRPV1⁺ neurons. Although TRPV1 is expressed as early as E12.5, expression levels are not complete until around post-natal day 2. Our previous experiments had shown that there was a transient change in fluorescence when Capsaicin was applied to the axonal compartment of E16.5 DRG neurons. In a similar way to the results observed following stimulation with KCL, axonal stimulation with capsaicin induced a rapid and transient increase in cytosolic Ca²⁺.

The time course analysis in figure 5.4.2A (below) shows how fluorescence of the control population and the treated cells had returned to a stable baseline by the end of a 60-second recording period. Following stimulation with capsaicin, the amplitude of the responses of cells treated with the non-targeting miRNA control probe or miR-138 inhibitor overlapped (figure 5.4.2A.)

There was no statistically significant difference between the amplitude of the response of the control treatment population, and those cells in which miR-138 was inhibited in the axons (figure 5.4.2B.) Moreover, there was no significant reduction in amplitude of the response compared with the axonal stimulation of empty microfluidic cultures (Chapter 4, figure 4.2.3 where average peak excitability was 0.23 Δ F.)

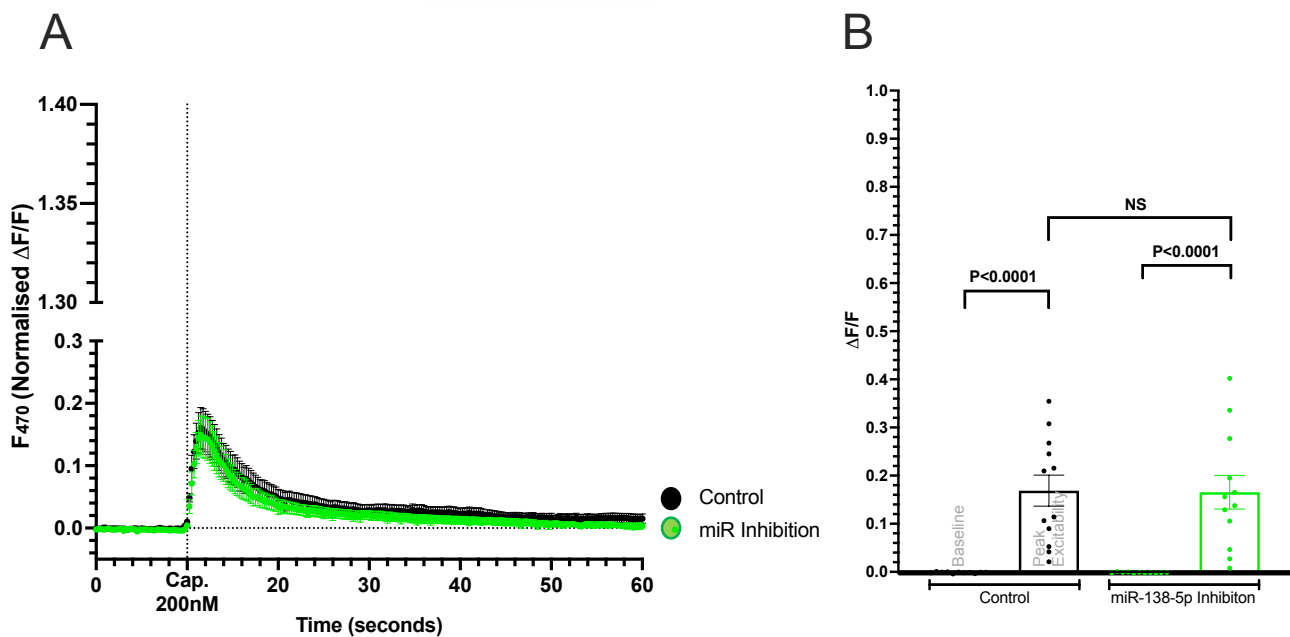
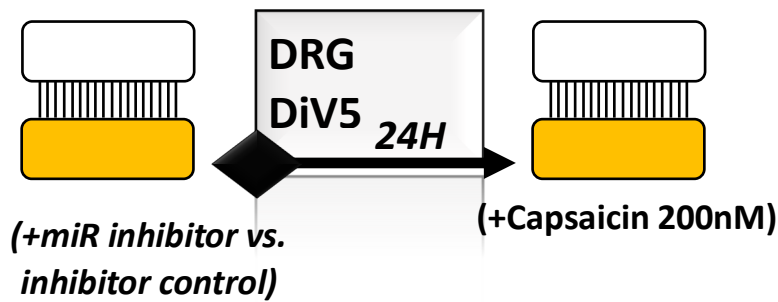


Figure 5.4.2: miR-138 inhibition in the axonal compartment did not induce a significant decrease in Ca²⁺ transients recorded in the soma following axonal stimulation with Capsaicin (200nM):

A) Time-course analysis with stimulation by Capsaicin shows that amplitude in response of cells incubated with a miR inhibitor was not significantly reduced relative to the control population. The change in fluorescence observed once again was used as a proxy for the change in excitability of the neurons.

B) Excitable response following stimulation was not significantly reduced following incubation with a miR-inhibitor and stimulation with Capsaicin. One-way ANOVA showed no statistically significant effect of miR-138 inhibition when stimulating the axonal compartment with capsaicin $F(3, 42) = 15.20$, where $P = 0.99$ as shown by multiple comparisons. Post-hoc Sidak's multiple comparison's also showed that the increase in excitability from baseline was always statistically significant ($P < 0.001$) irrespective of the axonal treatment. Representative of $N = 11$ biological repeats, where bars represent mean \pm SEM.

The results of figures 5.4.1 and 5.4.2 suggested a selective role for miR-138-5p in regulating the excitability of small diameter DRG neurons. The stimulation with Capsaicin did not demonstrate any significant difference in the excitability of cells incubated with or without the miR-138 inhibitor. Therefore, it was hypothesised that the effect of miR-138 was localised to neurons more closely resembling A-fibres.

It was also hypothesised that the effect of miR-138-5p was local to the axon. Therefore, it was predicted that inhibition of miR-138-5p in the soma would not induce a reduction in cell excitability following axonal stimulation of neurons. Microfluidic devices were cultured to DiV5, at which point the media was changed and the miR-138 inhibitor was added to the somal compartment for 24H. Following this, a stimulus was locally applied to the axonal compartment.

Figure 5.4.3 shows the resultant change in fluorescence following somal inhibition of miR-138 and subsequent axonal stimulation with KCL (25mM). The time-course in figure 5.4.3A shows that there was no difference in the KCL-evoked response when comparing the control group to those cells incubated with miR-138 inhibitor. Figure 5.4.3B shows that there was also no significant decrease in the KCL-evoked peak excitability of cells treated with a miR-138 inhibitor versus the negative control. It was also shown that axonal stimulation with KCL still evoked a significant increase in Ca^{2+} transients recorded from baseline. Therefore, the somal incubation with miR-138 inhibitor did not decrease viability of the neurons. This result further supported the evidence that miR-138-5p was only affecting the excitability of the cell by acting locally in the axon terminal.

The effect of Capsaicin-evoked neuronal excitability following somal incubation with the miR-138 inhibitor was also studied. Figure 5.4.3C shows that there was no significant difference in the peak excitability of neuronal cultures incubated with either the miR-138 inhibitor or the non-targeting control in the somal compartment.

5.4.3 Inhibition of miR-138-5p in the somal compartment did not reduce KCl or Capsaicin-evoked increase in neuronal excitability:

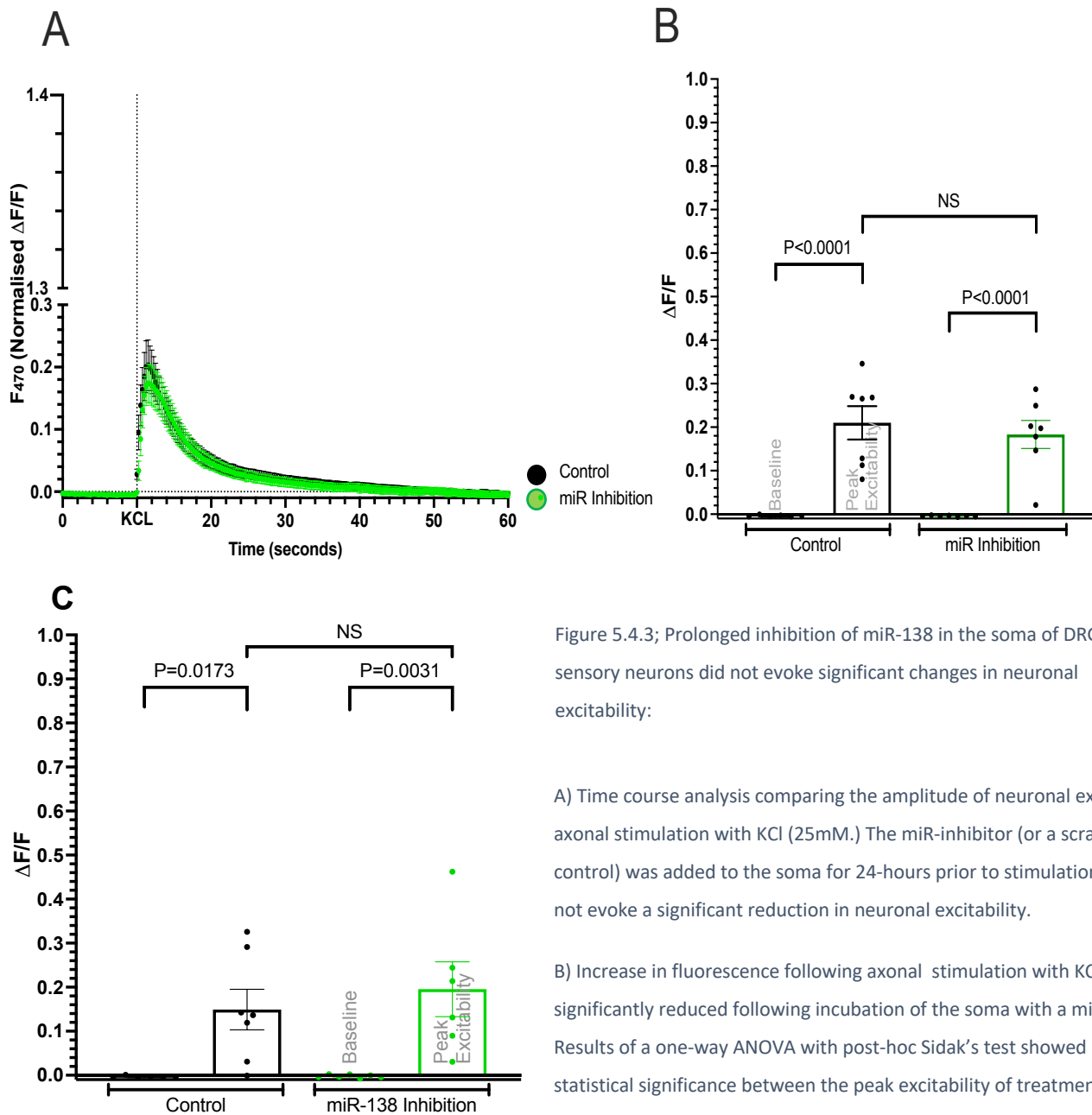
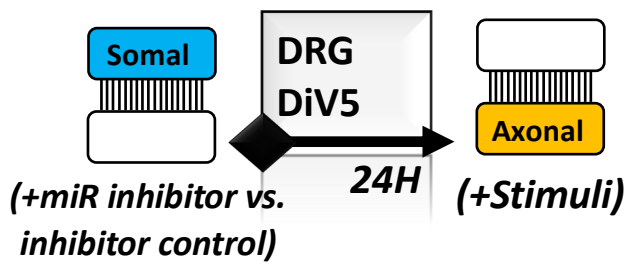


Figure 5.4.3; Prolonged inhibition of miR-138 in the soma of DRG sensory neurons did not evoke significant changes in neuronal excitability:

A) Time course analysis comparing the amplitude of neuronal excitability axonal stimulation with KCl (25mM.) The miR-inhibitor (or a scramble control) was added to the soma for 24-hours prior to stimulation and did not evoke a significant reduction in neuronal excitability.

B) Increase in fluorescence following axonal stimulation with KCl was not significantly reduced following incubation of the soma with a miR-inhibitor. Results of a one-way ANOVA with post-hoc Sidak's test showed no statistical significance between the peak excitability of treatments (NS) with P<0.05 significance threshold. N=7. Mean \pm SEM. F(3, 24)=21.79. Sidak's multiple comparisons showed a significant increase in fluorescence from baseline at P<0.0001 irrespective of the somal treatment.

(Legend continued overleaf)

Figure 5.4.3 C) Increase in fluorescence following axonal stimulation with Capsaicin was not significantly reduced following incubation of the soma with a miR-inhibitor. Results of a one-way ANOVA with post-hoc Sidak's test showed no statistical significance between the peak excitability of treatments (NS) with $P < 0.05$ significance threshold. $N=7$. Mean \pm SEM. $F(3, 23)=7.858$. Sidak's multiple comparisons showed a significant increase in fluorescence from baseline at $P=0.0031$ for somal incubation with the miR-inhibitor, versus $p=0.0173$ following incubation with a non-targeting inhibitor control probe..

In the final experimental setup, the somal compartment was incubated with miR-138 inhibitor for 24-hours prior to direct somal stimulation with either KCL at 25mM or Capsaicin at 200nM.

The time-course in figure 5.4.4A shows how there was a rapid increase in cell excitability following direct stimulation of the soma with KCL. The amplitude of the response was higher than the amplitude of KCL-evoked Ca^{2+} transients recorded at the soma following axonal stimulation (figure 5.4.4.) The increase in excitability from baseline was deemed significant irrespective of what treatment the soma were incubated with.

However, there was no significant difference between the peak excitabilities recorded following somal incubation with the miR-138 inhibitor or the non-targeting inhibitor control probe (figure 5.4.4B.) The direct stimulation of the soma with capsaicin following somal inhibition of miR-138-5p also did not induce a significant change in cell excitability relative to incubation with a non-targeting miRNA probe control (figure 5.4.4C.)

Somal inhibition of miR-138-5p demonstrated higher amplitude in response if stimulated with Capsaicin than KCL. The following conclusions can be drawn from this data:

miR-138-5p is involved in regulating excitability of the small fibres of the DRG. The effects of miR-138-5p most likely targets A-fibres since inhibition of miR-138 did not induce any significance changes in Capsaicin-evoked excitability (relative to treatment with a negative control). Based on this data it could be hypothesised that miR-138-5p has roles in regulating cellular excitability via local translation, most likely regulating neuronal conductance (e.g. potassium signalling) in small fibres of the DRG

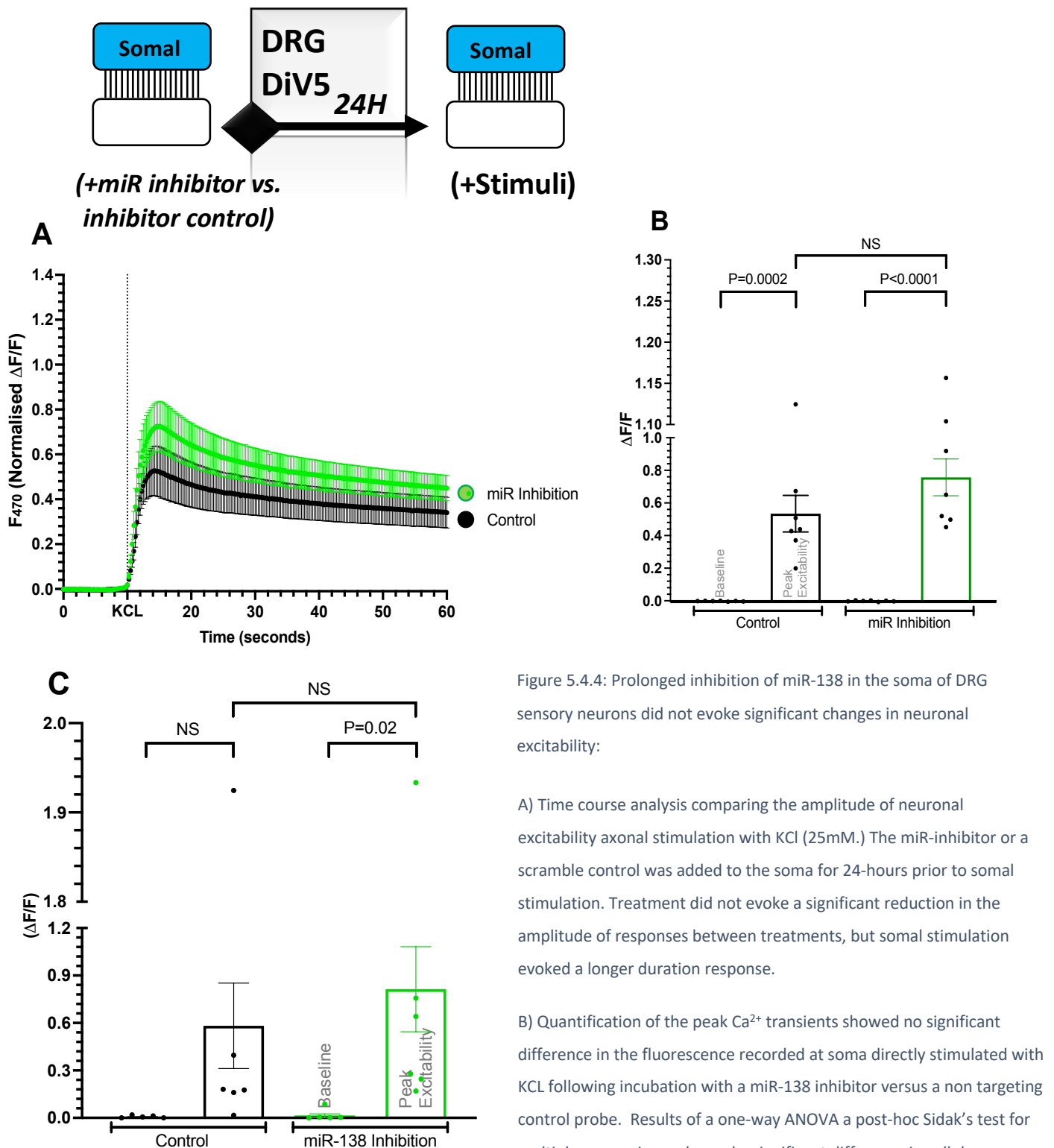


Figure 5.4.4: Prolonged inhibition of miR-138 in the soma of DRG sensory neurons did not evoke significant changes in neuronal excitability:

A) Time course analysis comparing the amplitude of neuronal excitability axonal stimulation with KCL (25mM.) The miR-inhibitor or a scramble control was added to the soma for 24-hours prior to somal stimulation. Treatment did not evoke a significant reduction in the amplitude of responses between treatments, but somal stimulation evoked a longer duration response.

B) Quantification of the peak Ca^{2+} transients showed no significant difference in the fluorescence recorded at soma directly stimulated with KCL following incubation with a miR-138 inhibitor versus a non targeting control probe. Results of a one-way ANOVA a post-hoc Sidak's test for multiple comparisons showed a significant difference in cellular excitability irrespective of the somal treatment with miR-138 inhibitor. As shown, $P=0.02$ following incubation with the miR-138 inhibitor. $F(3, 24)= 23.40$, with significance threshold at $P<0.05$. $N=7$ biological replicates showing mean \pm SEM.

Continued overleaf...

Figure 5.4.4 C) Quantification of the peak Ca²⁺ transients showed no significant difference in the fluorescence recorded at soma directly stimulated with Capsaicin following incubation with a miR-138 inhibitor versus a non targeting control probe. Results of a one-way ANOVA a post-hoc Sidak's test for multiple comparisons showed a significant difference in cellular excitability irrespective of the method of culture. As shown, P=0.02 following incubation with the miR-138 inhibitor. F(3, 23)= 4.314, with significance threshold at P<0.05. N=7 biological replicates showing mean ±SEM.

5.4.4 Bioinformatic prediction for targets with roles in regulating neuronal excitability by interaction with miR-138-5p:

Addition of the miR-138 inhibitor to compartmentalised microfluidic devices had demonstrated a clear role for miR-138-5p in regulating neuronal excitability. The inhibition of miR-138-5p only induced a significant decrease in neuronal excitability if the axonal compartment was incubated with the miR-138 inhibitor and the subsequent KCL stimulus was locally applied to the axons. As such it was hypothesised that miR-138-5p has roles in regulating neuronal excitability via local translation, most likely via regulation of membrane conductance. Since microRNAs are known to inhibit translation of mRNAs, a bioinformatic search was conducted to attempt to identify a protein target of interest that would help to explain the mechanism of miR-138-5p in regulating neuronal excitability.

Initial attempts to identify a target for miR-138-5p included a conservative search and comparison of multiple bioinformatic prediction tools, each of which uses a different algorithmic model. Preliminary searches included MirGate, Diana Tools microT-CDS at inclusion threshold 0.7, (Paraskevopoulou *et al.*, 2013a) Tarbase (26 targets,) (Karagkouni *et al.*, 2018) TargetScan v7.2 (Agarwal *et al.*, 2015) and miRTarBase (14 targets) (Hsu *et al.*, 2011).

At a threshold of 0.7, DIANA tools identified 556 targets potentially associated with miR-138-5p, where at 0.8 the predicted list was reduced to 267 targets. All targets that appeared in DIANA tools were converted from a transcript ID to a gene ID and cross-referenced with a list of results from a second bioinformatic database. When using TargetScan (v7.2) 630 transcripts were initially identified, although some of these were later identified as “false

positives” where the seed sequence was predicted but not present in the 3’UTR. Between TargetScan and DIANA tools, 122 targets overlapped. From here a species conservation list was produced, where each target was cross-referenced for prediction with rat and human tissue. This yielded a list of 16 targets:

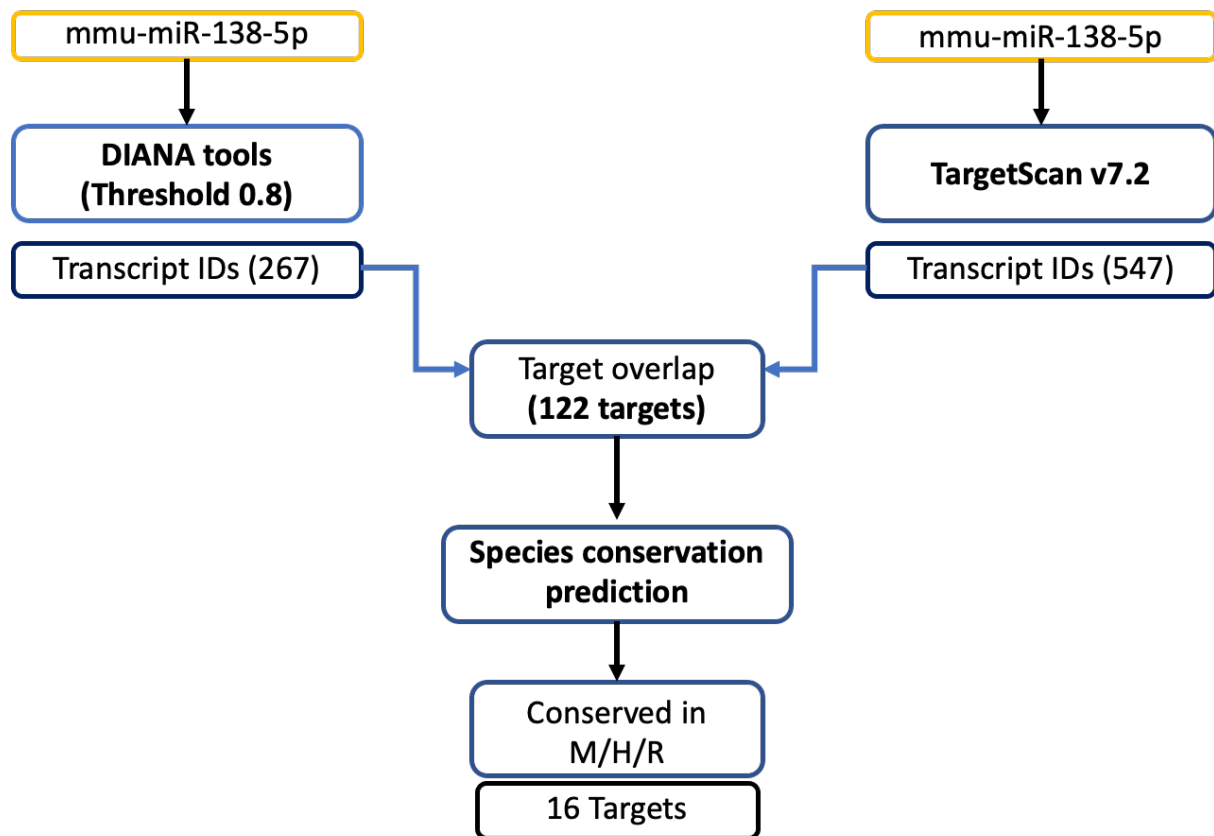


Figure 5.4.5: Developing a pipeline for bioinformatic searches of predicted targets overlapping with miR-138-5p.

From the 16 genes identified, the proteins identified were suggested to be involved in up to 45 biological processes including 4 genes involved in cell signalling and 4 genes involved in ‘response to stimulus.’ These included hits such as Calcipressin-2, involved in the signal transduction of calcium, and sodium channel beta subunits, which modulate channel conductance and action potential propagation. Furthermore, 7 protein classes were identified in this list, including intercellular signalling proteins, transmembrane signalling and transport proteins. Although the 16-targets identified appeared to have some roles in signal transduction, based on the results of the calcium assay previously described in this chapter, it was deemed that voltage-gated sensitive channels were potentially of high interest for this project, with particular regards to peripheral sensitisation. With the capacity to change the

search parameters of DIANA tools (Paraskevopoulou *et al.*, 2013b) to include even those targets most lowly predicted targets, a second more biased search was conducted based on the results observed with the miR-138-5p inhibitor in Ca²⁺ signalling assays. A target was only deemed suitable if it was endogenously expressed by E16.5, where protein expression often begins in the embryo, but may not peak until post-natal development.

This time the parameters on Diana tools microT-CDS were widened to include a prediction threshold of 0.1, in order to locate all potential voltage-gated targets containing the seed sequence of miR-138-5p. This search included calcium, potassium and sodium channels in line with the hypothesis that miR-138-5p has roles in signal transduction, and potentially regulates membrane conductance during states of hyperalgesia.

A list of potential targets was created based upon reported expression of a) the seed sequence for miR-138-5p in the 3'UTR, and b) known expression of the relevant protein on fibres of the DRG. Only those channels with multiple predicted seed sequences in the 3'UTR were carried forward, and the 3'UTR was manually searched to confirm expression of the sequence. It was noticeable that the DIANA prediction did not always accurately reflect the presence of the seed sequence in the 3'UTR. Those targets highlighted on figure 5.4.6 below were deemed the most appropriate for this study based on selective and localised expression throughout the DRG fibres.

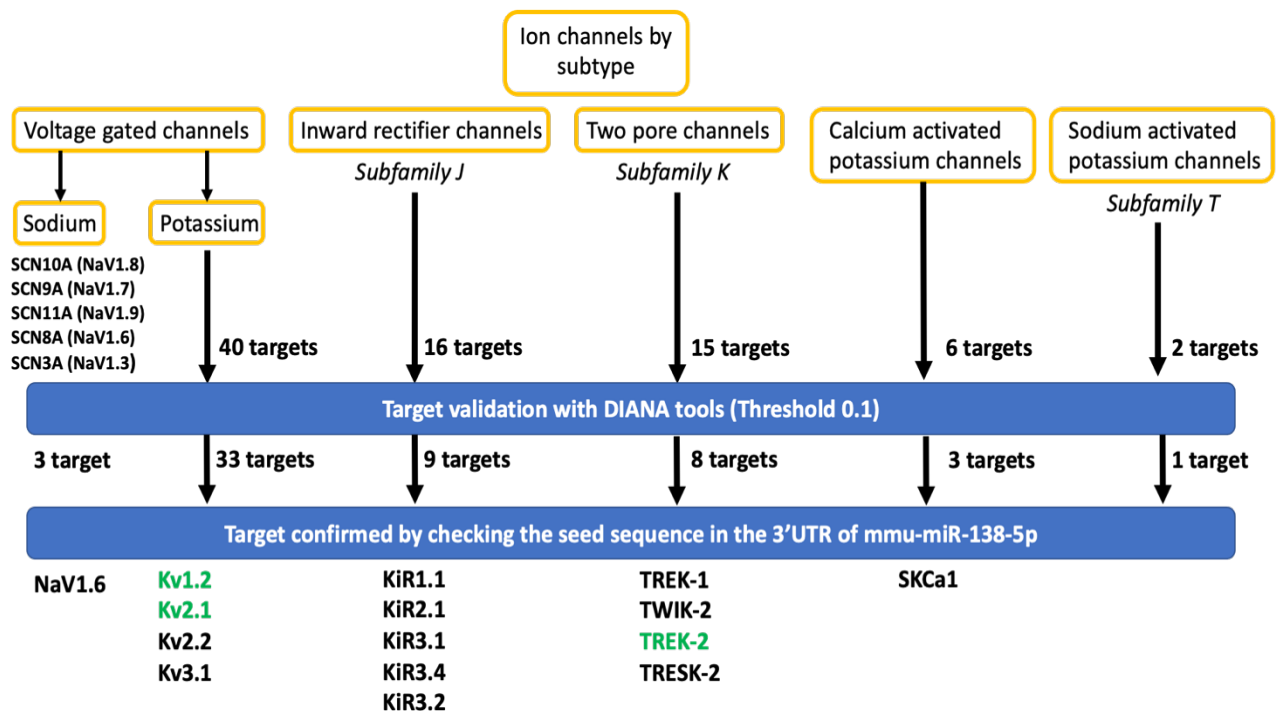


Figure 5.4.6: Based on seed sequence expression in the 3'UTR, ion channels of interest were shortlisted and subsequently validated as predicted targets of miR-138-5p.

5.4.4.1 Identifying which channels to investigate:

The work by Tsantoulas and McMahon described in Chapter 1, figure 1.4 (Tsantoulas and McMahon, 2014) gives a comprehensive overview of the suggested expression patterns of multiple voltage-gated channels throughout the DRG fibre subtypes. In Chapter 1.7 I have also discussed the role for different subtypes of both Kv and NaV channels throughout the changing phases of the action potential. Understanding which channels are affected by a nociceptive stimulus may help to determine how miR-138-5p potentially regulates neuronal excitability of the DRGs.

5.4.4.2 SCN family:

There are 13 members of the genes incorporating voltage-gated sodium channel family (SCN genes) including the large α -subunit and a potential additional β -subunit. These voltage-gated sodium channels are essential in the initiation and propagation of action potentials, although they can be further sub-categorized dependent on the chromosomal expression (Yu and

Catterall, 2003) and sensitivity to tetrodotoxin (TTX). In adult neurons the roles of NaV1.1, NaV1.6, NaV1.7, NaV1.8 and NaV1.9 have been established in regulating sensory neuron excitability in pain-based signalling. Furthermore, changes to the expression pattern or alterations to genetic variants of NaV1.7, NaV1.8 and NaV1.9 have all been linked to small fibre neuropathies. However, in those channels screened, the seed sequence for miR-138-5p was only identified in the 3'UTR of NaV1.6.

5.4.4.3 KCN family:

In a similar way, proteins of the voltage-gated potassium channel family were screened for known association with miR-138-5p. Of a total 40 channels screened, miR-138-5p was predicted to be associated with the regulation of 30 potassium channels. The 3'UTR for these candidates was manually searched to locate the seed sequence for miR-138-5p. Those channels showing multiple seed sequence expression for miR-138 were marked a good candidate for a luciferase assay.

Also included in this screening process was potassium activated calcium channels, voltage gated calcium channels, potassium inward rectifier channels and two-pore potassium channels.

A shortlist of candidate genes can be seen in table 5.4.1 below. Target genes were selected based on a) the TargetScan prediction with miR-138-5p, b) the expression of the seed sequence in the 3'UTR for miR-138-5p, c) the number of seed sequences expressed in the 3'UTR and d) literature based on the role of the target in nociception or neuronal excitability. For example, where Kv1.2 (KCNA2) has been documented to be selectively expressed in the A-fibres, TREK-2 (KCNK10) has been localised to IB4 positive C-fibres only. The DIANA tools

microT-CDS prediction is also included here, although the prediction rate does not always correlate with the prevalence of the seed sequence in the 3'UTR.

Predicted Targets with multiple seed sequences:			DIANA	Seed sequence in 3'UTR?	How many?		A fibres			C fibres		
							Peripheral terminals	Axon	Soma	Peripheral terminals	Axon	Soma
Voltage gated calcium channels	CACNG2	mmu-miR-138-5p	0.54820608	Y	2							
	CACNA1B	mmu-miR-138-5p	0.455010117	Y	2							
Voltage gated potassium channels	KCNA2	mmu-miR-138-5p	0.369008272	Y	5	Kv1.2	Y	Y	Y	N	N	N
	KCNB1	mmu-miR-138-5p	0.356515772	Y	2	Kv2.1	N	Y	Y	N	Y	Y
	KCNG1	mmu-miR-138-5p	0.528618788	Y	2	Kv6.1	N	N	N	N	N	N
Inward rectifier channels	KCNJ2	mmu-miR-138-5p	0.479757316	Y	2	Kir2.1						
	KCNJ9	mmu-miR-138-5p	0.358318028	Y	2	Kir3.3						
	KCNJ10	mmu-miR-138-5p	0.688974321	Y	2	Kir4.1						
Two pore channels	KCNK10	mmu-miR-138-5p	0.46439312	Y	4	TREK-2					Y	Y
	KCNK18	mmu-miR-138-5p	0.431115307	Y	1	TRESK-2						

Table 5.4.1: Shortlisted target genes for interactions with mmu-miR-138-5p. 4 potassium channels of interest have been highlighted based on expression in the A/C fibres of the DRG and predicted number of seed sequences in the 3'UTR.

Those targets used for cloning into the pmIRGlo vector have been highlighted in the table above. Only the targets highlighted in green (KCNK10/ KCNA2) were successfully cloned into the reporter and used in the luciferase assay with a miR-138-5p mimic.

5.4.4.4 Kv1.2:

The shaker protein Kv1.2 belongs to the delayed rectifier family of voltage-gated channels, which rapidly induce repolarization of the cell membrane following conduction of the action potential. Furthermore, there is evidence to demonstrate that the Kv1.2 protein is widely conserved between species including rat, human and mouse. The distribution of the Kv1.2 channel in murine neurons has been demonstrated to be uniform throughout the axons, terminals and cell body. However, as shown in Chapter 1 (Tsantoulas and McMahon, 2014) in mice these channels have been shown to be selectively expressed on the A-fibres of the DRG neurons.

Figure 5.4.7 below shows high levels of Kv1.2 expression both at the axonal terminals, and throughout the axon of the DRG neurons, although *in vivo* Kv1.2 is known to only localise to A-fibre subtype DRGs.

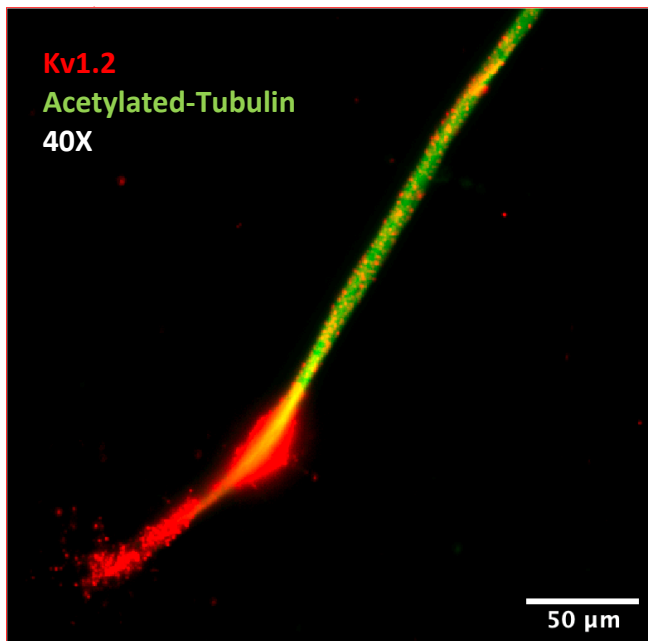


Figure 5.4.7: Dual staining immunofluorescence from a dissociated plate-based culture of DRG neurons at DiV5 showing high relative expression of Kv1.2 at the terminals (40X.)

Following axonal injury, the juxtaparanodal region becomes exposed and there is a high expression of Kv1 channels in this area. This may lead to a reduction in conduction velocity of these damaged neurons, as well as a potential sensory loss of function. Reduced functionality of channels in the Kv1 family potentially induces peripheral hyperexcitability where the axon does not repolarize as efficiently.

5.4.4.5 Two pore potassium channels:

Since one of the targets investigated (TREK-2, KCNK10) belongs to the two-pore- potassium channel family, I have further discussed the role of these channels in maintaining resting membrane potential. Where voltage-gated potassium channels are elucidated in the movement of potassium out of a depolarised membrane, the two-pore channel domain is predominantly determined by the electrochemical gradient of K^+ ions in the cell. Therefore, the K2P channels have a role in contributing to maintaining the background membrane potential (O'Connell, Morton and Hunter, 2002). Although there is relatively little homology between the intracellular N- and C- termini of the K2P channels, the short sequence of amino

acids forming the channel pores are highly conserved. These region makes the channel selective for K⁺ ion sensitivity, whilst allowing fast movement of ions across the cell membrane. Although not directly voltage-dependent, the K2P channel family are affected by a range of physiochemical variables. This is included but not limited to, changes in membrane potential, pH and surrounding temperature (Enyedi and Czirják, 2010). The first channel in the K2P family was identified in yeast in 1995 (Ketchum *et al.*, 1995), although since the TOK1 channel expresses eight transmembrane segments and is strongly outward rectifying, it is considered largely different from other members of the K2P channel family. In contrast, these channels, such as TREK-2, are acknowledged to possess 4-transmbrane domains and 2-channel pore forming subunits. As a “background K⁺ current” channel, the probability of these channels opening is not altered in response to changes in the membrane potential. Although K2P channels are weakly voltage-dependent they are predominantly considered ‘leak’ channels.

The first member of the TREK (TWIK-related K⁺ channel) family of proteins was discovered in 1996, followed by two further proteins including TREK-2 (Fink *et al.*, 1996) although the group is functionally diverse due to the presence of several splice variants. In particular alternative translation initiation in TREK-2 induces a long segment of the intracellular termini missing on this channel, and as such can affect the biophysical properties of the channel activity (Y. Kim *et al.*, 2001). Crucially, evidence has demonstrated that the TREK-2 channel is conserved between species, and is selectively expressed on the IB4-positive C-fibres of the DRGs (Acosta *et al.*, 2014; Viatchenko-Karpinski, Ling and Gu, 2018) making this protein a good candidate for a small-fibre pain-based study. Evidence from siRNA knockdown of the TREK-2 channel in *in vivo* murine studies demonstrated a role for TREK-2 in the hyperpolarization of the membrane of IB4-positive C-fibres (Acosta *et al.*, 2014). Moreover, *in vitro* studies demonstrated the expression of TREK2 as early as 2-days *in vitro*, suggesting the channel is not only expressed in mature DRG fibres.

5.4.5 Luciferase reporter assay:

Following the identification of predicted targets for miR-138-5p it was important to functionally validate these targets. The first step was cloning the 3'UTR region of interest into

the pmiRGlo vector containing the complementary seed sequence for miR-138-5p (as described in Chapter 2.4.4.1.) Following sequencing to confirm insertion of the primer into the pmiRGlo vector, a dual-luciferase reporter assay was carried out to confirm the interaction of miR-138-5p with the predicted target site in the 3'UTR.

Of the primers shown in Chapter 2.4.4.1, seven predicted target sites were eventually investigated for the capacity to act as functional targets using the luciferase assay (see chapter 2.4.4.2.2.)

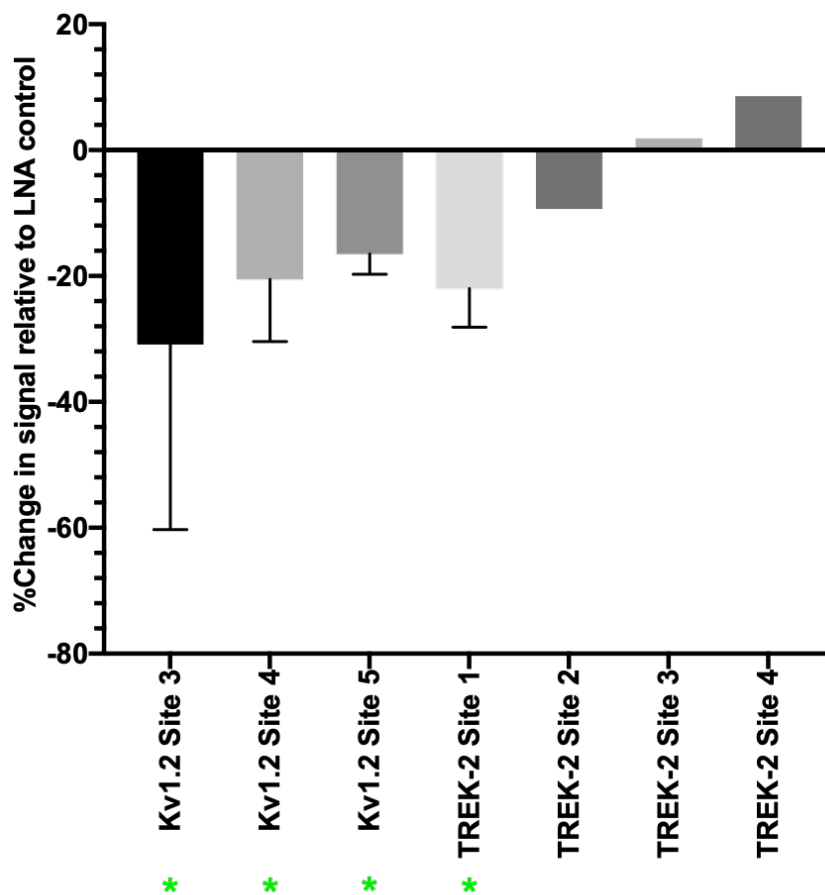


Figure 5.4.8: Preliminary results from a luciferase reporter assay at N=1: Results show %Change in fluorescence detected when cells were treated with 50nM miR-138 mimic for 48-hours. All 7-targets were previously validated using Sanger sequencing to locate the sequence of interest inserted into the pmiRGlo vector. Only the 4-targets marked with an asterisk were carried forward to N=4, where they showed reduction in fLuc activity in the dual luciferase reporter assay.

Cells were transfected with DNA inserted into pmiRGlo and treated with either the miR-138 mimic or a miR-control at 50nM for 48-hours prior to quantification of firefly luciferase signal. Preliminary tests included Kv1.2 site 3, Kv1.2 site 4, Kv1.2 site 5 and TREK-2 sites 1-4 as shown in figure 5.4.8. However, 3 target sites were identified as statistical outliers, demonstrating

very little (or a positive) change in fluorescence of the mimic relative to the control. Only 4 targets were carried forwards to investigate statistical significance of target interaction with miR-138-5p, as shown later in figure 5.4.9.

Of the 4 targets taken forward only two showed a statistically significant reduction in firefly luciferase activity, suggesting the miR-138 mimic was bound to the target site and protein translation was either repressed or degraded (see figure 5.4.9 A-D). The luciferase reporter assay was repeated to a minimum N=3 repeats to determine statistical significance of the reduction in firefly luciferase activity in each condition. Figure 5.4.9 below shows that only Kv1.2 site 4 and site 5 demonstrated a statistically significant decrease in fLuc activity. Since Kv1.2 is only expressed in A-fibres *in vivo*, this data further supported the hypothesis that miR-138-5p regulates excitability of the DRG neurons via local translation in A-fibres.

Following the preliminary validation of two target sites of interest via luciferase reporter, the primers for these target sites were mutated at the seed sequence to confirm the interaction with miR-138-5p. Via PCR the mutated primers were re-inserted into pmiR-Glo for use in a site directed mutagenesis recovery assay.

In the mutagenesis recovery assay, nucleotides in the seed sequence of miRNA interaction were replaced, but primers were designed according to standard melting point and GC%

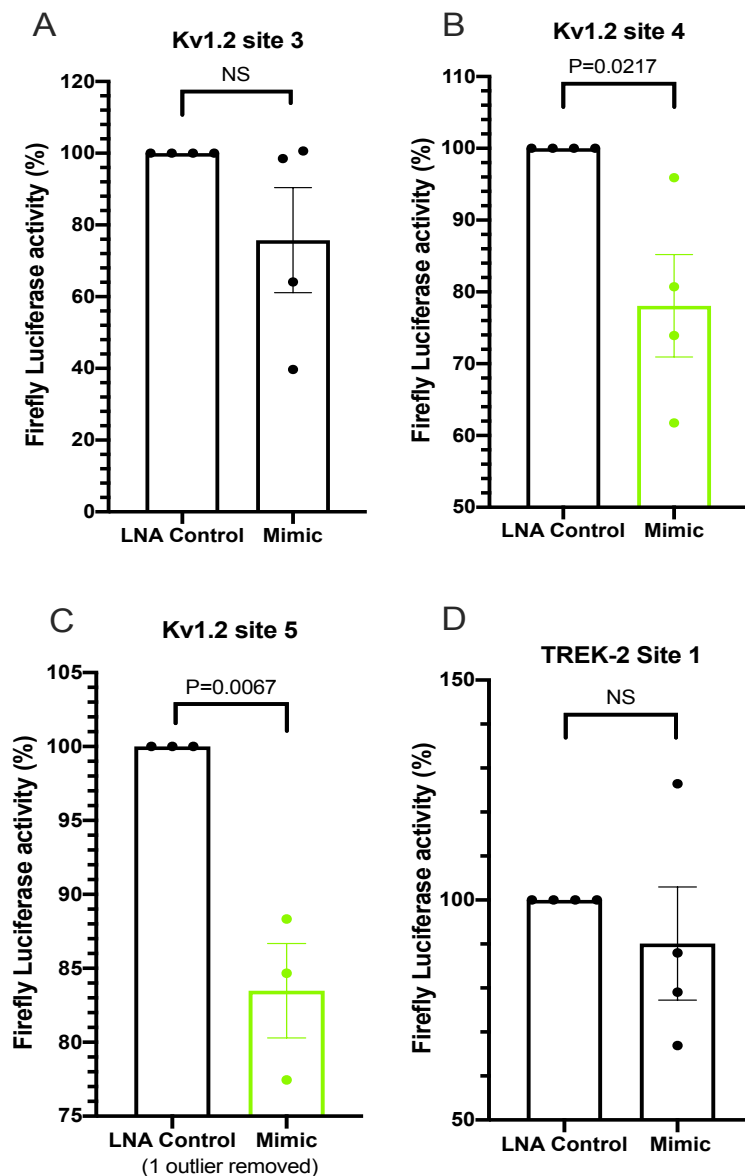


Figure 5.4.9: Transfection with miR-138 mimic and pmiRGlo with the target site inserted showed a reduction in firefly luciferase activity for four targets of interest.

Significance was determined using unpaired t-tests, where $P < 0.05$ was deemed statistically significant. Figures 5.4.9B (N=4) and figure 5.4.9C (N=3, 1 outlier removed) demonstrated a significant reduction in fLuc activity, and validated these as targets for miR-138-5p.

parameters. If the miRNA was truly targeting the Kv1.2 sites of interest, it was hypothesised that by mutating nucleotides in the seed sequence, the luciferase activity would be recovered following transfection with a mutated DNA sample.

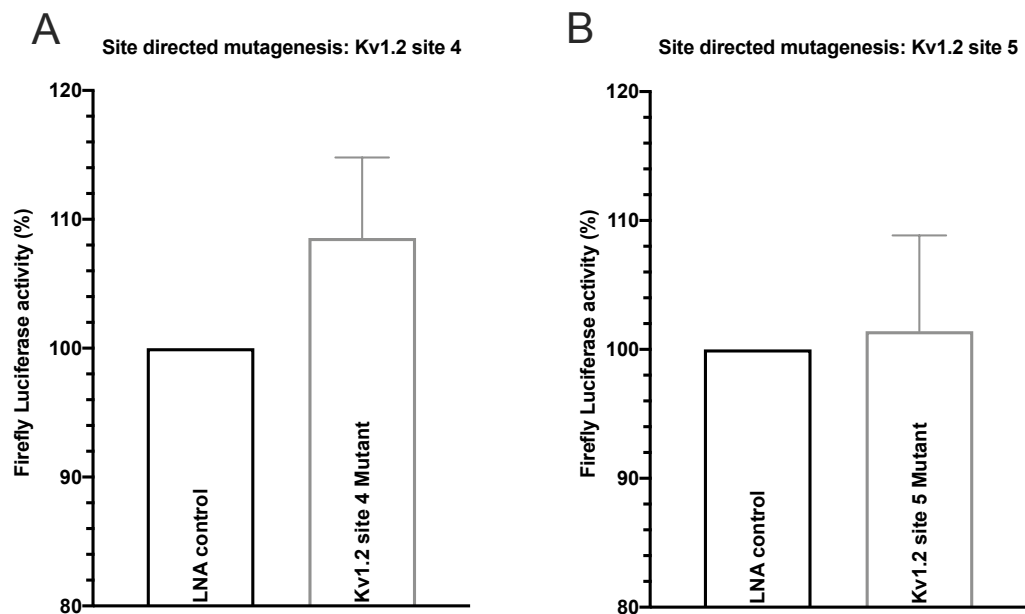


Figure 5.4.10: A site-directed mutagenesis assay demonstrated a loss of function with mutation of the seed sequence for miR-138-5p in the 3'UTR. Transfection with the miR-138 mimic and the mutated DNA sequenced did not induce a reduction in firefly luciferase activity in the dual luciferase assay, (N=3.) No significant difference in fLuc activity was detected between the LNA control and the SDM miR-138-5p targets, therefore validating the presence of a binding site in the 3'UTR of Kv1.2 for miR-138-5p.

Figure 5.4.10 demonstrates that the mutation in the seed sequence led to a reduction in miR-138-5p interaction with the target site on pmiRGlo, and confirmed the validity of the interaction of Kv1.2 with miR-138-5p. This was characterised by the increase in firefly luciferase activity to equal that of the results observed for the LNA control. This 'rescue' effect by mutation of the seed sequence of miR-138-5p, validated Kv1.2 as a target of interest. It was likely that in this context, the mutation in the seed sequence led to reduced interaction of the miR-138 mimic with the target mRNA, and consequentially reduced degradation the target mRNA.

5.4.6 Treatment of axons with small interfering RNA (siRNA) for Kv1.2 demonstrated partial rescue of the decrease in excitability induced by miR-138-5p inhibition:

At this point we had identified suitable target(s) of interest that could interact with miR-138-5p in the 3'UTR, and used molecular biology to validate Kv1.2 at multiple binding sites. It was previously demonstrated that axonal addition of the miR-138 inhibitor alone led to a reduction in cellular excitability compared to addition of the non-targeting microRNA control probe (see figure 5.4.1.) Additional evidence from the literature had also suggested that *in vivo* Kv1.2 is primarily located in the A-fibres of the DRG neurons (Tsantoulas and McMahon, 2014). Since microRNA is involved in translational repression or the degradation of target mRNA (Bartel, 2004; Jackson and Standart, 2007) it was deduced that miR-138-5p could regulate DRG excitability via repression of mRNA for ion channels regulating conductance of the action potential.

In this experiment, small interfering RNA (siRNA, see Chapter 2.4.2) for Kv1.2 was added to the axons of neurons cultured in microfluidics. Unlike miR-138-5p, which most likely targets repression or degradation of multiple proteins in the axon, the siRNA for Kv1.2 only targets degradation of mRNA for Kv1.2.

It was hypothesised that downregulation of the target of interest (Kv1.2) would lead to changes in the resting membrane potential, and increased excitability of the cell. If Kv1.2 was a real target for miR-138-5p, then knockdown of Kv1.2 in the axon was hypothesised to mimic the effects of miR-138-5p on neuronal excitability. To investigate this hypothesis, siRNA for Kv1.2 was added to the axons to selectively induce reduction of Kv1.2 expression.

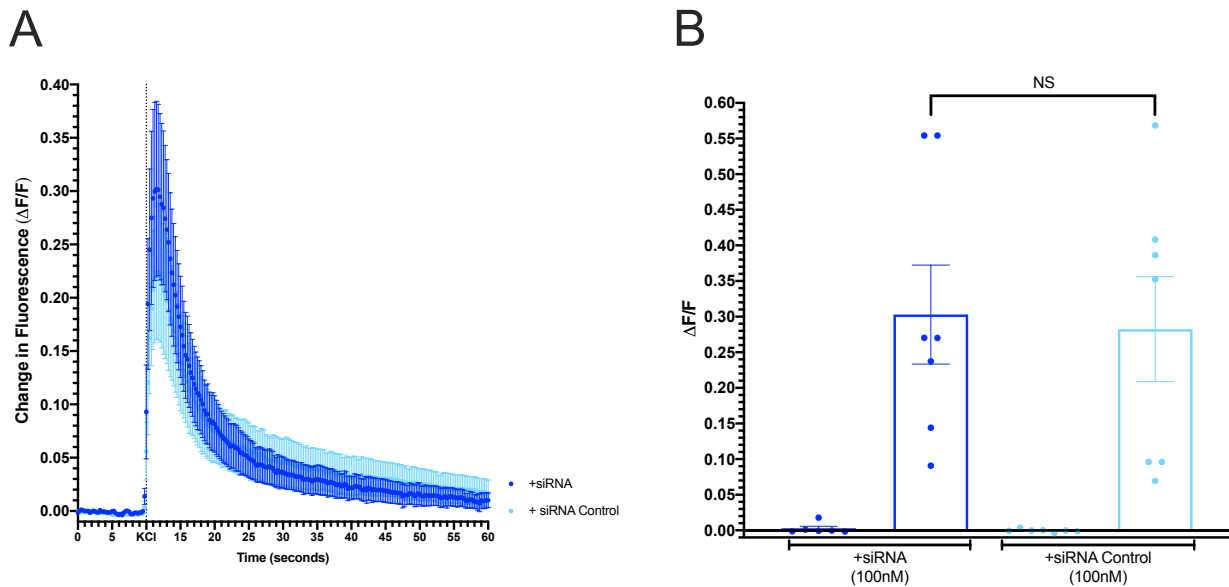


Figure 5.4.11: Prolonged incubation of the axonal compartment (24-hours) with 100nM siRNA for Kv1.2 evoked small changes in neuronal excitability relative to the non-targeting siRNA control sequence. Evoked change in excitability was not deemed statistically significant at N=7 biological replicates

A) Time course analysis comparing the amplitude of neuronal excitability following axonal stimulation with KCl (25mM.) siRNA for Kv1.2 or the non-targeting smartpool siRNA control was added to the axonal compartment for 24-hours prior to axonal stimulation. Treatment did not evoke a significant difference in the amplitude of responses between treatments.

B) Increase in fluorescence following stimulation increased following axonal incubation with siRNA for Kv1.2 or the non-targeting siRNA control. Results of an unpaired t-test showed no significant difference between the evoked Ca^{2+} response between conditions. N=7, Bars show mean \pm SEM.

The time course analysis in figure 5.4.11A shows that there was a rapid increase in fluorescence observed upon stimulation with KCL. The treatment with the siRNA for Kv1.2 (and subsequent knockdown of Kv1.2) did not reduce viability of the cells or render the neurons unresponsive to stimulation by KCL. The amplitude of the response following axonal stimulation with KCL was not significantly different if the axons had been exposed to the siRNA for Kv1.2 or the siRNA non-targeting probe (figure 5.4.11B.)

For reference, the peak excitability of the neurons incubated with siRNA for Kv1.2 was $0.30\Delta F$, compared to $0.20\Delta F$ following axonal incubation with a miR-138 power inhibitor (figure 5.4.1) and $0.64\Delta F$ in untreated microfluidics (figure 4.2.2.)

In these preliminary experiments knock-down of Kv1.2 in the axon did not appear to modulate excitability, so at the moment it does not appear to be the only target of miR-138-5p in this process. There was potential for this experiment to be development further focusing on

different concentrations of siRNA, a longer incubation period with siRNA or the co-incubation with a second siRNA of interest (for example where Kv1.1 and 1.2 are often seen to form heterotetramers.)

In line with the objectives for this chapter, the following conclusions can be drawn from these studies:

1. miR-138-5p regulates excitability of DRG neurons via local translation in the axon.
2. Two target sites for Kv1.2 were validated as targets for binding with miR-138-5p via bioinformatics, luciferase reporter and site directed mutagenesis

Future works could have been to confirm the interaction between miR-138-5p and Kv1.2. It was hypothesised that the reduction in cell excitability observed by treatment with a miR-138 inhibitor could be rescued by the dual addition of the miR-138 inhibitor and siRNA for Kv1.2.

5.4.7 Discussion and Chapter Conclusions:

The results of parts A and B of this chapter suggested that miR-138-5p is more likely involved in local translation and regulation of proteins such as potassium channels on the peripheral terminals of the small fibre DRG neurons, as opposed to the TRPV1 receptor. Some changes in excitability were detected when miR-138-5p was inhibited in the presence of inflammatory mediators. However, the somal upregulation of miR-138-5p in the cell associated with exposure to inflammatory mediators was not deemed to be significant. On the contrary, the localised inhibition of miR-138-5p in the axonal compartment induced a significant decrease in cellular excitability when axons were stimulated with KCL. Therefore, the role of miR-138-5p in local translation of Kv channels was investigated.

At a molecular level, pathologies such as pain are linked to changes in the way in which excitable cells signal. For example, in a state of hyperalgesia the exposure of the nerve terminals to an inflammatory stimulus has induced a state of increased excitability. Rapid evoked firing of the sensory nerves makes the terminals more sensitive to stimulation, and as such a noxious stimulus is often detected as more painful than it was before. At the centre of research on mechanisms of inflammatory pain have often been the VGSCs, specifically NaV1.7

and NaV1.8, where the exposure to inflammatory mediators induces phosphorylation of sodium channels and increased ectopic firing of DRG fibres (Cummins, Sheets and Waxman, 2007; Hameed, 2019).

In this work I have proposed a mechanism by which altered expression of voltage gated potassium channels, specifically Kv1.2 can be elucidated in the development of a state of increased excitability of DRG fibres. Voltage-gated potassium channels (Kv) have been shown to regulate both the amplitude and the duration of the action potential, as well as frequency of neuronal firing in response to membrane depolarization, and undoubtedly maintaining the resting membrane potential (Hille, 2001). The transmembrane Kv family are activated by depolarization of the membrane, and are responsible for the repolarization of the membrane potential to resting state (Kim and Nimigean, 2016). Therefore, it is understandable that the activation of these channels is dependent on the influx of sodium into the axon when the membrane is depolarized.

The propagation of the action potential is dependent on sequential activation of K⁺ channels, as depicted in figure 1.4.3, chapter 1. In sensory neurons of the PNS, such as the DRG neurons, the Kv1 family of channels are largely expressed in medium to large diameter neurons (Rasband *et al.*, 2001). The Kv1.2 channel is well documented to have roles in maintaining the resting membrane potential, as well as mediating repolarization of the neuron following firing of an action potential (Long, Campbell and MacKinnon, 2005). The heterotetrameric Kv1.2 channels are slow to activate in order to rectify depolarization of the membrane (Manis, 2014), and their role in modulation of the resting membrane potential is well documented (Trimmer, 2015). The inactivation of these delayed rectifier channels is not deemed to be dependent on a change in the driving force, and some evidence has also suggested that Kv1 in the DRG neurons channels may cluster at the juxta-paranodal regions with other Kv (e.g. Kv1.1 and Kv1.4) subtypes to help modulate downstream action potential propagation (Rasband, 2010).

Mutations in Kv1.2 have previously been observed *in vivo* with regards to both gain-of-function and loss-of-function (Syrbe *et al.*, 2015). At a single cell level it has become evident that loss of function of Kv1.2 can result in impaired membrane repolarisation and neuronal hyperexcitability (Kearney, 2015). There is even evidence to support the theory that different

variants of the Kv1.2 channel can be expressed, supporting a “gain-of-function” mutation and inducing hyperexcitability of neuronal networks in the CNS (Niday and Tzingounis, 2018). Evidence of Kv1.2 having a significant effect on peripheral nerve fibres is more limited. Although the Kv1.2 channel is well characterised in sensory neurons, especially the larger diameter A-fibres of the DRG (Tsantoulas and McMahon, 2014) it is often hard to pin-point a pathological effect arising from changes in expression in one protein *in vivo*.

It has been suggested, that the down-regulation of these channels is partly responsible for increased ectopic firing of DRG neurons in a neuropathic pain state (Fan *et al.*, 2014). In a CCI model in rats, there was shown to be a concomitant link between knockdown of Kv1.2 and upregulation of a different microRNA of interest (Zhang *et al.*, 2020). This work was completed in adult rats rather than embryonic mice, and studied changes in protein expression at the level of L4-L6 in the spinal cord following nerve injury. As anticipated, CCI at L4/L5 induced rapid reductions in the paw withdrawal threshold, and animals displayed signs of mechanical allodynia. This corresponded with a significant decrease in protein expression of Kv1.2 as determined by western blot (Zhang *et al.*, 2020). However, given that Kv1.2 is implicated in neuropathic pain, and is known to be expressed on the select fibres of the DRG neurons it was considered a good target for miR-138 in this study.

In a recent study it was shown that there was a link between long non coding RNA silencing of Kv1.2 in DRG neurons and the development of a neuropathic pain state by increased membrane depolarization (Zhao *et al.*, 2013). On the contrary the role of short, non-coding RNA such as microRNAs have not been widely investigated with regards to the expression of Kv1.2.

Based on the results of this work it could be hypothesised that miR-138-5p contributes to the regulation of neuronal excitability, potentially via translational repression of ion channels such as Kv1.2 on the terminals of sensory neurons. However, given that the addition of siRNA for Kv1.2 alone did not induce a significant increase in neuronal excitability, it is unlikely to be the only target for miR-138-5p involved in regulation of membrane excitability.

6 General Discussion and Conclusions

6.1 Role of the DRG neurons in peripheral neuropathy:

As described in Chapter 1.5.3 and 3.1.2 the development of chronic pain is concomitant with the peripheral nociceptor neurons of the DRG fibres becoming irreversibly sensitised. The molecular mechanisms underlying development of some pathologies including neuropathic pain are still being elucidated. Animal models have demonstrated that there is more than one peripheral and central component underlying the onset of painful neuropathies. At present there are several *in vivo* models that have been shown to successfully model behavioural characteristics of neuropathic pain. For example chronic constriction injury (CCI) models have shown the hyperexcitability of axotomized DRG neurons, and the eventual onset of central sensitisation (Chung and Chung, 2002). Other models include the use of spinal nerve ligations (SNL) to demonstrate onset of paw withdrawal resultant from reduction in thermal or mechanical threshold for stimulation (Wang and Wang, 2003; Jaggi, Jain and Singh, 2011).

Until recently *in vitro* modelling has been less successful at studying the molecular mechanisms underlying the development of pain. Largely this was due to the limited capacity of standard culture techniques to replicate the polarized nature of neurons *in vitro* (see Chapter 1.2 and 3.1.3.). The results from Chapter 3 showed that the use of compartmentalised microfluidic chambers described in this thesis enabled the development of an *in vitro* model that can replicate some of the key aspects of neuronal excitability as seen *in vivo*. Although direct co-culture of macrophages and DRG neurons was not deemed possible in this format, the use of cytokine rich media led to the development of a flexible model for quantifying changes in neuronal excitability. Given that this work was carried out *in vitro*, it is important to re-iterate that this was not directly a model of pain, but modelled changes in excitability as a proxy for nociceptive neuron function.

The results of live cell imaging in Chapters 4 and 5 have discussed that the amplitude and duration of a neuronal response was lower when only the axons were stimulated in microfluidic devices. These results highlighted how microfluidic chambers present advantages in terms of temporal responses, but also provide the capacity to modulate processes localised to the axon. Previous efforts by the Dajas-Bailador lab have used compartmentalised

microfluidic cultures to highlight the polarised nature of neurons and local protein expression in the axon (Lucci *et al.*, 2020). The model described in this thesis brings a dynamic dimension where function of excitability was studied locally by quantifying evoked changes in Ca^{2+} . Local translation is known to play a role in pain (Ferrari *et al.*, 2013) but has largely been ignored so far due to the inaccessibility of local axons *in vivo* and inability of standard *in vitro* models to do it. In conclusion, compartmentalised microfluidic models such as ours provide a novel technique for studying local protein expression in the axon using *in vitro* models.

6.2 Investigation of inflammation on the amplitude of evoked Ca^{2+} transients in the soma of sensory neurons:

Following insult to the nerve, the onset of inflammation indirectly regulates excitability of the DRG neurons, most likely via the modulation of membrane conductance. In states of inflammation, the axons of the DRG neurons become “stressed” and depleted of mitochondrial stores (Jha *et al.*, 2015; Misgeld and Schwarz, 2017). Neurons are highly metabolically active and the continual replenishment of ATP is essential for regulation of basic cellular functions. This includes resolving inflammation, regulating propagation of the action potential and regulation of membrane conductance. It has been shown that in the onset of peripheral sensitisation associated with inflammation, there is a rapid influx of M1-like macrophages to the damaged tissue (Godai *et al.*, 2014). Furthermore, during the resolution of inflammatory pain (in mice) the M2-like macrophages infiltrate the nerve terminals of the DRG, concurrent with increased levels of oxidative phosphorylation in the neurons.

In vivo, intraplantar injection of carrageenan into the hindpaw of mice shows rapid development of hyperalgesia (Winter, Risley and Nuss, 1962; Whiteley and Dalrymple, 2001) that can be measured using behavioural analysis such as ‘dynamic weight bearing.’ In a recent study it was shown that when macrophages were selectively depleted from mice, they still showed the rapid onset of pain in response to carrageenan, but critically this pain response did not resolve (Raouf *et al.*, 2020).

The work in this thesis has also investigated the role of inflammatory modulation on the terminals of sensory DRG neurons. The results in chapter 3 showed the development and characterisation of two populations of inflammatory macrophages. The results in Chapter 4

showed that the exposure of the neuronal terminals to the polarized media did not initiate a state of hyperalgesia, instead the cytokine-rich media reduced the overall excitability of the DRGs. In Section 1.8.2 the dynamic nature of macrophage cells was discussed, and *in vivo* studies have demonstrated that it is the metabolic nature of the inflammatory cell that contributes to the development of pain states such as hyperalgesia. For example, *in vivo*, the M1-macrophages are known to be glycolytic cells, whilst the M2-like cells are dependent on oxidative phosphorylation (Rath *et al.*, 2014b; Angajala *et al.*, 2018; Hobson-Gutierrez and Carmona-Fontaine, 2018). In chronic pain it has been demonstrated that where oxidative phosphorylation is impaired (Duggett, Griffiths and Flatters, 2017) so is Ca²⁺ buffering in the cell, and consequently action potential propagation. It was hypothesised that in a similar way that cortical neurons uptake mitochondria from surrounding astrocytes following a stroke (Hayakawa *et al.*, 2016), so do the DRGs uptake mitochondria from surrounding M2-like macrophages in the resolution phase of inflammatory pain (Raouf *et al.*, 2020).

Therefore, it could be hypothesised that the decrease in excitability of neurons exposed to cytokine-rich media *in vitro* was a response to the exposure of the cytokines present in the media, and not resultant from exposure to the macrophages themselves. Although the results of this model did not directly mirror what can be observed *in vivo*, this setup demonstrated the flexibility microfluidic modelling, with potential for the model described here to be developed further.

6.3 The role of microRNA in regulation of sensory neuron excitability:

In vivo the onset of pain and neuronal hypersensitivity is often associated with underlying changes in protein expression. For example, as described in Chapter 1.5.2, the sensitisation of peripheral nociceptors may be caused by translational regulation of receptors on the terminals of the DRG neurons. Given that microRNAs target translational repression (or degradation) of multiple mRNAs, it is hypothesised that microRNAs expressed in the sensory DRG nerves regulate local protein translation, and thus contribute towards regulation of neuronal excitability. Several studies have previously implicated the role of microRNAs in regulation of DRG excitability, often in the context of neuropathic pain (Aldrich *et al.*, 2010, Zhao *et al.*, 2010, Sakai *et al.*, 2013.).

In an SNL model of neuropathic pain, it was observed that there was a significant down-regulation of miR-183 in the ipsilateral L5 DRG, corresponding with the onset of mechanical hypersensitivity (Aldrich, et al., 2010). Furthermore, microarray analysis using total RNA isolated from L5 DRGs in rats implicated the downregulation of microRNAs such as miR-7a in the hyperexcitability of sensory neurons, arising from upregulation of voltage-gated channels (Sakai *et al.*, 2013).

In vivo loss of function studies have also previously elucidated the upregulation voltage-gated channels such as NaV1.8 in hyperexcitability of the DRG neurons in neuropathic pain models (Thakor *et al.*, 2009). In a spared nerve injury model of neuropathic pain, the down-regulation of miR-182 correlated with the upregulation of the NaV1.7 channel on nociceptive DRG fibres, and the onset of neuropathic pain behaviours. The selective over-expression of miR-182 at L4-L6 was shown to reverse this change over-expression of NaV1.7 and reduce the hyperexcitability of the DRG neurons (Cai, et al., 2018).

One advantage of the microfluidically isolated culture used in this thesis was the capacity to study changes in excitability at a molecular level. One mechanism of which has been explored in Chapter 5, investigating the effect of microRNA on excitability of small diameter DRG neurons. Of particular interest to this project was the role of miR-138-5p in regulating neuronal excitability in the context of pain. MiR-138-5p is a widely reported microRNA, with evidence for roles in suppression of axonal regeneration in the CNS (Liu, et al., 2013) and has also been implicated in inflammation and tumour suppression (Bai, et al., 2018). Chapter 5.1.2 describes the upregulation of miR-138-5p in a model of hyperalgesic priming. However, several other works have implicated miR-138-5p in pain. For example, in a recent CCI model for neuropathic pain in adult mice 125 microRNAs were differentially expressed in the sciatic nerve. This included a significant decrease in miR-138-5p corresponding with the onset of mechanical allodynia (Wilkerson, et al., 2020).

The microfluidic nature of the devices used in our model showed that localised inhibition of miR-138-5p in the axons of microfluidic culture of DRG neurons led to a decrease in neuronal excitability. As discussed in Chapter 5, bioinformatic targets searches combined with the results of the Ca²⁺ signalling assay suggested the role for miR-138-5p in specific inhibition of potassium channels.

6.4 Dysregulation of potassium channels in disease and neuropathy:

Excitability is a key function of neurons, both with regards to homeostatic function and development of pathologies such as pain. This has been discussed at length in Section 4.1.1, and supported by the results shown in Chapters 4 and 5. Neuronal excitability is regulated by subcellular expression and localization of ion channels, with evidence showing that ion channels form 'clusters' at different sites throughout the axon (Rasband, 2010). The tight regulation of the conduction and propagation of an action potential along the axon is essential for normal neuronal function. Underlying this control of membrane excitability is the expression of multiple ion channels on the nerve terminals and along the axonal membrane. Perhaps one of the most well documented examples of this are the voltage-gated ion channels. The dual signalling between sodium and potassium is key in maintaining the resting potential of the neuron. But what happens when this signalling goes awry?

It has been suggested, that down-regulation of the voltage-gated ion channels involved in regulating membrane conductance is partly responsible for increased ectopic firing of DRG neurons in a neuropathic pain state (Fan *et al.*, 2014). In particular the down-regulation of Kv1.1 and Kv1.2, both of which are expressed on the juxta-paranodal regions of DRG neurons, has demonstrated hyperexcitability of cells in loss-of-function studies (Tsantoulas and McMahon, 2014). For example, in a CCI model in rats, there was shown to be a concomitant link between knockdown of Kv1.2 and upregulation of a different microRNA of interest (Zhang *et al.*, 2020). This work was completed in adult rats rather than embryonic mice, and studied changes in protein expression at the level of L4-L6 in the spinal cord following nerve injury. As anticipated, CCI at L4/L5 induced rapid reductions in the paw withdrawal threshold, and animals displayed signs of mechanical allodynia. This corresponded with a significant decrease in protein expression of Kv1.2 as determined by western blot (Zhang *et al.*, 2020). However, given that Kv1.2 is implicated in neuropathic pain, and is known to be expressed on the select fibres of the DRG neurons it was considered a good target for miR-138 in this study.

6.5 Concluding remarks:

The work in this thesis details the use of compartmentalised microfluidic cultures to model changes in excitability of sensory DRG neurons. It was possible to utilise the microfluidic

isolation of the device to expose the axons and the soma of the DRG to separate micro-environments. Of particular interest to the study of nociception was the exposure of the axonal compartment to inflammatory stimuli. A unique set of *in-house* stimuli were developed from the culture and polarization of bone marrow derived macrophages.

The model described was flexible and could be repeated with different sets of inflammatory mediators if desired. For example, protocols for culture and polarization of spinal cord derived microglial cells were also developed, which could be used to investigate changes in DRG excitability resulting from changes in signalling from the CNS.

In our model, the use of live-cell imaging was particularly important to quantify changes in neuronal excitability, with the nature of microfluidic modelling providing the capacity to monitor changes in evoked Ca^{2+} transients at the soma as a result from axonal stimulation. This unique property of the microfluidic devices also permitted the investigation of local translation of protein. Neurons are highly polarised cells, and it was evident that localised stimulation of the axonal terminals with KCL induced a rapid and significant increase in neuronal excitability. Therefore, the effects of small non-coding RNA on translational repression in the axons were investigated. Kv1.2 was identified as a target for miR-138-5p, where inhibition of miR-138-5p in the axons induced a reduction of neuronal excitability in microfluidic cultures. It was hypothesised in Chapter 5 that Kv1.2 was a target for miR-138-5p, with bioinformatic predictions showing 5 potential binding sites for miR-138-5p in the 3'UTR (see Appendix, figure 7.7.1.) However, we were also able to validate some of these interactions between miR-138-5p and Kv1.2 using a dual luciferase reporter assay and site directed mutagenesis assays.

In our final pilot studies, knock-down of Kv1.2 mRNA in the axon did not show a significant increase in neuronal excitability. Several other studies have investigated the role of Kv1.2 in hyperexcitability and development of pain-states such as neuropathic pain (Everill and Kocsis, 2000; Xiuli *et al.*, 2013; Laumet *et al.*, 2015; Zhao *et al.*, 2017). The majority of these pain-based studies were conducted *in vivo*, due to the limited capacity of most *in vitro* models to replicate the complex morphology of the DRG neurons and surrounding non-neuronal cells. However, microfluidic model such as the one described in this work can overcome these hurdles. Of course, unlike siRNA, miRNAs target the translational repression of multiple mRNAs, and therefore it is unlikely that *in vivo* miR-138-5p only inhibits the expression of Kv1.2 at the axonal terminals of the DRG neurons. The results from the final experiment with

siRNA for Kv1.2 described in this thesis did not conclusively link upregulation of protein to miR-138-5p. The results of a bioinformatic target search also highlighted inward rectifiers and two-pore potassium channels such as TREK-2 as targets of interest. It could be hypothesised that miR-138-5p has roles in regulating the expression of multiple subtypes of potassium channels. The combined effect of miR-138-5p on multiple ion channels of interest could demonstrate a more significant effect on regulating membrane excitability (LaMotte & Ma, 2007).

6.6 Implications of this study on future work:

In order to discover more effective medicine for pain, there is an ever-present need for biologically relevant *in vitro* models. Microfluidic models provide the necessary tool for reproducible culture *in vitro* that replicate the polarity of the cells observed *in vivo*. This could help to lead to the development of *in vitro* models for the study of pain, that are more predictable to the response observed in humans.

The model described in this thesis provided the capacity to investigate the excitability of DRG neurons following localised exposure of the axons to a range of stimuli and molecular manipulations. Critically, the microfluidic nature of the devices meant that the DRG neurons retained their polarised morphology when cultured *in vitro*. The work in this thesis has already led to advances in the optimisation of the method of culture used in the lab, as well as the development of high throughput templates for analysis of Ca²⁺ signalling. As with the development of any model, there are still unanswered questions for future studies. The identification of future work would be dependent on the question being asked of the model. Here I have provided a few examples of how the model I have described could be further progressed in future works:

6.6.1 Investigation of neuronal excitability on inflammation:

Future works could involve the development of a model involving the use of triple channel devices (as show in schematic 3.1.2.) In the same way in which this project has modelled changes in excitability of the DRGs induced by changes in peripheral inflammatory cells, it could be interesting to investigate the downstream effect of this neuronal modulation on cells of the CNS such as microglia. This work also developed a protocol for the isolation and

characterization of populations of microglial cells *in vitro*. It could be hypothesized that for additional complexity, the next stage would be to investigate how the induced changes in neuronal excitability observed in this project could affect the morphology and phagocytic activity of spinal cord derived microglial cells.

6.6.2 Investigation of the targets for miR-138-5p in regulating neuronal excitability:

The preliminary study of siRNA for Kv1.2 on excitability of DRG neurons did not show a significant increase relative to the control at N=6. Expansion of the work shown in this project could include further development of the siRNA study, which time-permitting would have most likely been the next investigation of this Thesis. Using siRNA in co-incubation with a cell permeable miR-138-5p inhibitor, the decreased excitability induced by miR-138-5p inhibition could be potentially 'rescued'.

Other options could also include the development of the microfluidic model as a 'screen' for other targets regulated by miR-138-5p (or other microRNAs of interest.)

7 Appendices

7.1 Reduction in the concentration of GDNF did not prevent non-neuronal cell migration

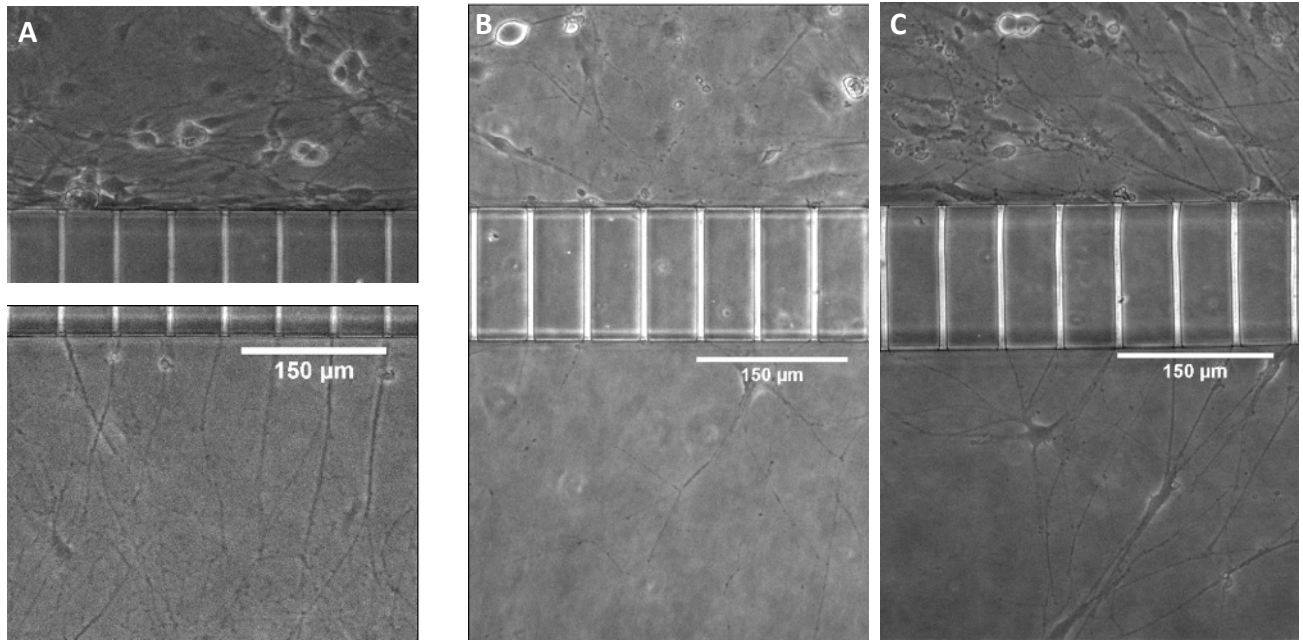


Figure 6.6.1: Measuring non-neuronal cell migration in microfluidic cultures;

A) DIV3 E18 rat DRGs . B) DIV4 P2 rat DRGs. C) DiV4 P2 Rat cells cultured with additional anti-mitotics.

7.2 Composition of polarized macrophage media:

Although 40 targets were tested relative to an endogenous positive control, a negative control and a blank control, the preliminary fold changes in select target of interest are displayed below. The positive control was provided by biotin-conjugated IgG printed directly onto the array membrane in the upper-left and lower-right corners. The negative control spots were printed with the same buffer used to dilute antibodies printed on the array. Therefore, the signal intensities of the negative controls represented the background plus non-specific binding to the printed spots and could be used for background correction of the signal.

The fold change of each target was measured relative to the endogenous positive control provided on the membrane. As part of a preliminary approach to investigate cytokine

regulation, this assay was replicated once, using 2 samples for each polarized media, and where each repeat was extracted from a different batch of polarized cells.

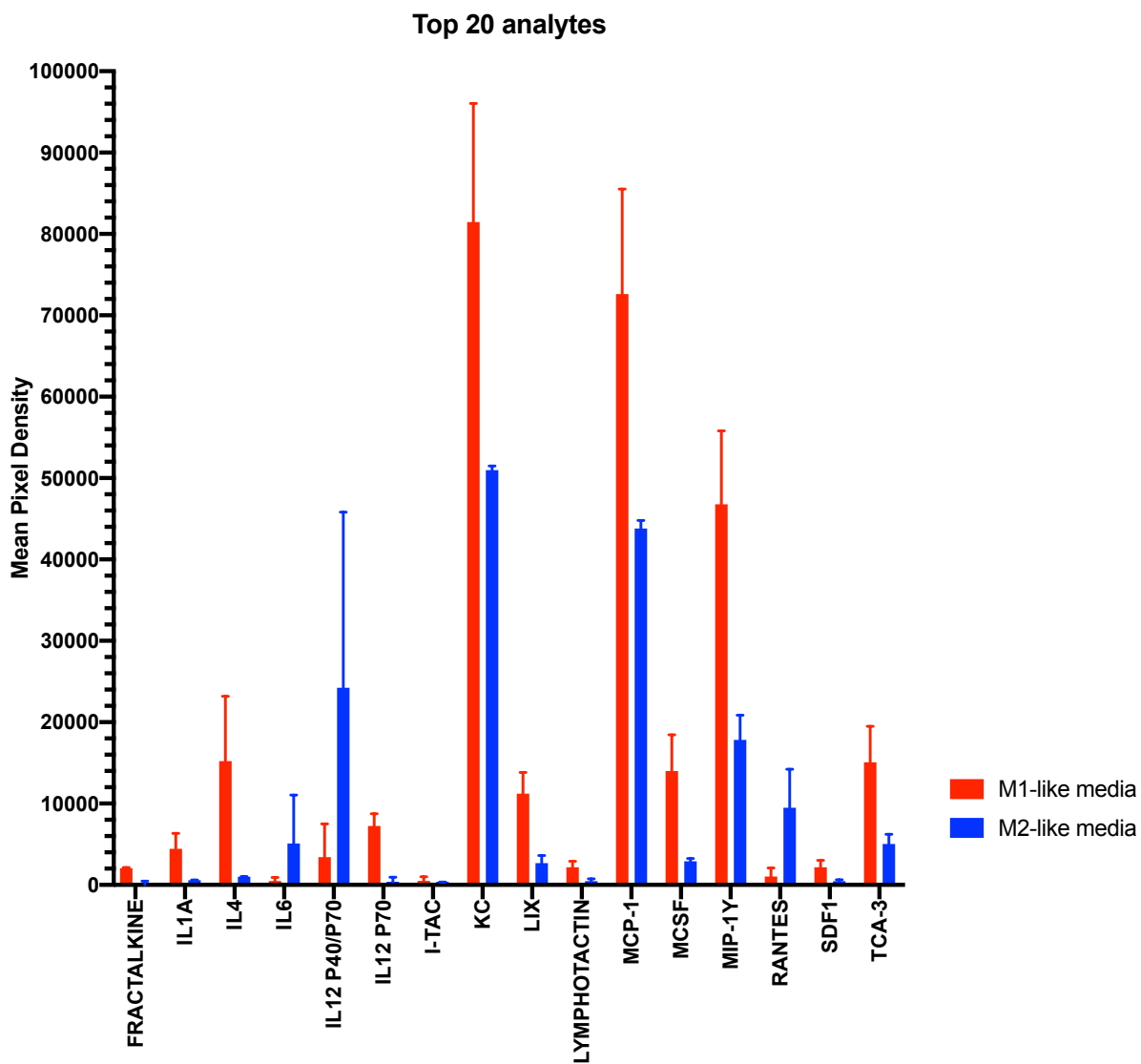


Figure 7.2.1: Results of a 40-target cytokine array using inverted densitometry for a semi-quantitative analysis of the fold change in the most highly expressed cytokines present in different media subtypes. N=2, error bars representing the standard deviation of the fold change.

Luminescence was then used to detect the relative concentration of each antigen in the media. In this instance both conditions were exposed for 10 minutes for direct comparison, although it was noticeable that the M2-like media displayed lower raw integrated density, particularly with relevance to the positive control. For this reason, results are shown as the raw integrated density (in pixels) with the fold change of each cytokine relative to the endogenous positive control. On each membrane, the most highly expressed chemokine was used to select the area for analysis.

Two batches of media were tested, from different dates of bone marrow extraction, and subsequent polarization. Although each batch of media show variation in the expression of specific markers there was some overlap between the most highly detected markers in both analysis formats. This is demonstrated by the prism analyses included above (figure 7.2.1). There was some initial concern by the low levels in expression of cytokines that have been heavily documented in inflammatory studies. However, it is important to note that different cytokines appear at different time points throughout the pro-inflammatory and resolution phase of injuries (Melton *et al.*, 2015).

It was unlikely that the protocol for polarizing macrophages generated two discrete populations of cells. The M1/M2 nomenclature is useful for defining the two populations of cells produced but fails to acknowledge the presence of intermediate polarization stages. Results of the cytokine array demonstrated that despite expected overlaps, the populations of polarized macrophages present clear shifts in cytokine profiles, and helps to define the inflammatory state (Orecchioni *et al.*, 2019; Zajd *et al.*, 2020). However, the M2 population in particular was unlikely to be purely an M2a phenotype. In order to better understand the results of the array, I have highlighted the importance of some of the most highly expressed cytokines.

CCL2 (MCP-1):

CCL2 (formerly MCP-1) is an inflammatory chemokine produced by monocytic cells, as well as fibroblasts and epithelial cells during the innate immune response (Deshmane *et al.*, 2009). There is vast evidence for the role of CCL2 as a pro-inflammatory chemokine that is involved in the influx of macrophages and fibroblasts to a site of injury or inflammation. However, the role of CCL2 as an innate polarizing signal for macrophages remains somewhat unclear. A high level of CCL2 production can be indicative of a shift towards the M2-like phenotype, where blockade of CCL2 binding shows a decrease in anti-inflammatory cytokine production in *in vivo* modelling of inflammation (deSchoolmeester *et al.*, 2003). However, CCL2 is also implicated in disease pathologies such as rheumatoid arthritis where macrophages are observed polarized towards an M1-like phenotype. For example, it has been demonstrated that stimulation by LPS induced polarization towards the M1-like phenotype, and correlated

with high levels of MCP-1 (CCL2.) Moreover, the level of CCL2 in the blood correlated with other markers of rheumatoid arthritis, and could therefore be considered a biomarker (Liou *et al.*, 2013). Our results also showed that CCL2 was highly expressed in both M1-like and M2-like cells relative to the positive control, although the release from M2-like cells appeared to be higher than that of the M1 population. Therefore, the role of CCL2 in driving cytokine-specific immune responses is both complex and dynamic.

RANTES (CCL5):

CCL5 was detected at a 2.2x increase in the M2-like population of cells, despite widely being regarded as a pro-inflammatory cytokine. However, it has also been demonstrated that some M2-like cells produce high levels of CCL5 in order to recruit other inflammatory cells (neutrophils, monocytes etc.) in a regulatory inflammatory response (Atri, Guerfali and Laouini, 2018). There is evidence to support the release of CCL2 (and CCL5) from both M1-like and M2-like cells in bone marrow derived cultures (Zajd *et al.*, 2020) although the relative concentrations of cytokines present will always be dependent on the microenvironment of the cell culture. This may have been affected by the time at which the media was removed from the cells for testing, or the length of initial exposure to a stimulus, or even the type of media cells were cultured in (Murray *et al.*, 2014a).

IL-6:

Other important examples include the small increase in IL-6 (0.97X) observed in the M2-like culture. IL-6 is a pleiotropic cytokine, with roles in modulating both pro- and anti-inflammatory pathways. However, it is acknowledged that the presence of IL-4 (the stimulus used to induce the M2-like phenotype) can cause downstream release of IL6 from M2-cells (Casella *et al.*, 2016).

7.3 Microglial Phagocytosis assay:

Having demonstrated that it was possible to detect changes in the phenotype of the spinal cord derived microglial culture, the next step was to investigate if this led to a functional change in the induction of phagocytosis, typical of polarized microglia cells (see figure 7.3.1 below for images acquired at 63X magnification). By incubating pre-polarized cells with yellow-fluorescent latex beads (1 μ M diameter, Sigma L1030) the average number of beads ingested in a set time period was used as a measure of phagocytic activity. This assay is ideally completed using confocal microscopy to confirm the bead has been phagocytosed. Without access to this equipment, we used widefield imaging and z-stacks confirmation to determine overlap of the bead with the image of the cell suggests migration towards the cell body.

Cells were exposed to the latex beads on separate occasions for either 24 or 48 hours, to quantify how quickly a microglial phenotype would begin to ingest a foreign body. In order to analyse these findings, the number of beads versus the number of cells in a single frame (20X magnification) was manually counted. From here, the number of beads overlapping with the cell body (stained with iba-1) was calculated and used to estimate the average number of beads phagocytosed per cell. After 24-hours exposure, results showed that the number of beads overlapping with the microglial cell body was highest in the M1-like population (20.2 ± 15.8) compared to only 14.12 ± 14.1 in the M2-like cells, see figure 7.3.1C. Since this metric did not demonstrate a significant difference in the number of beads ingested between the phenotypes used. Therefore, it was decided not to take this metric forward for further analysis.

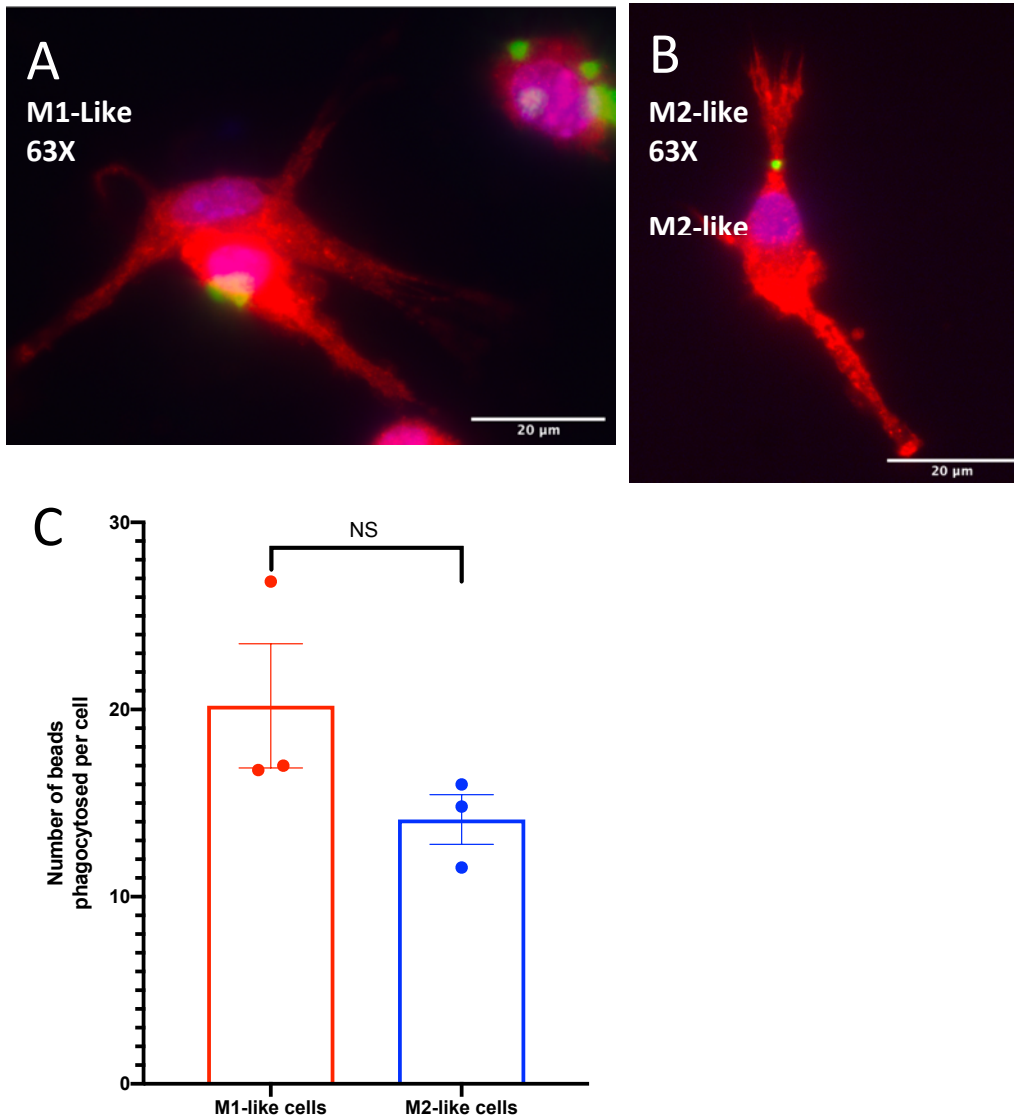


Figure 7.3.1: Looking at the overlay between Iba-1 and the green latex bead as a marker for how the phagocytic activity of microglial cells is dependent on phenotype.

A) M1-like cells. B) M2-like cells. Green= Latex fluorescent beads, Blue= DAPI nuclear stain, Red= Iba-1. C) Comparing average number of beads 'ingested' over 24-hours by M1-like cells vs. M2-like cells. $P=0.1644$ (NS), at $N=3$ coverslips, 5x ROI minimum.

7.4 Analysing changes in morphology dependent on cellular phenotype:

Feret's diameter is measured by the greatest distance between two points along the diameter of the cell. The equation for the transformation index is as follows:

$$\left[\frac{\text{perimeter of the cell } (\mu\text{M}^2)}{4\pi[\text{cell area } (\mu\text{M}^2)]} \right] \text{ (Fujita et al., 1996)}$$

This equation can be used to calculate microglial ramification state, based on phenotype of the cell. A cell with long processes and a small soma, such as the standard “anti-inflammatory” phenotype, has a large index value, and vice versa. It is also important to note that this index is only dependent on cell shape, not on cell size. Figure 7.3.1 (above) at 63X magnification clearly demonstrates distinct morphological changes of the microglial culture, dependent on the polarisation state and subsequent ramification.

The images acquired from the phagocytosis assay were also used to calculate Feret’s diameter:

	M1-like	M2-like
63X	30.35125	52.612
20X	28.0848	27.60432
Average area (μM)	29.218025	40.10816

Table 7.1.: Morphological changes of microglial cultures as determined by a Feret’s diameter calculation

In total 10 replicate images from the phagocytosis assay were used to calculate Feret’s diameter. (5x replicate images at 63X magnification and 5x images at 20X magnification.)

7.5 The stimulation of axons by cytokines used to polarize macrophages did not evoke a significant increase Ca^{2+} transients:

It was demonstrated that acute exposure of the axonal compartment to media extracted from polarized macrophages elicited a transient, but small increase in cellular excitability. Although the contents of the polarized media had been semi-quantified using the cytokine array in chapter 3 (supplementary figure 7.2.1) it had not yet been determined whether the stimuli used to polarize the macrophages would also induce a change in the excitability of the DRG neurons. When media was extracted from the polarized macrophages and used to stimulate the axonal compartment of a microfluidic device, it is likely that there was still a low level of cytokine in circulation, even following replacement of fresh media.

For this reason, cytokines such as IFN γ and IL-4 were diluted directly into complete imaging buffer and used to stimulate the axonal compartment of microfluidic devices (N=3.)

The exposure to the cytokines shown did not induce significant release of Ca²⁺ transients in the soma. The average peak excitability recorded is shown in the table shown below for the relative stimuli used:

Stimulus	ΔF Max
M1 (NPR 2H fresh)	0.053
LPS	0.05
IFNγ	0.1
M2 (NPR 2H fresh)	0.099
IL-4	0.02

Table 7. 2: Peak excitability induced following axonal exposure to stimuli shown

The response to M1-like media was very close to that of LPS and less than that of IFN γ . On the contrary, if cells were stimulated solely with IL-4, the average peak excitability was lower than if the cells were stimulated with the media containing the cytokines released from anti-inflammatory like macrophages. The increases in excitability were negligible with respect to Capsaicin or KCL and were not further investigated.

7.6 QPCRs from Pooled samples:

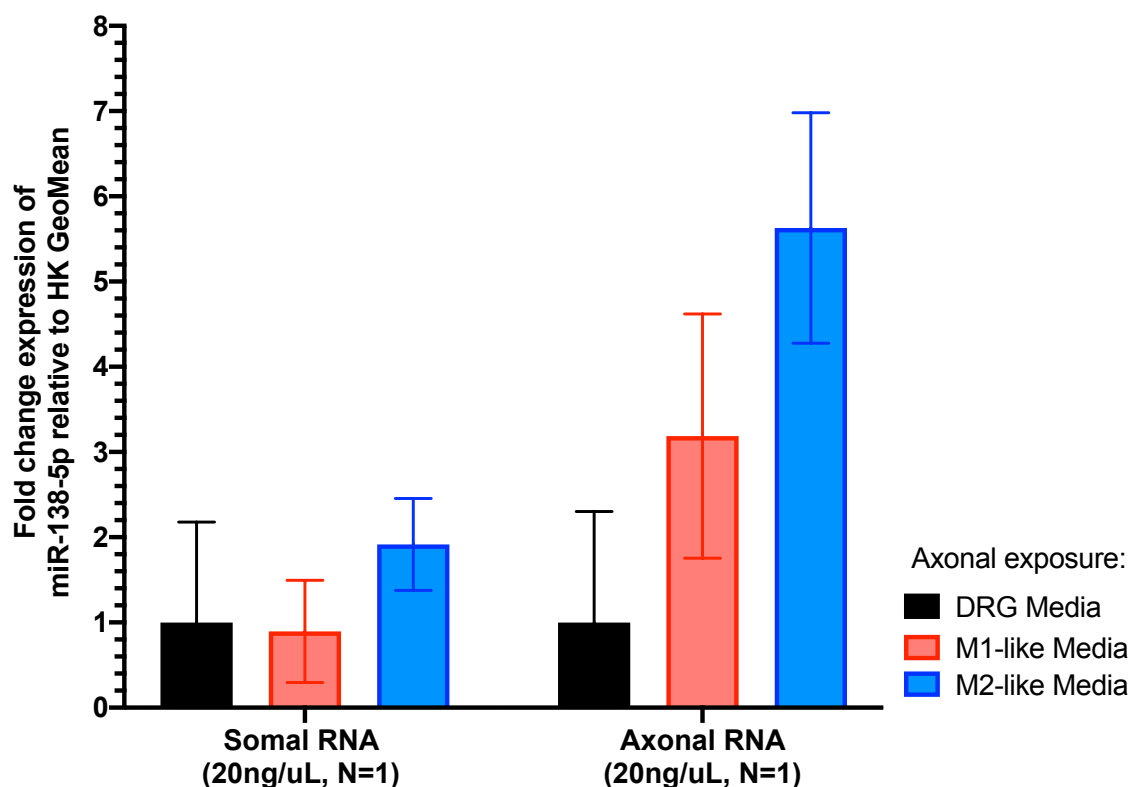


Figure 7.5.1: Quantification of localised effects of inflammatory mediators on expression of miR-138-5p in pooled samples of RNA

Figure 7.4.1 shows an N=1, where 3 biological replicates of RNA extractions were pooled prior to qPCR reactions.

Result of two-way ANOVAs, where the mean fold-change has been compared with the other averages for the same compartment of the insert. In this way an 'adjusted' P-value was calculated allowing for inter-sample variation. Results showed that there was no statistical significant increase in miR-138-5p expression in either the somal compartments in either the M1-media exposed cells or the M2-media exposed culture. It was hypothesised that by pooling the samples the significance was lost by reducing the N-number to 1. The data in supplementary figure 7.4.1 demonstrated a 0.9X change in miR-138-5p in axons exposed to M1-like media, relative to a 1.91X increase in miR-138-5p if cells were exposed to M2-like media. Evidence also showed that there was an increase in miR-138-5p in the soma relative to the DRG control media, irrespective of whether the axons were supplemented with M1-

like media (3.92X increase) or M2-like media (5.68X increase.) However, only if the neurons were exposed to M2-like media was an increase in miR-138-5p observed both in the somal RNA and the axonal RNA extracted from the cells.

7.7 pmiRGlo Plasmid Map (Promega):

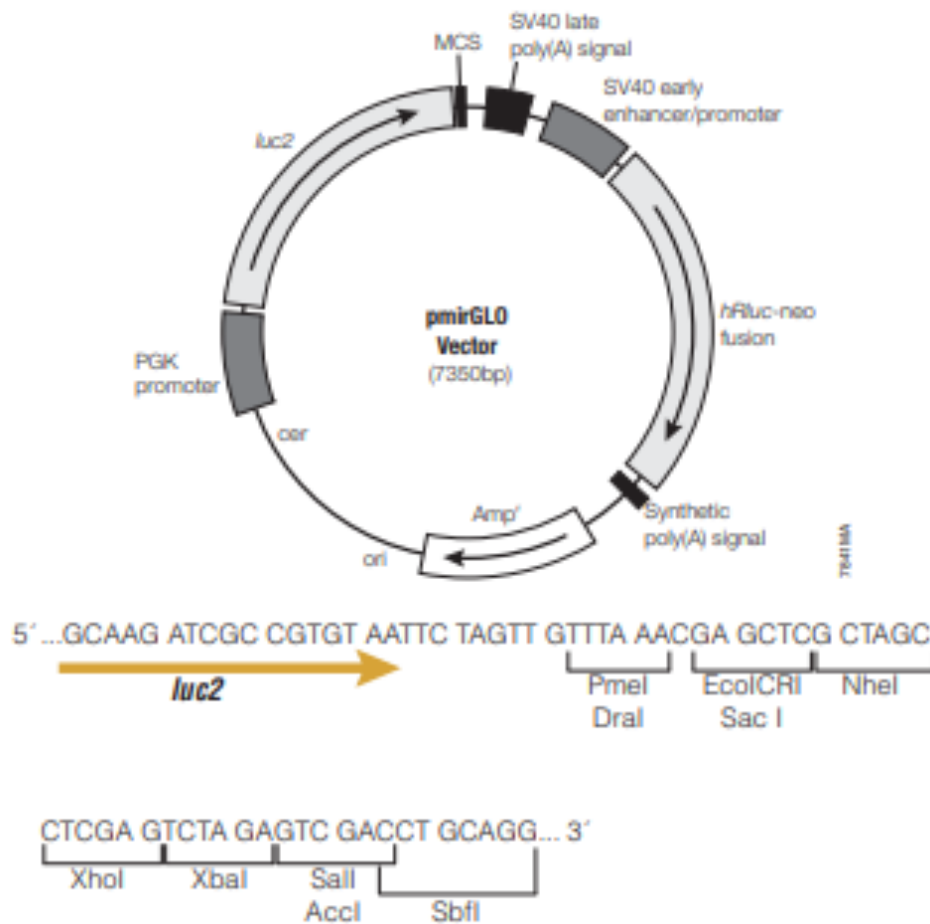


Figure 7.7.1: Plasmid map for pmiRGlo (Promega)

7.8 miR-138-5p binding sites in the 3'UTR of Kv1.2:

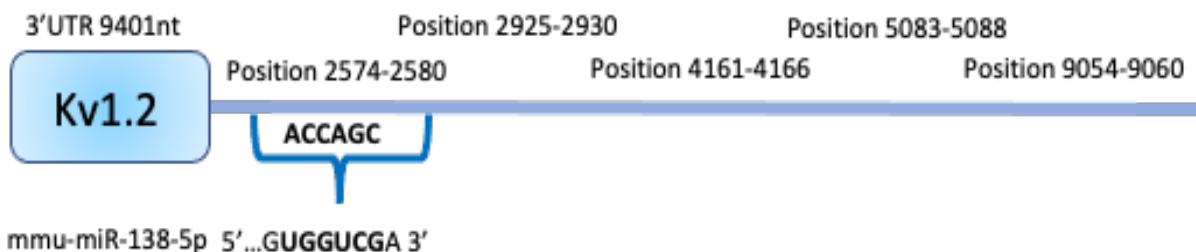


Figure 7.7.2; mmu-miR-138-5p binding sites in Kv1.2 as predicted by Ensembl.

Bibliography

- Abrahamsen, B. *et al.* (2008) 'The cell and molecular basis of mechanical, cold, and inflammatory pain', *Science*. doi: 10.1126/science.1156916.
- Abdiche, Y. N., Malashock, D. S. and Pons, J. (2008) "Probing the binding mechanism and affinity of tanezumab, a recombinant humanized anti-NGF monoclonal antibody, using a repertoire of biosensors," *Protein Science*, 17(8). doi: 10.1110/ps.035402.108.
- Abraira, V. E. and Ginty, D. D. (2013) 'The sensory neurons of touch', *Neuron*. doi: 10.1016/j.neuron.2013.07.051.
- Acosta, C. *et al.* (2014) 'TREK2 expressed selectively in IB4-binding C-fiber nociceptors hyperpolarizes their membrane potentials and limits spontaneous pain', *Journal of Neuroscience*. doi: 10.1523/JNEUROSCI.4528-13.2014.
- Agarwal, V. *et al.* (2015) 'Predicting effective microRNA target sites in mammalian mRNAs', *eLife*. doi: 10.7554/eLife.05005.
- Akiyama, H. and McGeer, P. L. (1990) 'Brain microglia constitutively express β -2 integrins', *Journal of Neuroimmunology*. doi: 10.1016/0165-5728(90)90055-R.
- Akopian, A. N., Sivilotti, L. and Wood, J. N. (1996) 'A tetrodotoxin-resistant voltage-gated sodium channel expressed by sensory neurons', *Nature*. doi: 10.1038/379257a0.
- Aldrich, B. T. *et al.*, 2010. Changes in expression of sensory organ-specific microRNAs in rat dorsal root ganglia in association with mechanical hypersensitivity induced by spinal nerve ligation. *Neuroscience*, 162(2), pp. 711-723.
- Alles, J. *et al.* (2019) 'An estimate of the total number of true human miRNAs', *Nucleic Acids Research*. doi: 10.1093/nar/gkz097.
- Altman, J. and Das, G. D. (1965) 'Autoradiographic and histological evidence of postnatal hippocampal neurogenesis in rats', *Journal of Comparative Neurology*. doi: 10.1002/cne.901240303.
- Ambros, V. *et al.* (2003) 'A uniform system for microRNA annotation', *RNA*. doi: 10.1261/rna.2183803.
- Amici, S. A., Dong, J. and Guerau-de-Arellano, M. (2017) 'Molecular mechanisms modulating the phenotype of macrophages and microglia', *Frontiers in Immunology*. doi: 10.3389/fimmu.2017.01520.
- Amir, R., Michaelis, M. and Devor, M. (1999) 'Membrane potential oscillations in dorsal root

ganglion neurons: Role in normal electrogenesis and neuropathic pain', *Journal of Neuroscience*. doi: 10.1523/jneurosci.19-19-08589.1999.

Andersen, H. H., Duroux, M. and Gazerani, P. (2014) 'MicroRNAs as modulators and biomarkers of inflammatory and neuropathic pain conditions', *Neurobiology of Disease*. doi: 10.1016/j.nbd.2014.08.003.

Andresen, M. (2019) 'Understanding diverse TRPV1 signaling – an update [version 1; peer review: 4 approved]', *F1000Research*. doi: 10.12688/f1000research.20795.1.

Angajala, A. *et al.* (2018) 'Diverse roles of mitochondria in immune responses: Novel insights into immuno-metabolism', *Frontiers in Immunology*. doi: 10.3389/fimmu.2018.01605.

Arnold, C. E. *et al.* (2014) 'A critical role for suppressor of cytokine signalling 3 in promoting M1 macrophage activation and function in vitro and in vivo', *Immunology*. doi: 10.1111/imm.12173.

Atri, C., Guerfali, F. Z. and Laouini, D. (2018) 'Role of human macrophage polarization in inflammation during infectious diseases', *International Journal of Molecular Sciences*. doi: 10.3390/ijms19061801.

Austin, P. J. *et al.* (2015) 'Evidence for a distinct neuro-immune signature in rats that develop behavioural disability after nerve injury', *Journal of Neuroinflammation*. doi: 10.1186/s12974-015-0318-4.

Azevedo, F. A. C. *et al.* (2009) 'Equal numbers of neuronal and nonneuronal cells make the human brain an isometrically scaled-up primate brain', *Journal of Comparative Neurology*. doi: 10.1002/cne.21974.

Baccei, M. L. and Kocsis, J. D. (2000) 'Voltage-gated calcium currents in axotomized adult rat cutaneous afferent neurons', *Journal of Neurophysiology*. doi: 10.1152/jn.2000.83.4.2227.

Bai, G. *et al.* (2007) 'Downregulation of selective microRNAs in trigeminal ganglion neurons following inflammatory muscle pain', *Molecular Pain*. doi: 10.1186/1744-8069-3-15.

Bai, X.-Z. *et al.*, 2018. MicroRNA-138 Aggravates Inflammatory Responses of Macrophages by Targeting SIRT1 and Regulating the NF- κ B and AKT Pathways. *Cellular Physiology and Biochemistry*, 49(2), pp. 489-500.

Bailey, J. D. *et al.* (2020) 'Isolation and culture of murine bone marrow-derived macrophages for nitric oxide and redox biology', *Nitric Oxide - Biology and Chemistry*. doi: 10.1016/j.niox.2020.04.005.

Bandeira, F., Lent, R. and Herculano-Houzel, S. (2009) 'Changing numbers of neuronal and

non-neuronal cells underlie postnatal brain growth in the rat', *Proceedings of the National Academy of Sciences of the United States of America*. doi: 10.1073/pnas.0804650106.

Bandell, M. *et al.* (2004) 'Noxious cold ion channel TRPA1 is activated by pungent compounds and bradykinin', *Neuron*. doi: 10.1016/S0896-6273(04)00150-3.

Bao, L. (2015) 'Trafficking regulates the subcellular distribution of voltage-gated sodium channels in primary sensory neurons', *Molecular Pain*. doi: 10.1186/s12990-015-0065-7.

Baral, P., Udit, S. and Chiu, I. M. (2019) 'Pain and immunity: implications for host defence', *Nature Reviews Immunology*. doi: 10.1038/s41577-019-0147-2.

Barker, P. A. *et al.* (2020) "Nerve Growth Factor Signaling and Its Contribution to Pain," *Journal of Pain Research*, Volume 13. doi: 10.2147/JPR.S247472.

Bartel, D. P. (2004) 'MicroRNAs: Genomics, Biogenesis, Mechanism, and Function', *Cell*. doi: 10.1016/S0092-8674(04)00045-5.

Bartel, D. P. (2009) 'MicroRNAs: Target Recognition and Regulatory Functions', *Cell*, pp. 215–233. doi: 10.1016/j.cell.2009.01.002.

von Bartheld, C. S., Bahney, J. and Herculano-Houzel, S. (2016) 'The search for true numbers of neurons and glial cells in the human brain: A review of 150 years of cell counting', *Journal of Comparative Neurology*. doi: 10.1002/cne.24040.

Basbaum, A. I. *et al.* (2009) 'Cellular and Molecular Mechanisms of Pain', *Cell*, pp. 267–284. doi: 10.1016/j.cell.2009.09.028.

Bassell, G. J. *et al.* (1998) 'Sorting of β -actin mRNA and protein to neurites and growth cones in culture', *Journal of Neuroscience*. doi: 10.1523/jneurosci.18-01-00251.1998.

Baudet, M. L. *et al.* (2012) 'MiR-124 acts through CoREST to control onset of Sema3A sensitivity in navigating retinal growth cones', *Nature Neuroscience*. doi: 10.1038/nn.2979.

Bautista, D. M. *et al.* (2006) 'TRPA1 Mediates the Inflammatory Actions of Environmental Irritants and Proalgesic Agents', *Cell*. doi: 10.1016/j.cell.2006.02.023.

Bazzan, E. *et al.* (2017) 'Dual polarization of human alveolar macrophages progressively increases with smoking and COPD severity', *Respiratory Research*. doi: 10.1186/s12931-017-0522-0.

Bazzini, A. A., Lee, M. T. and Giraldez, A. J. (2012) 'Ribosome profiling shows that miR-430 reduces translation before causing mRNA decay in Zebrafish', *Science*. doi: 10.1126/science.1215704.

Beland, B. and Fitzgerald, M. (2001) 'Influence of Peripheral Inflammation on the Postnatal

Maturation of Primary Sensory Neuron Phenotype in Rats', *The Journal of Pain*, 2(1), pp. 36–45. doi: 10.1054/jpai.2001.17697.

Bergmann, O. *et al.* (2012) 'The Age of Olfactory Bulb Neurons in Humans', *Neuron*. doi: 10.1016/j.neuron.2012.03.030.

Berridge, M. J., Bootman, M. D. and Roderick, H. L. (2003) 'Calcium signalling: Dynamics, homeostasis and remodelling', *Nature Reviews Molecular Cell Biology*. doi: 10.1038/nrm1155.

Berridge, M. J., Lipp, P. and Bootman, M. D. (2000) 'The versatility and universality of calcium signalling', *Nature Reviews Molecular Cell Biology*. doi: 10.1038/35036035.

Billiau, A. and Matthys, P. (2001) 'Modes of action of Freund's adjuvants in experimental models of autoimmune diseases.', *Journal of leukocyte biology*. doi: 10.1189/jlb.70.6.849.

Blair, N. T. and Bean, B. P. (2002) 'Roles of tetrodotoxin (TTX)-sensitive Na⁺ current, TTX-resistant Na⁺ current, and Ca²⁺ current in the action potentials of nociceptive sensory neurons', *Journal of Neuroscience*. doi: 10.1523/JNEUROSCI.22-23-10277.2002.

Bos, T. J. *et al.* (2016) 'Tethered function assays as tools to elucidate the molecular roles of RNA-binding proteins', in *Advances in Experimental Medicine and Biology*. doi: 10.1007/978-3-319-29073-7_3.

Bramsen, J. B. *et al.* (2007) 'Improved silencing properties using small internally segmented interfering RNAs', *Nucleic Acids Research*. doi: 10.1093/nar/gkm548.

Bretag, A. H. (1969) 'Synthetic interstitial fluid for isolated mammalian tissue', *Life Sciences*. doi: 10.1016/0024-3205(69)90283-5.

Briken, V. and Mosser, D. M. (2011) 'Editorial: Switching on arginase in M2 macrophages', *Journal of Leukocyte Biology*. doi: 10.1189/jlb.0411203.

Brundu S, F. A. (2015) 'Polarization and Repolarization of Macrophages', *Journal of Clinical and Cellular Immunology*. doi: 10.4172/2155-9899.1000319.

Burgin, K. E. *et al.* (1990) 'In situ hybridization histochemistry of Ca²⁺/calmodulin-dependent protein kinase in developing rat brain', *Journal of Neuroscience*. doi: 10.1523/jneurosci.10-06-01788.1990.

Burgoyne, R. D. and Haynes, L. P. (2015) 'Sense and specificity in neuronal calcium signalling', *Biochimica et Biophysica Acta - Molecular Cell Research*. doi: 10.1016/j.bbamcr.2014.10.029.

Burnstock, G. (2000) 'P2X receptors in sensory neurones', *British Journal of Anaesthesia*. doi:

10.1093/oxfordjournals.bja.a013473.

Burnstock, G. *et al.* (2009) 'Cytokine and Chemokine Regulation of Sensory Neuron Function', *Handbook of Experimental Pharmacology*. doi: 10.1007/978-3-642-28863-0_9.

Butovsky, O. *et al.* (2012) 'Modulating inflammatory monocytes with a unique microRNA gene signature ameliorates murine ALS', *Journal of Clinical Investigation*. doi: 10.1172/JCI62636.

Cai, W. *et al.*, 2018. MicroRNA-182 Alleviates Neuropathic Pain by Regulating Nav1.7 Following Spared Nerve Injury in Rats. *Nature: Scientific Reports*, 1803(16750).

Esposito, M. F., Malayil, R., Hanes, M. & Deer, T., 2019 . Unique Characteristics of the Dorsal Root Ganglion as a Target for Neuromodulation. *Pain Medicine*, Volume 20, pp. S23-S30.

Caldeira, C. *et al.* (2014) 'Microglia change from a reactive to an age-like phenotype with the time in culture', *Frontiers in Cellular Neuroscience*. doi: 10.3389/fncel.2014.00152.

Caldwell, J. H. *et al.* (2000) 'Sodium channel Nav1.6 is localized at nodes of Ranvier, dendrites, and synapses', *Proceedings of the National Academy of Sciences of the United States of America*. doi: 10.1073/pnas.090034797.

Campana, W. M. (2007) 'Schwann cells: Activated peripheral glia and their role in neuropathic pain', *Brain, Behavior, and Immunity*. doi: 10.1016/j.bbi.2006.12.008.

Campbell, J. N. and Meyer, R. A. (2006) 'Mechanisms of Neuropathic Pain', *Neuron*. doi: 10.1016/j.neuron.2006.09.021.

Campenot, R. B. (1982) 'Development of sympathetic neurons in compartmentalized cultures. II. Local control of neurite survival by nerve growth factor', *Developmental Biology*. doi: 10.1016/0012-1606(82)90233-0.

Casella, G. *et al.* (2016) 'IL4 induces IL6-producing M2 macrophages associated to inhibition of neuroinflammation in vitro and in vivo', *Journal of Neuroinflammation*. doi: 10.1186/s12974-016-0596-5.

Caterina, M. J. *et al.* (1997) 'The capsaicin receptor: A heat-activated ion channel in the pain pathway', *Nature*. doi: 10.1038/39807.

Caterina, M. J. *et al.* (2000) 'Impaired nociception and pain sensation in mice lacking the capsaicin receptor', *Science*. doi: 10.1126/science.288.5464.306.

Celada, A. *et al.* (1984) 'Evidence for a gamma-interferon receptor that regulates macrophage tumoricidal activity', *Journal of Experimental Medicine*. doi: 10.1084/jem.160.1.55.

- Celik, M. *et al.* (2020) 'IL-4 induces M2 macrophages to produce sustained analgesia via opioids', *JCI Insight*. doi: 10.1172/jci.insight.133093.
- Chen, C. *et al.* (2019) 'Long-term imaging of dorsal root ganglia in awake behaving mice', *Nature Communications*. doi: 10.1038/s41467-019-11158-0.
- Chen, G. *et al.* (2018) 'Sex-Dependent Glial Signaling in Pathological Pain: Distinct Roles of Spinal Microglia and Astrocytes', *Neuroscience Bulletin*. doi: 10.1007/s12264-017-0145-y.
- Chen, J. (Steven) and Sehdev, J. S. (2019) *Physiology, Pain, StatPearls*.
- Chen, X. *et al.* (2011a) 'TNF- α enhances the currents of voltage gated sodium channels in uninjured dorsal root ganglion neurons following motor nerve injury', *Experimental Neurology*. doi: 10.1016/j.expneurol.2010.11.017.
- Chen, X. *et al.* (2011b) 'TNF- α enhances the currents of voltage gated sodium channels in uninjured dorsal root ganglion neurons following motor nerve injury', *Experimental Neurology*. doi: 10.1016/j.expneurol.2010.11.017.
- Chen, Y. and Huang, L. Y. M. (2017) 'A simple and fast method to image calcium activity of neurons from intact dorsal root ganglia using fluorescent chemical Ca²⁺ indicators', *Molecular Pain*. doi: 10.1177/1744806917748051.
- Cheng, J.-K. and Ji, R.-R. (2008) "Intracellular Signaling in Primary Sensory Neurons and Persistent Pain," *Neurochemical Research*, 33(10). doi: 10.1007/s11064-008-9711-z.
- Chiu, I. M. *et al.* (2013) 'A neurodegeneration-specific gene-expression signature of acutely isolated microglia from an amyotrophic lateral sclerosis mouse model', *Cell Reports*. doi: 10.1016/j.celrep.2013.06.018.
- Chung, J. M. and Chung, K. (2002) 'Importance of Hyperexcitability of DRG Neurons in Neuropathic Pain', *Pain Practice*. doi: 10.1046/j.1533-2500.2002.02011.x.
- Clapham, D. E. (2007) *Calcium signaling, Calcium Signaling, Second Edition*. doi: 10.1201/9781420038231.
- Classen, A., Lloberas, J. and Celada, A. (2009) 'Macrophage activation: Classical vs. alternative', *Methods in Molecular Biology*. doi: 10.1007/978-1-59745-396-7_3.
- Commission, E. (2010) *Of mice and men – are mice relevant models for human disease ?*, *European Commission Workshop*.
- Corey, D. P. (2003) 'New TRP channels in hearing and mechanosensation', *Neuron*. doi: 10.1016/S0896-6273(03)00505-1.
- Coutaux, A. *et al.* (2005) 'Hyperalgesia and allodynia: Peripheral mechanisms', *Joint Bone*

Spine. doi: 10.1016/j.jbspin.2004.01.010.

Cowan, W. *et al.* (1984) 'Regressive events in neurogenesis', *Science*. doi: 10.1126/science.6474175.

Cregg, R. *et al.* (2010) 'Pain channelopathies', *Journal of Physiology*. doi: 10.1113/jphysiol.2010.187807.

Crowley, C. *et al.* (1994) 'Mice lacking nerve growth factor display perinatal loss of sensory and sympathetic neurons yet develop basal forebrain cholinergic neurons', *Cell*. doi: 10.1016/0092-8674(94)90378-6.

Cummins, T. R., Sheets, P. L. and Waxman, S. G. (2007) 'The roles of sodium channels in nociception: Implications for mechanisms of pain', *Pain*. doi: 10.1016/j.pain.2007.07.026.

Cunha, T. M. *et al.* (2008) 'Crucial role of neutrophils in the development of mechanical inflammatory hypernociception', *Journal of Leukocyte Biology*. doi: 10.1189/jlb.0907654.

Dajas-Bailador, F. *et al.* (2012) 'MicroRNA-9 regulates axon extension and branching by targeting Map1b in mouse cortical neurons', *Nature Neuroscience*. doi: 10.1038/nn.3082.

Davalos, D. *et al.* (2005) 'ATP mediates rapid microglial response to local brain injury in vivo', *Nature Neuroscience*. doi: 10.1038/nn1472.

Davis, H. P. and Squire, L. R. (1984) 'Protein synthesis and memory: A review', *Psychological Bulletin*. doi: 10.1037/0033-2909.96.3.518.

Davis, M. J. *et al.* (2013) 'Macrophage M1 / M2 Polarization Dynamically Adapts to Changes in', *MBio*, 4(3), pp. 1–10. doi: 10.1128/mBio.00264-13.Editor.

Denli, A. M. *et al.* (2004) 'Processing of primary microRNAs by the Microprocessor complex', *Nature*. doi: 10.1038/nature03049.

deSchoolmeester, M. L. *et al.* (2003) 'Absence of CC Chemokine Ligand 2 Results in an Altered Th1/Th2 Cytokine Balance and Failure to Expel *Trichuris muris* Infection', *The Journal of Immunology*. doi: 10.4049/jimmunol.170.9.4693.

Deshmane, S. L. *et al.* (2009) 'Monocyte chemoattractant protein-1 (MCP-1): An overview', *Journal of Interferon and Cytokine Research*. doi: 10.1089/jir.2008.0027.

Deuis, J. R., Dvorakova, L. S. and Vetter, I. (2017) 'Methods used to evaluate pain behaviors in rodents', *Frontiers in Molecular Neuroscience*. doi: 10.3389/fnmol.2017.00284.

Dib-Hajj, S. D. *et al.* (1999) 'Plasticity of sodium channel expression in DRG neurons in the chronic constriction injury model of neuropathic pain', *Pain*. doi: 10.1016/S0304-3959(99)00169-4.

Dib-Hajj, S. D. *et al.* (2010) 'Sodium Channels in Normal and Pathological Pain', *Annual Review of Neuroscience*. doi: 10.1146/annurev-neuro-060909-153234.

Dib-Hajj, S. D., Geha, P. and Waxman, S. G. (2017) 'Sodium channels in pain disorders: Pathophysiology and prospects for treatment', *Pain*. doi: 10.1097/j.pain.0000000000000854.

Dickensheets, H. *et al.* (2007) 'Suppressor of cytokine signaling-1 is an IL-4-inducible gene in macrophages and feedback inhibits IL-4 signaling', *Genes and Immunity*. doi: 10.1038/sj.gene.6364352.

Dinh, N.-D. *et al.* (2013) 'Microfluidic construction of minimalistic neuronal co-cultures', *Lab on a Chip*, 13(7). doi: 10.1039/c3lc41224e.

Discovering the Brain (1992) *Discovering the Brain*. doi: 10.17226/1785.

Djoughri, L. and Lawson, S. N. (2004) 'A β -fiber nociceptive primary afferent neurons: A review of incidence and properties in relation to other afferent A-fiber neurons in mammals', in *Brain Research Reviews*. doi: 10.1016/j.brainresrev.2004.07.015.

Dörrbaum, A. R. *et al.* (2018) 'Local and global influences on protein turnover in neurons and glia', *eLife*. doi: 10.7554/eLife.34202.

Drachman, D. A. (2005) 'Do we have brain to spare?', *Neurology*. doi: 10.1212/01.WNL.0000166914.38327.BB.

Dubin, A. E. and Patapoutian, A. (2010) 'Nociceptors: The sensors of the pain pathway', *Journal of Clinical Investigation*, pp. 3760–3772. doi: 10.1172/JCI42843.

Duflocq, A. *et al.* (2008) 'Nav1.1 is predominantly expressed in nodes of Ranvier and axon initial segments', *Molecular and Cellular Neuroscience*. doi: 10.1016/j.mcn.2008.06.008.

Duggett, N. A., Griffiths, L. A. and Flatters, S. J. L. (2017) 'Paclitaxel-induced painful neuropathy is associated with changes in mitochondrial bioenergetics, glycolysis, and an energy deficit in dorsal root ganglia neurons', *Pain*, 158(8), pp. 1499–1508. doi: 10.1097/j.pain.0000000000000939.

Duncan, C. *et al.* (2013) 'Painful nerve injury decreases sarco-endoplasmic reticulum Ca²⁺-ATPase activity in axotomized sensory neurons', *Neuroscience*. doi: 10.1016/j.neuroscience.2012.11.055.

Edelstein, A. D. *et al.* (2014) 'Advanced methods of microscope control using μ Manager software', *Journal of Biological Methods*. doi: 10.14440/jbm.2014.36.

Edwards, J. P. *et al.* (2006) 'Biochemical and functional characterization of three activated

macrophage populations', *Journal of Leukocyte Biology*. doi: 10.1189/jlb.0406249.

Elliott, A. A. and Elliott, J. R. (1993) 'Characterization of TTX-sensitive and TTX-resistant sodium currents in small cells from adult rat dorsal root ganglia.', *The Journal of Physiology*. doi: 10.1113/jphysiol.1993.sp019583.

Elshazzly, M. and Caban, O. (2019) *Embryology, Central Nervous System, StatPearls*.

Emery, E. C. *et al.* (2018) 'Dorsal Root Ganglion Neuron Types and Their Functional Specialization', in *The Oxford Handbook of the Neurobiology of Pain*. doi: 10.1093/oxfordhb/9780190860509.013.4.

Enyedi, P. and Czirják, G. (2010) 'Molecular background of leak K⁺ currents: Two-pore domain potassium channels', *Physiological Reviews*. doi: 10.1152/physrev.00029.2009.

Eom, T. *et al.* (2003) 'Localization of a B-Actin Messenger Ribonucleoprotein Complex with Zipcode-Binding Protein Modulates the Density of Dendritic Filopodia and Filopodial Synapses', *Journal of Neuroscience*. doi: 10.1523/jneurosci.23-32-10433.2003.

Esquela-Kerscher, A. and Slack, F. J. (2006) 'Oncomirs - MicroRNAs with a role in cancer', *Nature Reviews Cancer*. doi: 10.1038/nrc1840.

Eulalio, A. *et al.* (2009) 'A C-terminal silencing domain in GW182 is essential for miRNA function', *RNA*. doi: 10.1261/rna.1605509.

Everill, B. and Kocsis, J. D. (1999) 'Reduction in potassium currents in identified cutaneous afferent dorsal root ganglion neurons after axotomy', *Journal of Neurophysiology*. doi: 10.1152/jn.1999.82.2.700.

Everill, B. and Kocsis, J. D. (2000) 'Nerve growth factor maintains potassium conductance after nerve injury in adult cutaneous afferent dorsal root ganglion neurons', *Neuroscience*. doi: 10.1016/S0306-4522(00)00263-3.

Everill, B., Rizzo, M. A. and Kocsis, J. D. (1998) 'Morphologically identified cutaneous afferent DRG neurons express three different potassium currents in varying proportions', *Journal of Neurophysiology*. doi: 10.1152/jn.1998.79.4.1814.

Fan, L. *et al.* (2014) 'Impaired neuropathic pain and preserved acute pain in rats overexpressing voltage-gated potassium channel subunit Kv1.2 in primary afferent neurons', *Molecular Pain*. doi: 10.1186/1744-8069-10-8.

Fang, J. *et al.* (2010) 'The role of TLR2, TLR3, TLR4, and TLR9 signaling in the pathogenesis of autoimmune disease in a retinal autoimmunity model', *Investigative Ophthalmology and Visual Science*. doi: 10.1167/iovs.09-4754.

Fang, X. *et al.* (2002) 'The presence and role of the tetrodotoxin-resistant sodium channel Nav1.9 (NaN) in nociceptive primary afferent neurons', *Journal of Neuroscience*. doi: 10.1523/JNEUROSCI.22-17-07425.2002.

Fang, X. *et al.* (2006) 'Intense isolectin-B4 binding in rat dorsal root ganglion neurons distinguishes C-fiber nociceptors with broad action potentials and high Nav1.9 expression.', *The Journal of neuroscience : the official journal of the Society for Neuroscience*. doi: 10.1523/JNEUROSCI.1072-06.2006.

Fenstermacher, S. J., Pazyra-Murphy, M. F. and Segal, R. A. (2015) 'Campenot cultures and microfluidics provide complementary platforms for spatial study of dorsal root ganglia neurons', in *Microfluidic and Compartmentalized Platforms for Neurobiological Research*. doi: 10.1007/978-1-4939-2510-0_6.

Ferrari, L. F. *et al.* (2013) 'Peripheral administration of translation inhibitors reverses increased hyperalgesia in a model of chronic pain in the rat', *Journal of Pain*. doi: 10.1016/j.jpain.2013.01.779.

Fink, M. *et al.* (1996) 'Cloning, functional expression brain localization of a novel unconventional outward rectifier K⁺ channel', *EMBO Journal*. doi: 10.1002/j.1460-2075.1996.tb01077.x.

Fischer, M. J. M., Mak, S. W. Y. and McNaughton, P. A. (2014) 'Sensitisation of Nociceptors – What are Ion Channels Doing?', *The Open Pain Journal*. doi: 10.2174/1876386301003010082.

Fitzgerald, M. (2005) 'The development of nociceptive circuits', *Nature Reviews Neuroscience*. doi: 10.1038/nrn1701.

Fjell, J. *et al.* (2000) 'Localization of the tetrodotoxin-resistant sodium channel NaN in nociceptors', *NeuroReport*. doi: 10.1097/00001756-200001170-00039.

Fornasiero, E. F. *et al.* (2018) 'Precisely measured protein lifetimes in the mouse brain reveal differences across tissues and subcellular fractions', *Nature Communications*. doi: 10.1038/s41467-018-06519-0.

Fregnan, F. *et al.* (2012) 'Role of inflammatory cytokines in peripheral nerve injury', *Neural Regeneration Research*. doi: 10.3969/j.issn.1673-5374.2012.29.003.

Fuchs, A., Rigaud, M. and Hogan, Q. H. (2007) 'Painful nerve injury shortens the intracellular Ca²⁺ signal in axotomized sensory neurons of rats', *Anesthesiology*. doi: 10.1097/01.anes.0000267538.72900.68.

Fujita, H. *et al.* (1996) 'Effects of GM-CSF and ordinary supplements on the ramification of microglia in culture: A morphometrical study', *GLIA*. doi: 10.1002/(SICI)1098-1136(199612)18:4<269::AID-GLIA2>3.0.CO;2-T.

Galagali, H. and Kim, J. K. (2018) 'miRISC Composition Determines Target Fates in Time and Space', *Developmental Cell*. doi: 10.1016/j.devcel.2018.10.009.

Garcez, P. P., Guillemot, F. and Dajas-Bailador, F. (2017) 'Study of miRNA function in the developing axons of mouse cortical neurons: Use of compartmentalized microfluidic chambers and in utero electroporation', in *Neuromethods*. doi: 10.1007/7657_2016_12.

García-Piqueras, J. *et al.* (2019) 'Ageing of the somatosensory system at the periphery: age-related changes in cutaneous mechanoreceptors', *Journal of Anatomy*. doi: 10.1111/joa.12983.

Garner, C. C., Tucker, R. P. and Matus, A. (1988) 'Selective localization of messenger RNA for cytoskeletal protein MAP2 in dendrites', *Nature*. doi: 10.1038/336674a0.

Ghasemlou, N. *et al.* (2015) 'CD11b+Ly6G- myeloid cells mediate mechanical inflammatory pain hypersensitivity', *Proceedings of the National Academy of Sciences of the United States of America*. doi: 10.1073/pnas.1501372112.

Ginhoux, F. *et al.* (2010) 'Fate mapping analysis reveals that adult microglia derive from primitive macrophages', *Science*. doi: 10.1126/science.1194637.

Ginhoux, F. and Prinz, M. (2015) 'Origin of microglia: Current concepts and past controversies', *Cold Spring Harbor Perspectives in Biology*. doi: 10.1101/cshperspect.a020537.

Giuditta, A., Dettbarn, W. D. and Brzin, M. (1968) 'Protein synthesis in the isolated giant axon of the squid.', *Proceedings of the National Academy of Sciences of the United States of America*. doi: 10.1073/pnas.59.4.1284.

Godai, K. *et al.* (2014) 'Peripheral administration of morphine attenuates postincisional pain by regulating macrophage polarization through COX-2-dependent pathway', *Molecular Pain*. doi: 10.1186/1744-8069-10-36.

Gold, M. S. and Gebhart, G. F. (2010) 'Nociceptor sensitization in pain pathogenesis', *Nature Medicine*. doi: 10.1038/nm.2235.

Goldman, D. E. (1943) 'Potential, impedance, and rectification in membranes', *Journal of General Physiology*. doi: 10.1085/jgp.27.1.37.

Goldmann, T. and Prinz, M. (2013) 'Role of microglia in CNS autoimmunity', *Clinical and*

Developmental Immunology. doi: 10.1155/2013/208093.

Golpich, M. *et al.* (2015) 'Glycogen synthase kinase-3 beta (GSK-3 β) signaling: Implications for Parkinson's disease', *Pharmacological Research*. doi: 10.1016/j.phrs.2015.03.010.

Gordon, S. and Martinez-Pomares, L. (2017) 'Physiological roles of macrophages', *Pflugers Archiv European Journal of Physiology*. doi: 10.1007/s00424-017-1945-7.

Görlitz, B. D. and Frey, H. H. (1972) 'Central monoamines and antinociceptive drug action', *European Journal of Pharmacology*. doi: 10.1016/0014-2999(72)90146-X.

Grienberger, C. and Konnerth, A. (2012a) 'Imaging calcium in neurons.', *Neuron*. doi: 10.1016/j.neuron.2012.02.011.

Grienberger, C. and Konnerth, A. (2012b) 'Imaging Calcium in Neurons', *Neuron*. doi: 10.1016/j.neuron.2012.02.011.

Griffin, J. W. *et al.* (1976) 'AXONAL TRANSPORT TO AND FROM THE MOTOR NERVE ENDING', *Annals of the New York Academy of Sciences*. doi: 10.1111/j.1749-6632.1976.tb47674.x.

Griffin, J. W., George, R. and Ho, T. (1993) 'Macrophage systems in peripheral nerves. A review', *Journal of Neuropathology and Experimental Neurology*. doi: 10.1097/00005072-199311000-00001.

Griffiths-Jones, S. (2004) 'The microRNA registry', *Nucleic Acids Research*. doi: 10.1093/nar/gkh023.

Grimson, A. *et al.* (2007) 'MicroRNA Targeting Specificity in Mammals: Determinants beyond Seed Pairing', *Molecular Cell*. doi: 10.1016/j.molcel.2007.06.017.

Guldager Kring Rasmussen, D. and Karsdal, M. A. (2016) 'Laminins', in *Biochemistry of Collagens, Laminins and Elastin: Structure, Function and Biomarkers*. doi: 10.1016/B978-0-12-809847-9.00029-5.

Gumy, L. F. *et al.* (2011) 'Transcriptome analysis of embryonic and adult sensory axons reveals changes in mRNA repertoire localization', *RNA*. doi: 10.1261/rna.2386111.

Guo, R. *et al.* (2013) 'Novel MicroRNA Reporter Uncovers Repression of Let-7 by GSK-3 β ', *PLoS ONE*. doi: 10.1371/journal.pone.0066330.

Gutman, G. A. *et al.* (2005) 'International Union of Pharmacology. LIII. Nomenclature and molecular relationships of voltage-gated potassium channels', *Pharmacological Reviews*. doi: 10.1124/pr.57.4.10.

Ha, M. and Kim, V. N. (2014) 'Regulation of microRNA biogenesis', *Nature Reviews Molecular Cell Biology*. doi: 10.1038/nrm3838.

Hafner, A. S. *et al.* (2019) 'Local protein synthesis is a ubiquitous feature of neuronal pre- And postsynaptic compartments', *Science*. doi: 10.1126/science.aau3644.

Hagenston, A. M. and Baing, H. (2011) 'Calcium signaling in synapse-to-nucleus communication', *Cold Spring Harbor Perspectives in Biology*. doi: 10.1101/cshperspect.a004564.

Hall, A. K. *et al.* (1997) 'The generation of neuronal heterogeneity in a rat sensory ganglion', *Journal of Neuroscience*. doi: 10.1523/jneurosci.17-08-02775.1997.

Hamburger, V. and Levi-Montalcini, R. (1949) 'Proliferation, differentiation and degeneration in the spinal ganglia of the chick embryo under normal and experimental conditions', *Journal of Experimental Zoology*. doi: 10.1002/jez.1401110308.

Hameed, S. (2019) 'Nav1.7 and Nav1.8: Role in the pathophysiology of pain', *Molecular Pain*. doi: 10.1177/1744806919858801.

Hamilton, S. G. and McMahon, S. B. (2000) 'ATP as a peripheral mediator of pain', *Journal of the Autonomic Nervous System*. doi: 10.1016/S0165-1838(00)00137-5.

Han, J. *et al.* (2004) 'The Drosha-DGCR8 complex in primary microRNA processing', *Genes and Development*. doi: 10.1101/gad.1262504.

Hao, J. *et al.* (2013) 'Kv1.1 channels act as mechanical brake in the senses of touch and pain', *Neuron*. doi: 10.1016/j.neuron.2012.12.035.

Hayakawa, K. *et al.* (2016) 'Transfer of mitochondria from astrocytes to neurons after stroke Neurons can release damaged mitochondria and transfer them to astrocytes for disposal and recycling', *Nature*. doi: 10.1038/nature18928.

He, X. H. *et al.* (2010) 'TNF- α contributes to up-regulation of Nav1.3 and Nav1.8 in DRG neurons following motor fiber injury', *Pain*. doi: 10.1016/j.pain.2010.06.005.

von Hehn, C. A., Baron, R. and Woolf, C. J. (2012) 'Deconstructing the Neuropathic Pain Phenotype to Reveal Neural Mechanisms', *Neuron*. doi: 10.1016/j.neuron.2012.02.008.

Heine, M. *et al.* (2019) 'Dynamic compartmentalization of calcium channel signalling in neurons', *Neuropharmacology*. doi: 10.1016/j.neuropharm.2019.02.038.

Helmut, K. *et al.* (2011) 'Physiology of microglia', *Physiological Reviews*. doi: 10.1152/physrev.00011.2010.

Hendricks, A. G. *et al.* (2010) 'Motor Coordination via a Tug-of-War Mechanism Drives Bidirectional Vesicle Transport', *Current Biology*. doi: 10.1016/j.cub.2010.02.058.

Heneka, M. T., Kummer, M. P. and Latz, E. (2014) 'Innate immune activation in

neurodegenerative disease', *Nature Reviews Immunology*. doi: 10.1038/nri3705.

Herculano-Houzel, S., Mota, B. and Lent, R. (2006) 'Cellular scaling rules for rodent brains', *Proceedings of the National Academy of Sciences of the United States of America*. doi: 10.1073/pnas.0604911103.

Hille, B. (2001) 'Potassium Channels and Chloride Channels', in *Ionic Channels of Excitable Membranes*.

Hillman, H. and Hillman, H. (1986) 'The Fine Structure of the Nervous System', in *The Cellular Structure of the Mammalian Nervous System*. doi: 10.1007/978-94-009-4922-5_10.

Hirst, J. A. *et al.* (2014) 'The need for randomization in animal trials: An overview of systematic reviews', *PLoS ONE*. doi: 10.1371/journal.pone.0098856.

Hjerling-Leffler, J. *et al.* (2007) 'Emergence of Functional Sensory Subtypes as Defined by Transient Receptor Potential Channel Expression', *Journal of Neuroscience*. doi: 10.1523/jneurosci.5614-06.2007.

Hobson-Gutierrez, S. A. and Carmona-Fontaine, C. (2018) 'The metabolic axis of macrophage and immune cell polarization', *DMM Disease Models and Mechanisms*. doi: 10.1242/dmm.034462.

Hodgkin, A. L. and Huxley, A. F. (1952a) 'A quantitative description of membrane current and its application to conduction and excitation in nerve', *The Journal of Physiology*. doi: 10.1113/jphysiol.1952.sp004764.

Hodgkin, A. L. and Huxley, A. F. (1952b) 'Currents carried by sodium and potassium ions through the membrane of the giant axon of Loligo', *The Journal of Physiology*. doi: 10.1113/jphysiol.1952.sp004717.

Hodgkin, A. L. and Katz, B. (1949) 'The effect of sodium ions on the electrical activity of the giant axon of the squid', *The Journal of Physiology*. doi: 10.1113/jphysiol.1949.sp004310.

Hogan, Q. *et al.* (2000) 'PAINFUL NEUROPATHY DECREASES MEMBRANE CALCIUM CURRENT IN MAMMALIAN PRIMARY AFFERENT NEURONS', *Journal of the Peripheral Nervous System*. doi: 10.1046/j.1529-8027.2000.00022-34.x.

Holmes, F. E. *et al.* (2000) 'Targeted disruption of the galanin gene reduces the number of sensory neurons and their regenerative capacity', *Proceedings of the National Academy of Sciences of the United States of America*. doi: 10.1073/pnas.210221897.

Holt, C. E., and Schuman, E. M. (2013) 'The central dogma decentralized: new perspectives on RNA function and local translation in neurons.', *Neuron*, 80, pp. 648–657. doi: doi:

10.1016/j.neuron.2013.10.036.

Honma, Y. *et al.* (2010) 'Axonal projections of mechanoreceptive dorsal root ganglion neurons depend on Ret', *Development*. doi: 10.1242/dev.046995.

Hsu, S. Da *et al.* (2011) 'MiRTarBase: A database curates experimentally validated microRNA-target interactions', *Nucleic Acids Research*. doi: 10.1093/nar/gkq1107.

Huang, S., Hong, S. and De Schutter, E. (2015) 'Non-linear leak currents affect mammalian neuron physiology', *Frontiers in Cellular Neuroscience*. doi: 10.3389/fncel.2015.00432.

Huang, W. J., Chen, W. W. and Zhang, X. (2017) 'Multiple sclerosis: Pathology, diagnosis and treatments (review)', *Experimental and Therapeutic Medicine*. doi: 10.3892/etm.2017.4410.

Huang, X. *et al.* (2018) 'Polarizing macrophages in vitro', in *Methods in Molecular Biology*. doi: 10.1007/978-1-4939-7837-3_12.

Huebner, E. A. and Strittmatter, S. M. (2009) 'Axon regeneration in the peripheral and central nervous systems', *Results and Problems in Cell Differentiation*. doi: 10.1007/400_2009_19.

HYDEN, H. (1962) 'The neuron and its glia-a biochemical and functional unit.', *Endeavour*.

Iosub, R. *et al.* (2015) 'Calcium-induced calcium release during action potential firing in developing inner hair cells', *Biophysical Journal*. doi: 10.1016/j.bpj.2014.11.3489.

Ipsaro, J. J. and Joshua-Tor, L. (2015) 'From guide to target: Molecular insights into eukaryotic RNA-interference machinery', *Nature Structural and Molecular Biology*. doi: 10.1038/nsmb.2931.

Jackson, R. J. and Standart, N. (2007) 'How do microRNAs regulate gene expression?', *Science's STKE : signal transduction knowledge environment*. doi: 10.1126/stke.3672007re1.

Jacobs, K. M. *et al.* (2012) 'GSK-3 β : A bifunctional role in cell death pathways', *International Journal of Cell Biology*. doi: 10.1155/2012/930710.

Jaggi, A. S., Jain, V. and Singh, N. (2011) 'Animal models of neuropathic pain', *Fundamental and Clinical Pharmacology*. doi: 10.1111/j.1472-8206.2009.00801.x.

Jančálek, R. *et al.* (2010) 'Bilateral changes of TNF- α and IL-10 protein in the lumbar and cervical dorsal root ganglia following a unilateral chronic constriction injury of the sciatic nerve', *Journal of Neuroinflammation*. doi: 10.1186/1742-2094-7-11.

Jennings, E. and Fitzgerald, M. (1998) 'Postnatal changes in responses of rat dorsal horn cells to afferent stimulation: A fibre-induced sensitization', *Journal of Physiology*. doi: 10.1111/j.1469-7793.1998.859bm.x.

Jessen, K. R. and Arthur-Farraj, P. (2019) 'Repair Schwann cell update: Adaptive reprogramming, EMT, and stemness in regenerating nerves', *GLIA*. doi: 10.1002/glia.23532.

Jessen, K. R. and Mirsky, R. (2005) 'The origin and development of glial cells in peripheral nerves', *Nature Reviews Neuroscience*. doi: 10.1038/nrn1746.

Jha, M. K. *et al.* (2015) 'Metabolic Connection of Inflammatory Pain: Pivotal Role of a Pyruvate Dehydrogenase Kinase-Pyruvate Dehydrogenase-Lactic Acid', *Journal of Neuroscience*, 35(42), pp. 14353–14369. doi: 10.1523/JNEUROSCI.1910-15.2015.

Ji, R.-R., Chamesian, A. and Zhang, Y.-Q. (2016) 'Pain regulation by non-neuronal cells and inflammation', *Science*, 354(6312), pp. 572–577. doi: 10.1126/science.aaf8924.

Ji, R. R., Chamesian, A. and Zhang, Y. Q. (2016) 'Pain regulation by non-neuronal cells and inflammation', *Science*. doi: 10.1126/science.aaf8924.

Ji, R. R. and Strichartz, G. (2004) 'Cell signaling and the genesis of neuropathic pain.', *Science's STKE : signal transduction knowledge environment*. doi: 10.1126/stke.2522004re14.

Jin, X. and Gereau IV, R. W. (2006) 'Acute p38-mediated modulation of tetrodotoxin-resistant sodium channels in mouse sensory neurons by tumor necrosis factor- α ', *Journal of Neuroscience*. doi: 10.1523/JNEUROSCI.3858-05.2006.

Jin, Y. *et al.* (2013) 'Evaluating the MicroRNA targeting sites by luciferase reporter gene assay', *Methods in Molecular Biology*. doi: 10.1007/978-1-62703-083-0_10.

Jo, M. H. *et al.* (2015) 'Human Argonaute 2 Has Diverse Reaction Pathways on Target RNAs', *Molecular Cell*. doi: 10.1016/j.molcel.2015.04.027.

Johnston, J., Forsythe, I. D. and Kopp-Scheinflug, C. (2010) 'Going native: Voltage-gated potassium channels controlling neuronal excitability', in *Journal of Physiology*. doi: 10.1113/jphysiol.2010.191973.

Jonas, R. *et al.* (2020) 'TTX-Resistant Sodium Channels Functionally Separate Silent From Polymodal C-nociceptors', *Frontiers in Cellular Neuroscience*. doi: 10.3389/fncel.2020.00013.

Jonas, S. and Izaurralde, E. (2015) 'Towards a molecular understanding of microRNA-mediated gene silencing', *Nature Reviews Genetics*. doi: 10.1038/nrg3965.

Jow, F. *et al.* (2004) 'Functional coupling of intracellular calcium and inactivation of voltage-gated Kv1.1/Kv β 1.1 A-type K⁺ channels', *Proceedings of the National Academy of Sciences of the United States of America*. doi: 10.1073/pnas.0402081101.

Jung, H., Yoon, B. C. and Holt, C. E. (2012) 'Axonal mRNA localization and local protein

synthesis in nervous system assembly, maintenance and repair', *Nature Reviews Neuroscience*. doi: 10.1038/nrn3210.

Karagkouni, D. *et al.* (2018) 'DIANA-TarBase v8: A decade-long collection of experimentally supported miRNA-gene interactions', *Nucleic Acids Research*. doi: 10.1093/nar/gkx1141.

El Kasmi, K. C. *et al.* (2008) 'Toll-like receptor-induced arginase 1 in macrophages thwarts effective immunity against intracellular pathogens', *Nature Immunology*. doi: 10.1038/ni.1671.

Katz, J. and Rosenbloom, B. N. (2015) 'The golden anniversary of Melzack and Wall's gate control theory of pain: Celebrating 50 years of pain research and management', *Pain Research and Management*, pp. 285–286. doi: 10.1155/2015/865487.

Kazuhide, I. and Makoto, T. (2009) 'Microglia and neuropathic pain', *GLIA*. doi: 10.1002/glia.20871.

Kearney, J. A. (2015) 'KCNA2-Related Epileptic Encephalopathy', *Pediatric Neurology Briefs*. doi: 10.15844/pedneurbriefs-29-4-2.

Ketchum, K. A. *et al.* (1995) 'A new family of outwardly rectifying potassium channel proteins with two pore domains in tandem', *Nature*. doi: 10.1038/376690a0.

Khallou-Laschet, J. *et al.* (2010) 'Macrophage plasticity in experimental atherosclerosis', *PLoS ONE*. doi: 10.1371/journal.pone.0008852.

Kim, H. H., Kim, P., Phay, M., and Yoo, S. (2015) 'Identification of precursor microRNAs within distal axons of sensory neuron.', *Journal of Neurochemistry*, 134, pp. 193–199. Available at: doi: 10.1111/jnc.13140.

Kim, C. H. *et al.* (2001) 'The changes in expression of three subtypes of TTX sensitive sodium channels in sensory neurons after spinal nerve ligation', *Molecular Brain Research*. doi: 10.1016/S0169-328X(01)00226-1.

Kim, C. H. *et al.* (2002) 'Changes in three subtypes of tetrodotoxin sensitive sodium channel expression in the axotomized dorsal root ganglion in the rat', *Neuroscience Letters*. doi: 10.1016/S0304-3940(02)00127-1.

Kim, D. M. and Nimigean, C. M. (2016) 'Voltage-gated potassium channels: A structural examination of selectivity and gating', *Cold Spring Harbor Perspectives in Biology*. doi: 10.1101/cshperspect.a029231.

Kim, H. H. *et al.* (2015) 'Identification of precursor microRNAs within distal axons of sensory neuron', *Journal of Neurochemistry*. doi: 10.1111/jnc.13140.

- Kim, S. U. and De Vellis, J. (2005) 'Microglia in health and disease', *Journal of Neuroscience Research*. doi: 10.1002/jnr.20562.
- Kim, V. N. (2005) 'Small RNAs: classification, biogenesis, and function.', *Molecules and cells*, 19(1), pp. 1–15. doi: 806 [pii].
- Kim, V. N., Han, J. and Siomi, M. C. (2009) 'Biogenesis of small RNAs in animals', *Nature Reviews Molecular Cell Biology*, pp. 126–139. doi: 10.1038/nrm2632.
- Kim, Y. *et al.* (2001) 'Localization of $trkA$ channel domains that regulate channel kinetics and sensitivity to pressure, fatty acids and pH ', *Pflügers Archiv European Journal of Physiology*. doi: 10.1007/s004240100626.
- Koerber, H. R., Druzinsky, R. E. and Mendell, L. M. (2017) 'Properties of somata of spinal dorsal root ganglion cells differ according to peripheral receptor innervated', *Journal of Neurophysiology*. doi: 10.1152/jn.1988.60.5.1584.
- Koerber, H. R., Mirnics, K. and Mendell, L. M. (2017) 'Properties of regenerated primary afferents and their functional connections', *Journal of Neurophysiology*. doi: 10.1152/jn.1995.73.2.693.
- Kozlowski, C. and Weimer, R. M. (2012) 'An automated method to quantify microglia morphology and application to monitor activation state longitudinally in vivo', *PLoS ONE*. doi: 10.1371/journal.pone.0031814.
- Kozomara, A. and Griffiths-Jones, S. (2014) 'MiRBase: Annotating high confidence microRNAs using deep sequencing data', *Nucleic Acids Research*, 42(D1), pp. 68–73. doi: 10.1093/nar/gkt1181.
- Krames, E. S. (2014) 'The role of the dorsal root ganglion in the development of neuropathic pain', *Pain Medicine (United States)*. doi: 10.1111/pme.12413.
- Krames, E. S. (2015) 'The dorsal root ganglion in chronic pain and as a target for neuromodulation: A review', *Neuromodulation*, 18(1), pp. 24–32. doi: 10.1111/ner.12247.
- Krol, J., Loedige, I. and Filipowicz, W. (2010) 'The widespread regulation of microRNA biogenesis, function and decay', *Nature Reviews Genetics*. doi: 10.1038/nrg2843.
- Krukowski, K. *et al.* (2016) 'CD8+ T cells and endogenous IL-10 are required for resolution of chemotherapy-induced neuropathic pain', *Journal of Neuroscience*. doi: 10.1523/JNEUROSCI.3708-15.2016.
- Kuner, R. (2010) 'Central mechanisms of pathological pain', *Nature Medicine*. doi: 10.1038/nm.2231.

- Kwan, K. Y. *et al.* (2006) 'TRPA1 Contributes to Cold, Mechanical, and Chemical Nociception but Is Not Essential for Hair-Cell Transduction', *Neuron*. doi: 10.1016/j.neuron.2006.03.042.
- Kwon, M. J. *et al.* (2015) 'CCL2 mediates neuron-macrophage interactions to drive proregenerative macrophage activation following preconditioning injury', *Journal of Neuroscience*. doi: 10.1523/JNEUROSCI.1924-15.2015.
- Kwong, K. and Carr, M. J. (2015) 'Voltage-gated sodium channels', *Current Opinion in Pharmacology*. doi: 10.1016/j.coph.2015.04.007.
- Lakke, E. A. (1997) 'The projections to the spinal cord of the rat during development: a timetable of descent.', *Advances in anatomy, embryology, and cell biology*. doi: 10.1007/978-3-642-60601-4.
- LaMotte, R. & Ma, C., 2007. Multiple Sites for Generation of Ectopic Spontaneous Activity in Neurons of the Chronically Compressed Dorsal Root Ganglion. *Journal of Neuroscience*, 27(51), p. 14059–14068..
- Larson, C. M., Wilcox, G. L. and Fairbanks, C. A. (2019) 'The Study of Pain in Rats and Mice', *Comparative medicine*. doi: 10.30802/AALAS-CM-19-000062.
- Lasek, R. J., Dabrowski, C. and Nordlander, R. (1973) 'Analysis of axoplasmic RNA from invertebrate giant axons', *Nature New Biology*. doi: 10.1038/newbio244162a0.
- Latremoliere, A. and Woolf, C. J. (2009) 'Central Sensitization: A Generator of Pain Hypersensitivity by Central Neural Plasticity', *Journal of Pain*. doi: 10.1016/j.jpain.2009.06.012.
- Laumet, G. *et al.* (2015) 'G9a is essential for epigenetic silencing of K⁺ channel genes in acute-to-chronic pain transition', *Nature Neuroscience*. doi: 10.1038/nn.4165.
- Lawson, S. N. (2002) 'Phenotype and function of somatic primary afferent nociceptive neurones with C-, A δ - or A α / β -fibres', *Experimental Physiology*. doi: 10.1113/eph8702350.
- Lawson, S. N., Fang, X. and Djouhri, L. (2019) 'Nociceptor subtypes and their incidence in rat lumbar dorsal root ganglia (DRGs): focussing on C-polymodal nociceptors, A β -nociceptors, moderate pressure receptors and their receptive field depths', *Current Opinion in Physiology*. doi: 10.1016/j.cophys.2019.10.005.
- Lechner, S. G. *et al.* (2009) 'Developmental waves of mechanosensitivity acquisition in sensory neuron subtypes during embryonic development', *EMBO Journal*. doi: 10.1038/emboj.2009.73.
- Lee, R. C., Feinbaum, R. L. and Ambros, V. (1993) 'The *C. elegans* heterochronic gene *lin-4*

encodes small RNAs with antisense complementarity to lin-14', *Cell*, 75(5), pp. 843–854. doi: 10.1016/0092-8674(93)90529-Y.

Lee, S. H. *et al.* (2018) 'Targeting macrophage and microglia activation with colony stimulating factor 1 receptor inhibitor is an effective strategy to treat injury-triggered neuropathic pain', *Molecular Pain*. doi: 10.1177/1744806918764979.

Lee, Y. *et al.* (2003) 'The nuclear RNase III Drosha initiates microRNA processing', *Nature*. doi: 10.1038/nature01957.

Lei, W. *et al.* (2019) 'Non-engineered and engineered adult neurogenesis in mammalian brains', *Frontiers in Neuroscience*. doi: 10.3389/fnins.2019.00131.

Leo, M. *et al.* (2015) 'Modulation of Voltage-Gated Sodium Channels by Activation of Tumor Necrosis Factor Receptor-1 and Receptor-2 in Small DRG Neurons of Rats', *Mediators of Inflammation*. doi: 10.1155/2015/124942.

Leong, S. -K and Ling, E. -A (1992) 'Amoeboid and ramified microglia: Their interrelationship and response to brain injury', *Glia*. doi: 10.1002/glia.440060106.

Levi-Montalcini, R. (1987) 'The nerve growth factor 35 years later', *Science*. doi: 10.1126/science.3306916.

Levinson, S. R., Luo, S. and Henry, M. A. (2012) 'The role of sodium channels in chronic pain', *Muscle and Nerve*. doi: 10.1002/mus.23314.

Lewis, B. P. *et al.* (2003) 'Prediction of Mammalian MicroRNA Targets', *Cell*. doi: 10.1016/S0092-8674(03)01018-3.

Li, Y. *et al.* (2004) 'Determination of the critical concentration of neutrophils required to block bacterial growth in tissues', *Journal of Experimental Medicine*. doi: 10.1084/jem.20040725.

Lian, H., Roy, E. and Zheng, H. (2016) 'Microglial Phagocytosis Assay', *BIO-PROTOCOL*. doi: 10.21769/bioprotoc.1988.

Di Liegro, C. M., Schiera, G. and Di Liegro, I. (2014) 'Regulation of mRNA transport, localization and translation in the nervous system of mammals (Review)', *International Journal of Molecular Medicine*. doi: 10.3892/ijmm.2014.1629.

Lin, A. C. and Holt, C. E. (2008) 'Function and regulation of local axonal translation', *Current Opinion in Neurobiology*. doi: 10.1016/j.conb.2008.05.004.

Lindborg, J. A., Mack, M. and Zigmond, R. E. (2017) 'Neutrophils are critical for myelin removal in a peripheral nerve injury model of wallerian degeneration', *Journal of*

Neuroscience. doi: 10.1523/JNEUROSCI.2085-17.2017.

Liou, L. bang *et al.* (2013) 'Blood Monocyte Chemotactic Protein-1 (MCP-1) and Adapted Disease Activity Score28-MCP-1: Favorable Indicators for Rheumatoid Arthritis Activity', *PLoS ONE*. doi: 10.1371/journal.pone.0055346.

Liu, B. L. *et al.* (2014) 'Increased severity of inflammation correlates with elevated expression of TRPV1 nerve fibers and nerve growth factor on interstitial Cystitis/Bladder pain syndrome', *Urologia Internationalis*. doi: 10.1159/000355175.

Liu, C. M. *et al.* (2013) 'MicroRNA-138 and SIRT1 form a mutual negative feedback loop to regulate mammalian axon regeneration', *Genes and Development*. doi: 10.1101/gad.209619.112.

Liu, W. and Wang, X. (2019) 'Prediction of functional microRNA targets by integrative modeling of microRNA binding and target expression data', *Genome Biology*. doi: 10.1186/s13059-019-1629-z.

Liu, X. J. *et al.* (2016) 'TLR signaling adaptor protein MyD88 in primary sensory neurons contributes to persistent inflammatory and neuropathic pain and neuroinflammation', *Scientific Reports*. doi: 10.1038/srep28188.

Livak, K. J. and Schmittgen, T. D. (2001) 'Analysis of relative gene expression data using real-time quantitative PCR and the 2- $\Delta\Delta$ CT method', *Methods*. doi: 10.1006/meth.2001.1262.

Lock, J. T. *et al.* (2015) 'Imaging Local Ca²⁺ Signals in Cultured Mammalian Cells', *Journal of Visualized Experiments*. doi: 10.3791/52516.

Lock, J. T., Parker, I. and Smith, I. F. (2015) 'A comparison of fluorescent Ca²⁺ indicators for imaging local Ca²⁺ signals in cultured cells', *Cell Calcium*. doi: 10.1016/j.ceca.2015.10.003.

Long, S. B., Campbell, E. B. and MacKinnon, R. (2005) 'Crystal structure of a mammalian voltage-dependent Shaker family K⁺ channel', *Science*. doi: 10.1126/science.1116269.

Louw, A., Nijs, J. and Puentedura, E. J. (2017) 'A clinical perspective on a pain neuroscience education approach to manual therapy', *Journal of Manual and Manipulative Therapy*. doi: 10.1080/10669817.2017.1323699.

Low, L. K. and Cheng, H. J. (2006) 'Axon pruning: An essential step underlying the developmental plasticity of neuronal connections', *Philosophical Transactions of the Royal Society B: Biological Sciences*. doi: 10.1098/rstb.2006.1883.

Lu, H. L. *et al.* (2018) 'Activation of M1 macrophages plays a critical role in the initiation of acute lung injury', *Bioscience Reports*. doi: 10.1042/BSR20171555.

- Lu, S.-G. and Gold, M. S. (2008) 'Inflammation-Induced Increase in Evoked Calcium Transients in Subpopulations of Rat DRG Neurons', *Neuroscience*, 153(1), pp. 279–288. doi: 10.1016/j.neuroscience.2008.02.006.
- Lu, S. G. *et al.* (2010) 'Persistent inflammation alters the density and distribution of voltage-activated calcium channels in subpopulations of rat cutaneous DRG neurons', *Pain*. doi: 10.1016/j.pain.2010.08.030.
- Lu, X. and Richardson, P. M. (1993) 'Responses of macrophages in rat dorsal root ganglia following peripheral nerve injury', *Journal of Neurocytology*. doi: 10.1007/BF01195557.
- Lucci, C. *et al.* (2020) 'Spatiotemporal regulation of GSK3 β levels by miRNA-26a controls axon development in cortical neurons', *Development (Cambridge)*. doi: 10.1242/dev.180232.
- Lugli, G. *et al.* (2012) 'Primary microRNA precursor transcripts are localized at post-synaptic densities in adult mouse forebrain', *Journal of Neurochemistry*. doi: 10.1111/j.1471-4159.2012.07921.x.
- Lytle, J. R., Yario, T. A. and Steitz, J. A. (2007) 'Target mRNAs are repressed as efficiently by microRNA-binding sites in the 5' UTR as in the 3' UTR', *Proceedings of the National Academy of Sciences*, 104(23), pp. 9667–9672. doi: 10.1073/pnas.0703820104.
- Lyu, Y. S. *et al.* (2000) 'Low dose of tetrodotoxin reduces neuropathic pain behaviors in an animal model', *Brain Research*. doi: 10.1016/S0006-8993(00)02451-3.
- Ma, C., Greenquist, K. W. and LaMotte, R. H. (2006) 'Inflammatory mediators enhance the excitability of chronically compressed dorsal root ganglion neurons', *Journal of Neurophysiology*. doi: 10.1152/jn.00748.2005.
- MacInnis, B. L. and Campenot, R. B. (2002) 'Retrograde support of neuronal survival without retrograde transport of nerve growth factor', *Science*. doi: 10.1126/science.1064913.
- Maday, S. *et al.* (2014) 'Axonal Transport: Cargo-Specific Mechanisms of Motility and Regulation', *Neuron*. doi: 10.1016/j.neuron.2014.10.019.
- Madden, J. F. *et al.* (2020) 'Functional and Molecular Analysis of Proprioceptive Sensory Neuron Excitability in Mice', *Frontiers in Molecular Neuroscience*. doi: 10.3389/fnmol.2020.00036.
- Manis, P. B. (2014) 'Delayed Rectifier and A-Type Potassium Channels', in *Encyclopedia of Computational Neuroscience*. doi: 10.1007/978-1-4614-7320-6_227-1.
- Mantovani, A. *et al.* (2004) 'The chemokine system in diverse forms of macrophage

activation and polarization', *Trends in Immunology*. doi: 10.1016/j.it.2004.09.015.

Martinez, F. O. *et al.* (2008) 'Macrophage activation and polarization', *Frontiers in Bioscience*. doi: 10.2741/2692.

Martinez, F. O. and Gordon, S. (2014) 'The M1 and M2 paradigm of macrophage activation: time for reassessment', *F1000Prime Reports*, 6. doi: 10.12703/P6-13.

Martucci, C. *et al.* (2008) 'The purinergic antagonist PPADS reduces pain related behaviours and interleukin-1 β , interleukin-6, iNOS and nNOS overproduction in central and peripheral nervous system after peripheral neuropathy in mice', *Pain*. doi: 10.1016/j.pain.2007.08.017.

Massier, J. *et al.* (2015) 'Effects of differently activated rodent macrophages on sensory neurons: Implications for arthritis pain', *Arthritis and Rheumatology*. doi: 10.1002/art.39134.

McGrath, J. C. *et al.* (2010) 'Editorial: Guidelines for reporting experiments involving animals: The ARRIVE guidelines', *British Journal of Pharmacology*. doi: 10.1111/j.1476-5381.2010.00873.x.

McKemy, D. D., Neuhauser, W. M. and Julius, D. (2002) 'Identification of a cold receptor reveals a general role for TRP channels in thermosensation', *Nature*. doi: 10.1038/nature719.

Meier, P., Finch, A. and Evan, G. (2000) 'Apoptosis in development', *Nature*. doi: 10.1038/35037734.

Melton, D. W. *et al.* (2015) 'Temporal phenotypic features distinguish polarized macrophages in vitro', *Autoimmunity*. doi: 10.3109/08916934.2015.1027816.

Menassa, D. A. and Gomez-Nicola, D. (2018) 'Microglial dynamics during human brain development', *Frontiers in Immunology*. doi: 10.3389/fimmu.2018.01014.

Mercurio, A. M. and Shaw, L. M. (1988) 'Macrophage interactions with laminin: PMA selectively induces the adherence and spreading of mouse macrophages on a laminin substratum.', *Journal of Cell Biology*.

Merianda, T. T. *et al.* (2009) 'A functional equivalent of endoplasmic reticulum and Golgi in axons for secretion of locally synthesized proteins', *Molecular and Cellular Neuroscience*. doi: 10.1016/j.mcn.2008.09.008.

Michael, M. *et al.* (2019) 'TRPV1 activation alters the function of A δ and C fiber sensory neurons that innervate bone', *Bone*, 123, pp. 168–175. doi: <https://doi.org/10.1016/j.bone.2019.03.040>.

Michelucci, A. *et al.* (2009) 'Characterization of the microglial phenotype under specific pro-inflammatory and anti-inflammatory conditions: Effects of oligomeric and fibrillar amyloid- β ', *Journal of Neuroimmunology*. doi: 10.1016/j.jneuroim.2009.02.003.

Miller, R. J. *et al.* (2009) 'Cytokine and chemokine regulation of sensory neuron function', *Handbook of Experimental Pharmacology*. doi: 10.1007/978-3-540-79090-7_12.

Milligan, E. D. *et al.* (2006) 'Intrathecal polymer-based interleukin-10* gene delivery for neuropathic pain', *Neuron Glia Biology*. doi: 10.1017/S1740925X07000488.

Mills, C. D. *et al.* (2000) 'M-1/M-2 Macrophages and the Th1/Th2 Paradigm', *The Journal of Immunology*. doi: 10.4049/jimmunol.164.12.6166.

Mills, C. D. (2012) 'M1 and M2 macrophages: Oracles of health and disease', *Critical Reviews in Immunology*. doi: 10.1615/CritRevImmunol.v32.i6.10.

Ming, G. li and Song, H. (2011) 'Adult Neurogenesis in the Mammalian Brain: Significant Answers and Significant Questions', *Neuron*. doi: 10.1016/j.neuron.2011.05.001.

Misgeld, T. and Schwarz, T. L. (2017) 'Mitostasis in Neurons: Maintaining Mitochondria in an Extended Cellular Architecture', *Neuron*. doi: 10.1016/j.neuron.2017.09.055.

Moalem, G. and Tracey, D. J. (2006a) 'Immune and inflammatory mechanisms in neuropathic pain', *Brain Research Reviews*, pp. 240–264. doi: 10.1016/j.brainresrev.2005.11.004.

Moalem, G. and Tracey, D. J. (2006b) 'Immune and inflammatory mechanisms in neuropathic pain', *Brain Research Reviews*. doi: 10.1016/j.brainresrev.2005.11.004.

Molliver, D. C. *et al.* (1997) 'IB4-binding DRG neurons switch from NGF to GDNF dependence in early postnatal life', *Neuron*. doi: 10.1016/S0896-6273(00)80966-6.

Molliver, D. C. and Snider, W. D. (1997) 'Nerve growth factor receptor TrkA is down-regulated during postnatal development by a subset of dorsal root ganglion neurons', *Journal of Comparative Neurology*. doi: 10.1002/(SICI)1096-9861(19970519)381:4<428::AID-CNE3>3.0.CO;2-4.

Montell, C. (2005) 'The TRP superfamily of cation channels.', *Science's STKE : signal transduction knowledge environment*. doi: 10.1126/stke.2722005re3.

de Moraes, E. R., Kushmerick, C. and Naves, L. A. (2017) 'Morphological and functional diversity of first-order somatosensory neurons', *Biophysical Reviews*. doi: 10.1007/s12551-017-0321-3.

Morgan, M. *et al.* (2019) 'TRPV1 activation alters the function of A δ and C fiber sensory

neurons that innervate bone', *Bone*. doi: 10.1016/j.bone.2019.03.040.

Moss, A. *et al.* (2007) 'Spinal microglia and neuropathic pain in young rats', *Pain*. doi: 10.1016/j.pain.2006.09.018.

Mosser, D. M. and Edwards, J. P. (2008) 'Exploring the full spectrum of macrophage activation', *Nature Reviews Immunology*, pp. 958–969. doi: 10.1038/nri2448.

Mosser, D. M. and Zhang, X. (2008) 'Activation of murine macrophages.', *Current protocols in immunology / edited by John E. Coligan ... [et al.]*, Chapter 14, p. Unit 14.2. doi: 10.1002/0471142735.im1402s83.

Mueller, M. *et al.* (2003) 'Macrophage response to peripheral nerve injury: The quantitative contribution of resident and hematogenous macrophages', *Laboratory Investigation*. doi: 10.1097/01.LAB.0000056993.28149.BF.

Mulay, S. R. *et al.* (2016) 'Monocyte and macrophage heterogeneity', *Nature Communications*. doi: nri1733 [pii]\r10.1038/nri1733.

Murray, P. J. *et al.* (2014a) 'Macrophage Activation and Polarization: Nomenclature and Experimental Guidelines', *Immunity*. doi: 10.1016/j.immuni.2014.06.008.

Murray, P. J. *et al.* (2014b) 'Macrophage Activation and Polarization: Nomenclature and Experimental Guidelines', *Immunity*, pp. 14–20. doi: 10.1016/j.immuni.2014.06.008.

Murray, P. J. (2017) 'Macrophage Polarization', *Annual Review of Physiology*. doi: 10.1146/annurev-physiol-022516-034339.

Nahrendorf, M. *et al.* (2007) 'The healing myocardium sequentially mobilizes two monocyte subsets with divergent and complementary functions', *Journal of Experimental Medicine*. doi: 10.1084/jem.20070885.

Natera-Naranjo, O. *et al.* (2010) 'Identification and quantitative analyses of microRNAs located in the distal axons of sympathetic neurons', *RNA*. doi: 10.1261/rna.1833310.

Nave, K. A. and Salzer, J. L. (2006) 'Axonal regulation of myelination by neuregulin 1', *Current Opinion in Neurobiology*. doi: 10.1016/j.conb.2006.08.008.

Neher, E. and Sakaba, T. (2008) 'Multiple Roles of Calcium Ions in the Regulation of Neurotransmitter Release', *Neuron*. doi: 10.1016/j.neuron.2008.08.019.

Neto, E. *et al.* (2016) 'Compartmentalized microfluidic platforms: The unrivaled breakthrough of in vitro tools for neurobiological research', *Journal of Neuroscience*. doi: 10.1523/JNEUROSCI.1748-16.2016.

Niday, Z. and Tzingounis, A. V. (2018) 'Potassium Channel Gain of Function in Epilepsy: An

Unresolved Paradox', *Neuroscientist*. doi: 10.1177/1073858418763752.

Nolan, T., Hands, R. E. and Bustin, S. A. (2006) 'Quantification of mRNA using real-time RT-PCR', *Nature Protocols*. doi: 10.1038/nprot.2006.236.

O'Brien, J. *et al.* (2018) 'Overview of microRNA biogenesis, mechanisms of actions, and circulation', *Frontiers in Endocrinology*. doi: 10.3389/fendo.2018.00402.

O'Connell, A. D., Morton, M. J. and Hunter, M. (2002) 'Two-pore domain K⁺ channels - Molecular sensors', in *Biochimica et Biophysica Acta - Biomembranes*. doi: 10.1016/S0005-2736(02)00597-7.

Obara, I., Géranton, S. M. and Hunt, S. P. (2012) "Axonal protein synthesis: a potential target for pain relief?," *Current Opinion in Pharmacology*, 12(1). doi: 10.1016/j.coph.2011.10.005.

Ocaña, M. *et al.* (2004) 'Potassium channels and pain: Present realities and future opportunities', *European Journal of Pharmacology*. doi: 10.1016/j.ejphar.2004.07.026.

Okun, A. *et al.* (2011) 'Transient inflammation-induced ongoing pain is driven by TRPV1 sensitive afferents', *Molecular Pain*. doi: 10.1186/1744-8069-7-4.

Omana-Zapata, I. *et al.* (1997) 'QX-314 inhibits ectopic nerve activity associated with neuropathic pain', *Brain Research*. doi: 10.1016/S0006-8993(97)00770-1.

Oprée, A. and Kress, M. (2000) 'Involvement of the proinflammatory cytokines tumor necrosis factor- α , IL-1 β , and IL-6 but not IL-8 in the development of heat hyperalgesia: Effects on heat-evoked calcitonin gene-related peptide release from rat skin', *Journal of Neuroscience*. doi: 10.1523/jneurosci.20-16-06289.2000.

Orecchioni, M. *et al.* (2019) 'Macrophage polarization: Different gene signatures in M1(Lps+) vs. Classically and M2(LPS-) vs. Alternatively activated macrophages', *Frontiers in Immunology*. doi: 10.3389/fimmu.2019.01084.

Parada, C. A. *et al.* (2003) 'Transient attenuation of protein kinase C ϵ can terminate a chronic hyperalgesic state in the rat', *Neuroscience*. doi: 10.1016/S0306-4522(03)00267-7.

Paraskevopoulou, M. D. *et al.* (2013a) 'DIANA-microT web server v5.0: service integration into miRNA functional analysis workflows.', *Nucleic acids research*. doi: 10.1093/nar/gkt393.

Paraskevopoulou, M. D. *et al.* (2013b) 'DIANA-microT web server v5.0: service integration into miRNA functional analysis workflows.', *Nucleic acids research*. doi: 10.1093/nar/gkt393.

Paredes, R. M. *et al.* (2008) 'Chemical calcium indicators', *Methods*. doi: 10.1016/j.ymeth.2008.09.025.

Paredes, R. M. *et al.* (2009) 'Chemical Calcium Indicators R.', *Imaging*. doi:

10.1016/j.ymeth.2008.09.025.Chemical.

Park, J. W. *et al.* (2006) 'Microfluidic culture platform for neuroscience research', *Nature Protocols*. doi: 10.1038/nprot.2006.316.

Pasquinelli, A. E. *et al.* (2000) 'Conservation of the sequence and temporal expression of let-7 heterochronic regulatory RNA', *Nature*. doi: 10.1038/35040556.

Passlick, B., Flieger, D. and Loms Ziegler-Heitbrock, H. W. (1989) 'Identification and characterization of a novel monocyte subpopulation in human peripheral blood', *Blood*. doi: 10.1182/blood.v74.7.2527.bloodjournal7472527.

Patapoutian, A. *et al.* (2003) 'Thermotrp channels and beyond: Mechanisms of temperature sensation', *Nature Reviews Neuroscience*. doi: 10.1038/nrn1141.

Patapoutian, A., Tate, S. and Woolf, C. J. (2009) 'Transient receptor potential channels: Targeting pain at the source', *Nature Reviews Drug Discovery*. doi: 10.1038/nrd2757.

Pereira, J. A., Lebrun-Julien, F. and Suter, U. (2012) 'Molecular mechanisms regulating myelination in the peripheral nervous system', *Trends in Neurosciences*. doi: 10.1016/j.tins.2011.11.006.

Perlin, J. R. *et al.* (2011) 'Neuronal Neuregulin 1 type III directs Schwann cell migration', *Development*, 138(21), pp. 4639–4648. doi: 10.1242/dev.068072.

Perry, V. H., Hume, D. A. and Gordon, S. (1985) 'Immunohistochemical localization of macrophages and microglia in the adult and developing mouse brain', *Neuroscience*. doi: 10.1016/0306-4522(85)90215-5.

Peterson, S. M. *et al.* (2014) 'Common features of microRNA target prediction tools', *Frontiers in Genetics*. doi: 10.3389/fgene.2014.00023.

Pettersen, J. S. *et al.* (2011) 'Tumor-associated macrophages in the cutaneous SCC microenvironment are heterogeneously activated', *Journal of Investigative Dermatology*, 131(6), pp. 1322–1330. doi: 10.1038/jid.2011.9.

Piesla, M. J. *et al.* (2009) 'Abnormal gait, due to inflammation but not nerve injury, reflects enhanced nociception in preclinical pain models', *Brain Research*. doi: 10.1016/j.brainres.2009.07.091.

Pillai, R. S., Artus, C. G. and Filipowicz, W. (2004) 'Tethering of human Ago proteins to mRNA mimics the miRNA-mediated repression of protein synthesis', *RNA*. doi: 10.1261/rna.7131604.

Pinho-Ribeiro, F. A., Verri, W. A. and Chiu, I. M. (2016) 'Nociceptor Sensory Neuron–Immune

Interactions in Pain and Inflammation Modulation of Pain Sensitivity by Immune Cells', *Trends in Immunology*. doi: 10.1016/j.it.2016.10.001.

Pinto, L. G. *et al.* (2019) 'Non-Peptidergic Nociceptive Neurons Are Essential for Mechanical Inflammatory Hypersensitivity in Mice', *Molecular Neurobiology*. doi: 10.1007/s12035-019-1494-5.

Pitzer, C., Kuner, R. and Tappe-Theodor, A. (2016) 'Voluntary and evoked behavioral correlates in neuropathic pain states under different social housing conditions', *Molecular Pain*. doi: 10.1177/1744806916656635.

Popescu, B. F. G. and Lucchinetti, C. F. (2012) 'Pathology of Demyelinating Diseases', *Annual Review of Pathology: Mechanisms of Disease*. doi: 10.1146/annurev-pathol-011811-132443.

Prinz, M. and Mildner, A. (2011) 'Microglia in the CNS: Immigrants from another world', *GLIA*. doi: 10.1002/glia.21104.

Raddant, A. C. and Russo, A. F. (2011) 'Calcitonin gene-related peptide in migraine: intersection of peripheral inflammation and central modulation', *Expert Reviews in Molecular Medicine*. doi: 10.1017/s1462399411002067.

Raffaello, A. *et al.* (2016) 'Calcium at the Center of Cell Signaling: Interplay between Endoplasmic Reticulum, Mitochondria, and Lysosomes', *Trends in Biochemical Sciences*. doi: 10.1016/j.tibs.2016.09.001.

Rajamäki, K. *et al.* (2013) 'Extracellular acidosis is a novel danger signal alerting innate immunity via the NLRP3 inflammasome', *Journal of Biological Chemistry*. doi: 10.1074/jbc.M112.426254.

RANDALL, L. O. and SELITTO, J. J. (1957) 'A method for measurement of analgesic activity on inflamed tissue', *Archives internationales de pharmacodynamie et de thérapie*.

Randolph, G. J. *et al.* (1999) 'Differentiation of phagocytic monocytes into lymph node dendritic cells in vivo', *Immunity*. doi: 10.1016/S1074-7613(00)80149-1.

Ransohoff, R. M. (2016) 'A polarizing question: Do M1 and M2 microglia exist', *Nature Neuroscience*. doi: 10.1038/nn.4338.

Rao, X. *et al.* (2013) 'An improvement of the $2^{-\Delta\Delta CT}$ method for quantitative real-time polymerase chain reaction data analysis', *Biostat Bioinforma Biomath*. doi: 10.1016/j.micinf.2011.07.011.Innate.

Raouf, R. *et al.* (2020) 'Macrophages transfer mitochondria to sensory neurons to resolve inflammatory pain', *Cold Spring Harbor Perspectives in Biology*, Preprint. doi:

<https://doi.org/10.1101/2020.02.12.940445>.

Rasband, M. N. *et al.* (1998) 'Potassium channel distribution, clustering, and function in remyelinating rat axons', *Journal of Neuroscience*. doi: 10.1523/jneurosci.18-01-00036.1998.

Rasband, M. N. *et al.* (2001) 'Distinct potassium channels on pain-sensing neurons', *Proceedings of the National Academy of Sciences of the United States of America*. doi: 10.1073/pnas.231376298.

Rasband, M. N. (2010) 'Clustered K⁺ channel complexes in axons', *Neuroscience Letters*. doi: 10.1016/j.neulet.2010.08.081.

Rasband, M. N. and Peles, E. (2016) 'The nodes of Ranvier: Molecular assembly and maintenance', *Cold Spring Harbor Perspectives in Biology*. doi: 10.1101/cshperspect.a020495.

Rath, M. *et al.* (2014a) 'Metabolism via arginase or nitric oxide synthase: Two competing arginine pathways in macrophages', *Frontiers in Immunology*. doi: 10.3389/fimmu.2014.00532.

Rath, M. *et al.* (2014b) 'Metabolism via arginase or nitric oxide synthase: Two competing arginine pathways in macrophages', *Frontiers in Immunology*. doi: 10.3389/fimmu.2014.00532.

Reichling, D. B. and Levine, J. D. (2009) 'Critical role of nociceptor plasticity in chronic pain', *Trends in Neurosciences*, pp. 611–618. doi: 10.1016/j.tins.2009.07.007.

Reid, G., Kirschner, M. B. and van Zandwijk, N. (2011) 'Circulating microRNAs: Association with disease and potential use as biomarkers', *Critical Reviews in Oncology/Hematology*. doi: 10.1016/j.critrevonc.2010.11.004.

De Rie, D. *et al.* (2017) 'An integrated expression atlas of miRNAs and their promoters in human and mouse', *Nature Biotechnology*. doi: 10.1038/nbt.3947.

Rieske, E. and Kreutzberg, G. W. (1977) 'Long-term cell culture of electrically active sensory neurons free of glial cells', *Neuroscience Letters*. doi: 10.1016/0304-3940(77)90039-8.

Rink, T. J. and Merritt, J. E. (1990) 'Calcium signalling', *Current Opinion in Cell Biology*. doi: 10.1016/0955-0674(90)90007-2.

Del Rio-Hortega, P. (1919) 'El tercer elemento de los centros nerviosos', *Bio Soc Esp Biol*.

Rios, J. C. *et al.* (2003) 'Paranodal interactions regulate expression of sodium channel subtypes and provide a diffusion barrier for the node of ranvier', *Journal of Neuroscience*. doi: 10.1523/jneurosci.23-18-07001.2003.

van Rooij, E. and Kauppinen, S. (2014) 'Development of microRNA therapeutics is coming of age.', *EMBO molecular medicine*, 6(7), pp. 851–64. doi: 10.15252/emmm.201100899.

Rosenbaum Emir, T. L. (2017) *Neurobiology of TRP Channels, Neurobiology of TRP Channels*. doi: 10.4324/9781315152837.

Roszer, T. (2015) 'Understanding the mysterious M2 macrophage through activation markers and effector mechanisms', *Mediators of Inflammation*. doi: 10.1155/2015/816460.

Rotem, N. et al. (2017) 'ALS along the Axons - Expression of coding and noncoding RNA differs in axons of ALS models', *Scientific Reports*. doi: 10.1038/srep44500.

Ruscheweyh, R. et al. (2007) 'Modification of classical neurochemical markers in identified primary afferent neurons with A β -, A δ -, and C-fibers after chronic constriction injury in mice', *Journal of Comparative Neurology*. doi: 10.1002/cne.21311.

Sacerdote, P. et al. (2008) 'Transient early expression of TNF- α in sciatic nerve and dorsal root ganglia in a mouse model of painful peripheral neuropathy', *Neuroscience Letters*. doi: 10.1016/j.neulet.2008.03.023.

Sakai, A. et al. (2013) 'MiR-7a alleviates the maintenance of neuropathic pain through regulation of neuronal excitability', *Brain*. doi: 10.1093/brain/awt191.

Sakai, A. and Suzuki, H. (2014) 'Emerging roles of microRNAs in chronic pain', *Neurochemistry International*, pp. 58–67. doi: 10.1016/j.neuint.2014.05.010.

Saldanha, G. et al. (1999) "Decreased CGRP, but preserved Trk A immunoreactivity in nerve fibres in inflamed human superficial temporal arteries," *Journal of Neurology, Neurosurgery & Psychiatry*, 66(3). doi: 10.1136/jnnp.66.3.390.

Salzer, J. L. (2003) 'Polarized domains of myelinated axons', *Neuron*. doi: 10.1016/S0896-6273(03)00628-7.

Salzer, J. L. and Zalc, B. (2016) 'Myelination', *Current Biology*. doi: 10.1016/j.cub.2016.07.074.

Samways, D. S. K. et al. (2016) 'Measurement of relative Ca²⁺ permeability during sustained activation of TRPV1 receptors', *Pflügers Archiv European Journal of Physiology*. doi: 10.1007/s00424-015-1741-1.

Sandkühler, J. (2009) 'Models and mechanisms of hyperalgesia and allodynia', *Physiological Reviews*. doi: 10.1152/physrev.00025.2008.

Schäfers, M. et al. (2003) 'Spinal nerve ligation induces transient upregulation of tumor necrosis factor receptors 1 and 2 in injured and adjacent uninjured dorsal root ganglia in the

rat', *Neuroscience Letters*. doi: 10.1016/S0304-3940(03)00695-5.

Scheib, J. and Höke, A. (2013) 'Advances in peripheral nerve regeneration', *Nature Reviews Neurology*. doi: 10.1038/nrneurol.2013.227.

Schindelin, J. *et al.* (2012) 'Fiji: An open-source platform for biological-image analysis', *Nature Methods*. doi: 10.1038/nmeth.2019.

Schmidt, M. *et al.* (2009) 'Various signals involved in nociception regulate TRPA1 levels at the plasma membrane', *Neuron*. doi: 10.1016/j.neuron.2009.09.030.Various.

Scholz, J. and Woolf, C. J. (2007) 'The neuropathic pain triad: neurons, immune cells and glia', *Nature Neuroscience*, 10(11), pp. 1361–1368. doi: 10.1038/nn1992.

Schwaller, B. (2010) 'Cytosolic Ca²⁺ buffers.', *Cold Spring Harbor perspectives in biology*. doi: 10.1101/cshperspect.a004051.

Shachar, I. and Karin, N. (2013) 'The dual roles of inflammatory cytokines and chemokines in the regulation of autoimmune diseases and their clinical implications', *Journal of Leukocyte Biology*. doi: 10.1189/jlb.0612293.

Shimada, N. *et al.* (2020) 'M1 macrophage infiltration exacerbate muscle/bone atrophy after peripheral nerve injury', *BMC Musculoskeletal Disorders*. doi: 10.1186/s12891-020-3069-z.

Siegel, G. *et al.* (2009) 'A functional screen implicates microRNA-138-dependent regulation of the depalmitoylation enzyme APT1 in dendritic spine morphogenesis', *Nature Cell Biology*. doi: 10.1038/ncb1876.

Silos-Santiago, I. *et al.* (1995) 'Non-TrkA-expressing small DRG neurons are lost in TrkA deficient mice', *Journal of Neuroscience*. doi: 10.1523/jneurosci.15-09-05929.1995.

Simon, T. and Bromberg, J. S. (2017) 'Regulation of the Immune System by Laminins', *Trends in Immunology*. doi: 10.1016/j.it.2017.06.002.

Singh, K. K. and Miller, F. D. (2005) 'Activity regulates positive and negative neurotrophin-derived signals to determine axon competition', *Neuron*. doi: 10.1016/j.neuron.2005.01.049.

Soifer, H. S. *et al.* (2012) 'Silencing of gene expression by gymnotic delivery of antisense oligonucleotides', *Methods in Molecular Biology*. doi: 10.1007/978-1-61779-424-7_25.

Sotelo-Silveira, J. R. *et al.* (2006) 'RNA trafficking in axons', *Traffic*. doi: 10.1111/j.1600-0854.2006.00405.x.

Staud, R. and Smitherman, M. L. (2002) 'Peripheral and central sensitization in fibromyalgia: pathogenetic role.', *Current pain and headache reports*. doi: 10.1007/s11916-002-0046-1.

Stein, C. A. *et al.* (2009) 'Efficient gene silencing by delivery of locked nucleic acid antisense oligonucleotides, unassisted by transfection reagents', *Nucleic Acids Research*. doi: 10.1093/nar/gkp841.

Stein, C., Millan, M. J. and Herz, A. (1988) 'Unilateral inflammation of the hindpaw in rats as a model of prolonged noxious stimulation: Alterations in behavior and nociceptive thresholds', *Pharmacology, Biochemistry and Behavior*. doi: 10.1016/0091-3057(88)90372-3.

Stein, M. *et al.* (1992) 'Interleukin 4 potently enhances murine macrophage mannose receptor activity: A marker of alternative immunologic macrophage activation', *Journal of Experimental Medicine*. doi: 10.1084/jem.176.1.287.

Stevens, C. F. and Wesseling, J. F. (1998) 'Activity-dependent modulation of the rate at which synaptic vesicles become available to undergo exocytosis', *Neuron*. doi: 10.1016/S0896-6273(00)80550-4.

Steward, O. and Ribak, C. E. (1986) 'Polyribosomes associated with synaptic specializations on axon initial segments: Localization of protein-synthetic machinery at inhibitory synapses', *Journal of Neuroscience*. doi: 10.1523/jneurosci.06-10-03079.1986.

Stoll G *et al.* (1989) 'Wallerian degeneration in the peripheral nervous system: participation of both Schwann cells and macrophages in myelin degradation.', *Journal of Neurocytology*, 18(5), pp. 671–683.

Story, G. M. *et al.* (2003) 'ANKTM1, a TRP-like channel expressed in nociceptive neurons, is activated by cold temperatures', *Cell*. doi: 10.1016/S0092-8674(03)00158-2.

Stucky, C. L. and Lewin, G. R. (1999) 'Isolectin B4-positive and -negative nociceptors are functionally distinct', *Journal of Neuroscience*. doi: 10.1523/jneurosci.19-15-06497.1999.

Su, W. F. *et al.* (2019) 'Overexpression of P2X4 receptor in Schwann cells promotes motor and sensory functional recovery and remyelination via BDNF secretion after nerve injury', *GLIA*. doi: 10.1002/glia.23527.

Subtelny, A. O. *et al.* (2014) 'Poly(A)-tail profiling reveals an embryonic switch in translational control', *Nature*. doi: 10.1038/nature13007.

Susuki, K. (2010) 'Myelin: a specialized membrane for cell communication', *Nature Education*.

Sutton, M. A. and Schuman, E. M. (2006) 'Dendritic Protein Synthesis, Synaptic Plasticity, and Memory', *Cell*. doi: 10.1016/j.cell.2006.09.014.

Syrbe, S. *et al.* (2015) 'De novo loss-or gain-of-function mutations in KCNA2 cause epileptic encephalopathy', *Nature Genetics*. doi: 10.1038/ng.3239.

Takahashi, M. *et al.* (2004) 'Cyclooxygenase-2 expression in Schwann cells and macrophages in the sciatic nerve after single spinal nerve injury in rats', *Neuroscience Letters*. doi: 10.1016/j.neulet.2004.03.040.

Tandrup, T. (2004) 'Unbiased estimates of number and size of rat dorsal root ganglion cells in studies of structure and cell survival', *Journal of Neurocytology*. doi: 10.1023/B:NEUR.0000030693.91881.53.

Tarique, A. A. *et al.* (2015) 'Phenotypic, Functional and Plasticity Features of Classical and Alternatively Activated Human Macrophages.', *American journal of respiratory cell and molecular biology*, 53(5), pp. 676–688. doi: 10.1165/rcmb.2015-0012OC.

Taylor, A. M. *et al.* (2005) 'A microfluidic culture platform for CNS axonal injury, regeneration and transport', *Nature Methods*. doi: 10.1038/nmeth777.

Tender, G. C., Li, Y. Y. and Cui, J. G. (2008) 'Vanilloid receptor 1-positive neurons mediate thermal hyperalgesia and tactile allodynia', *Spine Journal*. doi: 10.1016/j.spinee.2007.08.005.

Thacker, M. A. *et al.* (2007) 'Pathophysiology of peripheral neuropathic pain: Immune cells and molecules', *Anesthesia and Analgesia*. doi: 10.1213/01.ane.0000275190.42912.37.

Thakor, D. *et al.* (2009) 'Increased peripheral nerve excitability and local NaV1.8 mRNA up-regulation in painful neuropathy', *Molecular Pain*. doi: 10.1186/1744-8069-5-14.

Thomas, A. C. and Mattila, J. T. (2014) "'Of mice and men": Arginine metabolism in macrophages', *Frontiers in Immunology*. doi: 10.3389/fimmu.2014.00479.

Thomas, D. *et al.* (2000) 'A comparison of fluorescent Ca²⁺ indicator properties and their use in measuring elementary and global Ca²⁺ signals', *Cell Calcium*. doi: 10.1054/ceca.2000.0152.

Thomson, C. E. *et al.* (2008) 'Myelinated, synapsing cultures of murine spinal cord - Validation as an in vitro model of the central nervous system', *European Journal of Neuroscience*. doi: 10.1111/j.1460-9568.2008.06415.x.

Timmerman, R., Burm, S. M. and Bajramovic, J. J. (2018) 'An overview of in vitro methods to study microglia', *Frontiers in Cellular Neuroscience*. doi: 10.3389/fncel.2018.00242.

Todd, A. J. (2010) 'Neuronal circuitry for pain processing in the dorsal horn', *Nature Reviews Neuroscience*. doi: 10.1038/nrn2947.

- Toews, A. D., Barrett, C. and Morell, P. (1998) 'Monocyte chemoattractant protein 1 is responsible for macrophage recruitment following injury to sciatic nerve', *Journal of Neuroscience Research*. doi: 10.1002/(SICI)1097-4547(19980715)53:2<260::AID-JNR15>3.0.CO;2-A.
- Trimmer, J. S. (2015) 'Subcellular localization of K⁺ channels in mammalian brain neurons: Remarkable precision in the midst of extraordinary complexity', *Neuron*. doi: 10.1016/j.neuron.2014.12.042.
- Tsantoulas, C. *et al.* (2012) 'Sensory neuron downregulation of the Kv9.1 potassium channel subunit mediates neuropathic pain following nerve injury', *Journal of Neuroscience*. doi: 10.1523/JNEUROSCI.3561-12.2012.
- Tsantoulas, C. *et al.* (2013) 'Probing functional properties of nociceptive axons using a microfluidic culture system', *PLoS ONE*. doi: 10.1371/journal.pone.0080722.
- Tsantoulas, C. and McMahon, S. B. (2014) 'Opening paths to novel analgesics: The role of potassium channels in chronic pain', *Trends in Neurosciences*. doi: 10.1016/j.tins.2013.12.002.
- Tsuchida, M. A. *et al.* (2014) 'Advanced methods of microscope control using μ Manager software', *Journal of Biological Methods*. doi: 10.14440/jbm.2014.36.
- Tsuda, M. *et al.* (2003) 'P2X4 receptors induced in spinal microglia gate tactile allodynia after nerve injury', *Nature*. doi: 10.1038/nature01786.
- Tsuda, M. *et al.* (2009) 'Behavioral phenotypes of mice lacking purinergic P2X4 receptors in acute and chronic pain assays', *Molecular Pain*. doi: 10.1186/1744-8069-5-28.
- Tsuda, M., Tozaki-Saitoh, H. and Inoue, K. (2010) 'Pain and purinergic signaling', *Brain Research Reviews*. doi: 10.1016/j.brainresrev.2009.11.003.
- Tüfekci, K. U. *et al.* (2014) 'The role of microRNAs in human diseases', *Methods in Molecular Biology*. doi: 10.1007/978-1-62703-748-8_3.
- Tushev, G. *et al.* (2018) 'Alternative 3' UTRs Modify the Localization, Regulatory Potential, Stability, and Plasticity of mRNAs in Neuronal Compartments', *Neuron*. doi: 10.1016/j.neuron.2018.03.030.
- Uceyler, N., Tschärke, A. and Sommer, C. (2007) '399 EARLY CYTOKINE EXPRESSION IN MOUSE SCIATIC NERVE AFTER CHRONIC CONSTRICTION NERVE INJURY DEPENDS ON CALPAIN', *European Journal of Pain*. doi: 10.1016/j.ejpain.2007.03.414.
- Ueno, M. *et al.* (2013) 'Layer v cortical neurons require microglial support for survival during

postnatal development', *Nature Neuroscience*. doi: 10.1038/nn.3358.

Uncini, A. and Kuwabara, S. (2015) 'Nodopathies of the peripheral nerve: An emerging concept', *Journal of Neurology, Neurosurgery and Psychiatry*. doi: 10.1136/jnnp-2014-310097.

Unsain, N. *et al.* (2014) 'Production and Isolation of Axons from Sensory Neurons for Biochemical Analysis Using Porous Filters', *Journal of Visualized Experiments*. doi: 10.3791/51795.

Vandewauw, I., Owsianik, G. and Voets, T. (2013) 'Systematic and quantitative mRNA expression analysis of TRP channel genes at the single trigeminal and dorsal root ganglion level in mouse', *BMC Neuroscience*. doi: 10.1186/1471-2202-14-21.

Vega-Avelaira, D., Ballesteros, J. J. and López-García, J. A. (2013) 'Inflammation-induced hyperalgesia and spinal microglia reactivity in neonatal rats', *European Journal of Pain (United Kingdom)*. doi: 10.1002/j.1532-2149.2013.00308.x.

Vega-Avelaira, D., Géranton, S. M. and Fitzgerald, M. (2009) 'Differential Regulation of Immune Responses and Macrophage/Neuron Interactions in the Dorsal Root Ganglion in Young and Adult Rats following Nerve Injury', *Molecular Pain*, 5, pp. 1744-8069-5-70. doi: 10.1186/1744-8069-5-70.

Viatchenko-Karpinski, V., Ling, J. and Gu, J. G. (2018) 'Characterization of temperature-sensitive leak K⁺ currents and expression of TRAAK, TREK-1, and TREK2 channels in dorsal root ganglion neurons of rats', *Molecular Brain*. doi: 10.1186/s13041-018-0384-5.

Vysokov, N., McMahon, S. B. and Raouf, R. (2019) 'The role of NaV channels in synaptic transmission after axotomy in a microfluidic culture platform', *Scientific Reports*. doi: 10.1038/s41598-019-49214-w.

Wager, C. M. L. and Wormley, F. L. (2014) 'Classical versus alternative macrophage activation: The Ying and the Yang in host defense against pulmonary fungal infections', *Mucosal Immunology*. doi: 10.1038/mi.2014.65.

Wagner, R. and Myers, R. R. (1996) 'Schwann cells produce tumor necrosis factor alpha: Expression in injured and non-injured nerves', *Neuroscience*. doi: 10.1016/0306-4522(96)00127-3.

Wang, B. *et al.* (2015) 'FMRP-Mediated Axonal Delivery of miR-181d Regulates Axon Elongation by Locally Targeting Map1b and Calm1', *Cell Reports*. doi: 10.1016/j.celrep.2015.11.057.

- Wang, H. *et al.* (1993) 'Heteromultimeric K⁺ channels in terminal and juxtaparanodal regions of neurons', *Nature*. doi: 10.1038/365075a0.
- Wang, H. and Wessendorf, M. W. (2001) 'Equal proportions of small and large DRG neurons express opioid receptor mRNAs', *Journal of Comparative Neurology*. doi: 10.1002/1096-9861(20010122)429:4<590::AID-CNE6>3.0.CO;2-V.
- Wang, J. G. *et al.* (2007) 'Local inflammation in rat dorsal root ganglion alters excitability and ion currents in small-diameter sensory neurons', *Anesthesiology*. doi: 10.1097/01.anes.0000270761.99469.a7.
- Wang, Jiaying *et al.* (2019) 'Targeting microglia and macrophages: A potential treatment strategy for multiple sclerosis', *Frontiers in Pharmacology*. doi: 10.3389/fphar.2019.00286.
- Wang, L. X. and Wang, Z. J. (2003) 'Animal and cellular models of chronic pain', *Advanced Drug Delivery Reviews*. doi: 10.1016/S0169-409X(03)00098-X.
- Waxman, S. G., Kocsis, J. D. and Black, J. A. (1994) 'Type III sodium channel mRNA is expressed in embryonic but not adult spinal sensory neurons, and is reexpressed following axotomy', *Journal of Neurophysiology*. doi: 10.1152/jn.1994.72.1.466.
- Weiss, P. (1967) 'Neuronal dynamics and axonal flow. 3. Cellulifugal transport of labeled neuroplasm in isolated nerve preparations.', *Proceedings of the National Academy of Sciences of the United States of America*. doi: 10.1073/pnas.57.5.1239.
- Weng, X. *et al.* (2012) 'Chronic inflammatory pain is associated with increased excitability and hyperpolarization-activated current (I_h) in C- but not A δ -nociceptors', *Pain*. doi: 10.1016/j.pain.2012.01.019.
- Whiteley, P. E. and Dalrymple, S. A. (2001) 'Models of Inflammation: Carrageenan-Induced Paw Edema in the Rat', in *Current Protocols in Pharmacology*. doi: 10.1002/0471141755.ph0504s00.
- Wightman, B., Ha, I. and Ruvkun, G. (1993) 'Posttranscriptional regulation of the heterochronic gene *lin-14* by *lin-4* mediates temporal pattern formation in *C. elegans*', *Cell*, 75(5), pp. 855–862. doi: 10.1016/0092-8674(93)90530-4.
- Winter, C. A., Risley, E. A. and Nuss, G. W. (1962) 'Carrageenin-Induced Edema in Hind Paw of the Rat as an Assay for Antiinflammatory Drugs', *Proceedings of the Society for Experimental Biology and Medicine*. doi: 10.3181/00379727-111-27849.
- Wirkner, K., Sperlagh, B. and Illes, P. (2007) 'P2X₃ receptor involvement in pain states', *Molecular Neurobiology*. doi: 10.1007/s12035-007-0033-y.

- Woolf, C. J. *et al.* (1994) 'Nerve growth factor contributes to the generation of inflammatory sensory hypersensitivity', *Neuroscience*, 62(2), pp. 327–331. doi: 10.1016/0306-4522(94)90366-2.
- Woolf, C. J. *et al.* (1998) 'Towards a mechanism-based classification of pain?', *Pain*. doi: 10.1016/S0304-3959(98)00099-2.
- Xian, X. C. and Nicol, G. D. (2007) 'Manipulation of the potassium channel Kv1.1 and its effect on neuronal excitability in rat sensory neurons', *Journal of Neurophysiology*. doi: 10.1152/jn.00437.2007.
- Xie, M. *et al.* (2013) 'Mammalian 5'-capped microRNA precursors that generate a single microRNA', *Cell*. doi: 10.1016/j.cell.2013.11.027.
- Xie, M. and Steitz, J. A. (2014) 'Versatile microRNA biogenesis in animals and their viruses', *RNA Biology*. doi: 10.4161/rna.28985.
- Xiuli, Z. *et al.* (2013) 'A long noncoding RNA contributes to neuropathic pain by silencing Kcna2 in primary afferent neurons.', *Nature Neuroscience*.
- Xuan, F.-L. *et al.* (2019) 'Differences of Microglia in the Brain and the Spinal Cord', *Frontiers in Cellular Neuroscience*. doi: 10.3389/fncel.2019.00504.
- Xue, Q. *et al.* (2006) "Transcription of rat TRPV1 utilizes a dual promoter system that is positively regulated by nerve growth factor," *Journal of Neurochemistry*, 101(1). doi: 10.1111/j.1471-4159.2006.04363.x.
- Yam, M. F. *et al.* (2018) 'General pathways of pain sensation and the major neurotransmitters involved in pain regulation', *International Journal of Molecular Sciences*. doi: 10.3390/ijms19082164.
- Yang, F. and Zheng, J. (2017) 'Understand spiciness: mechanism of TRPV1 channel activation by capsaicin', *Protein and Cell*. doi: 10.1007/s13238-016-0353-7.
- Yang, J. S. and Lai, E. C. (2011) 'Alternative miRNA Biogenesis Pathways and the Interpretation of Core miRNA Pathway Mutants', *Molecular Cell*. doi: 10.1016/j.molcel.2011.07.024.
- Yang, Z. and Ming, X. F. (2014) 'Functions of arginase isoforms in macrophage inflammatory responses: Impact on cardiovascular diseases and metabolic disorders', *Frontiers in Immunology*. doi: 10.3389/fimmu.2014.00533.
- Yu, F. H. and Catterall, W. A. (2003) 'Overview of the voltage-gated sodium channel family', *Genome Biology*. doi: 10.1186/gb-2003-4-3-207.

Yuan, J., Lipinski, M. and Degterev, A. (2003) 'Diversity in the mechanisms of neuronal cell death', *Neuron*. doi: 10.1016/S0896-6273(03)00601-9.

Yurchenco, P. D. (2011) 'Basement membranes: Cell scaffoldings and signaling platforms', *Cold Spring Harbor Perspectives in Biology*. doi: 10.1101/cshperspect.a004911.

Zajd, C. M. *et al.* (2020) 'Bone Marrow-Derived and Elicited Peritoneal Macrophages Are Not Created Equal: The Questions Asked Dictate the Cell Type Used', *Frontiers in Immunology*. doi: 10.3389/fimmu.2020.00269.

Zanier, E. R. *et al.* (2015) 'Shape descriptors of the "never resting" microglia in three different acute brain injury models in mice', *Intensive Care Medicine Experimental*. doi: 10.1186/s40635-015-0039-0.

Zeilhofer, H. U. *et al.* (2020) 'Dorsal Horn Pain Mechanisms', in *The Oxford Handbook of the Neurobiology of Pain*. doi: 10.1093/oxfordhb/9780190860509.013.23.

Zhang, H. *et al.* (2013) 'Induction of monocyte chemoattractant protein-1 (mcp-1) and its receptor ccr2 in primary sensory neurons contributes to paclitaxel-induced peripheral neuropathy', *Journal of Pain*. doi: 10.1016/j.jpain.2013.03.012.

Zhang, J. *et al.* (2020) 'Epigenetic restoration of voltage-gated potassium channel Kv1.2 alleviates nerve injury-induced neuropathic pain', *Journal of Neurochemistry*. doi: 10.1111/jnc.15117.

Zhang, X., Goncalves, R. and Mosser, D. M. (2008) 'The isolation and characterization of murine macrophages', *Curr Protoc Immunol*. doi: 10.1002/0471142735.im1401s83.The.

Zhang, Y. *et al.* (2015) 'MicroRNAs in the axon locally mediate the effects of chondroitin sulfate proteoglycans and cGMP on axonal growth', *Developmental Neurobiology*. doi: 10.1002/dneu.22292.

Zhao, J., Lee, M. C., *et al.* (2010) 'Small RNAs control sodium channel expression, nociceptor excitability, and pain thresholds', *Journal of Neuroscience*. doi: 10.1523/JNEUROSCI.1980-10.2010.

Zhao, J., Lee, M.-C., *et al.* (2010) 'Small RNAs Control Sodium Channel Expression, Nociceptor Excitability, and Pain Thresholds', *Journal of Neuroscience*. doi: 10.1523/JNEUROSCI.1980-10.2010.

Zhao, J. Y. *et al.* (2017) 'DNA methyltransferase DNMT3a contributes to neuropathic pain by repressing Kcna2 in primary afferent neurons', *Nature Communications*. doi: 10.1038/ncomms14712.

- Zhao, Q. *et al.* (2016) 'TRPV1 and neuropeptide receptor immunoreactivity and expression in the rat lung and brainstem after lung ischemia-reperfusion injury', *Journal of Surgical Research*. doi: 10.1016/j.jss.2016.03.050.
- Zhao, S. *et al.* (2004) 'Human, mouse, and rat genome large-scale rearrangements: Stability versus speciation', *Genome Research*. doi: 10.1101/gr.2663304.
- Zhao, X. *et al.* (2013) 'A long noncoding RNA contributes to neuropathic pain by silencing Kcna2 in primary afferent neurons', *Nature Neuroscience*. doi: 10.1038/nn.3438.
- Zheng, J. Q. *et al.* (2001) 'A functional role for intra-axonal protein synthesis during axonal regeneration from adult sensory neurons', *Journal of Neuroscience*. doi: 10.1523/jneurosci.21-23-09291.2001.
- Zhou, T. *et al.* (2017) 'Microglia polarization with M1/M2 phenotype changes in rd1 mouse model of retinal degeneration', *Frontiers in Neuroanatomy*. doi: 10.3389/fnana.2017.00077.
- Zhou, X. *et al.* (2016) 'MicroRNA-138 Inhibits Periodontal Progenitor Differentiation under Inflammatory Conditions.', *Journal of dental research*. United States, 95(2), pp. 230–237. doi: 10.1177/0022034515613043.
- Zigmond, R. E. and Echevarria, F. D. (2019) 'Macrophage biology in the peripheral nervous system after injury', *Progress in Neurobiology*. doi: 10.1016/j.pneurobio.2018.12.001.
- Zimmermann, K. *et al.* (2007) 'Sensory neuron sodium channel Nav1.8 is essential for pain at low temperatures', *Nature*. doi: 10.1038/nature05880.
- Zuchero, J. B. (2014) 'Purification and culture of dorsal root ganglion neurons', *Cold Spring Harbor Protocols*. doi: 10.1101/pdb.top073965.